Elucidation of fibroblast growth factor 1 and 2 effects on the adipogenesis and osteogenesis of primary human bone marrow stromal cells

---

Aufklärung der Effekte von Fibroblasten-Wachstumsfaktor 1 und 2 auf die Adipogenese und Osteogenese von primären humanen Knochenmark-Stroma-Zellen

Doctoral thesis for a doctoral degree at the
Graduate School of Life Sciences (GSLS),
Julius-Maximilians-Universität Würzburg,
Section Biomedicine

submitted by

Meike Simann
born in Soltau

Würzburg 2015

Submitted on: June 19, 2015

Members of the thesis committee:

Chairperson: Prof. Dr. Markus Engstler

Primary supervisor: Prof. Dr. Norbert Schütze

Supervisor (second): Prof. Dr. Ricardo Benavente

Supervisor (third): Prof. Dr. Franz Jakob

Date of public defense: September 10, 2015

Date of receipt of certificates: _____

Affidavit

I hereby confirm that my thesis entitled 'Elucidation of fibroblast growth factor 1 and 2 effects on the adipogenesis and osteogenesis of primary human bone marrow stromal cells' is the product of my own work. I did not receive any help or support from commercial consultants. All sources and/or materials applied are listed and specified in the thesis.

Furthermore, I confirm that this thesis has not yet been submitted as part of another examination process neither in identical nor in similar form.

Würzburg

June 18, 2015 _____

(Meike Simann)

Eidesstattliche Erklärung

Hiermit erkläre ich an Eides statt, die Dissertation "Aufklärung der Effekte von Fibroblasten-Wachstumsfaktor 1 und 2 auf die Adipogenese und Osteogenese von primären humanen Knochenmark-Stroma-Zellen" eigenständig, d.h. insbesondere selbständig und ohne Hilfe eines kommerziellen Promotionsberaters, angefertigt und keine als die angegebenen Hilfsmittel verwendet zu haben.

Ich erkläre außerdem, dass die Dissertation weder in gleicher noch in ähnlicher Form bereits in einem anderen Prüfungsverfahren vorgelegen hat.

Würzburg

June 18, 2015 _____

(Meike Simann)

Contents

Acknowledgments

The present doctoral thesis was conducted in the laboratory for Molecular Orthopedics and Cell Biology, which is integrated in the Orthopedic Center for Musculoskeletal Research (OZMF) and the Musculoskeletal Center Würzburg (MCW). Besides, a part of the work was accomplished at the premises of the institute of Tissue Engineering and Regenerative Medicine (TERM) chaired by Prof. Dr. Heike Walles. It is my pleasure to thank all my colleagues of the OZMF and the MCW as well as the members of the TERM for sharing their technical equipment and experimental know-how.

Additionally, I had the chance to assign to the Graduate School of Life Sciences (GSLS) and the Integrated Graduate College SFB Transregio 17 (TR17), which organized excellent workshops on scientific and transferable skills as well as mentoring activities.

I am grateful to Dr. Tatjana Schilling, who laid the foundation for the present study with her previous work on MSC differentiation and transdifferentiation. My work was funded by the German Research Foundation (DFG), grant number Schi 1071/3-1.

I thank my primary supervisor Prof. Dr. Norbert Schütze for giving me the chance to work on this interesting scientific topic and for the numerous opportunities to present and discuss my work at national and international conferences.

I acknowledge my second supervisor Prof. Dr. Ricardo Benavente of the Faculty of Biology, who accepted the position of a reviewer, thereby enabling this scientific dissertation at the GSLS.

I am greatly indebted to Prof. Dr. Franz Jakob, my third supervisor, for his broad scientific expertise, the visions concerning my project, and most fruitful discussions concerning not only this work, but also the preceding journal publication and the successful GSLS stipend application.

In addition, I acknowledge the professional support of my colleagues Beate Geyer, Viola Zehe, Susanne Wiesner, and Jutta Schneidereit, who created an excellent working atmosphere against all odds. Moreover, I highly appreciated to supervise my bachelor student Verena Schneider. Most special thanks go to my doctoral fellows Sylvia Hondke, Solange Le Blanc, Julia Dotterweich, and Bettina Hafen. They encouraged and supported me in various ways on the professional as well as the personal level. Particular thanks go to Sylvia for careful and critical proof reading of this manuscript.

Finally, my most profound thanks go to my mother Renate Simann, who always encouraged me to find and follow my own direction. Furthermore, I am very grateful to my sister Sandra for her deeply inspirational attitude. At last, I thank my boyfriend Andreas for his consistency and understanding.

Abstract

Regulating and reverting the adipo-osteogenic lineage decision of trabecular human bone marrow stromal cells (hBMSCs) represents a promising approach for osteoporosis therapy and prevention. Fibroblast growth factor 1 (FGF1) and its subfamily member FGF2 were scored as lead candidates to exercise control over lineage switching processes (conversion) in favor of osteogenesis previously. However, their impact on differentiation events is controversially discussed in literature. Hence, the present study aimed to investigate the effects of these FGFs on the adipogenic and osteogenic differentiation and conversion of primary hBMSCs. Moreover, involved downstream signaling mechanisms should be elucidated and, finally, the results should be evaluated with regard to the possible therapeutic approach.

This study clearly revealed that culture in the presence of FGF1 strongly prevented the adipogenic differentiation of hBMSCs as well as the adipogenic conversion of pre-differentiated osteoblastic cells. Lipid droplet formation was completely inhibited by a concentration of $25\,\mathrm{ng}\,\mu\mathrm{L}^{-1}$. Meanwhile, the expression of genetic markers for adipogenic initiation, peroxisome proliferator-activated receptor $\gamma 2$ (PPAR$\gamma 2$) and CCAAT/enhancer binding protein α (C/EBPα), as well as subsequent adipocyte maturation, fatty acid binding protein 4 (FABP4) and lipoprotein lipase (LPL), were significantly downregulated. Yet, the genetic markers of osteogenic commitment and differentiation were not upregulated during adipogenic differentiation and conversion under FGF supplementation, not supporting an event of osteogenic lineage switching.

Moreover, when examining the effects on the osteogenic differentiation of hBMSCs and the osteogenic conversion of pre-differentiated adipocytic cells, culture in the presence of FGF1 markedly decreased extracellular matrix (ECM) mineralization. Additionally, the gene expression of the osteogenic marker alkaline phosphatase (ALP) was significantly reduced and ALP enzyme activity was decreased. Furthermore, genetic markers of osteogenic commitment, like the master regulator runt-related transcription factor 2 (RUNX2) and bone morphogenetic protein 4 (BMP4), as well as markers of osteogenic differentiation and ECM formation, like collagen 1 A1 (COL1A1) and integrin-binding sialoprotein (IBSP), were downregulated. In contrast, genes known to inhibit ECM mineralization, like ANKH inorganic pyrophosphate transport regulator (ANKH) and osteopontin (OPN), were upregulated. ANKH inhibition revealed that its transcriptional elevation was not crucial for the reduced matrix mineralization, perhaps due to decreased expression of ectonucleotide pyrophosphatase/phosphodiesterase 1 (ENPP1) that likely annulled ANKH upregulation. Like FGF1, also the culture in the presence of FGF2 displayed a marked anti-adipogenic and anti-osteogenic effect.

The FGF receptor 1 (FGFR1) was found to be crucial for mediating the described FGF effects in adipogenic and osteogenic differentiation and conversion. Yet, adipogenic conversion displayed a lower involvement of the FGFR1. For adipogenic differentiation and osteogenic differentiation/conversion, downstream signal transduction involved the extracellular signal-regulated kinases 1 and 2 (ERK1/2) and the mitogen-activated protein kinase (MAPK)/ERK kinases 1 and 2 (MEK1/2), probably via the phosphorylation of FGFR docking protein FGFR substrate 2α (FRS2α) and its effector Ras/MAPK. The c-Jun N-terminal kinase (JNK), p38-MAPK, and protein kinase C (PKC) were not crucial for the signal transduction, yet were in part responsible for the rate of adipogenic and/or osteogenic differentiation itself, in line with current literature.

Taken together, to the best of our knowledge, our study was the first to describe the strong impact of FGF1 and FGF2 on both the adipogenic and osteogenic differentiation and conversion processes of primary hBMSCs in parallel. It clearly revealed that although both FGFs were not able to promote the differentiation and lineage switching towards the osteogenic fate, they strongly prevented adipogenic differentiation and lineage switching, which seem to be elevated during osteoporosis. Our findings indicate that FGF1 and FGF2 entrapped hBMSCs in a pre-committed state. In conclusion, these agents could be applied to potently prevent unwanted adipogenesis *in vitro*. Moreover, our results might aid in unraveling a pharmacological control point to eliminate the increased adipogenic differentiation and conversion as potential cause of adipose tissue accumulation and decreased osteoblastogenesis in bone marrow during aging and especially in osteoporosis.

Zusammenfassung

Die Regulation und Umkehr des adipogenen und osteogenen Commitments von trabekulären humanen Knochenmarks-Stroma Zellen (hBMSCs) stellt einen vielversprechenden Ansatz für die Prävention und Therapie der Knochenerkrankung Osteoporose dar. Der Fibroblasten-Wachstumsfaktor 1 (FGF1) und sein Proteinfamilien-Mitglied FGF2 wurden in einer vorhergehenden Studie als Hauptkandidaten bezüglich der Kontrolle einer Konversion (Schicksalsänderung) von hBMSCs in die osteogene Richtung bewertet. Der Effekt von FGF1 und FGF2 auf die Differenzierung von hBMSCs wird jedoch in der Literatur kontrovers diskutiert. Folglich zielte die aktuelle Studie darauf ab, die Effekte dieser Faktoren auf die adipogene und osteogene Differenzierung und Konversion von primären hBMSCs zu untersuchen. Außerdem sollten die nachgeschalteten Signalmechanismen aufgeklärt und die Ergebnisse abschließend bezüglich des angestrebten Therapieansatzes bewertet werden.

Die vorliegende Studie zeigte eindeutig, dass die adipogene Differenzierung von hBMSCs sowie die adipogene Konversion von vordifferenzierten osteoblastischen Zellen durch die Kultur in Gegenwart von FGF1 stark inhibiert wurde. Die typische Bildung von intrazellulären Fetttropfen war bei einer Konzentration von $25\,\mathrm{ng}\,\mu\mathrm{L}^{-1}$ vollständig inhibiert, während die Genexpression von frühen und späten adipogenen Markern signifikant herunterreguliert war. Die osteogenen Marker waren jedoch während der adipogenen Differenzierung und Konversion unter FGF-Zugabe nicht hochreguliert, was eine etwaige Schicksalsänderung zugunsten der osteogenen Richtung nicht unterstützte.

Bei der Untersuchung der osteogenen Differenzierung von hBMSCs und der osteogenen Konversion von vordifferenzierten adipozytischen Zellen bewirkte die Zugabe von FGF1 zum Differenzierungsmedium eine deutliche Verminderung der Mineralisierung der extrazellulären Matrix (ECM). Darüber hinaus war die Genexpression der alkalischen Phosphatase (ALP) signifikant reduziert; außerdem wurde die ALP Enzymaktivität erniedrigt. Sowohl Marker des osteogenen Commitments einschließlich des osteogenen Master-Transkriptionsfaktors RUNX2 (Runt-related transcription factor 2), als auch Marker der weiterführenden osteogenen Differenzierung waren herunterreguliert. Im Kontrast dazu waren Inhibitoren der ECM-Mineralisierung hochreguliert. Die Hochregulation von ANKH (ANKH inorganic pyrophosphate transport regulator) schien hierbei jedoch keine direkte Auswirkung auf die Reduzierung der Mineralisierung zu haben; seine Wirkung wurde wahrscheinlich durch die Herunterregulation von ENPP1 (Ectonucleotide pyrophosphatase/ phosphodiesterase 1) aufgehoben. Wie FGF1 zeigte auch FGF2 eine anti-adipogene und anti-osteogene Wirkung.

Der FGF Rezeptor 1 (FGFR1) war für die Weiterleitung der beschriebenen FGF-Effekte entscheidend, wobei die adipogene Konversion eine erniedrigte Beteiligung dieses Rezeptors zeigte. Bei der adipogenen Differenzierung und der osteogenen Differenzierung und Konversion waren die nachgeschalteten Signalwege ERK1/2 (Extracellular signal-regulated kinases 1 and 2) bzw. MEK1/2 (Mitogen-activated protein kinase (MAPK)/ ERK kinases 1 and 2) involviert, vermutlich über eine Phosphorylierung des FGFR Substrats FRS2α (FGFR substrate 2α) und der Ras/MAP Kinase. Im Gegensatz dazu waren die c-Jun N-terminale Kinase (JNK), die p38-MAP Kinase und die Proteinkinase C (PKC) nicht an der Weiterleitung des FGF-Signals beteiligt. Sie zeigten sich jedoch, in Übereinstimmung mit der aktuellen Literatur, verantwortlich für das Ausmaß der adipogenen bzw. osteogenen Differenzierung selbst.

Zusammenfassend war die vorliegende Studie nach unserem besten Wissen die erste, die den starken Einfluss von FGF1 und FGF2 parallel sowohl auf die adipogene als auch die osteogene Differenzie-

rung und Konversion von primären hBMSCs untersucht hat. Sie zeigte deutlich, dass, obwohl beide FGFs nicht die Differenzierung und Konversion zum osteogenen Zellschicksal hin unterstützen konnten, sie dennoch wirkungsvoll die adipogene Differenzierung und Konversion verhinderten, die whrend der Osteoporose erhht zu sein scheinen. Unsere Ergebnisse lassen den Schluss zu, dass hBMSCs durch FGF1 und FGF2 in einem Stadium vor dem Schicksals-Commitment festgehalten werden. Folglich könnten diese Proteine verwendet werden, um eine ungewollte Adipogenese *in vitro* zu verhindern. Außerdem könnten unsere Ergebnisse helfen, einen pharmakologischen Kontrollpunkt zur Eliminierung der gesteigerten adipogenen Differenzierung und Konversion aufzudecken, welche potentielle Gründe für die Fettakkumulation und die reduzierte Osteoblastogenese im Knochenmark während des Alterns und besonders in der Osteoporose sind.

Part I

Introduction

1 Osteoporosis and the adipose tissue accumulation in bone marrow

1.1 Bone disorder of high clinical relevance

Osteoporosis ('fragile or porous bones', from Greek: 'ostoun: bone' and 'poros: pore') is characterized by the decrease of bone mass and density, which predisposes to an increased fracture risk[1]. This progressive bone disorder is clinically highly relevant. It is the most common skeletal disease in persons from 50 years upwards with a female to male ration of 4 to 1. Approximately 30% of all postmenopausal women develop osteoporosis, which is attributable to the decrease in estrogen production. In addition to this primary osteoporosis subtype, which is not resulting from another predisposing disease, the secondary osteoporosis occurs due to chronic medical problems or the prolonged use of medications such as glucocorticoids. In summary, osteoporosis is responsible for millions of fractures per year, which typically affect the vertebral column, hip, rib, and wrist. Especially vertebral and hip fractures result in increased morbidity and mortality and cause enormous healthcare costs. This is of particular importance since the global trend of increasing longevity results in aging populations and a rise of this skeletal disorder.

The World Health Organization (WHO) defines osteoporosis as bone mineral density (BMD) of 2.5 standard deviations or more below the mean peak bone mass of young and healthy adults, measured by dual-energy X-ray absorptiometry[1]. While BMD decreases, the trabecular bone micro-architecture progressively deteriorates leading to decreased bone strength and quality (Fig. 1.1). The underlying mechanism is an imbalance between the two processes characterizing the bone remodeling cycle, the resorption of old and the formation of new bone[2].

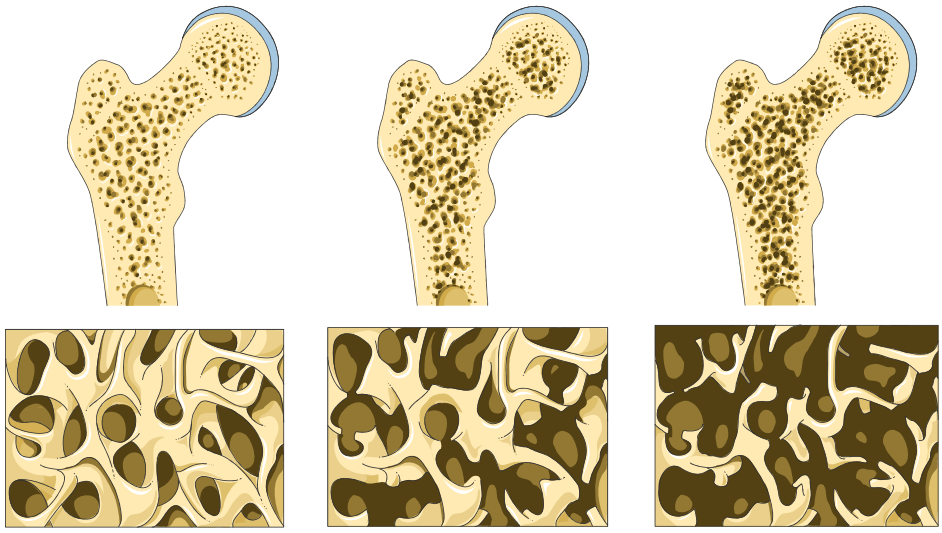

Figure 1.1: Osteoporosis deteriorates the micro-architecture of trabecular bone. Normal trabecular or spongy bone is structured in well-connected plates or broad bands providing great strength and flexibility at the same time. During osteoporosis, these bands are weakened and disrupted so that they can no longer contribute to bone strength, thereby predisposing to an increased fracture risk. This affects especially the spine, wrist, and hip, where trabecular bone predominates. Figure adapted from Servier Medical Art (`http://www.servier.com/Powerpoint-image-bank`).

1.2 Bone resorption and new formation

In healthy bone, the remodeling of bone matrix occurs constantly so that up to 10% of total bone mass undergo this process at any time point. It allows the repair of major injuries as well as small bone fractures occurring from daily physical activities; moreover, bone is adjusted to altered needs of physical activity and loading.

Bone consists of two major components, the inorganic bone mineral hydroxyapatite and the organic component that comprises bone matrix proteins. As recently reviewed[3], during the bone remodeling cycle (Fig. 1.2) the bone-degrading osteoclast dissolves the bone mineral and secretes enzymes to degrade the bone matrix proteins[4], thereby creating pits in the bone surface. During a brief reversal phase, the resorption pit is occupied by osteoblast precursors. Then, the bone-forming osteoblast newly synthesizes and secretes extracellular matrix (ECM)-associated proteins like i.e. collagen type 1, osteopontin (OPN), integrin-binding sialoprotein (IBSP), and osteocalcin (OC). This extracellular layer of organic components forms the unmineralized, flexible osteoid on which the osteoblasts reside. Furthermore, osteoblast-derived matrix vesicles, which contain alkaline phosphatases (ALP), locally release inorganic phosphate. In combination with the abundant calcium in the extracellular fluid, this leads to the new formation of hydroxyapatite $Ca_{10}(PO_4)_6(OH)_2$ crystals[5], which are deposited along the collagenous fibrilar scaffolds[6]. These processes are also referred to as ECM formation and mineralization.

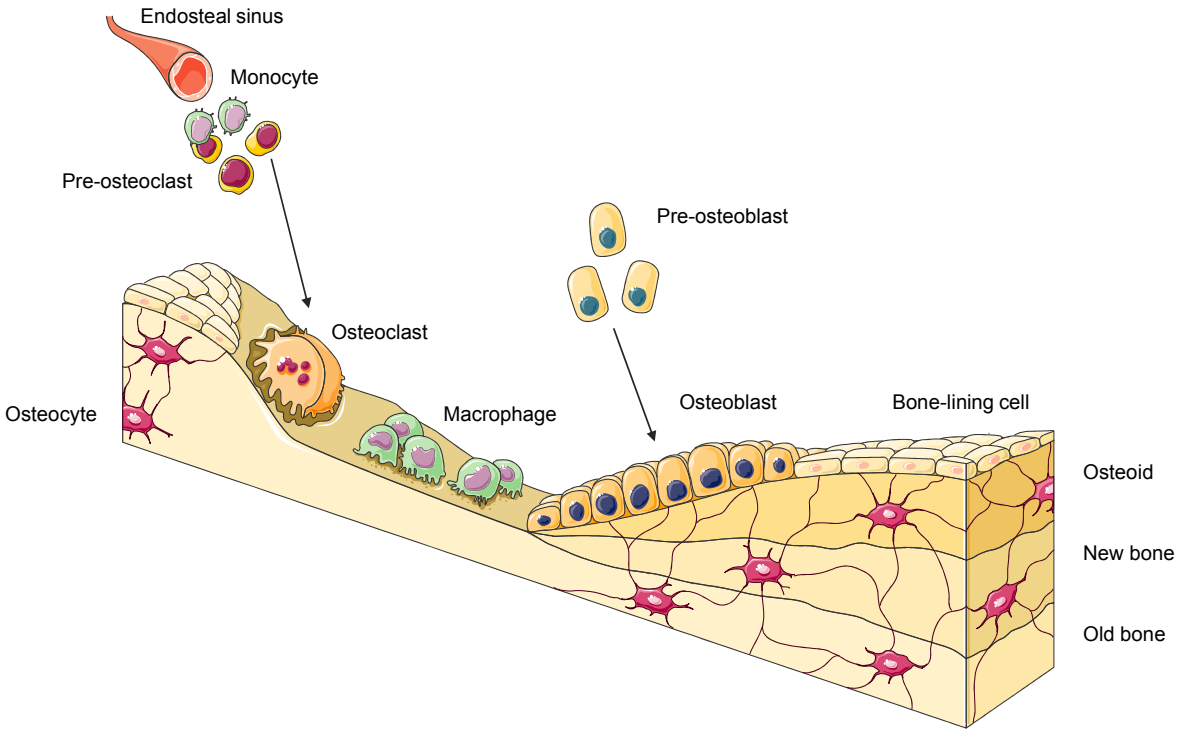

Figure 1.2: The bone remodeling cycle consists of the two processes bone resorption and new bone formation. After osteoclasts degrade the inorganic and organic components of the extracellular bone matrix (bone resorption), osteoblasts synthesize new bone matrix proteins and facilitate subsequent ECM mineralization (new bone formation). Osteoblasts can mature into osteocytes residing in the mineralized bone matrix or bone-lining cells seated on the bone surface. Figure adapted from Servier Medical Art (`http://www.servier.com/Powerpoint-image-bank`).

While osteoclasts die by apoptosis after approximately two weeks, most osteoblasts mature into osteocytes after a lifespan of about three months[3]. Osteocytes become incorporated into the bone matrix and depict the most abundant bone cell type with 95%. During this maturation, osteoblast morphology markedly changes and thin extensions build intercellular connections to other osteocytes as well as to osteoblasts on the bone surface, forming the osteocyte network. When sensing mechanical and metabolic stimuli, osteocytes transmit signals through this network to influence the activity of osteoclasts and osteoblasts[7]. Besides, other osteoblasts develop into flattened bone-lining cells on the surface, which are suggested to couple bone resorption to bone formation[8] by possibly defining physical compartments of bone remodeling[9].

1.3 Preferential adipogenesis and fat accumulation

With aging and especially during osteoporosis, bone resorption exceeds bone formation (that is either normal or also deficient) resulting in net bone loss. While bone resorption increases probably as a result of sex hormone deprivation, bone formation is diminished because of the reduction of the cell number, activity, and the life span of osteoblasts[2]. Several specific reasons are discussed for the reduced number of mature osteoblasts. Firstly, it is likely to be caused by a decrease in the proliferative and/or bone forming capacity of pre-osteoblastic cells[10,11].

Secondly, the preferential differentiation of bone marrow stromal cells (BMSCs) into adipocytes may most probably account for the reduced osteoblastogenesis since BMSCs are the common precursor for osteoblasts as well as adipocytes[2]. Based on scientific publications as well as clinical observations, evidence suggests an inverse relationship between adipogenesis and osteogenesis[12–18]. For example, the canonical Wnt/β-catenin pathway inhibits adipogenesis and induces osteoblastogenesis, while the transcription factor and key inducer of adipogenesis peroxisome proliferator-activated receptor γ2 (PPARγ2) inhibits osteoblastogenesis[19]. Moreover, the pharmacological inactivation of PPARγ2 increases osteoblast differentiation and bone formation in mice[20]. Intriguingly, osteoporosis is commonly accompanied by an increased accumulation of adipose tissue in the bone marrow, referred to as 'fatty degeneration'. That is why, osteoporosis has been discussed as the obesity of bone[21]. Furthermore, higher marrow fat is associated with a lower BMD and prevalent vertebral fractures[22].

In addition to the favored adipogenic differentiation of BMSCs, the plasticity between pre-differentiated cells of the adipogenic and osteogenic lineage has been described by us and others[23,24]. Thus, the lineage switching of pre-differentiated osteoblastic cells into adipocytes (adipogenic conversion) might increase the adipogenic outcome at the expense of osteogenesis.

Taken together, the shifted balance between adipogenic and osteogenic BMSC differentiation towards adipogenesis may probably account for the fatty degeneration. In conclusion, controlling this lineage decision in favor of osteogenesis depicts a novel and highly interesting approach for future osteoporosis therapy and prevention. In contrast to the common medications that mostly focus on decreasing bone resorption, this therapeutic approach would aim for increasing osteoblastogenesis and therefore bone formation while counteracting the fatty degeneration of the bone marrow that is connected to a poorer outcome.

2 Human bone marrow stromal cells

2.1 Differentiation into the adipocytic and osteoblastic lineage

Human bone marrow stromal cells (hBMSCs), also termed mesenchymal stem cells (MSCs), are multipotent cells. They are able to differentiate into the lineages of mesenchymal tissue including bone, cartilage, fat, tendon, and muscle[25–27]. Hence, they are the common precursor of the adipogenic as well as the osteogenic lineage. hBMSCs are key players in the bone remodeling process since they are the progenitors of pre-osteoblasts and, subsequently, the bone-forming osteoblasts. Thus, the osteogenic differentiation of hBMSCs is the prerequisite for the formation of bone matrix proteins and ensuing ECM mineralization by the osteoblasts as described earlier. However, the preferential differentiation into the adipogenic lineage is likely one of the main reasons for the decreased osteoblast cell number during aging and especially in osteoporosis, which is elucidated by the increased fat accumulation in and the fatty degeneration of the bone marrow, respectively.

The hBMSC differentiation process is controlled by a multitude of cytokines regulating the expression of cell-lineage specific sets of transcription factors (Fig 2.1). During the onset of differentiation, master transcription factors determine the cell fate, like PPARγ2 for adipogenic differentiation and runt-related transcription factor 2 (RUNX2) for osteogenic differentiation[28–30]. On the one side, the initial adipogenic commitment of hBMSCs is driven by the CCAAT/enhancer binding protein (C/EBP) family with its members C/EBPδ and β, which promote C/EBPα and PPARγ2 transcription[31]. The further differentiation into mature adipocytes is characterized by the expression of fatty acid binding protein 4 (FABP4) and lipoprotein lipase (LPL) accompanied by the formation of lipid droplets, which occupy most of the intracellular space while the nucleus is located at the cell margin.

On the other side, the osteogenic commitment is initiated by the expression of the master transcription factor RUNX2 and its co-activator the transcriptional co-activator with PDZ-binding motif (TAZ)[32]. Moreover, ALP and bone morphogenetic proteins (BMPs) like BMP4 comprise early osteogenic markers. Furthermore, the osteogenic differentiation and maturation is characterized by the expression of collagen 1 A1 (COL1A1), IBSP, OC, and OPN, which are components of the bone ECM. Then, ANKH inorganic pyrophosphate transport regulator (ANKH), ectonucleotide pyrophosphatase/ phosphodiesterase 1 (ENPP1), and ALP facilitate the ECM mineralization. While ALP is considered to be an early marker, OC is recognized as a late marker for osteoblast differentiation.

2.2 Lineage plasticity and conversion

Apart from the commitment and subsequent differentiation of undifferentiated hBMSCs, plasticity between pre-differentiated cells of the adipogenic and osteogenic lineage was reported by us and others *in vitro*. The conversion of osteoblastic cells into the adipocytic lineage[23,24,33–39] as well as the conversion of pre-differentiated adipocytes into the osteoblastic fate[23,24,39–44] was stated in current literature. As reviewed by Berendsen *et al.*, these lineage switches are able to take place after transcriptional modifications and through epigenetic mechanisms[45]. The process of conversion, also referred to as 'transdifferentiation' in earlier publications, is defined as one cell type being committed to and progressing along a specific developmental lineage switching into another cell type of a different lineage through genetic reprogramming[23].

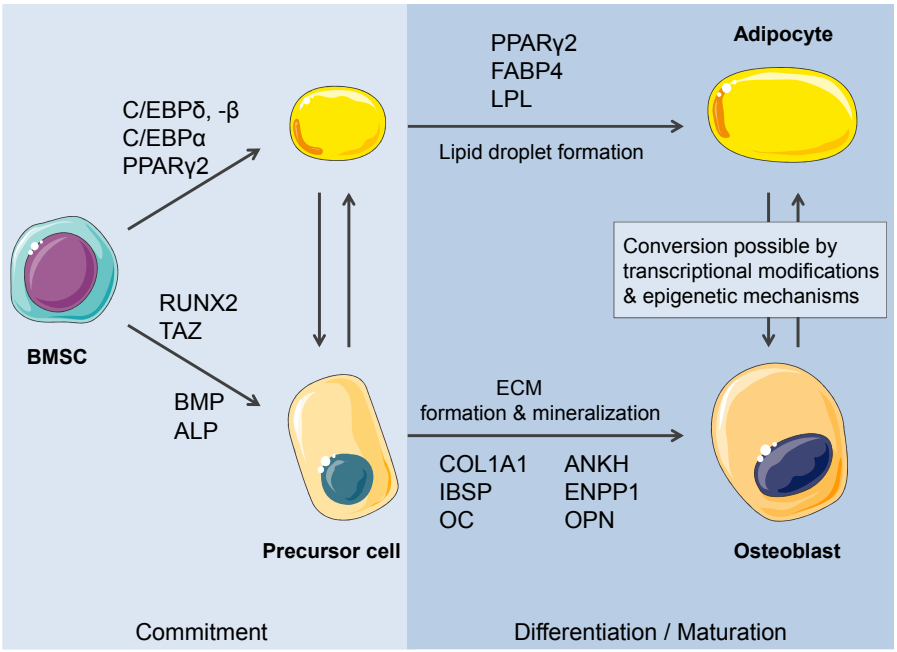

Figure 2.1: Adipogenic and osteogenic differentiation and conversion of hBMSCs. Adipogenic commitment is characterized by the expression of the early marker genes C/EBPδ, -β, and -α with the adipogenic key transcription factor PPARγ2. FABP4 and LPL expression followed by lipid droplet formation further designate adipocyte differentiation. Osteogenic commitment is driven by the expression of the master transcription factor RUNX2 and its co-activator TAZ. Whereas BMPs and ALP depict early osteogenic markers, COL1A1, IBSP, OC, and OPN are considered to be later markers of osteogenic differentiation and maturation involved in ECM formation. Then, ANKH, ENPP1, and OPN control ECM mineralization, a process fundamental for new bone formation (see above). Besides differentiation processes, the conversion of pre-differentiated cells was reported. This lineage plasticity might play a role in the increased adipogenesis in the skeletal disorder osteoporosis. Figure adapted from Servier Medical Art (`http://www.servier.com/Powerpoint-image-bank`).

2.3 *In vitro* model for hBMSC differentiation and conversion

The *in vitro* system deployed in the current study was established by Prof. Dr. Norbert Schütze and further modified by Dr. Tatjana Schilling previously. The adipogenic and osteogenic differentiation of hBMSCs was proven feasible as well as the conversion of adipogenically pre-differentiated cells into the osteogenic fate (osteogenic conversion) and vice versa (adipogenic conversion)[24]. This *in vitro* approach based on human primary cells was established to better reflect the bone marrow environment than available immortalized cell lines from human or other species. Moreover, it enables the investigation of the specific cell type of trabecular hBMSCs, which functions as a key player in bone formation and represents the common precursor for osteoblastic as well as adipocytic cells.

When comparing converted cells with normally differentiated cells by using microarray analysis, our group was able to elicit reproducibly regulated genes for adipogenic and osteogenic conversion[46]. By deploying a novel bioinformatic scoring scheme that ranked the genes according to reproducibility, regulation level, and reciprocity between the different directions of conversion, members of several signaling pathways like fibroblast growth factor (FGF), insulin-like growth factor (IGF), and Wnt signaling were identified as potential key factors associated with adipogenic and osteogenic conversion.

The study revealed that FGF1 was upregulated during osteogenic conversion and downregulated during adipogenic conversion. Pre-trials suggested an anti-adipogenic effect on hBMSC differentiation. In addition, FGF2 was downregulated during adipogenic conversion. Therefore, FGF1 and its

subfamily member FGF2 were scored as highly promising regulators of the initiation of conversion. However, the reports regarding the effects of FGF1 and FGF2 on adipogenic and osteogenic differentiation of mesenchymal precursors in current literature are controversial. As to our knowledge, no study has investigated the effects of FGF1 and FGF2 on the adipogenic and osteogenic conversion of pre-differentiated cells so far. In consequence, these signaling molecules needed to be characterized in detail regarding their effects on the adipogenic and osteogenic differentiation and conversion of trabecular hBMSCs.

3 Fibroblast growth factors and their receptors

3.1 Fibroblast growth factors

Fibroblast growth factors (FGFs) are a family of polypeptides that are found in vertebrates and invertebrates[47]. They serve essential roles in embryonic development and during organogenesis. In addition, FGFs regulate several important cellular processes in the adult like tissue maintenance, repair, regeneration, and metabolism, including angiogenesis and wound healing[48]. The FGF family comprises 22 structurally related members in human. Their molecular weight ranges from 17 to 34 kDa and they share a homologous internal core region[47]. The FGFs are divided into seven subfamilies grouped into the intracellular, the endocrine, and the canonical FGFs[49]. Whereas the intracellular, non-signaling FGFs (FGF11-14) serve as co-factors for voltage gated sodium channels and other molecules and have been well studied in neurons, the other FGFs are secreted signaling proteins that act via receptor tyrosine kinases. The endocrine, hormone-like FGFs (FGF15/19, FGF21, FGF23) mediate mineral, metabolic, energy, and bile acid homeostasis[50–54].

FGF1 and its subfamily member FGF2 are two of the most extensively studied canonical FGFs. In contrast to endocrine FGFs, the canonical FGFs function as autocrine or paracrine factors and control cell proliferation, differentiation, and survival[47,49,55–58]. They bind to heparin, heparan sulfates (HS) and cell-surface-associated heparan sulfate proteoglycans (HSPGs), which retain the polypeptides in the vicinity of their secreting cells, thereby enabling the autocrine and/or paracrine action[59,60]. Moreover, heparins are essential co-factors for the binding and activation of FGF receptors (FGFRs)[57,61–63] and regulate the specificity and affinity of the FGF-FGFR binding[64–67].

3.2 FGF receptors

FGFRs belong to the family of receptor tyrosine kinases. They consist of an extracellular ligand-binding domain that is linked to the intracellular catalytic tyrosine kinase core (TK) via a single-pass transmembrane domain[68]. The extracellular part is constituted of three immunoglobulin-type domains D1-D3[69]. FGFs interact with the D2 and D3 domain while HS bind to the D3 domain[62]. In mammals, four members of the FGFR family exist named FGFR1-4. The sequences of amino acids are highly conserved whereas ligand affinity and tissue distribution differ in each receptor[70]. In addition, alternative mRNA splicing results in specified variants of the D3 domain, giving rise to either the IIIb or IIIc isoform in FGFR1-3[71–75]. Whereas exon IIIb is expressed in epithelial lineages, exon IIIc is more inclined to be expressed in mesenchymal lineages[76–79]. This tissue-specific alternative splicing largely affects the ligand-receptor binding specificity[76–80].

Each FGFR is able to bind to a specific subset of FGFs. Similarly, most FGFs bind to several of the seven different FGFR subtypes, i.e. FGF1 is capable of activating all of them[74]. Upon ligand binding, a tertiary signaling complex is formed that consists of two FGFs, two heparin sulfate chains, and two FGFRs (Fig. 3.1)[81]. While each ligand binds to both receptors, the FGFRs make contact with one another via the D2 domain[57]. The receptor dimerization leads to a conformational shift in the receptor structure that releases the kinase auto-inhibition. This results in the trans-phosphorylation of intrinsic tyrosine residues of each receptor monomer[82–84]. In consequence, the docking protein FGFR substrate 2α (FRS2α) is phosphorylated, which leads to the recruitment of i.e. the adaptor protein growth

factor receptor-bound protein 2 (GRB2), the GRB2-associated-binding protein 1 (GAB1), the guanine nucleotide exchange factor son of sevenless homolog (SOS), and the protein tyrosine phosphatase, non-receptor type 11 (PTPN11 alias SHP2) (Fig. 3.1)[48]. This FRS2 complex serves as docking site for adaptor proteins that activate downstream signaling pathways, including Ras/mitogen-activated protein kinase (MAPK) and phosphoinositide 3-kinase (PI3K)/Akt[56,85,86].

The Ras/MAPK pathway constitutes the main downstream signaling pathway of FGF signaling and exercises control over cell proliferation and differentiation[48,87]. MAPKs regulate various cellular processes by responding to extracellular stimuli and act as serine/threonine-specific kinases. Downstream effectors of the Ras/MAPK pathway are the c-Jun N-terminal kinase (JNK), the p38-MAPK,

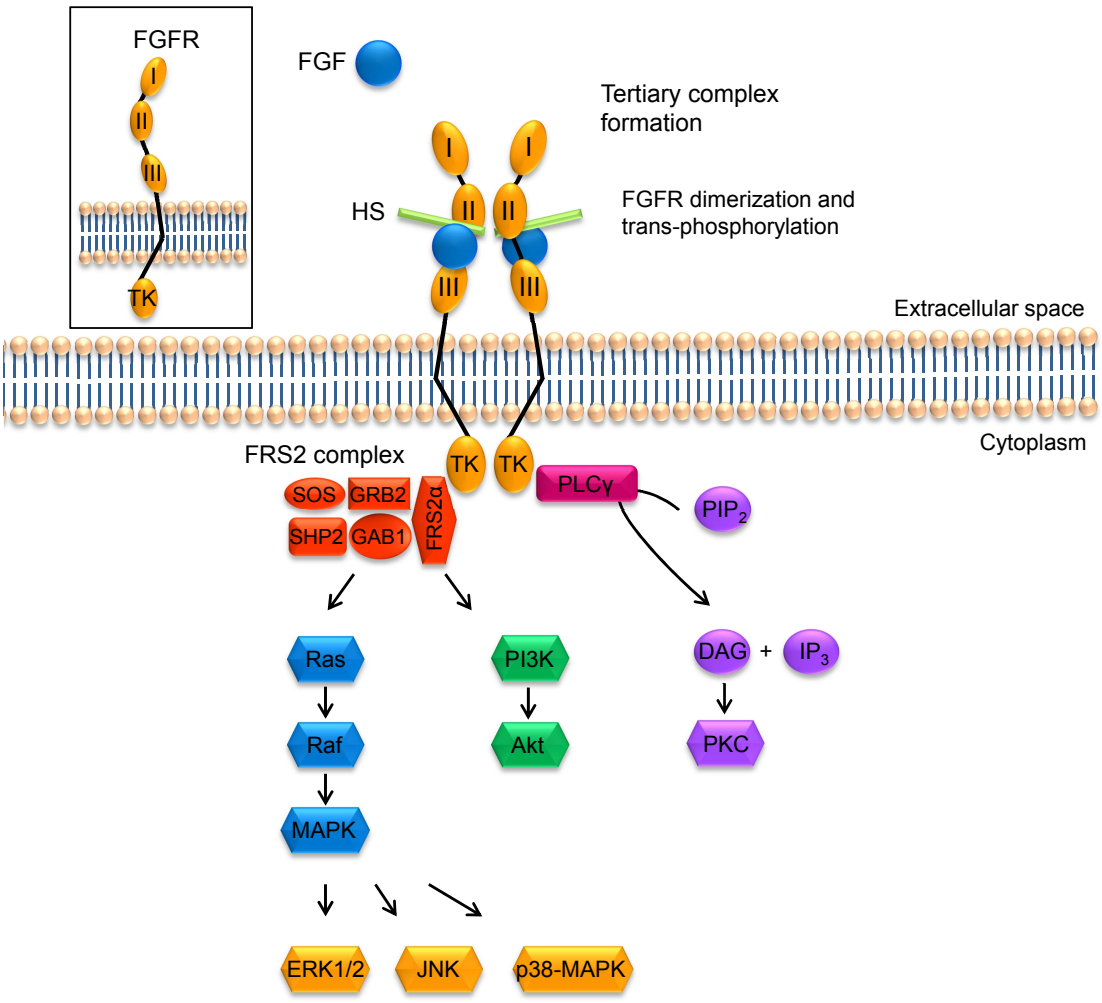

Figure 3.1: The FGF/FGFR signaling pathway. The signaling cascade is initialized upon the formation of the tertiary signaling complex consisting of two FGF ligands, two FGF receptors (FGFR), and two heparan sulfate (HS) molecules. The subsequent dimerization activates the intracellular FGFR tyrosine kinase domain (TK). The phosphorylation of the FGFR substrate (FRS) 2α and the subsequent recruitment of proteins like growth factor receptor-bound protein 2 (GRB2), GRB2-associated-binding protein 1 (GAB1), guanine nucleotide exchange factor son of sevenless homolog (SOS), and protein tyrosine phosphatase, non-receptor type 11 (PTPN11 alias SHP2) facilitate the initiation of downstream signaling cascades. The main downstream pathway Ras/mitogen-activated protein kinase (MAPK) as well as the phosphoinositide 3-kinase (PI3K)/Akt pathway are activated by this FRS2 complex. In contrast, phospholipase C (PLC) γ is directly activated by the FGFR and initiates protein kinase C (PKC) signaling. The c-Jun N-terminal kinase (JNK), the p38-MAPK, and the extracellular signal-regulated kinase (ERK) represent possible downstream pathways of Ras/MAPK signaling. Figure based on[48].

and the extracellular signal-regulated kinase (ERK) (Fig. 3.1)[48,88]. Besides Ras/MAPK, the PI3K/Akt pathway can be initiated by the FRS2 complex and is associated with cell survival and fate determination[48,81,89]. In addition, the phospholipase C (PLC) γ represents another target molecule of FGFR signaling. The PLCγ pathway affects cell morphology, migration, and adhesion[48,81,89]. Unlike the previously mentioned pathways, PLCγ is activated by direct binding to a phosphorylated site of the receptor[90]. Subsequent hydrolysis of phosphatidylinositol 4,5-bisphosphate (PIP_2) into diacylglycerol (DAG) and inositol triphosphate (IP_3) results in the activation of protein kinase C (PKC)[90].

Apart from this 'classical' FGFR signaling, it was reported that FGFR1-3 are capable of being internalized into the nucleus, where they might function in a different manner to receptor tyrosine kinase signaling[68]. After the binding and activation by the FGF ligand at the cell surface, the FGFR-FGF complex is internalized and translocated to the nucleus, i.e. in order to regulate cell proliferation[91–94].

3.3 Role in osteogenesis and bone formation

As mentioned in several studies, the FGF/FGFR signaling plays an important role in regulating prenatal and postnatal skeletal development[95–97]. Especially FGF2 has been reported to influence osteoblastogenesis and bone formation. On the one hand, it was stated that FGF2 positively affects bone formation[98,99]. Its bone anabolic effects have been demonstrated in several animal models including rat, mice, and rabbit[100–103]. FGF2 was also able to prevent trabecular bone loss in ovariectomized rats[104]. Moreover, the bone anabolic effect of BMP2 and parathyroid hormone (PTH) was shown to be in part dependent on endogenous FGF2 expression[105–107].

In line, the deletion of the FGF2 gene led to a marked decrease in bone mass and bone formation in $FGF2^{-/-}$ mice[108]. In addition, the trabecular micro-architecture was markedly impaired with loss of connecting rod-like structures and bone mineralization was diminished. Furthermore, the decreased mineralized nodule formation in $FGF2^{-/-}$ BMSC cultures *in vitro* was recovered by exogenously applied FGF2[109]. Besides, several *in vitro* studies on mesenchymal progenitors displayed a positive effect on osteogenic differentiation markers[110–115]. With high importance for our current study, FGF2 was also stated to control the switch between the adipogenic and osteogenic differentiation of BMSCs towards osteoblastogenesis[116].

On the other hand, FGF2 overexpression in transgenic mice resulted in impaired bone formation including shortening and flattening of long bones[117]. Moreover, FGF2 treatment *in vitro* was repeatedly reported to reduce the markers of osteogenic differentiation[118–128]. However, it was suggested that FGF2 might exert an early pro-proliferative role on osteoblast progenitors associated with a decrease in differentiation *in vitro*, but still have bone anabolic effects *in vivo* because of the creation of a larger pool of osteo-progenitor cells[97].

Apart from FGF2, also the FGFRs were reported to impact bone formation. Gain-of-function mutations in FGFR1 and FGFR2 were found in several craniosynostosis syndromes in human[49]. These autosomal dominant syndromes result in premature ossification and closure of the cranial suture and have various additional skeletal and soft tissue phenotypes. For example, Pfeiffer and Jackson-Weiss syndrome result from mutations in FGFR1 or FGFR2 whereas Apert and Crouzon syndrome are caused by missense mutations, deletions, and insertions in the FGFR2 gene[129–138]. These activating FGFR2 mutations were shown to promote osteoblast differentiation by increasing the expression of RUNX2 and osteogenic marker genes[95,139]. Moreover, mutations of FGFR3 cause achondroplasia, the most common form of human short-limbed dwarfism[140]. In addition, the process of bone formation was

shown to be dependent upon the interplay between the local expression of FGFs and the spatiotemporal expression of the FGFR1-4 and their splice variants[73,95,141,142].

4 Aim of my doctoral research

During aging and especially as a consequence of the skeletal disorder osteoporosis, the balance between bone resorption and new formation is disturbed. Cell number, activity, and life span of bone-forming osteoblasts are markedly decreased and adipose tissue accumulates in the bone marrow, referred to as 'fatty degeneration'. These alterations may be caused by the preferential adipogenic differentiation of trabecular hBMSCs at the expense of osteogenesis. Scientific evidence suggests an inverse relationship between the adipocytic and osteoblastic lineage, as both descend from the same precursor cell type. Moreover, plasticity has been shown between already committed and/or differentiated cells of these lineages, termed 'conversion' in the current study. Hence, the conversion of pre-differentiated osteoblastic cells into adipocytes *in vivo* might be a further cause of the fatty degeneration and the decreased osteoblast number.

Previous findings featuring microarray analysis followed by bioinformatic evaluation pointed at the members of the FGF signaling pathway FGF1 and FGF2 as most promising candidates for controlling hBMSC lineage decisions in order to favor the osteogenic over the adipogenic differentiation and conversion. This strategy may aid in finding novel pharmaceutical approaches for bone regeneration during aging and for the prevention and therapy of osteoporosis. Moreover, it may be advantageous for the *in vitro* engineering of calcified tissues. So far, there have been contradictory results on the effects of FGF1 and FGF2 on adipogenesis and osteogenesis in the literature and this subject is still a matter of scientific debate. Especially literature on primary human precursor cells from bone marrow origin is scarce.

In consequence, my doctoral research had three key aims: [1] to investigate the influence of FGF1 and FGF2 on adipogenic and osteogenic differentiation and conversion processes in primary trabecular hBMSCs; [2] to elucidate the involved downstream signaling cascades; and [3] to draw conclusions with regard to exercising control over the adipogenic and osteogenic differentiation and conversion processes.

Part II

Materials and Methods

5 Materials

5.1 Equipment

Table 5.1: Used equipment and corresponding suppliers

Equipment	Supplier
Abimed Single channel pipettes (10 µL, 100 µL, and 1000 µL)	Kinesis GmbH, Langenfeld, Germany
BioPhotometer	Eppendorf AG, Hamburg, Germany
C1000^{TM} Thermal Cycler with CFX 96 Real-Time System	Bio-Rad Laboratories GmbH, München, Germany
Centrifuge Biofuge Fresco	Thermo Electron LED GmbH, Langenselbold, Germany
Centrifuge Micro FugOne	Thermo Electron LED GmbH, Langenselbold, Germany
Centrifuge Multifuge X1R Heraeus	Thermo Electron LED GmbH, Langenselbold, Germany
Centrifuge Pico Heraeus	Thermo Electron LED GmbH, Langenselbold, Germany
CO_2 incubator CB 150	Binder GmbH, Tuttlingen, Germany
CO_2 incubator Kelvitron T	Thermo Electron LED GmbH, Langenselbold, Germany
CO_2 incubator HERAcell 240i	Thermo Electron LED GmbH, Langenselbold, Germany
Dishwasher	Miele & Co. KG, Gütersloh, Germany
Drier	Thermo Electron LED GmbH, Langenselbold, Germany
FluorChem Q (CCD Detection System for Western Blot Analysis)	Cell Biosciences, Santa Clara, USA
Freezer Economic (−20 °C)	Bosch GmbH, Gerlingen-Schillerhöhe, Germany
Freezer II Shin (−80 °C)	Nunc GmbH & Co. KG, Wiesbaden, Germany
Fridge Freshcenter	Bosch GmbH, Gerlingen-Schillerhöhe, Germany
Gel electrophoresis Mini Protean 3 cell	Bio-Rad Laboratories GmbH, München, Germany
Glassware	Schott, purchased from Hartenstein, Würzburg, Germany
Glass pipettes	A. Hartenstein, Würzburg, Germany
GloMax^{TM}-Multi Detection System microplate reader with fluorescence module	Promega, Mannheim, Germany
Heater	Medax, purchased from Hartenstein, Würzburg, Germany
Heater VWR analog heatblock	VWR International LLC., purchased from Peqlab Biotechnologie GmbH, Erlangen, Germany

Continued on next page

Table 5.1 – *Continued*

Equipment	**Suppliers**
Laminar air flow box Hera Safe KS12	Thermo Electron LED GmbH, Langenselbold, Germany
Laminar air flow Hera Safe 2020 1.8	Thermo Electron LED GmbH, Langenselbold, Germany
Magnetic stirrer	A. Hartenstein, Würzburg, Germany
Microscope Axiovert. A1 with AxioCam ICc1	Carl Zeiss Jena GmbH, Jena, Germany
Multistepper Handy Step	Brand GmbH & Co KG, Wertheim, Germany
Orion II Luminometer (chemiluminescence detection)	Berthold Detection Systems, Pforzheim, Germany
Peqstar 96 Universal Gradient PCR machine	Peqlab Biotechnologie GmbH, Erlangen, Germany
Peqstar 2x PCR machine	Peqlab Biotechnologie GmbH, Erlangen, Germany
PerfectBlue semi dry electroblotter	Peqlab Biotechnologie GmbH, Erlangen, Germany
pH meter inolab pH level 1	WTW, purchased from Hartenstein, Würzburg, Germany
Pipetboy Acu	IBS Integra Biosciences, Fernwald, Germany
Power Pac 300	Bio-Rad Laboratories GmbH, München, Germany
Scale PCB 1000-2 chemical balance	Kern und Sohn GmbH, purchased from Hartenstein, Würzburg, Germany
Scale (micro) ABS 220-4 electronic balance	Kern und Sohn GmbH, purchased from Hartenstein, Würzburg, Germany
Shaker DRS-12	Neolab, Heidelberg, Germany
Sonifier Branson Digital Sonifier® 250	Branson Ultrasonics Corporation, Danbury, CT, USA
Speed Vac SC 110	Savant, Thermo Electron LED GmbH, Langenselbold, Germany
Sunrise™ Microplate Absorbance Reader	Tecan Deutschland GmbH, Crailsheim, Germany
Thermal cycler PTC-200	Peltier, MJ Research, purchased from Biozym Scientific GmbH, Hessisch-Oldendorf, Germany
Vortexer Vortex-Genie 2	Scientific Industries, purchased from Hartenstein, Würzburg, Germany
Water bath WB7	Memmert GmbH & Co. KG, purchased from Hartenstein, Würzburg, Germany
Water bath WNB14	Memmert GmbH & Co. KG, purchased from Hartenstein, Würzburg, Germany

5.2 Software and online sources

Table 5.2: Utilized software and online sources

Software/Database	Company/URL
AmplifX software 1.7.0	http://crn2m.univ-mrs.fr/pub/recherche/equipe-t-brue/jullien-nicolas/programmation/amplifx/?lang=fr
Axiovision Rel. 4.8	Carl Zeiss Vision GmbH, Aalen, Germany
Bio-Rad CFX Manager 3.1	Bio-Rad Laboratories GmbH, München, Germany
BLASTn	(Altschul et al., 1990) http://www.ncbi.nlm.nih.gov/BLAST/Blast.cgi?CMD=Web&PAGE_TYPE=BlastHome
Dict	http://www.dict.cc/
FluorChemQ Software	Cell Biosciences, Santa Clara, USA
GenBank	(Thompson et al., 1997) http://www.ncbi.nlm.nih.gov/genbank/
GraphPad Prism version 6.04 for Windows	GraphPad Software, La Jolla, CA, USA, www.graphpad.com
Mendeley Desktop 1.11	Mendeley Ltd. http://www.mendeley.com
MiKTeX Version 2.9	http://miktex.org/
NCBI Pubmed	http://www.ncbi.nlm.nih.gov/pubmed
Photoshop 4.0®	Adobe Systems Inc., San Jose, CA, USA
Primer3Plus	http://primer3plus.com/cgi-bin/dev/primer3plus.cgi (Rozen and Skaletsky, 2000)
Servier Medical Art	http://www.servier.com/Powerpoint-image-bank; Servier Medical Art is licensed under the Creative Commons Attribution 3.0 Unported License (http://creativecommons.org/licenses/by/3.0/)
Sumatra PDF Viewer 2.4	http://sumatra-pdf.softonic.de/
TeXnic Center 2.02	The TeXnic Center Team www.texniccenter.org/
Wikipedia	http://www.wikipedia.org/

5.3 Consumables

Table 5.3: Consumables and their corresponding suppliers

Consumables	Supplier
Cell culture flasks (25 cm^2, 75 cm^2, 150 cm^2, and 175 cm^2)	Greiner Bio-One GmbH, Frickenhausen, Germany
Cell scraper	SPS Lifesciences, purchased from A. Hartenstein GmbH, Würzburg, Germany
Centrifugation tubes (15 mL and 50 mL)	Greiner Bio-One GmbH, Frickenhausen, Germany
Eppendorf micro test tubes	Greiner Bio-One GmbH, Frickenhausen, Germany
Multitips	Eppendorf AG, purchased from A. Hartenstein GmbH, Würzburg, Germany
Nitrocellulose transfer membrane Whatman Protran BA85	Whatman GmbH, purchased from A. Hartenstein GmbH, Würzburg, Germany
Pasteur pipettes	A. Hartenstein GmbH, Würzburg, Germany
PCR reaction tubes for qPCR	Biozym Scientific GmbH, Hessisch Oldendorf, Germany
PCR reaction tubes for RT-PCR	Greiner Bio-One GmbH, Frickenhausen, Germany
Pipette tips	Brandt, purchased from Laug & Scheller GmbH, Kürnach, Germany
Pipette tips, aseptic, with filters	STARLAB GmbH, Hamburg, Germany
Plastic pipettes (5 mL, 10 mL, and 25 mL)	Greiner Bio-One GmbH, Frickenhausen, Germany
Plates, non-sterile (96-well)	A. Hartenstein GmbH, Würzburg, Germany
Plates, non-sterile, black (96-well) for fluorescence, Cat.-no. 655076	Greiner Bio-One GmbH, Frickenhausen, Germany
Plates, non-sterile, white (96-well) for luminescence, Cat.-no. 655075	Greiner Bio-One GmbH, Frickenhausen, Germany
Plates, sterile (6-, 12-, 24-well)	Greiner Bio-One GmbH, Frickenhausen, Germany
Protran nitrocellulose transfer membrane	Whatman Schleicher & Schuell, purchased from A. Hartenstein GmbH, Würzburg, Germany
PVDF blotting membrane	Whatman GmbH, purchased from A. Hartenstein GmbH, Würzburg, Germany
Sterile filters	Carl Roth GmbH & Co. KG, Karlsruhe, Germany
UVettes	Eppendorf AG, purchased from A. Hartenstein GmbH, Würzburg, Germany

Continued on next page

Table 5.3 – *Continued*

Consumables	Suppliers
Whatman paper	Whatman GmbH, purchased from A. Hartenstein GmbH, Würzburg, Germany

5.4 Chemicals and reagents

Table 5.4: Chemicals and reagents and their corresponding suppliers

Chemicals and reagents	Supplier
Acetic acid anhydrous	Carl Roth GmbH & Co. KG, Karlsruhe, Germany
Acetone	AppliChem, purchased from A. Hartenstein GmbH, Würzburg, Germany
Agarose	Biozym Scientific GmbH, Hessisch-Oldendorf, Germany
Alizarin red S	Sigma-Aldrich Chemie GmbH, Schnelldorf, Germany
Ammonia solution (25%)	Merck KGaA, Darmstadt, Germany
Ammonium persulfate (APS)	PAA Laboratories GmbH, Pasching, Austria
L-Ascorbic acid 2-phosphate	Sigma-Aldrich Chemie GmbH, Schnelldorf, Germany
Bovine Serum Albumin (BSA), fatty acid free, low endotoxin (for cell culture)	Sigma-Aldrich Chemie GmbH, Schnelldorf, Germany
Bovine Serum Albumin (BSA) fraction V (for western blotting)	PAA Laboratories GmbH, Pasching, Austria
Bromphenole blue sodium salt	Carl Roth GmbH & Co. KG, Karlsruhe, Germany
Calphostin C (inhibitor of PKC, PKA, PKG and calcium channel proteins) CAS 121263-19-2, sc-3545A, Lot #G1112	Santa Cruz Biotechnology, Santa Cruz, CA, USA
Complete protease inhibitor cocktail	Roche Diagnostics GmbH, Mannheim, Germany
CSPD (Disodium 3-(4-methoxyspiro 1,2-dioxetane-3,2′-(5′-chloro)tricyclo [3.3.1.13,7]decan-4-yl)phenyl phosphate) ready-to-use solution	Roche Diagnostics GmbH, Mannheim, Germany

Continued on next page

Table 5.4 – *Continued*

Chemicals and reagents	**Suppliers**
Dexamethasone	Sigma-Aldrich Chemie GmbH, Schnelldorf, Germany
1α,25-Dihydroxyvitamin D_3 Cat.no. D1530	Sigma-Aldrich Chemie GmbH, Schnelldorf, Germany
Disodium carbonate	Carl Roth GmbH & Co. KG, Karlsruhe, Germany
Dimethylsulfoxide (DMSO)	Carl Roth GmbH & Co. KG, Karlsruhe, Germany
DNA from salmon sperm (Sigma D1626)	Sigma-Aldrich Chemie GmbH, Schnelldorf, Germany
DNA ladder (1 kb)	Peqlab Biotechnology GmbH, Erlangen, Germany
DNA ladder plus (100 bp)	Peqlab Biotechnology GmbH, Erlangen, Germany
Dulbecco's modified Eagle's medium (DMEM) high glucose with L-glutamine	Life Technologies GmbH, Darmstadt, Germany
Dulbecco's modified Eagle's medium with Ham's F12 nutrient mixture 1:1 (DMEM/Ham's F12) with Glutamax	Life Technologies GmbH, Darmstadt, Germany
Ethanol, absolute	AppliChem, purchased from A. Hartenstein GmbH, Würzburg, Germany
Ethanol (98%), denatured	Carl-Roth GmbH & Co. KG, Karlsruhe, Germany
Ethylenediaminetetraacetic acid (EDTA) tetrasodium salt dihydrate	AppliChem, purchased from A. Hartenstein GmbH, Würzburg, Germany
Fetal calf serum (FCS)	Biochrom GmbH, Berlin, Germany
Fibroblast growth factor 1 (FGF1, FGF acidic), recombinant human, E. coli derived Cat.no. 232-FA-025 (25 µg)	R&D Systems Inc., Minneapolis, USA
Fibroblast growth factor 2 (FGF2, FGF basic), recombinant human, E. coli derived Cat.no. 233-FB-025 (25 µg)	R&D Systems Inc., Minneapolis, USA
GelRed® 10 000x	Genaxxon BioScience GmbH, Ulm, Germany
Glycerol	Merck KGaA, Darmstadt, Germany
Glycerol gelatine	Sigma-Aldrich Chemie GmbH, Schnelldorf, Germany

Continued on next page

Table 5.4 – *Continued*

Chemicals and reagents	**Suppliers**
β-Glycerophosphate	Sigma-Aldrich Chemie GmbH, Schnelldorf, Germany
Glycine	Carl Roth GmbH & Co. KG, Karlsruhe, Germany
Heparin sodium salt	Biochrom GmbH, Berlin, Germany
HPLC-H_2O	Carl Roth GmbH & Co. KG, Karlsruhe, Germany
Indomethacin	Sigma-Aldrich Chemie GmbH, Schnelldorf, Germany
Insulin from bovine pancreas	Sigma-Aldrich Chemie GmbH, Schnelldorf, Germany
3-Isobutyl-1-methylxanthine (IBMX)	AppliChem, purchased from A. Hartenstein GmbH, Würzburg, Germany
Hydrochloric acid solution (1 mol L^{-1})	AppliChem, purchased from A. Hartenstein GmbH, Würzburg, Germany
Hydrochloric acid (37%)	Carl Roth GmbH & Co. KG, Karlsruhe, Germany
Loading dye (6x)	Peqlab Biotechnology GmbH, Erlangen, Germany
Lysispuffer 10x #9803 for protein isolation	Cell Signaling Technology Inc., purchased from New England Biolabs GmbH, Frankfurt am Main, Germany
Magnesium chloride	AppliChem, purchased from A. Hartenstein GmbH, Würzburg, Germany
2-Mercaptoethanol	AppliChem, purchased from A. Hartenstein GmbH, Würzburg, Germany
Methanol	AppliChem, purchased from A. Hartenstein GmbH, Würzburg, Germany
N,N,N-N-tetramethylethylene-diamine (TEMED)	Merck KGaA, Darmstadt, Germany
Oil red O	Sigma-Aldrich Chemie GmbH, Schnelldorf, Germany
Paraformaldehyde	Merck KGaA, Darmstadt, Germany
Penicillin/streptomycin solution (100x)	Life Technologies GmbH, Darmstadt, Germany
Phenylmethylsulfonylfluorid (PMSF)	Sigma-Aldrich Chemie GmbH, Schnelldorf, Germany

Continued on next page

Table 5.4 – *Continued*

Chemicals and reagents	**Suppliers**
Phosphate buffered saline (PBS) w/o Ca^{2+} and Mg^{2+}	Life Technologies GmbH, Darmstadt, Germany
Phosphatase inhibitor PhosSTOP (20x) #04906845001	Roche Diagnostics GmbH, Mannheim, Germany
Ponceaus S solution	Sigma-Aldrich Chemie GmbH, Schnelldorf, Germany
Probenecid (inhibitor of ANKH) CAS: 57-66-9, P 8761	Sigma-Aldrich Chemie GmbH, Schnelldorf, Germany
2-Propanol	Carl Roth GmbH & Co. KG, Karlsruhe, Germany
Protease inhibitor Complete, EDTA-free (25x) #04693132001	Roche Diagnostics GmbH, Mannheim, Germany
Quant-iT PicoGreen dsDNA Reagent	Life Technologies GmbH, Darmstadt, Germany
Rainbowmarker RPN 800	GE Healthcare Europe GmbH, München, Germany
Random hexamer primers	Invitrogen GmbH, Darmstadt, Germany
Roti Histofix 4%	Carl Roth GmbH & Co. KG, Karlsruhe, Germany
Roti-Quant (5x)	Carl Roth GmbH & Co. KG, Karlsruhe, Germany
Rotiphorese gel 40 acrylamide/bisacrylamide mix	Carl Roth GmbH & Co. KG, Karlsruhe, Germany
SB203580 (inhibitor of p38 MAPK) Cat.no. S1076, Lot. 04	Selleck Chemicals, Houston, TX, USA
Skim milk powder	AppliChem, purchased from A. Hartenstein GmbH, Würzburg, Germany
Sodium acetate	AppliChem, purchased from A. Hartenstein GmbH, Würzburg, Germany
Sodium chloride	AppliChem, purchased from A. Hartenstein GmbH, Würzburg, Germany
Sodium dodecyl sulfate (SDS)	Merck KGaA, Darmstadt, Germany
Sodium hydrogen carbonate	Carl Roth GmbH & Co. KG, Karlsruhe, Germany
Sodium hydroxide solution (1 mol L^{-1})	AppliChem, purchased from A. Hartenstein GmbH, Würzburg, Germany
Sodium hydoxide pellets	Merck KGaA, Darmstadt, Germany

Continued on next page

Table 5.4 – *Continued*

Chemicals and reagents	Suppliers
SP600125 (competitive inhibitor of JNK 1, 2 and 3) Cat.no. 1496, Batch No: 9B/148046	Tocris Bioscience, Bristol, UK
Thioglycolic acid	Sigma-Aldrich Chemie GmbH, Schnelldorf, Germany
Tris base	AppliChem, purchased from A. Hartenstein GmbH, Würzburg, Germany
Triton X-100	Carl Roth GmbH & Co. KG, Karlsruhe, Germany
Trypan blue (0.4%)	Sigma-Aldrich Chemie GmbH, Schnelldorf, Germany
Trypsin/EDTA (1x)	Life Technologies GmbH, Darmstadt, Germany
Tween 20	Merck KGaA, Darmstadt, Germany
U0126 (highly selective inhibitor of MEK1 and MEK2) #9903S, Ref:10/2013, Lot: 14	Cell Signaling Technology Inc., purchased from New England Biolabs GmbH, Frankfurt am Main, Germany

5.5 Buffers and solutions

5.5.1 Histology

Table 5.5: Established buffers and solutions used for histology

Buffers and solutions	Ingredients and preparation
1% Alizarin red S staining solution	0.25 g alizarin red S dissolve in 25 mL dist. H_2O add 250 µL 25% ammonia
ALP staining solution (according to manufacturer's protocol) made freshly	per 6-well: 20 µL FBB alkaline solution (included in the ALP kit) add 20 µL sodium nitrate solution (included) mix gently by inverting and incubate for 2 min add mixture to 900 µL dist. H_2O add 20 µL naphtol-AS-BI solution (included) mix thoroughly and protect from light

Continued on next page

Table 5.5 – *Continued*

Buffers and solutions	**Ingredients and preparation**
Citrate acetone formaldehyde fixing solution (for ALP staining) (according to manufacturer's protocol)	2.5 mL citrate solution (included in ALP Kit) add 6.5 mL acetone add 800 µL 37% formaldehyde store at 2 °C to 8 °C for up to 4 weeks
0.5% Oil red O stock solution	0.5 g Oil red O dissolve in 100 mL 99% 2-propanol
4% Paraformaldehyde	4 g paraformaldehyde dissolve in approx. 75 mL PBS (pH 7.4) heat to 60 °C, stir at 55 °C to 60 °C for 5 min (do not heat above 60 °C) add approx. 100 µL to 150 µL 1 N NaOH until solution becomes clear let cool to room temperature adjust pH to 7.4 with 1 N HCl PBS ad 100 mL store at room temperature

5.5.2 Alkaline phosphatase (ALP) assay

Table 5.6: Buffers and solutions used for ALP assay

Buffers and solutions	**Ingredients and preparation**
0.2 mol L^{-1} Carbonate buffer pH 10.2	200 mL 0.2 mol L^{-1} Na_2CO_3 add 100 mL 0.2 mol L^{-1} $NaHCO_3$ adjust pH to 10.2 and store at 4 °C
0.2 mol L^{-1} Na_2CO_3	4.2 g Na_2CO_3 dist. H_2O ad 200 mL
0.2 mol L^{-1} $NaHCO_3$	1.7 g $NaHCO_3$ dist. H_2O ad 100 mL
DNA standard stock solution (10 mg mL^{-1})	10 mg DNA from salmon sperm dissolve in 1 mL HPLC-H_2O aliquot and store at −20 °C
0.1% Triton X-100 in 0.2 mol L^{-1} carbonate buffer	45 mL 0.2 mol L^{-1} carbonate buffer add 5 mL 1% Triton X-100 mix well, store at 4 °C
1% Triton X-100	50 mL dist. H_2O add 500 µL Triton X-100 and mix thoroughly

5.5.3 Mineralization assay

Table 5.7: Solutions for calcification assay

Solution	Ingredients and preparation
0.5 mol L^{-1} (= 0.5 N) HCl	for 50 mL: 2.5 mL 37% HCl add 47.5 mL dist. H_2O filter sterile and store at 4 °C

5.5.4 RNA isolation and PCR

Table 5.8: Established buffers and solutions used for RNA isolation and PCR

Buffers and solutions	Ingredients and preparation
0.5 mol L^{-1} EDTA	19 g EDTA tetrasodium salt hydrate dist. H_2O ad 100 mL adjust pH to 8.0
TE buffer (10 mmol L^{-1} Tris, 1 mmol L^{-1} EDTA) autoclaved	0.12 g Tris base 0.029 g EDTA tetrasodium salt hydrate dist. H_2O ad 100 mL adjust pH to 7.5
10x TBE	108 g Tris base 55 g Boric acid 9.05 g EDTA tetrasodium salt hydrate dist. H_2O ad 1000 mL adjust pH to 8.3

5.5.5 Protein isolation

Table 5.9: Lysis buffer used for protein isolation

Buffers and solutions	Ingredients and preparation
PhosSTOP (20x)	1 tablet phosphatase inhibitor PhosSTOP dissolve in 500 µL HPLC-H_2O aliquot and store at −20 °C, stable for at least 6 months

Continued on next page

Table 5.9 – *Continued*

Buffers and solutions	**Ingredients and preparation**
PMSF (25x) (100 mmol L^{-1})	0.174 g Phenylmethylsulfonylfluoride dissolve in 10 mL DMSO aliquot and store at −20 °C
Protease inhibitor (25x)	1 tablet Protease inhibitor Complete, EDTA-free dissolve in 2 mL HPLC-H_2O aliquot and store at −20 °C, stable for at least 12 weeks
Protein lysis buffer (1x) (e.g. 4 mL)	400 µL Lysis buffer (10x) 3080 µL HPLC-H_2O 160 µL PMSF (100 mmol L^{-1}) 160 µL Protease inhibitor (25x) 200 µL PhosSTOP (20x)

5.5.6 SDS-PAGE

Table 5.10: Established buffers and solutions used for SDS-PAGE procedures

Buffers and solutions	**Ingredients**
0.5% Bromphenole blue	0.05 g Bromphenole blue sodium salt dist. H_2O ad 10 mL adjust pH to 8.0
10% APS	1 g Ammonium persulfate dist. H_2O ad 10 mL store aliquots at −20 °C
10% SDS	10 g Sodium dodecyl sulfate dist. H_2O ad 100 mL
Lower buffer, Stock solution (10x)	15.1 g Tris base 71.4 g Glycine dist. H_2O ad 500 mL
Lower buffer, Working solution	100 mL Stock solution (10x) dist. H_2O ad 1000 mL
Sample buffer, Stock solution (20x)	1.2 mL 0.5 mol L^{-1} Tris base (0.5 mol L^{-1}, pH 6.8) 1 mL Glycerol 2 mL 10% SDS 0.5 mL 0.5% Bromphenole blue dist. H_2O ad 500 mL
Sample buffer, Working solution	0.95 mL Stock solution (20x) 0.05 mL 2-Mercaptoethanol

Continued on next page

Table 5.10 – *Continued*

Buffers and solutions	Ingredients
Separating gel buffer, 3 mol L^{-1} Tris, pH 8.8	36.34 g Tris base add approx. 70 mL dist. H_2O adjust pH to 8.8 with 37% HCl dist. H_2O ad 100 mL
Stacking gel buffer, 0.5 mol L^{-1} Tris, pH 6.8	6.1 g Tris base dist. H_2O ad 100 mL adjust pH to 6.8 with 1 N HCl
Upper buffer, Stock solution (4x)	13.6 g Tris base 57.1 g Glycine 4 g SDS dist. H_2O ad 1000 mL
Upper buffer, Working solution	100 mL Stock solution (4x) 84 µL Thioglycolic acid dist. H_2O ad 500 mL

5.5.7 Western blotting

Table 5.11: Established buffers and solutions used for western blotting

Buffers and solutions	Ingredients
Stripping buffer (1x)	0.985 g Tris-HCl (62.5 mmol L^{-1}) 20 mL 10% SDS (2%) bi-dist. H_2O ad 100 mL For 30 mL per membrane add 210 µL 2-Mercaptoethanol (100 nmol L^{-1})
Transfer buffer (10x) for proteins larger than 100 kDa	30.35 g Tris base (250 mmol L^{-1}) 142.63 g Glycine (1.9 mol L^{-1}) 10 g SDS (1%) dist. H_2O ad 1000 mL
Transfer buffer (1x) for proteins larger than 100 kDa	100 mL Transfer buffer (10x) 100 mL Methanol dist. H_2O ad 1000 mL
Transfer buffer (10x) for proteins smaller than 100 kDa	30.35 g Tris base (250 mmol L^{-1}) 142.63 g Glycine (1.9 mol L^{-1}) dist. H_2O ad 1000 mL adjust pH with NaOH pellets to 10.0

Continued on next page

Table 5.11 – *Continued*

Buffers and solutions	Ingredients
Transfer buffer (1x) for proteins smaller than 100 kDa	100 mL Transfer buffer (10x) 200 mL Methanol dist. H_2O ad 1000 mL
TBS (10x)	24.2 g Tris base (200 mmol L^{-1}) 87.66 g NaCl (1.5 mol L^{-1}) 14 mL HCl dist. H_2O ad 1000 mL adjust pH to 7.6
10% Tween 20	90 mL bi-dist. H_2O 10 mL Tween 20 mix well by stirring
Washing buffer TBS-T (1x)	100 mL TBS (10x) 10 mL 10% Tween 20 (0.1%) dist. H_2O ad 1000 mL

5.6 Cell culture media and additives

Table 5.12: Media used for cultivation and differentiation of hBMSCs

Media	Ingredients and preparation
hBMSC cultivation medium	500 mL DMEM/Ham's F12 with Glutamax 50 mL FCS 5 mL Penicillin/streptomycin solution 100x 555 µL Ascorbic acid 2-phosphate (50 mg mL^{-1})
Basal medium	500 mL DMEM high glucose with L-glutamine 50 mL FCS 5 mL Penicillin/streptomycin solution 100x
Adipogenic medium (AM) (made freshly)	100 mL Basal medium 100 µL IBMX (500 mmol L^{-1}) 100 µL Indomethacin (100 mmol L^{-1}) 10 µL Insulin (2 mg mL^{-1}) 10 µL Dexamethasone (10 mmol L^{-1})
Osteogenic medium (OM) (made freshly)	100 mL Basal medium 1000 µL β-Glycerophosphate (1 mol L^{-1}) 100 µL Ascorbic acid 2-phosphate (50 mg mL^{-1}) 1 µL Dexamethasone (10 mmol L^{-1})

Continued on next page

Table 5.12 – *Continued*

Media	Ingredients and preparation
1x PBS (autoclaved)	9.55 g Dulbecco's PBS w/o Ca^{2+} and Mg^{2+} dist. H_2O ad 1000 mL adjust pH to 7.4

Table 5.13: Additives utilized for supplementation of cell culture media

Additives	Ingredients
Ascorbic acid 2-phosphate (M = 298.5 g mol^{-1}) Stock solution 50 mg mL^{-1}	2.5 g L-Ascorbic acid 2-phosphate sesquimagnesium salt dissolve in 50 mL bi-dist. H_2O filter sterile and store aliquots at −20 °C use 1:1000 for OM
0.1% BSA in PBS Mock for FGF supplementation	0.01 g BSA dissolve in 10 mL sterile PBS store aliquots at −20 °C
Calphostin C (M = 790.8 g mol^{-1}) Stock solution 1 mmol L^{-1}	1 mg Calphostin C dissolve in 1.2645 mL DMSO store aliquots at −20 °C
Dexamethasone (M = 392.5 g mol^{-1}) Stock solution 10 mmol L^{-1}	0.0393 g Dexamethasone dissolve in 10 mL Ethanol store aliquots at −80 °C use 1:10 000 for AM and 1:100 000 for OM
FGF1 (FGF acidic) (predicted molecular weight: 15.5 kDa) Stock solution 25 µg mL^{-1}	25 µg FGF1 dissolve in 1 mL 0.1% BSA in PBS store aliquots at −20 °C
FGF2 (FGF basic) (predicted molecular weight: 16.5 kDa) Stock solution 25 µg mL^{-1}	25 µg FGF2 dissolve in 1 mL 0.1% BSA in PBS store aliquots at −20 °C
β-Glycerophosphate (M = 216 g mol^{-1}) Stock solution 1 mol L^{-1}	2.16 g β-Glycerophosphate disodium salt hydrate dissolve in 10 mL bi-dist. H_2O filter sterile and store aliquots at −20 °C use 1:100 for OM
Indomethacin (M = 357.8 g mol^{-1}) Stock solution 100 mmol L^{-1}	0.035 78 g Indomethacin dissolve in 1 mL DMSO store aliquots at −20 °C use 1:1000 for AM

Continued on next page

Table 5.13 – *Continued*

Additives	Ingredients
Insulin (M = 5733.5 g mol^{-1}) Stock solution 2 mg mL^{-1}	mix 54 mL bi-dist. H_2O with 3 mL Acetic acid (anhydrous), pH 2-3 0.01 g Insulin from bovine pancreas dissolve in 5 mL diluted Acetic acid filter sterile and store aliquots at −20 °C use 1:10 000 for AM
3-Isobutyl-1-methylxanthine (IBMX) (M = 222.2 g mol^{-1}) Stock solution 500 mmol L^{-1}	0.5555 g 3-Isobutyl-1-methylxanthine dissolve in 5 mL DMSO store aliquots at −20 °C use 1:1000 for AM
Probenecid (M = 285.36 g mol^{-1}) Stock solution 0.175 mol L^{-1}	49.945 mg Probenecid dissolve in 1 mL 1 N NaOH store aliquots at −20 °C
Probenecid (M = 285.36 g mol^{-1}) Stock solution 0.875 mol L^{-1}	499.45 mg Probenecid dissolve in 2 mL 1 N NaOH store aliquots at −20 °C
SB203580 (M = 377.43 g mol^{-1}) Stock solution 10 mmol L^{-1}	25 mg SB203580 dissolve in 6.6237 mL DMSO store aliquots at −80 °C
SP600125 (M = 220.23 g mol^{-1}) Stock solution 10 mmol L^{-1}	10 mg SP600125 dissolve in 4.54 mL DMSO store aliquots at −20 °C in the dark (light-sensitive)
U0126 (M = 380.5 g mol^{-1}) Stock solution 10 mmol L^{-1}	5 mg U0126 dissolve in 1.31 mL DMSO store aliquots at −20 °C

5.7 Kits

Table 5.14: All kits and their respective suppliers

Kits	Suppliers
Alkaline Phosphatase (AP), Leucocyte Kit No. 86C	Sigma-Aldrich Chemie GmbH, Schnelldorf, Germany
QuantiChrom Calcium Assay Kit (DICA-500)	Biotrend GmbH, Köln, Germany
NucleoSpin® RNA Purification Kit	Macherey-Nagel GmbH & Co. KG, Düren, Germany

Continued on next page

Table 5.14 – *Continued*

Kits	Suppliers
Western Bright Chemiluminescence Substrate Sirius for CCD Systems	Advansta, Menlo Park, CA, USA

5.8 Primers

Primers were ordered as lyophilized and salt-free unmodified DNA oligonucleotides. They were reconstituted to a stock concentration of 100 pmol μL^{-1}. Working solutions consisted of stock solutions diluted 1:20 in autoclaved HPLC-H_2O (5 pmol μL^{-1}). Both stock and working solutions were stored at $-20\,^{\circ}C$. If not stated otherwise, primers were used for quantitative real-time PCR (qPCR) and primer efficiencies are stated in the table.

Table 5.15: Primers for housekeeping genes. Apart from sequences, annealing temperatures (Ann. temp.) and efficiencies (Effic.) are listed.

Primers	Sequence	Ann. temp.	Effic.
Eukaryotic translocation elongation factor 1α (EEF1α) (used only for RT-PCR)	aggtgattatcctgaaccatcc aaaggtggatagtctgagaagc	54 °C	–
Ribosomal protein, large, P0 (RPLP0 alias 36B4)	tgcatcagtaccccattctatcat aggcagatggatcagccaaga	60 °C	2.01
Ribosomal protein S 27a (RPS27A)	tcgtggtggtgctaagaaaa tctcgacgaaggcgactaat	60 °C	1.96

Table 5.16: Primers for target genes utilized in qPCR. Apart from sequences, annealing temperatures (Ann. temp.) and efficiencies (Effic.) are listed.

Primers	Sequence	Ann. temp.	Effic.
Alkaline phosphatase liver, bone, kidney (ALPL)	gtacgagctgaacaggaacaacg cttggcttttccttcatggtg	58 °C	1.83
ANKH inorganic pyrophosphate transport regulator (ANKH)	ttcacagtcacctggaatgc cagggatgatgtcgtgaatg	58 °C	1.97
Bone morphogenetic protein 4 (BMP4)	tacatgcgggatctttaccg atgttcttcgtggtggaagc	57 °C	2.06

Continued on next page

Table 5.16 – *Continued*

Primers	Sequence	Ann. temp.	Effic.
CCAAT/enhancer binding protein α (CEBPα)	ccagagagctccttggtcaag tcgggcaagcctcgagatc	60 °C	1.89
Collagen 1 A1 (COL1A1)	ccctggaaagaatggagatg ccatccaaaccactgaaacc	60 °C	1.88
Ectonucleotide pyrophosphatase/ phosphodiesterase 1 (ENPP1)	ttggctatggacctggattc taggagccggtgtcaaattc	60 °C	1.98
Fatty acid binding protein 4, adipocyte (FABP4)	tactgggccaggaatttgac gacacccccatctaaggttatg	60 °C	2.14
Fibroblast growth factor receptor 1 (FGFR1)	ctgggtagcaacgtggagtt accatgcaggagatgaggaa	58 °C	1.75
Fibroblast growth factor receptor 2 (FGFR2)	ggacccaaaatgggagtttc tccttgggcttgtctttgtc	60 °C	1.84
Integrin-binding sialoprotein (IBSP)	tgacagttcagaagaggaggag tccatagcccagtgttgtagc	58 °C	1.85
Lipoprotein lipase (LPL)	ccggtttatcaactggatgg tggtcagacttcctgcaatg	58 °C	2.00
Osteocalcin alias bone gamma-carboxyglutamate (Gla) protein (OC)	tgaccacatcggctttcag aaggggaagaggaaagaagg	60 °C	2.08
Osteopontin alias secreted phosphoprotein 1 (OPN)	tatgatggccgaggtgatag cattcaactcctcgctttcc	60 °C	1.80
Peroxisome proliferator-activated receptor γ2 (PPARγ2)	ccagaaagcgattccttcac acggagctgatcccaaag	58 °C	1.81
Runt-related transcription factor 2 (RUNX2)	cttcacaaatcctccccaag atgcgccctaaatcactgag	58 °C	1.91
Sclerostin (Sost)	caggcgttcaagaatgatgc tactcggacacgtctttggtc	60 °C	1.79

5.9 Enzymes

Table 5.17: Enzymes and their respective suppliers

Enzymes	Suppliers
BioScript^{TM} Reverse Transcriptase	Bioline, Luckenwalde, Germany
KAPA Sybr Fast qPCR Master Mix Universal (2x mix containing polymerase and buffer)	Peqlab Biotechnology GmbH, Erlangen, Germany
MangoTaq^{TM} DNA-polymerase and 5x buffer	Bioline, Luckenwalde, Germany

5.10 Antibodies

Table 5.18: Primary antibodies and blocking peptides and their respective suppliers

Primary antibodies and blocking peptides	Suppliers
Anti-β-Actin (13E5) rabbit monoclonal, #4970 stored at $-80\,^{\circ}C$	Cell Signaling Technology Inc., purchased from New England Biolabs GmbH, Frankfurt am Main, Germany
Anti-FGFR1, rabbit polyclonal, ab10646 stored at $-20\,^{\circ}C$	Abcam, Cambridge, UK
Anti-FGFR2, rabbit polyclonal, ab10648 stored at $-20\,^{\circ}C$	Abcam, Cambridge, UK
Anti-GAPDH (6C5), mouse monoclonal, GTX28245 stored at $-20\,^{\circ}C$	Genetex Inc., purchased from Biozol Diagnostica Vertrieb GmbH, Eching, Germany
Anti-Osteopontin, rabbit polyclonal, ab8448 Lot.no. GR52573-13 ($75\,000\,mg\,mL^{-1}$) stored at $-80\,^{\circ}C$	Abcam, Cambridge, UK
Anti-Phospho-FGFR1-4 (Y653/Y654), polyclonal rabbit reconstituted at 0.2 mg/mL in sterile PBS stored at $-20\,^{\circ}C$	R&D Systems Inc., Minneapolis, USA
Anti-Phosphotyrosine (2Q267), mouse monoclonal, ab17285 stored at $-20\,^{\circ}C$	Abcam, Cambridge, UK
Osteopontin peptide, human recombinant, ab65665 used as blocking peptide for ab8448 Lot.no. 727937 ($1000\,mg\,mL^{-1}$) stored at $-80\,^{\circ}C$	Abcam, Cambridge, UK

Table 5.19: Secondary antibodies and their respective suppliers

Secondary antibodies	Suppliers
Anti-Rabbit IgG peroxidase, goat, A0545used 1:5000	Sigma-Aldrich Chemie GmbH, Schnelldorf, Germany
Anti-Mouse IgG peroxidase, goat, A9917used 1:2000	Sigma-Aldrich Chemie GmbH, Schnelldorf, Germany

6 Methods

6.1 Cell Culture

6.1.1 Isolation of human bone marrow stromal cells

Human bone marrow stromal cells (hBMSCs) were isolated from trabecular bone of femoral heads as described previously[24,143] using a modified protocol originally published by Haynesworth and colleagues[144]. Patients were undergoing hip replacement surgery due to age-related or hip dysplasia-related attrition; they were otherwise healthy and did not receive medications with relation to bone metabolism. Cell isolation and further experiments were performed upon approval by the Local Ethics Committee of the University of Würzburg and informed consent from each patient (7 male patients aged 41-70 years).

In short, cells were washed out of spongiosa pieces with DMEM/Ham's F12 medium not containing any further supplements. The fat layer swimming on top of the suspension and existing bone fragments at its bottom were separated. After a centrifugation step at 270 *g* for 5 min, the cells were resuspended in cultivation medium. Cell number was determined using a hematocytometer according to Neubauer. Cells were seeded at a density of 4.6×10^6 to 5.7×10^6 per cm^2 (equal to 8×10^8 to 10^9 cells per T175 flask) in cultivation medium and incubated in a humidified atmosphere at 37 °C, 5% CO_2 and 95% air. First medium change was performed after 3-4 days, straight after the cells were washed once with sterile PBS.

6.1.2 Cultivation of primary hBMSCs

After isolation, hBMSCs were grown in cultivation medium consisting of DMEM/Ham's F12 with Glutamax that contained 10% FCS, 100 IU/mL penicillin, 100 µg mL^{-1} streptomycin, and 50 µg mL^{-1} ascorbic acid 2-phosphate. Cultures were maintained at 37 °C in a humidified atmosphere of 5% CO_2 and 95% air, and medium was changed every 3-4 days. When reaching confluence, hBMSCs were passaged 1:3 using 1x trypsin/EDTA solution containing 0.05% trypsin and 0.02% EDTA in PBS.

For the analysis of alkaline phosphatase activity, cells were seeded into 12-well plates with 24×10^4 cells per well. For lipid droplet quantification, mineralization assay, and RNA isolation, hBMSCs were seeded into 6-well plates with 6×10^5 cells per well. For protein isolation, cells were seeded into cell culture flasks with a surface area of 150 cm^2 or 175 cm^2 using 62 500 cells per cm^2. hBMSCs were cultivated to confluence again before starting differentiation and conversion procedures in passage 2.

6.2 Multipotency testing

Differentiation and conversion were induced according to Schilling *et al.*[24,46] in confluent hBMSCs using DMEM high glucose with L-glutamine that contained 10% FBS, 100 IU/mL penicillin, and 100 µg mL^{-1} streptomycin. To generate undifferentiated controls, hBMSCs were cultured in this basal medium without further supplements.

6.2.1 Adipogenic differentiation and conversion

Adipogenic differentiation and conversion was induced using basal medium supplemented with 500 µmol L^{-1} isobutylmethylxanthine, 100 µmol L^{-1} indomethacin, 0.2 µg mL^{-1} insulin and 1 µmol L^{-1} dexamethasone (modified after[24,25]) referred to as adipogenic medium. For adipogenic differentiation, hBMSCs were incubated in this adipogenic medium for 14 days (Fig. 6.1). To test the effect of FGF1 and FGF2, different concentrations (1 ng mL^{-1}, 4 ng mL^{-1}, 10 ng mL^{-1}, and 25 ng mL^{-1}) were added to the samples for the whole period of 14 days of conventional differentiation assays. Like in current literature, samples containing FGF1 were additionally supplemented with 20 IU/mL unfractionated heparin, whereas samples containing FGF2 were not further supplemented with heparin.

For adipogenic conversion, hBMSCs were first osteogenically pre-differentiated for 14 days in osteogenic medium (see below), followed by a medium switching and a further cultivation time of 14 days in adipogenic medium for the induction of lineage changing (Fig. 6.1). To test the effect of FGF1 and FGF2, the above mentioned concentrations were added starting from the day of media switching (day 14) until the end of the conversion on day 28. Again, FGF1 samples were additionally supplemented with 20 IU/mL unfractionated heparin. The osteogenic pre-differentiation period was carried out without any FGF administration. Differentiation and conversion samples not containing FGF1 or FGF2 were referred to as 'control' (ctrl). Differentiation and conversion status were controlled using the specific histological Oil red O staining to be covered below.

6.2.2 Osteogenic differentiation and conversion

Osteogenic differentiation and conversion cocktail consisted of basal medium supplemented with 10 mmol L^{-1} β-glycerophosphate, 100 nmol L^{-1} dexamethasone[145] and 50 µg mL^{-1} ascorbic acid 2-phosphate[146] referred to as osteogenic medium. For osteogenic differentiation, hBMSCs were incubated in osteogenic medium for 7 or 14 days (Fig. 6.1). To test the effects of FGF1 or FGF2 in the above mentioned concentrations, samples were additionally supplied with FGF1 plus 20 IU mL^{-1} heparin or with FGF2 for the whole period of 7 or 14 days of differentiation.

For osteogenic conversion, hBMSCs were first adipogenically pre-differentiated for 14 days in adipogenic medium (see 6.2.1), followed by a medium switching and a further cultivation time of 7 or 14 days in osteogenic medium for lineage changing (Fig. 6.1). In parallel to adipogenic set-ups, to test the effects of FGF1 or FGF2, samples were additionally supplied with FGF1 plus heparin or with FGF2; the above mentioned concentrations of 1 ng mL^{-1}, 4 ng mL^{-1}, 10 ng mL^{-1}, and 25 ng mL^{-1} were added starting from the day of media switching (day 14) until the end of the conversion on day 21 or 28. The adipogenic pre-differentiation period was carried out without any FGF administration. Differentiation and conversion samples not containing FGF1 or FGF2 were referred to as 'control' (ctrl). Differentiation and conversion status was controlled using specific histological stainings to be covered below.

6.3 Inhibitor experiments

To investigate involvement of signaling cascades, differentiations and conversions with specific inhibitors were performed. The following inhibitors were deployed: Probenecid for inhibition of ANKH inorganic pyrophosphate transport regulator, PD166866 for inhibition of FGFR1, SB203580 for p38-mitogen-activated protein kinase (p38-MAPK) inhibition, SP600125 for inhibition of c-Jun N-terminal

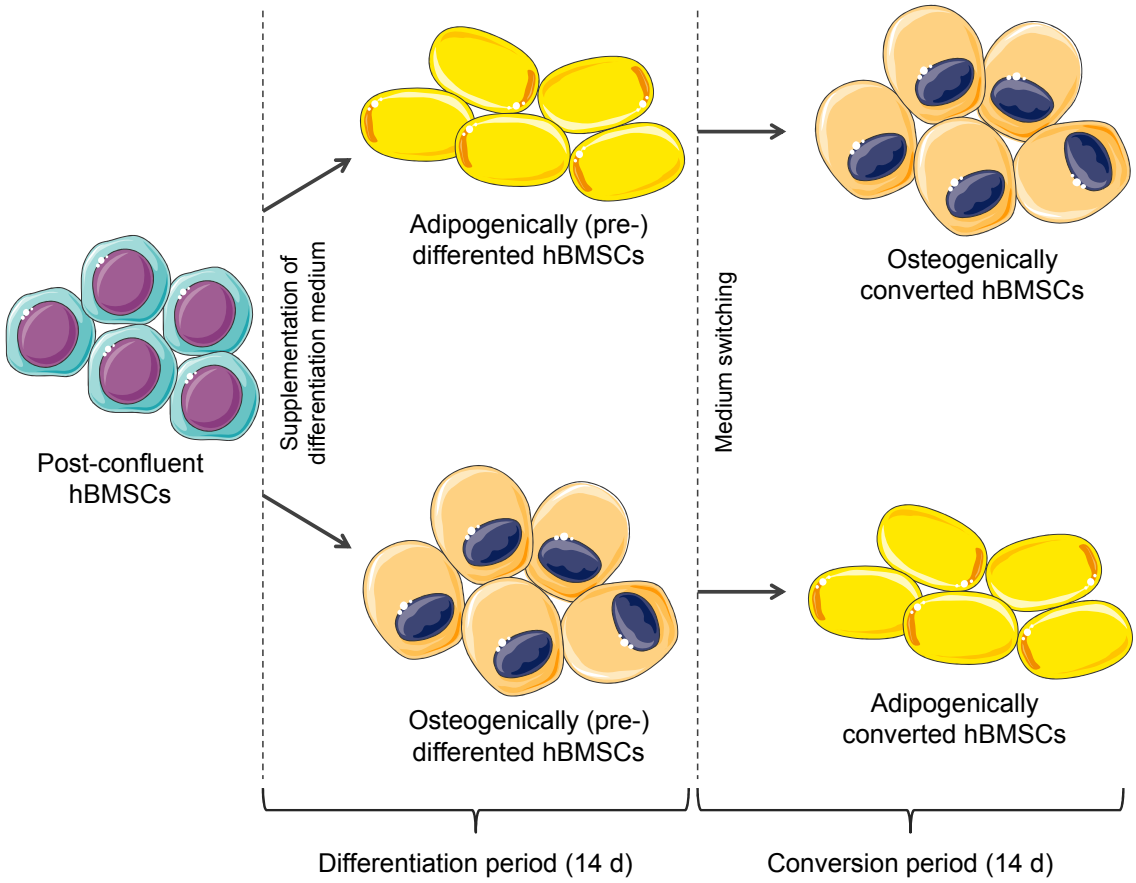

Figure 6.1: Schematic illustration of the experimental differentiation and conversion procedure. Post-confluent hBMSCs were differentiated by the addition of specific adipogenic or osteogenic medium for a standard period of 14 days. For further conversion, medium was switched to osteogenically convert the adipogenically pre-differentiated cells and to adipogenically convert the osteogenically pre-differentiated cells. FGFs were supplemented for the whole period of differentiation (for differentiation set-ups) and for the last 14 days of conversion (for conversion set-ups). Figure adapted from Servier Medical Art (`http://www.servier.com/Powerpoint-image-bank`).

kinase (JNK), Calphostin C for protein kinase C (PKC) inhibition, and U0126 for inhibition of mitogen-activated protein kinase kinase 1 and 2 (MAPKK1/2, also known as MEK1/2) to investigate the involvement of the extracellular signal-regulated kinases 1 and 2 (ERK1/2) signaling pathway. Prior to the start of differentiation, hBMSCs were always preincubated with the inhibitor for 2 h. Control set-ups were preincubated with the respective amount of inhibitor solvent (vehicle), either 1 N NaOH (for Probenecid only) or DMSO. Differentiation and conversion was performed as described above with the additional supplementation of inhibitor or vehicle. To ensure thorough mixing, inhibitor or vehicle was added to the media prior to the administration of the media onto the monolayers.

The inhibitor concentrations were chosen based on literature about previous experiments with MSCs. The deployed inhibitor concentrations were as follows: 0.25 mmol L^{-1}, 2 mmol L^{-1}, and 10 mmol L^{-1} Probenecid, 250 nmol L^{-1} PD166866, 5 µmol L^{-1} SB203580, 1 µmol L^{-1} SP600125, and 50 nmol L^{-1}, 100 nmol L^{-1}, 500 nmol L^{-1}, and 1000 nmol L^{-1} Calphostin C. As a concentration of 25 ng mL^{-1} was found to be most effective for FGF1, this concentration was used for all inhibitor experiments; additionally, differentiation media were supplemented with 20 IU/mL heparin.

6.4 Histological stainings

6.4.1 Oil red O staining

To visualize lipid droplet formation, adipogenically differentiated and converted hBMSCs were stained with Oil red O as described by Pittenger and colleagues[25]. In short, monolayers were washed once with PBS, then fixed in 4% paraformaldehyde or 4% Roti Histofix for 10 min. After washing once with dist. H_2O, monolayers were incubated with 60% 2-propanol for 5 min and subsequently in Oil red O working solution for 10 min. Working solution was mixed freshly on the previous day by diluting 6 parts of the Oil red O stock solution with 4 parts of dist. H_2O. The working solution was filtered before use. After staining, cells were washed once with 60% 2-propanol and dist. H_2O. Before discarding the last washing solution, microscopic pictures were taken with a magnification of 100x. At least six images were taken at random sites of the well to acquire representative areas from each incubation type. After having allowed the monolayers to dry, Oil red O dye was eluted to perform the lipid droplet quantification assay as described below.

6.4.2 ALP staining

To demonstrate the location of the enzyme activity of the osteogenic marker alkaline phosphatase (ALP), stainings were performed using the 'alkaline phosphatase, leucocyte kit no. 86C' according to the manufacturer's instructions. In short, citrate acetone formaldehyde fixing solution was equilibrated to room temperature before use. In the meantime, ALP staining solution was prepared freshly. After fixing for 30 s, and washing 3 times with dist. H_2O, monolayers were incubated with 900 µL staining solution per well of a 6-well plate for 15 min in the dark. Following another washing step of 3 times dist. H_2O, cells were mounted in the aqueous medium glycerol gelatine, evaluated light microscopically and photographed. Images were taken at random sites to acquire representative areas from each incubation type.

6.4.3 Alizarin red S staining

To visualize the location of calcified areas in osteogenic samples, the Alizarin red S protocol was performed to stain calcium hydrogen phosphate in the extracellular matrix. According to the laboratory's established protocol, monolayers were rinsed once with PBS, then fixed with ice cold methanol for 10 min. After washing once with dist. H_2O, the monolayers were covered with Alizarin red S and incubated for 2 min. Following another washing step of 3 times dist. H_2O, monolayers were mounted in glycerol-gelatine, evaluated light microscopically and photographed. Images were taken at random sites to acquire representative areas of each incubation type.

6.5 Specific assays quantifying differentiation and conversion

6.5.1 Lipid droplet assay

To quantify lipid droplet formation, adipogenically differentiated and converted hBMSCs were stained with Oil red O as described above. After acquiring microscopic images, stained monolayers were dried over night. Lipid-bound dye was eluted using 100% 2-propanol (500 µL per well of a 6-well

plate) by gentle shaking for 10 min. Absorbance was measured in a 96-well plate in technical triplicates of 90 µL per well at a wavelength of 492 nm using a microplate absorbance reader. The protocol was adapted from Zhang and colleagues[147]. The assay was carried out on day 14 for adipogenic differentiation and on day 28 for adipogenically converted samples (14 days of osteogenic pre-differentiation plus 14 days of adipogenic conversion). Relative Oil red O absorbance resembling lipid content was calculated by normalizing to differentiation and conversion controls of each donor, respectively.

6.5.2 ALP activity assay

Osteogenic samples were harvested on day 7 for differentiation and on day 21 for conversion (14 days of adipogenic pre-differentiation plus 7 days of osteogenic conversion) as preliminary experiments gave reason to expect the most conclusive differences at these time points. Cells were washed once with 0.2 mol L^{-1} carbonate buffer pH 10.2, then lysed with 0.1% Triton X-100 in 0.2 mol L^{-1} carbonate buffer and immediately frozen at −80 °C. Samples were freeze-thawed (−80 °C/37 °C) 3 times for mechanical cell disruption prior to measurements.

To determine ALP activity, 50 µL CSPD ready-to use solution was added using a multistepper to 50 µL aliquots of the cell lysates according to the manufacturers instructions. After shaking for 30 min at room temperature and an additional incubation for 5 min at 37 °C, chemiluminescence was measured in an appropriate, white 96-well plate in six technical replicates using an Orion II Luminometer. Measurement duration was set to 1 s, values were displayed as relative luminescence units (RLU) per s.

To overcome proliferation-dependent effects, ALP activity was normalized to DNA content. DNA quantification was carried out using Quant-iT^{TM} PicoGreen according to the manufacturers instructions. DNA standard solutions were produced freshly after diluting the DNA standard stock solution 1:100 in 0.1% Triton X-100/carbonate buffer (lysis buffer) as described in table 6.1. DNA standards were measured in triplicates whereas samples were measured in six technical replicates. A volume of 50 µL cell lysate or DNA standard solution per well was transferred into an appropriate, black 96-well plate. PicoGreen was diluted 1:200 in 10 mmol L^{-1} TE buffer and protected from light. Immediately before measuring, 50 µL PicoGreen solution were added per well. Fluorescence was determined at 538 nm (excitation at 485 nm) using a GloMax^{TM}-Multi Detection System microplate reader with fluorescence module.

Table 6.1: DNA standard solutions used for ALP assay

DNA conc. [µg mL^{-1}]	**DNA solution** [µL]	**Lysis buffer** [µL]	**Total volume** [µL]
8	80 (100 µg mL^{-1} solution)	920	1000 (A)
4	500 of A	500	1000 (B)
2	500 of B	500	1000 (C)
1	500 of C	500	1000 (D)
0.5	500 of D	500	1000 (E)
0.25	500 of E	500	1000
0	0	500	500

conc.: concentration

6.5.3 Mineralization assay

To quantify the calcium deposition in osteogenic samples, cells were harvested on day 14 for differentiation and on day 28 for conversion (14 days of adipogenic pre-differentiation plus 14 days of osteogenic conversion). Samples were washed twice with PBS, then 500 µL 0.5 N HCl per well of a 6-well plate were added and monolayers were disrupted with a cell scraper. Calcium ions were dissolved from the extracellular matrix by shaking at 4 °C for 4 h. After the solution was transferred into 1.5 mL reaction tubes, samples were centrifuged at 1000 *g* and 4 °C for 5-10 min. Supernatants were collected into fresh reaction tubes and stored at 4 °C until calcium measurements were performed.

To determine calcium content, the QuantiChrom™ Calcium Assay Kit (DICA-500) was used according to the manufacturer's protocol. In short, included calcium standard solution (20 mg dL^{-1}) was diluted as described in table 6.2 and stored at 4 °C for future use. A volume of 5 µL per well of each sample and of each standard solution was pipetted into a 96-well plate and 200 µL working solution were added per well. The working solution was freshly prepared by combining equal volumes of reagent A and reagent B and equilibrating to room temperature before use. After an incubation period of 10-15 min while shaking, measurements of the absorbance at 620 nm were carried out using the Tecan microplate reader. Calcium content was determined in technical triplicates. Protein content was measured as well in technical triplicates using Roti®-Quant according to the manufacturer's instructions. Calcium concentrations were normalized to relative protein content.

Table 6.2: Calcium standard solutions used for mineralization assay

Ca^{2+} conc. [mg dL^{-1}]	**Calcium solution** [µL]	**dist. H_2O** [µL]	**Total volume** [µL]
20	100	0	100
16	80	20	100
12	60	40	100
8	40	60	100
6	30	70	100
4	20	80	100
2	10	90	100
0	0	100	100

conc.: concentration

6.6 mRNA expression analysis

6.6.1 RNA isolation

Total RNA was isolated using the NucleoSpin® RNA Purification Kit according to the manufacturer's protocol. In detail, cells were carefully washed with PBS once, and the lysis buffer RA1 mixed 1:100 with 2-mercaptoethanol was added onto the monolayers after aspirating the PBS thoroughly. To generate sufficient amounts of RNA while avoiding waste of human and chemical material, RNA isolation was generally performed in 6-well plates using 350 µL lysis buffer per well. After monolayers were

detached with a cell scraper and transferred into reaction tubes, samples were snap frozen in liquid nitrogen and stored at −80 °C until further processing.

To reduce viscosity, samples were filtrated through violet columns included in the kit by centrifugation at 11 000 *g* for 1 min. Then, an equal volume of 70% ethanol was added and lysates were transferred onto the blue columns for RNA binding followed by another centrifugation step at 11 000 *g* for 30 s. Silica membranes were desalted and dried through an equal volume of membrane desalting buffer (MDB) and spinned again at 11 000 *g* for 1 min. In the meantime, 10 µL reconstituted DNase were diluted in 90 µL reaction buffer (per sample) and mixed by snapping the vial carefully since the enzyme is sensitive to mechanical stress. Beforehand, lyophylized DNase was reconstituted by adding 550 µL of RNase free water (included in the kit) and carefully inverting the vial of enzyme; aliquots of 50 µL were stored at −20 °C. For DNase digestion, 95 µL DNase reaction mix were transferred onto the middle of each column and incubated for 15 min at room temperature. After that, silica membranes were washed with 200 µL buffer RA2 to inactivate DNase, followed by centrifugation at 11 000 *g* for 1 min. Subsequently, 600 µL buffer RA3 were added, followed by centrifugation at 11 000 *g* for 30 s. Then, 250 µL RA3 were applied in the final washing step, followed by centrifugation at 11 000 *g* for 2 min to completely dry the silica membranes. RNA was eluted by pipetting 30 µL to 60 µL RNase free water (from the kit) directly onto each column, followed by the final centrifugation step at 11 000 *g* for 1 min. RNA samples were placed on ice immediately and stored at −80 °C.

RNA concentration and purity were determined by diluting 2 µL RNA sample in 48 µL 10 mmol L^{-1} Tris base and measuring the absorbance at 206 nm and 280 nm at the BioPhotometer. Only samples with an absorbance ratio A_{260}/A_{280} near 2.0 were considered reliable and taken for further examination, since lower values indicate protein contamination whereas higher values display the presence of degraded RNA and/or the excess of free nucleotides.

6.6.2 Reverse transcription

After defrosting RNA samples on ice, the respective volume of 1 µg RNA per sample was mixed with HPLC-H_2O to a final volume of 11 µL. 1 µL random primers (1 µg µL^{-1}) were added and the reaction mix was incubated at 70 °C for 5 min to denature RNA secondary structures. To assure primer binding, samples were incubated on ice for another 5 min. Then, a master mix was prepared to provide 1 µL 10 mmol L^{-1} dNTPs and 0.25 µL 200 U/µL BioScript™ Reverse Transcriptase in 4 µL 5x reaction buffer and 2.75 µL HPLC-H_2O for each sample. After incubation at room temperature for 10 min, reverse transcription was performed at 42 °C for 60 min. The enzyme was inactivated at 70 °C for 10 min. Finally, 30 µL HPLC-H_2O were added to the samples to make a final volume of 50 µL and stored at −20 °C.

6.6.3 Semiquantitative reverse transcriptase PCR (RT-PCR)

To check the quality of reverse transcription, semiquantitative polymerase chain reaction was performed using reverse transcripts as templates (RT-PCR). Primer pairs for the housekeeping genes eukaryotic translocation elongation factor 1α (EEF1α) or ribosomal protein S27a (RPS27A) were deployed. Table 6.3 reflects a standard protocol and corresponding reaction steps; according to the cDNA quality, amplification was performed for 20-25 cycles. The master mix was prepared for all cDNA samples and the negative control. PCR products were separated by gel electrophoresis on a 1% agarose gel containing GelRed®. Band size was determined using UV light.

Table 6.3: Reagents and standard reaction steps of RT-PCR

Reagent	Vol. [µL]	Reaction step		Temp. [°C]	Time [min]
HPLC-H_2O, autocl.	18.7	1^{st}	Initial denaturation	94	3
5x Mango buffer	6	2^{nd}	Denaturation	94	0.5
$MgCl_2$ (50 mmol L^{-1})	1	3^{rd}	Annealing	54	0.5
dNTPs (10 mmol L^{-1})	1	4^{th}	Elongation	72	0.5
Primer forward (5 pmol μL^{-1})	1	5^{th}	Repeat steps 2-4	-	-
Primer reverse (5 pmol μL^{-1})	1	6^{th}	Final elongation	72	1
MangoTaq Polymerase (5000 U/mL)	0.3	7^{th}	Cooling	4	inf
cDNA template	1				

Autocl.: autoclaved; Temp.: temperature; Vol.: volume; inf: infinite

6.6.4 Quantitative real-time reverse transcriptase PCR (qPCR)

After having checked the quality of cDNA synthesis, qPCR of the reverse transcripts was performed for target genes. Therefore, cDNA samples were amplified using KAPA Sybr Fast Universal 2x qPCR Master Mix and 0.25 pmol μL^{-1} sequence-specific primers as described in table 6.4. Amplification was generally repeated 40 times, every cycle being followed by a plate read.

To determine the specificity of amplification, a DNA melting curve was recorded by heating from 65 °C to 95 °C with increments of 0.5 °C for 5 s being followed by a plate read. Relative target gene expression was calculated using the Pfaffl method, i.e. based on primer efficiency and the ΔC_t values of sample versus control and normalized to the reference gene expression of RPS27A and ribosomal protein, large, P0 (RPLP0 alias 36B4), which were as well amplified via qPCR [148,149].

Table 6.4: Reagents and standard reaction steps of qPCR

Reagent	Vol. [µL]	Reaction step		Temp. [°C]	Time
HPLC-H_2O, autocl.	8.5	1^{st}	Initial denaturation	94	3 min
KAPA Sybr Fast Universal Mix	10	2^{nd}	Denaturation	94	10 s
Primer forward (5 pmol μL^{-1})	0.5	3^{rd}	Annealing	57-61	10 s
Primer reverse (5 pmol μL^{-1})	0.5	4^{th}	Elongation	72	20 s
cDNA template	0.5	5^{th}	Plate read	-	-
		6^{th}	Repeat steps 2-4 for 40 cycles	-	-
		7^{th}	Melting curve with 0.5 °C increment + Plate read	65-95	5 s

Autocl.: autoclaved; Temp.: temperature; Vol.: volume

6.6.5 Primer design and establishment for qPCR

To exclude any false-positive detection of DNA contaminants, intron-spanning primers were designed using either Primer3 Plus software employing the settings for qPCR as mentioned in[150] or AmplifX software version 1.7.0. When designed with AmplifX software, primer length was set to 19-24 base pairs with a maximum melting temperature difference of 3 °C, maximum primer quality of 90. Transcript sequences were extracted from GenBank and one primer was generally placed in the exon containing the coding DNA sequence (CDS) if applicable. Suggested primer pairs without secondary structures were checked via BLASTn.

Annealing temperature was determined employing a temperature gradient from 58 °C to 61 °C for a pooled positive and a negative control. After that, efficiency was defined by amplifying dilutions of the pooled positive control, plotting C_t values versus $\log_{(\text{DNA dilution})}$ as $y = a * x + b$ and calculating efficiency E as:

$$E = 10^{\frac{1}{a}}$$

Values between 1.75 and 2.2 were defined as satisfying, whereby primers with efficiencies around 2.0 were preferred.

6.7 Protein expression analyses

6.7.1 Protein isolation

Protein samples from differentiated and converted monolayers were generated to further analyze protein expression and phosphorylation status via Western blotting procedure. Therefore, protein lysis buffer was prepared freshly containing PMSF as well as a commercial protease inhibitor and a phosphatase inhibitor (PhosStop). All isolation steps were implemented on ice if possible. In detail, after being washed with ice cold PBS once, monolayers were scraped off in PBS (5 mL per T175 flask) using a cell scraper. After that, flasks were washed with a further volume of PBS. Following centrifugation at 270 *g* for 5 min, cell pellets were resuspended in ice cold protein lysis buffer (approx. 500 µL per T175 flask). Lysates were incubated on ice for 10 min with occasional vortexing. Then, lysates were sonicated with 70% power, 10 s pulsing with 1 s pulse and 1 s pause. After being centrifuged at 13 700 *g* for 15 min at 4 °C, supernatants were aliquoted and stored at −80 °C until further analysis.

6.7.2 Western blotting

For the analysis of protein expression and phosphorylation status, lysates were introduced to Western blotting. In short, protein concentrations were determined using Roti-Quant 5x solution according to the manufacturer's protocol. In general, 30 µg total protein were added to the appropriate amount of 6x sample buffer and distilled water to make a 1x solution that was heated to 95 °C for 5 min. Samples were separated by SDS-PAGE for 1 h at 150 V, the gel concentration being adapted to the expected size of the target protein(s) (table 6.5).

After the run, proteins were blotted onto a nitrocellulose (standard) or PVDF membrane (for analysis of phospho-proteins) for 2 h with 150 mA per membrane using a semi-dry blotting device. To check the performance of the blotting procedure, membranes were stained with Ponceau S solution. The

dye was rinsed out using tap water. Membranes were blocked using 3-5% solutions of skim milk or BSA in TBS-T according to the manufacturer's instructions. Primary antibodies for target proteins were applied over night at 4 °C in blocking solution, whereas antibodies for housekeeping proteins like GAPDH and β-Actin were applied for 1 h at room temperature. After washing the membranes 3 times for 5-15 min with TBS-T, horse radish peroxidase (HRP)-conjugated secondary antibodies were employed in established concentrations: goat anti-rabbit IgG with 1:5000 and goat anti-mouse IgG with 1:2000 in blocking solution.

Following another washing step of 3 times 5-10 min with TBS-T, horse radish peroxidase signals were detected using the Western Bright Chemiluminescence Kit for CCD Systems as described in the manufacturer's protocol. Signals were recorded and further analyzed densitometrically using the FluorChemQ software. Therefore, the target protein signals of samples were set in relation to the signal of the control and normalized to housekeeping protein amounts.

To assure equal protein concentrations for the detection of target and housekeeping proteins, membranes were first developed with target protein antibody, then stripped, and examined for the housekeeping proteins. For membrane stripping, membranes were incubated at 50 °C in pre-heated stripping buffer for 30 min. Followed by a 3 times washing step with TBS-T for 5min, blocking procedure and respective antibody incubation were performed as described above.

Table 6.5: Standard composition for two SDS acrylamide gels

Reagent	**5% stacking gel** [mL]	**12.5% separating gel** [mL]
H_2O dest.	2.4	4.8
Rotiphorese gel 40 Acryl-amide/bisacrylamide mix	0.5	3.75
Stacking gel buffer	1.0	-
Separating gel buffer	-	1.25
10% SDS	0.04	0.1
TEMED	0.004	0.004
10% APS	1.04	0.10

6.8 Statistical analysis

Experiments were performed at least in triplicates. If not stated otherwise, results are displayed as means $\tilde{x} \pm$ standard error of the mean (SEM). Results were considered significant when $p \leq 0.05$. Statistical analysis was performed using GraphPad Prism version 6.04 for Windows based on consultation of the statistics department of the university of Würzburg.

Experiments concerning the concentration-dependent effect of FGFs on differentiation and conversion were analyzed using one-way ANOVA (for independent samples). This was followed by multiple comparison tests of each sample to the respective differentiation and conversion control that was not supplemented with FGFs. Thereby, Dunnett's correction was deployed.

In parallel, set-ups determining the effect of different inhibitors were analyzed through one-way ANOVA. Afterwards, the sample differentiated with FGF1 plus inhibitor was compared to the respective control containing FGF1 plus vehicle. Comparisons were corrected using the Sidak test.

Part III

Results

7 FGF1 and FGF2 prevent adipogenic differentiation and conversion

To investigate the effect of fibroblast growth factor 1 (FGF1) and FGF2 on the adipogenic differentiation and conversion of trabecular human bone marrow stromal cells (hBMSCs), different experimental approaches were conducted. Based on the literature, hBMSCs were cultured in the presence of different concentrations of 1 ng mL^{-1}, 4 ng mL^{-1}, 10 ng mL^{-1}, and 25 ng mL^{-1} FGF1 and FGF2.

Firstly, the extent of adipogenic outcome was quantified by lipid droplet assays. Then, mRNA expression of early as well as later adipogenic marker genes was characterized using quantitative real-time PCR (qPCR) to gain a deeper insight into transcriptional changes. Finally, the course of the expression of key osteogenic marker genes was analyzed via qPCR to unravel possible effects on the balance between adipogenesis and osteogenesis on the transcriptional level.

7.1 Formation of lipid droplets

7.1.1 FGF1 completely inhibits lipid droplet formation

Following 14 days of adipogenic differentiation, hBMSCs exhibited distinct lipid droplet formation stained via Oil red O (Fig. 7.1 A, 'ctrl'). Interestingly, culture in the presence of FGF1 strongly reduced the formation of lipid droplets in a concentration-dependent manner compared to the non-FGF containing control (Fig. 7.1 A, 'FGF1'). In contrast, undifferentiated hBMSCs cultured in basal medium without differentiation supplements did not display any formation of lipid vesicles (Fig. 7.1 A, 'undiff') and therefore zero lipid accumulation in the lipid droplet quantification assay was detected. No signs of spontaneous adipogenic differentiation occurred in our cell culture model.

The inhibitory effect of FGF1 seen after Oil red O staining was further examined by lipid droplet quantification: hBMSCs, which were adipogenically differentiated in the presence of 1 ng mL^{-1}, 4 ng mL^{-1}, 10 ng mL^{-1}, and 25 ng mL^{-1} FGF1 had a significantly reduced amount of lipid accumulation (Fig. 7.2 A '+FGF1'). The concentration of 1 ng mL^{-1} FGF1 exhibited a slight, yet non-significant lipid droplet reduction down to 0.83. The higher concentrations of 4 ng mL^{-1}, 10 ng mL^{-1}, and 25 ng mL^{-1} FGF1 displayed highly significant reductions in fat droplet formation in the range of 0.03 to 0.08. The most effective concentration of 10 ng µL^{-1} FGF1 reduced lipid droplet values to 0.03, which was not significantly different from the undifferentiated control sample (Fig. 7.2 A 'undiff').

After adipogenic conversion consisting of 14 days of osteogenic pre-differentiation plus another 14 days of conversion in adipogenic medium (28 days in total), the hBMSCs showed a marked lipid droplet formation (Fig. 7.1 B, 'ctrl'). As expected, the osteogenically differentiated cells neither showed any signs of lipid vesicle formation (Fig. 7.1 B, 'ost prediff') nor any lipid accumulation in the quantitative assay (Fig. 7.2 B).

Analogous to the differentiation set-ups, FGF1 administration reduced the formation of lipid vesicles during conversion (Fig. 7.1 B, 'FGF1'). The quantification via lipid droplet assay displayed a decrease intensifying with increasing concentrations. It ranged from 0.86 over 0.42 and 0.13 to 0.05 (1 ng mL^{-1}, 4 ng mL^{-1}, 10 ng mL^{-1}, and 25 ng mL^{-1} FGF1), the last three values being highly significant (Fig. 7.2 B '+FGF1').

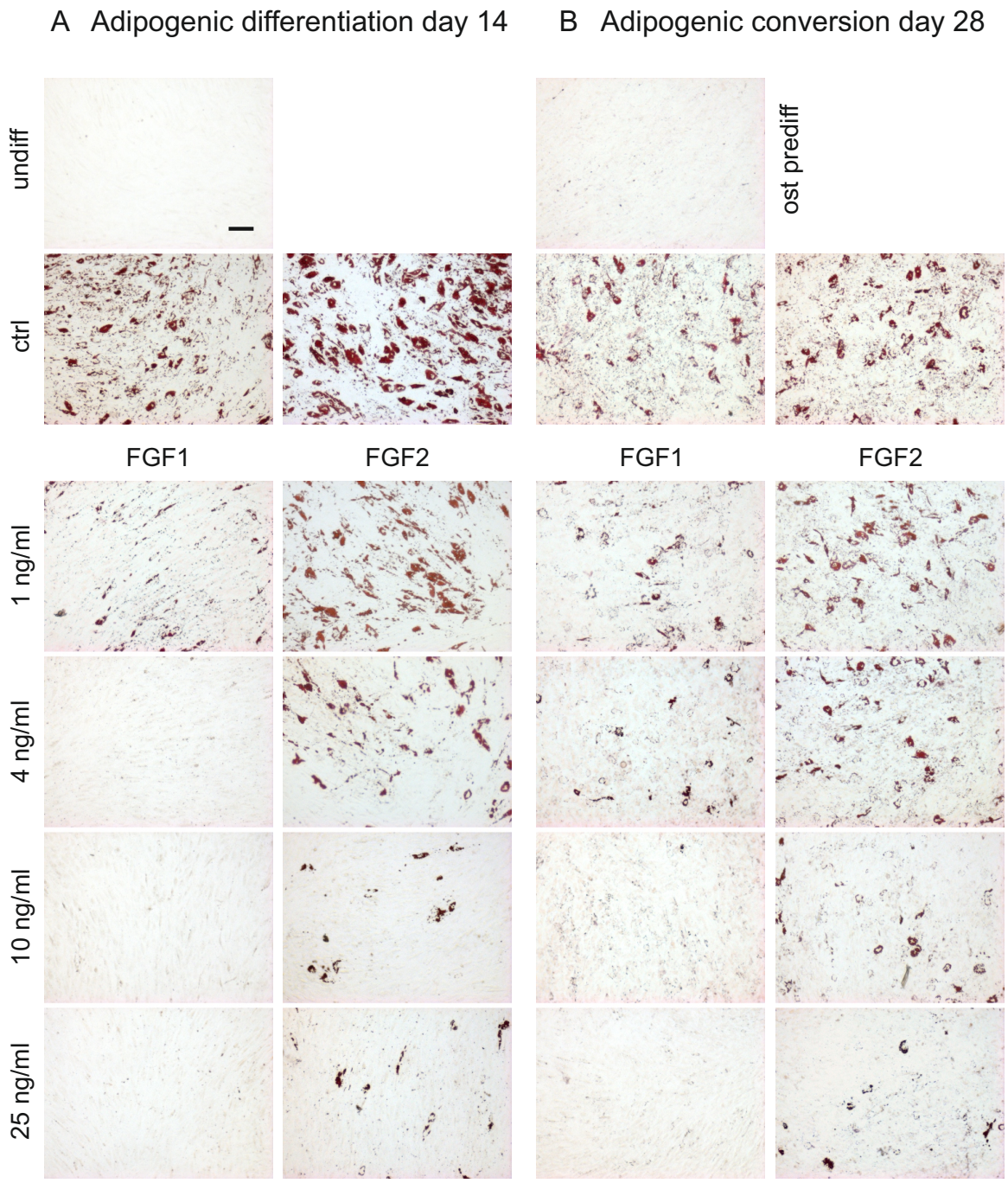

Figure 7.1: Oil red O staining of adipogenic differentiation (A) and conversion (B) in the presence of different concentrations of FGF1 and FGF2. Representative donor. undiff: hBMSCs incubated in basal medium without differentiation supplements; ctrl: hBMSCs incubated in adipogenic medium for differentiation (A) or conversion (B) without FGF1 and FGF2; 1 ng mL^{-1}, 4 ng mL^{-1}, 10 ng mL^{-1}, and 25 ng mL^{-1} FGF1 or FGF2: hBMSCs differentiated or converted in adipogenic medium supplemented with the respective concentration of FGF1 or FGF2; ost prediff: hBMSCs pre-differentiated in osteogenic medium for 14 days without further adipogenic conversion. Conversion samples were osteogenically pre-differentiated for 14 days, then converted in adipogenic medium for another 14 days. Scale bar represents 100 µm.

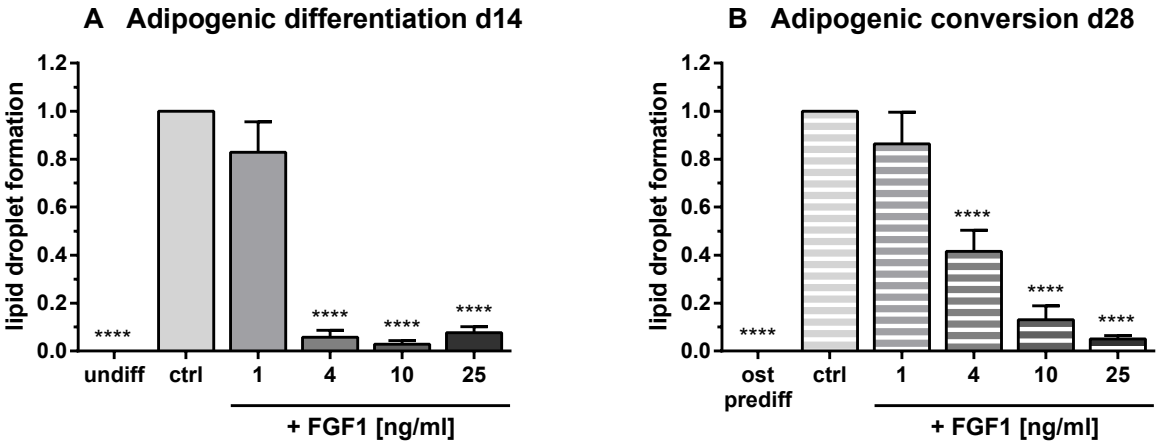

Figure 7.2: Lipid droplet assay during adipogenic differentiation (A) and conversion (B) supplemented with different concentrations of FGF1. undiff: hBMSCs incubated in basal medium without differentiation supplements; ctrl: hBMSCs incubated in adipogenic medium without FGF1 for adipogenic differentiation (A) or conversion (B); 1 ng mL^{-1}, 4 ng mL^{-1}, 10 ng mL^{-1}, and 25 ng mL^{-1} FGF1: hBMSCs differentiated or converted in adipogenic medium supplemented with the respective FGF1 concentration; ost prediff: hBMSCs pre-differentiated in osteogenic medium for 14 days without further adipogenic conversion. Conversion samples were osteogenically pre-differentiated for 14 days, then converted in adipogenic medium for another 14 days. For statistical analysis, samples were compared to the respective differentiation (ctrl, A) or conversion control (ctrl, B). $\tilde{x} \pm$ SEM; n = 4. **** $p < 0.0001$.

7.1.2 FGF2 distinctly reduces lipid droplet formation

After 14 days of adipogenic differentiation in the presence of different FGF2 concentrations, hBMSCs displayed a concentration-dependent reduction in lipid vesicle formation (Fig. 7.1 A, 'FGF2'). The effect was apparent in the higher concentrations of 10 ng mL^{-1} and 25 ng mL^{-1}. The quantifying assay exhibited no decrease at 1 ng mL^{-1} FGF2 (Fig. 7.3 A '+FGF2'). The concentration of 4 ng mL^{-1} reduced lipid droplet formation to 0.83, whereas 10 ng mL^{-1} FGF2 decreased the value to 0.54 and 25 ng mL^{-1} down to 0.56. The two highest concentrations represent highly significant differences.

Following adipogenic conversion, FGF2 supplementation demonstrated a decrease in lipid droplet formation, which was promoted by higher concentrations (Fig. 7.1 B, 'FGF2'). It ranged from 0.90 with 1 ng mL^{-1} over 0.71 using 4 ng mL^{-1} and 0.41 with 10 ng mL^{-1} to 0.31 at 25 ng mL^{-1} (Fig. 7.3 B '+FGF2'). Here, the results of 10 ng mL^{-1} and 25 ng mL^{-1} FGF2 were highly significant.

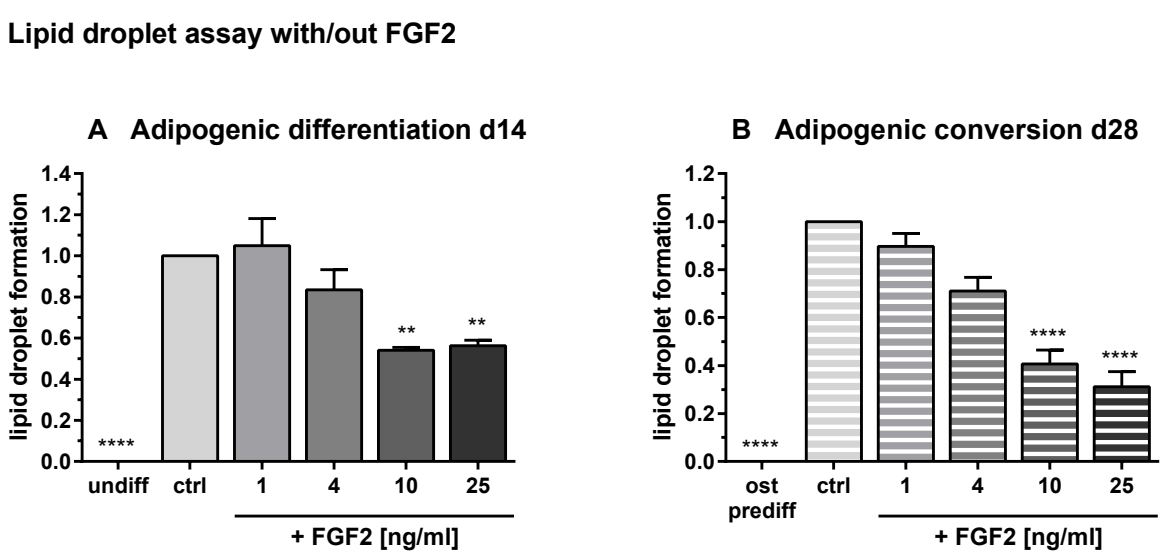

Figure 7.3: Lipid droplet assay during adipogenic differentiation and conversion supplemented with different concentrations of FGF2. undiff: hBMSCs incubated in basal medium without differentiation supplements; ctrl: hBMSCs incubated in adipogenic medium without FGF2 for adipogenic differentiation (A) or conversion (B); 1 ng mL^{-1}, 4 ng mL^{-1}, 10 ng mL^{-1}, and 25 ng mL^{-1} FGF2: hBMSCs differentiated or converted in adipogenic medium supplemented with the respective FGF2 concentration; ost prediff: hBMSCs pre-differentiated in osteogenic medium for 14 days without further adipogenic conversion. Conversion samples were osteogenically pre-differentiated for 14 days, then converted in adipogenic medium for another 14 days. For statistical analysis, samples were compared to the respective differentiation (ctrl, A) or conversion control (ctrl, B). $\tilde{x} \pm$ SEM; n = 4. ** $p < 0.005$; **** $p < 0.0001$.

7.2 Expression profile of adipogenic marker genes

To further investigate the reduction of lipid formation by FGF1 and FGF2 addition, we were prompted to gain deeper insight into the mRNA expression of adipogenic marker genes. To realize a profound overview throughout the progression of adipogenic differentiation and conversion, early as well as later marker genes were pursued. Hence, we concentrated on gene expression analysis of peroxisome proliferator-activated receptor γ 2 (PPARγ2) and CCAAT/enhancer binding protein α (C/EBPα) (considered as the two early key adipogenic markers) plus fatty acid binding protein 4 (FABP4) and lipoprotein lipase (LPL) (considered as later key markers of adipogenesis).

7.2.1 FGF1 completely prevents adipogenic marker mRNA expression

After 14 days of differentiation, the expression of adipogenic marker genes was markedly upregulated in comparison to the undifferentiated sample ('ctrl' vs. 'undiff'). The early marker PPARγ2 displayed a 910-fold increase, whereas C/EBPα was up-regulated by 8.22-fold. The later markers FABP4 and LPL were enhanced by 21 739-fold and 58 824-fold, respectively (Fig. 7.4). The additional supplementation with FGF1 decreased the early adipogenic marker gene expression distinctly and highly significantly in a concentration-dependent manner. PPARγ2 expression was downregulated to 0.45, 0.05, 0.02, and 0.01 (1 ng mL^{-1}, 4 ng mL^{-1}, 10 ng mL^{-1}, and 25 ng mL^{-1} FGF1), respectively (Fig. 7.4 A). The expression of C/EBPα declined to 0.61 by 1 ng mL^{-1} FGF1, further down to 0.07 by 4 ng mL^{-1}, to 0.03 via 10 ng mL^{-1} and reached 0.02 through 25 ng mL^{-1} FGF1 (Fig. 7.4 B '+FGF1').

Likewise, the later adipogenic marker genes were highly significantly downregulated in a concentration dependent manner. FABP4 decreased to values between 0.39 and 0.01 (1 ng mL^{-1} and 25 ng mL^{-1}) (Fig. 7.4 C '+FGF1'). The expression of LPL declined to values ranging from 0.32 to 0.00 (1 ng mL^{-1} to 25 ng mL^{-1}) (Fig. 7.4 D '+FGF1').

In parallel to adipogenic differentiation, the effect of FGF1 was examined during conversion. After 28 days (consisting of 14 days of osteogenic pre-differentiation plus 14 days of conversion under adipogenic conditions), hBMSCs displayed a distinct up-regulation of all four adipogenic marker genes compared to the non-converted sample (referred to as 'ost prediff'). PPARγ2 exhibited an 315-fold increase, while C/EBPα was enhanced by 46-fold. FABP4 and LPL were up-regulated by 14 286-fold and 2710-fold, respectively (Fig. 7.5, 'ost prediff' vs. 'ctrl').

The addition of FGF1 led to a highly significant and concentration-dependent downregulation of all examined adipogenic marker genes. PPARγ2 was decreased to values between 0.60 (1 ng mL^{-1}) and 0.03 (25 ng mL^{-1}) (Fig. 7.5 A '+FGF1'). Meanwhile, C/EBPα expression declined to values ranging from 0.67 (1 ng mL^{-1}) and 0.04 (25 ng mL^{-1}) (Fig. 7.5 B '+FGF1'). FABP4 values reached from 0.51 (1 ng mL^{-1}) to a minimum of 0.03 (25 ng mL^{-1}) (Fig. 7.5C '+FGF1'). The results of LPL ranged from 0.53 (1 ng mL^{-1}) to 0.01 (25 ng mL^{-1}) (Fig. 7.5 D '+FGF1').

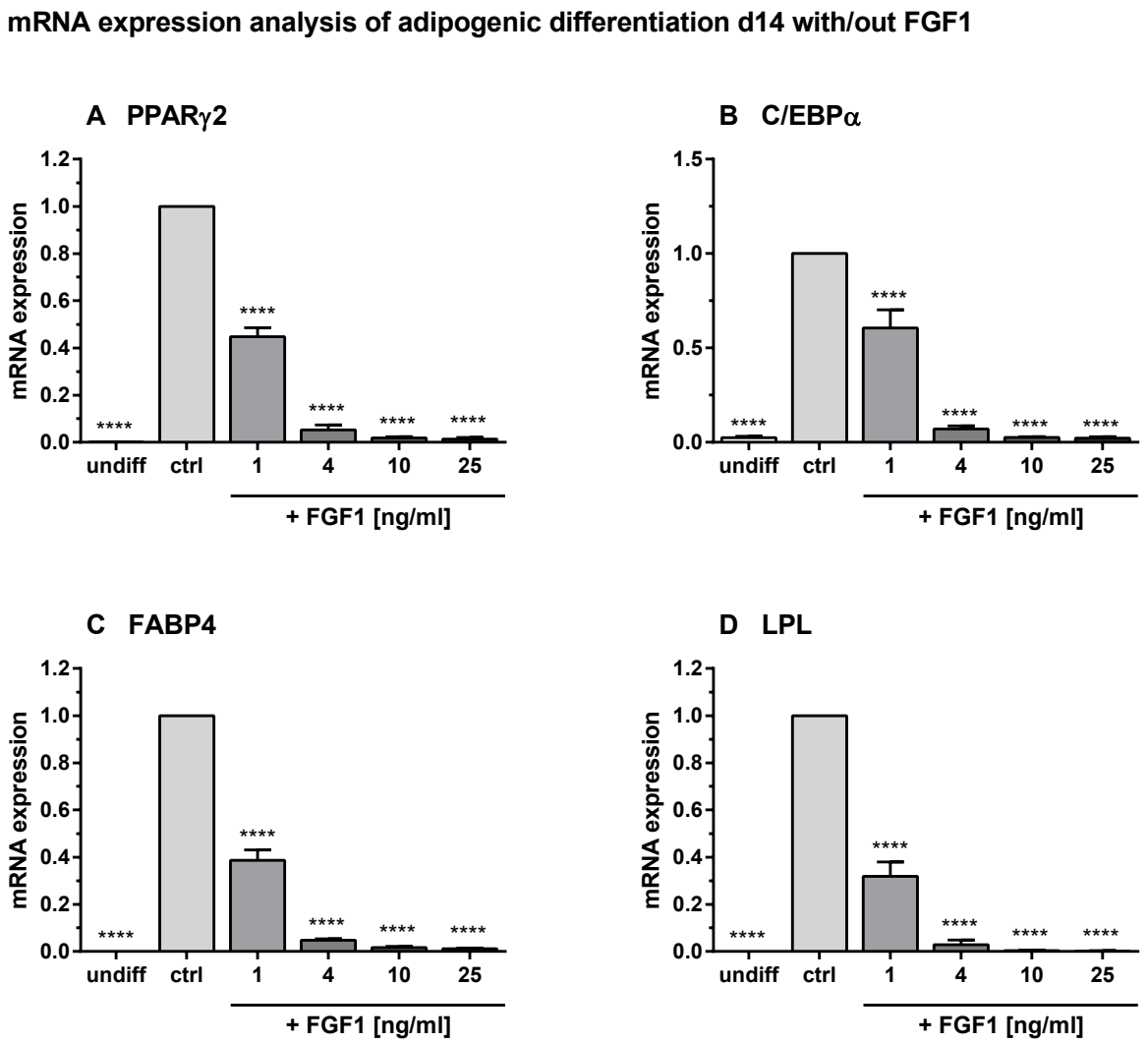

Figure 7.4: FGF1 effects on mRNA expression of early (A,B) and late adipogenic marker genes (C,D) during adipogenic differentiation on day 14. undiff: hBMSCs incubated in basal medium without differentiation supplements; ctrl: hBMSCs differentiated in adipogenic medium without FGF1; 1 ng mL^{-1}, 4 ng mL^{-1}, 10 ng mL^{-1}, and 25 ng mL^{-1} FGF1: hBMSCs differentiated in adipogenic medium supplemented with the respective FGF1 concentration. For statistical analysis, samples were compared to the differentiation control (ctrl). $\tilde{x} \pm$ SEM; n = 4 except for C/EBPα: n = 3. **** $p < 0.0001$.

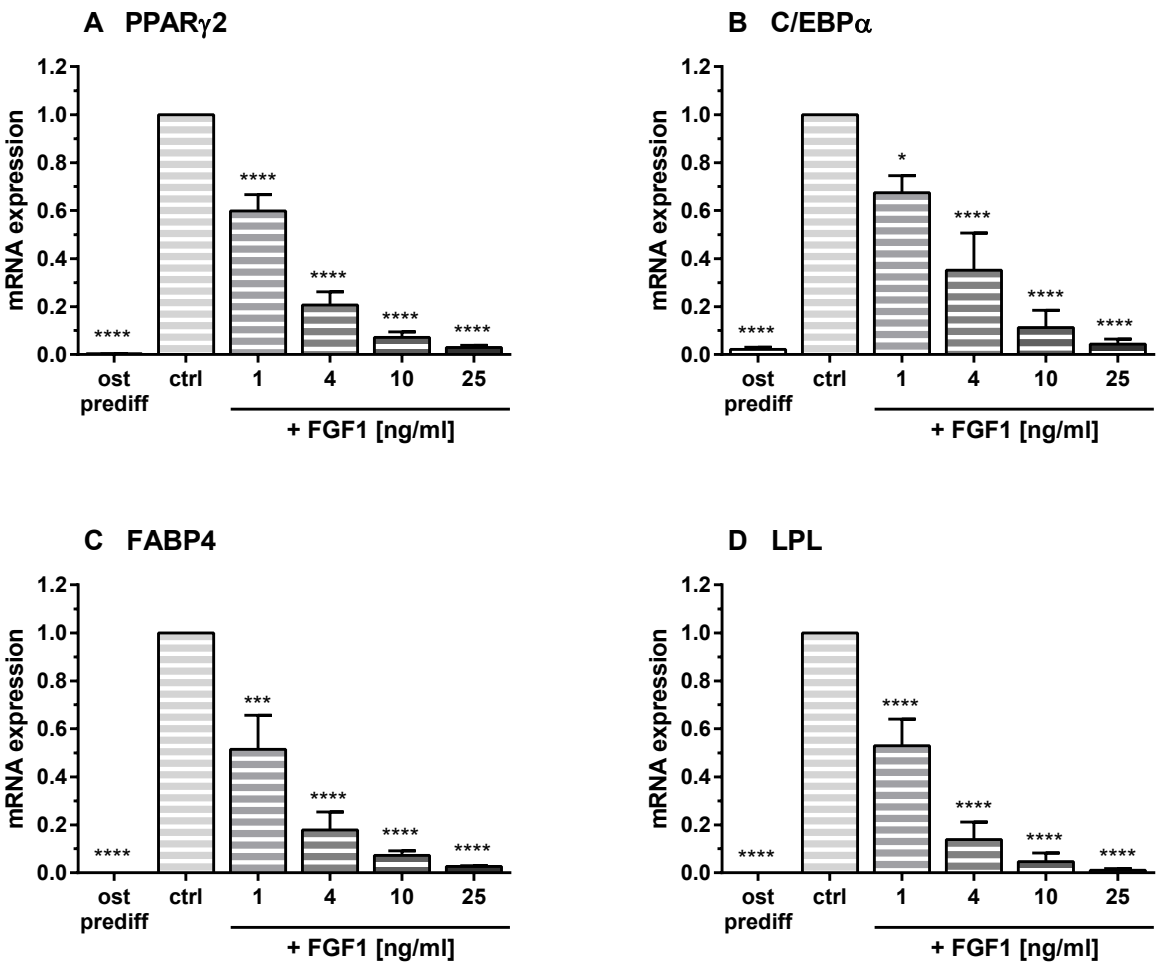

Figure 7.5: FGF1 effects on mRNA expression of early (A,B) and late adipogenic marker genes (C,D) during adipogenic conversion on day 28. ost prediff: hBMSCs pre-differentiated in osteogenic medium for 14 days without further adipogenic conversion; ctrl: hBMSCs osteogenically pre-differentiated for 14 days, then converted in adipogenic medium without FGF1 for another 14 days; 1 ng mL^{-1}, 4 ng mL^{-1}, 10 ng mL^{-1}, and 25 ng mL^{-1} FGF1: hBMSCs osteogenically pre-differentiated for 14 days, then converted in adipogenic medium supplemented with the respective FGF1 concentration for another 14 days. For statistical analysis, samples were compared to the conversion control (ctrl). $\tilde{x} \pm$ SEM; n = 4. * $p < 0.05$; *** $p < 0.001$; **** $p < 0.0001$.

7.2.2 FGF2 markedly reduces adipogenic marker mRNA expression

Analogous to the FGF1 set-ups, the effect of FGF2 on adipogenic marker gene expression was examined. As a proof of principle for adipogenic differentiation, marker gene expression rose similar to formerly described results: PPARγ2 (1212-fold), C/EBPα (48-fold), FABP4 (20 833-fold), and LPL (28 571-fold) (Fig. 7.6, 'undiff' vs. 'ctrl').

The addition of different concentrations of FGF2 to the adipogenic medium during differentiation decreased marker gene expression highly significantly. Values of PPARγ2 ranged from 0.54 (25 ng mL^{-1}) to 0.19 (10 ng mL^{-1} and 25 ng mL^{-1}) (Fig. 7.6 A '+FGF2'). C/EBPα was down-regulated to 0.91 (1 ng mL^{-1}) and 0.15 (25 ng mL^{-1}), respectively (Fig. 7.6 B '+FGF2'). Meanwhile, FABP4 declined to values between 0.71 (1 ng mL^{-1}) to 0.17 (25 ng mL^{-1}) (Fig. 7.6 C '+FGF2'). The expression of LPL decreased to 0.40 (1 ng mL^{-1}) and 0.09 (25 ng mL^{-1}) (Fig. 7.6 D '+FGF2').

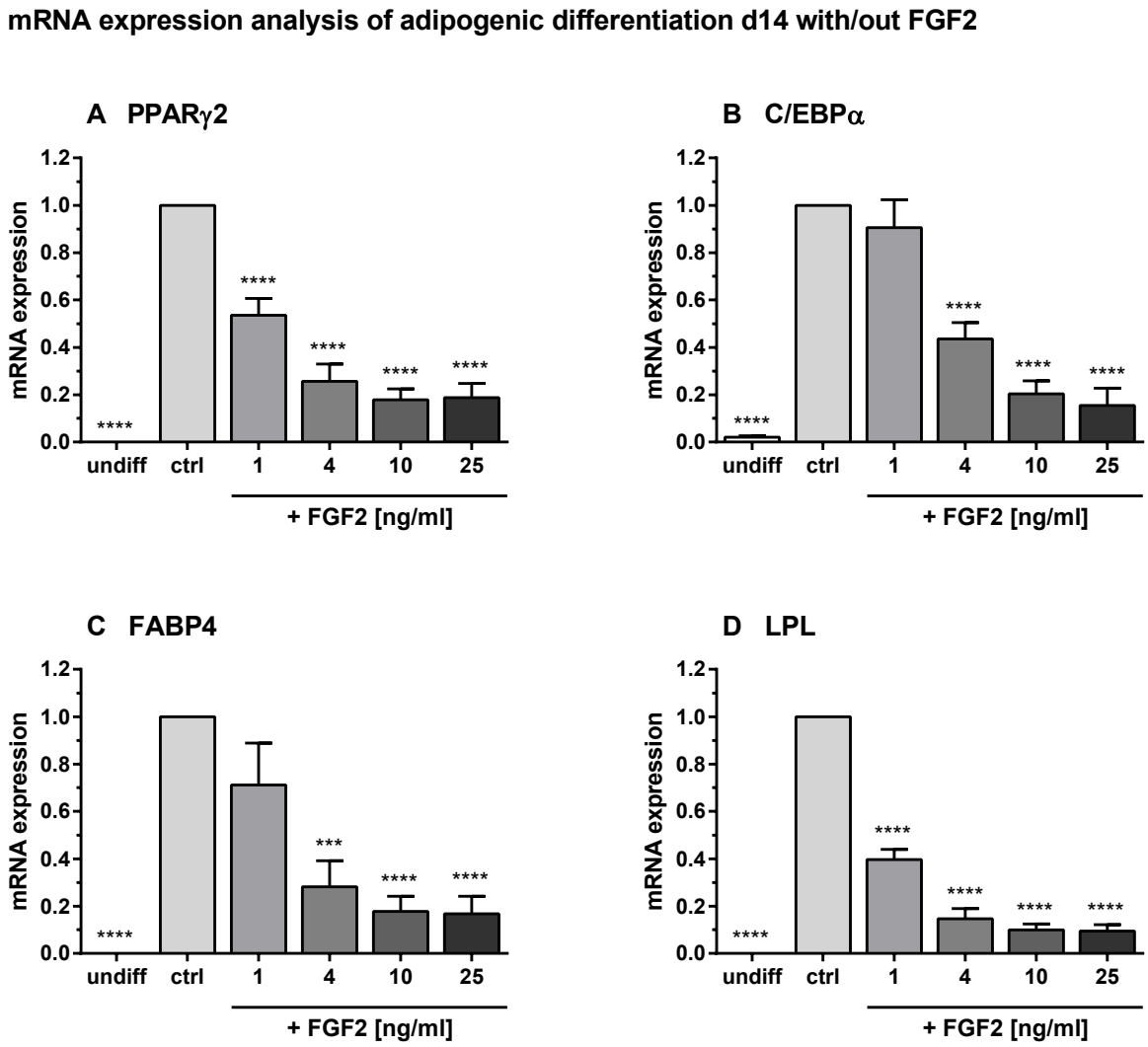

Figure 7.6: FGF2 effects on mRNA expression of early (A,B) and late adipogenic marker genes (C,D) during adipogenic differentiation on day 14. undiff: hBMSCs incubated in basal medium without differentiation supplements; ctrl: hBMSCs differentiated in adipogenic medium without FGF2; 1 ng mL^{-1}, 4 ng mL^{-1}, 10 ng mL^{-1}, and 25 ng mL^{-1} FGF2: hBMSCs differentiated in adipogenic medium supplemented with the respective FGF2 concentration. For statistical analysis, samples were compared to the differentiation control (ctrl). $\tilde{x} \pm$ SEM; n = 4. *** $p < 0.001$; **** $p < 0.0001$.

Adipogenic conversion performed with and without FGF2 supplementation led to similar results. On day 28, the expression of marker genes in the adipogenically converted control sample was markedly up-regulated in comparison to osteogenically pre-differentiated hBMSCs. Fold changes varied from 46 (C/EBPα) over 344 (PPARγ2) and 2506 (LPL) to 12 346 (FABP4) (Fig. 7.7, 'ost prediff' vs. 'ctrl').

Following FGF2 addition, adipogenic marker gene expression was markedly reduced. PPARγ2 expression decreased to values between 0.78 ($1\,\mathrm{ng\,mL^{-1}}$) and 0.10 ($25\,\mathrm{ng\,mL^{-1}}$) (Fig. 7.7 A '+ FGF2'). C/EBPα declined to 0.67 ($1\,\mathrm{ng\,mL^{-1}}$) and 0.04 ($25\,\mathrm{ng\,mL^{-1}}$) (Fig. 7.7 B '+ FGF2'). FABP4 expression varied between 0.64 ($1\,\mathrm{ng\,mL^{-1}}$) and 0.10 ($25\,\mathrm{ng\,mL^{-1}}$) (Fig. 7.7 C '+ FGF2'). Values of LPL declined to 0.69 ($1\,\mathrm{ng\,mL^{-1}}$) and 0.07 ($25\,\mathrm{ng\,mL^{-1}}$) (Fig. 7.7 D '+ FGF2').

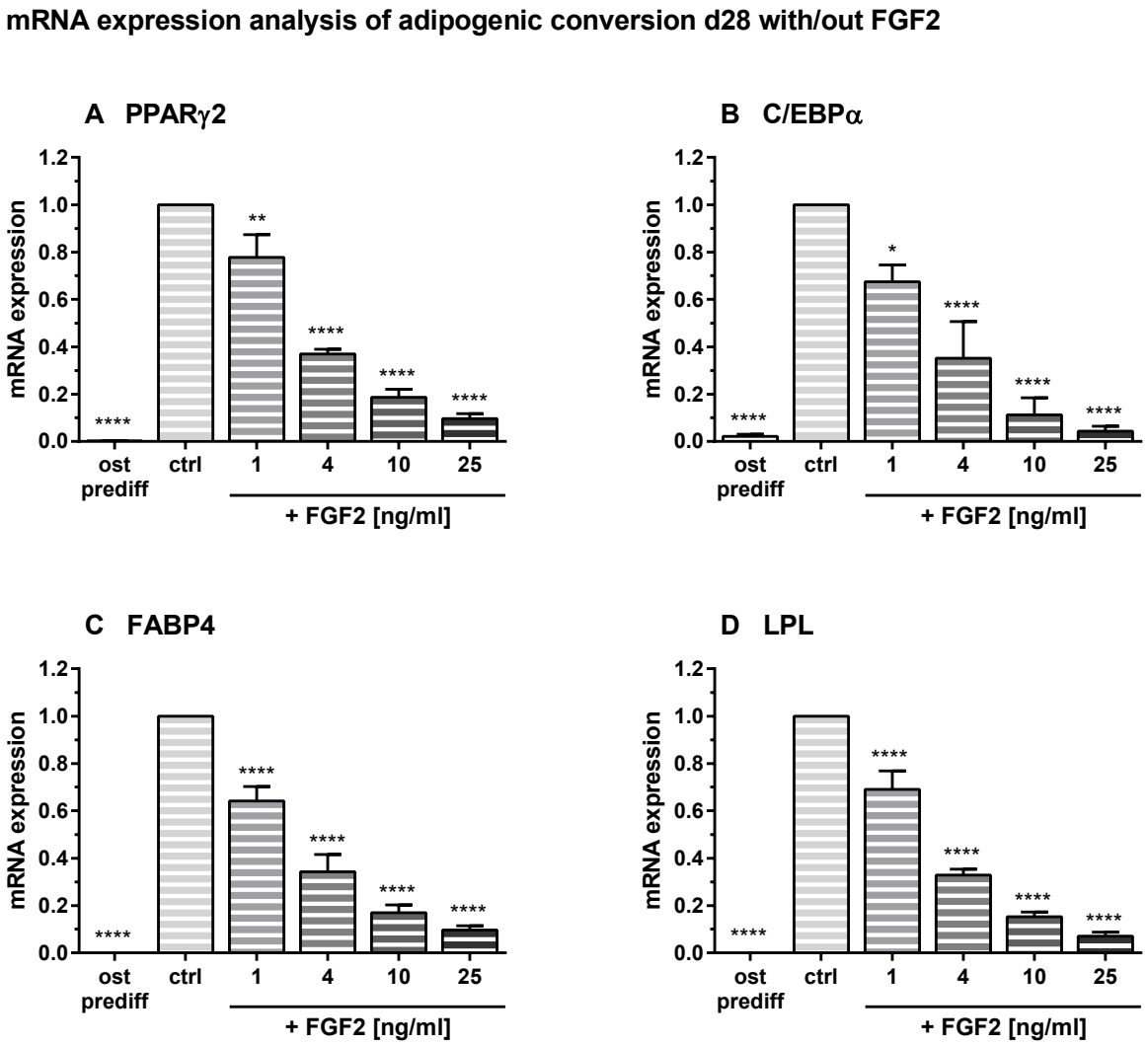

Figure 7.7: FGF2 effects on mRNA expression of early (A, B) and late adipogenic marker genes (C, D) during adipogenic conversion on day 28. ost prediff: hBMSCs pre-differentiated in osteogenic medium for 14 days without further adipogenic conversion; ctrl: hBMSCs osteogenically pre-differentiated for 14 days, then converted in adipogenic medium without FGF2 for another 14 days; $1\,\mathrm{ng\,mL^{-1}}$, $4\,\mathrm{ng\,mL^{-1}}$, $10\,\mathrm{ng\,mL^{-1}}$, and $25\,\mathrm{ng\,mL^{-1}}$ FGF2: hBMSCs osteogenically pre-differentiated for 14 days, then converted in adipogenic medium supplemented with the respective FGF2 concentration for another 14 days. For statistical analysis, samples were compared to the conversion control (ctrl). $\tilde{x} \pm$ SEM; n = 4. * $p \leq 0.05$; ** $p < 0.01$; **** $p < 0.0001$.

7.3 Expression of osteogenic markers during adipogenesis

Since preliminary results pointed at a supportive impact of the culture in the presence of FGF1 and FGF2 on osteogenesis, a broad range of early and late osteogenic markers as well as marker genes concerning extracellular matrix (ECM) mineralization were analyzed during adipogenic differentiation and conversion.

7.3.1 Adipogenic conversion downregulates osteogenic key markers

Inducing the conversion of pre-differentiated osteoblastic cells towards the adipogenic fate resulted in a marked downregulation of different sets of osteogenic markers. The expression of the early osteogenic key transcription factor runt-related transcription factor 2 (RUNX2) and bone morphogenetic protein 4 (BMP4) was markedly reduced by adipogenic conversion itself (Fig. 7.8 A, B, 'ost prediff' vs. 'ctrl'). However, additional supplementation with FGF1 and FGF2 did not alter RUNX2 and BMP4 transcription (Fig. 7.8 A, B and 7.9 A, B). The same was observed for the later osteogenic marker genes collagen 1 A1 (COL1A1) and osteocalcin (OC), which were also significantly downregulated by adipogenic conversion itself but not further altered by FGF1 or FGF2 administration (Fig. 7.8 C, D and 7.9 C, D).

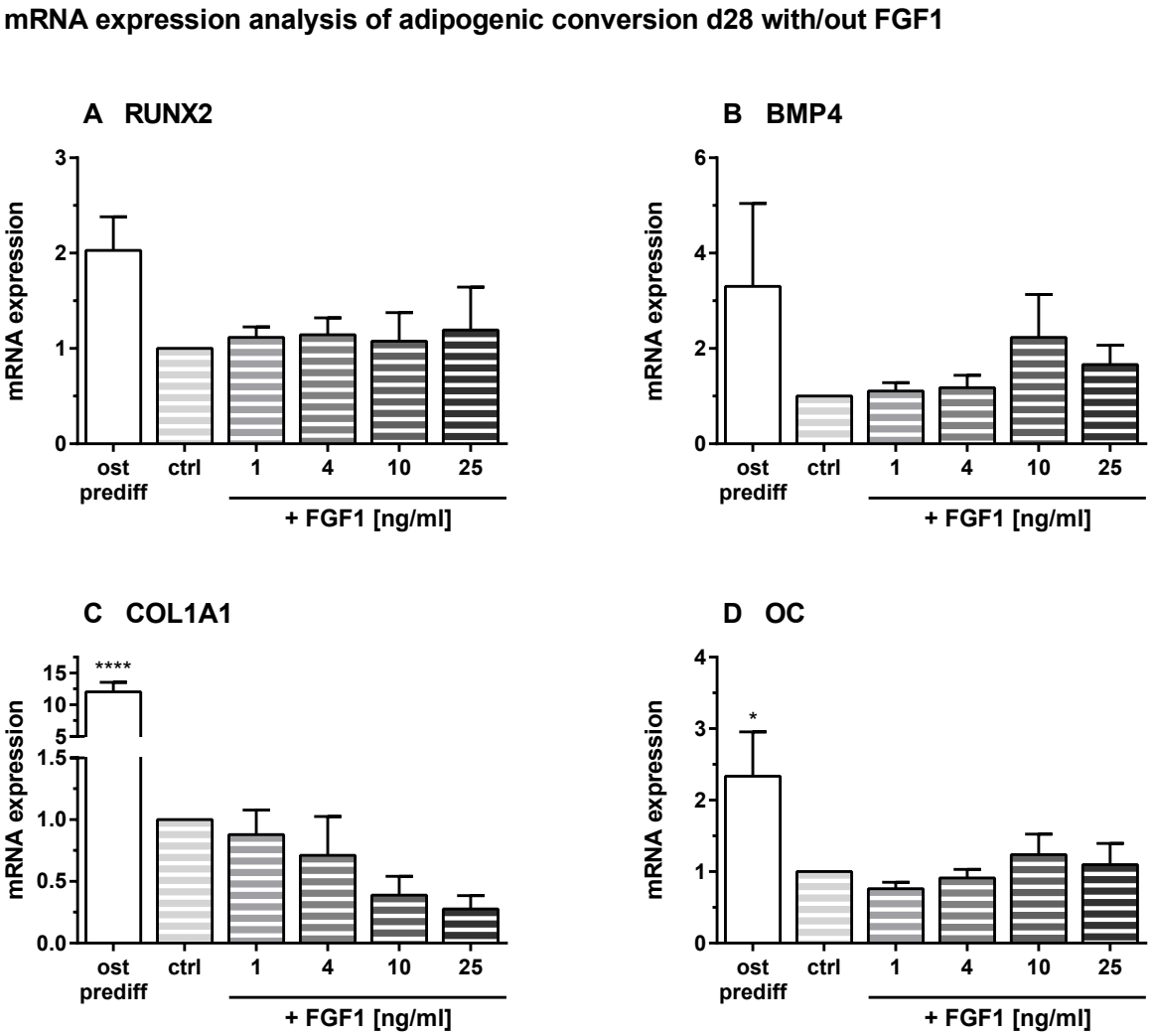

Figure 7.8: Effects of adipogenic conversion and FGF1 administration on mRNA expression of early and late osteogenic markers RUNX2, BMP4, COL1A1, and OC. ost prediff: hBMSCs pre-differentiated in osteogenic medium for 14 days without further adipogenic conversion; ctrl: hBMSCs osteogenically pre-differentiated for 14 days, then converted in adipogenic medium without FGF1 for another 14 days; 1 ng mL^{-1}, 4 ng mL^{-1}, 10 ng mL^{-1}, and 25 ng mL^{-1} FGF1: hBMSCs osteogenically pre-differentiated for 14 days, then converted in adipogenic medium supplemented with the respective FGF1 concentration for another 14 days. For statistical analysis, samples were compared to the conversion control (ctrl). $\tilde{x} \pm$ SEM; n = 4. * $p \leq 0.05$; **** $p < 0.0001$.

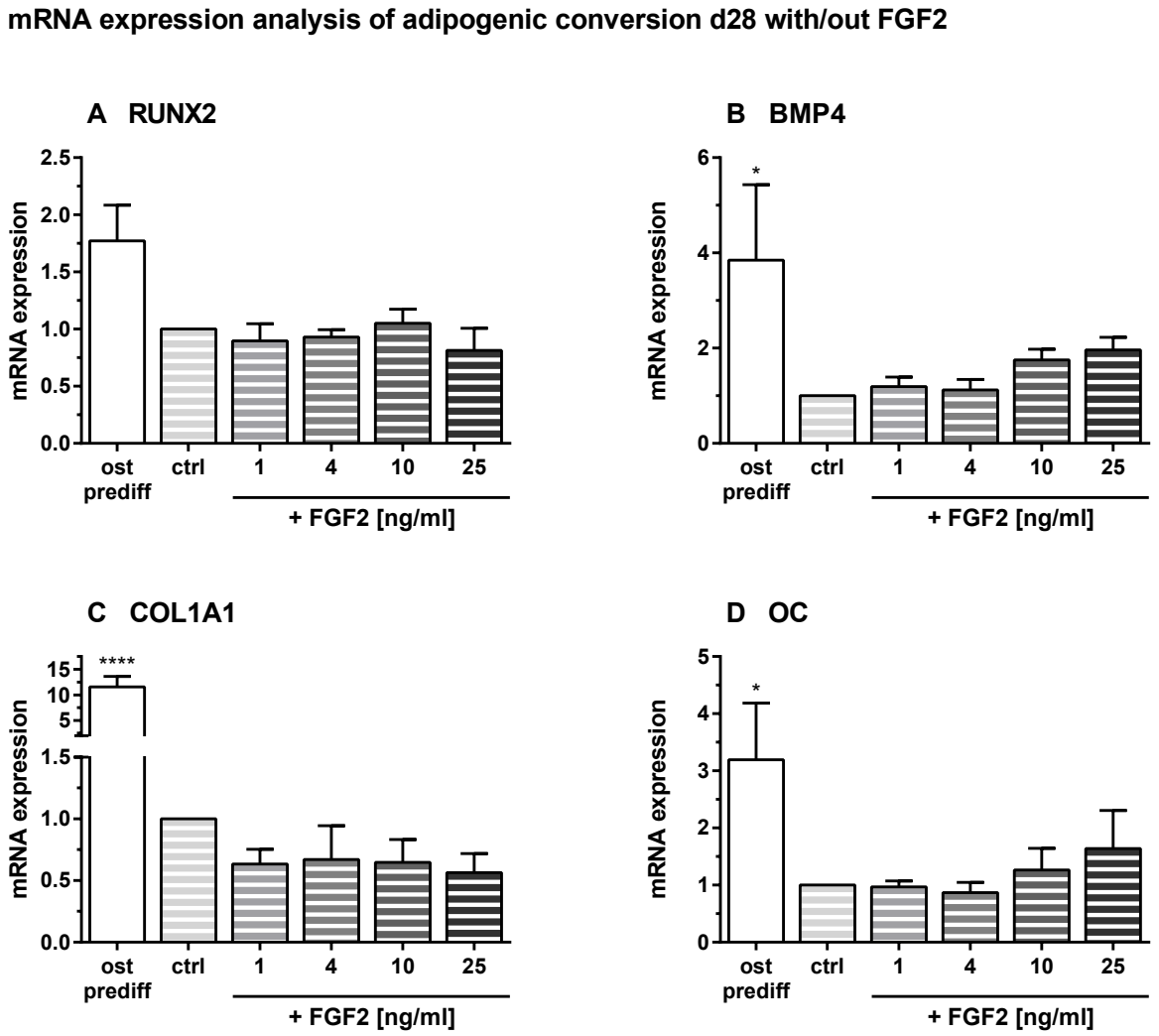

Figure 7.9: Effects of adipogenic conversion and FGF2 administration on mRNA expression of early and late osteogenic markers RUNX2, BMP4, COL1A1, and OC. ost prediff: hBMSCs pre-differentiated in osteogenic medium for 14 days without further adipogenic conversion; ctrl: hBMSCs osteogenically pre-differentiated for 14 days, then converted in adipogenic medium without FGF2 for another 14 days; 1 ng mL^{-1}, 4 ng mL^{-1}, 10 ng mL^{-1}, and 25 ng mL^{-1} FGF2: hBMSCs osteogenically pre-differentiated for 14 days, then converted in adipogenic medium supplemented with the respective FGF2 concentration for another 14 days. For statistical analysis, samples were compared to the conversion control (ctrl). $\tilde{x} \pm$ SEM; n = 4. * $p \leq 0.05$; **** $p < 0.0001$.

7.3.2 FGF1 upregulates inhibitory mineralization marker genes

In contrast to the key marker genes of osteogenic onset and maturation, which were not changed by FGF addition, we found a transcriptional regulation of genes crucial for ECM mineralization. The ANKH inorganic pyrophosphate transport regulator (ANKH) was downregulated through adipogenic differentiation itself by 4.32-fold (Fig. 7.10 A, 'undiff' vs. 'ctrl'). The additional administration of progressive concentrations of FGF1 increased ANKH expression to 1.55 (4 ng mL^{-1}), 3.62 (10 ng mL^{-1}), and 9.55 (25 ng mL^{-1}). The last value exceeded the basal expression level in undifferentiated hBMSCs and was highly significant (Fig. 7.10 A '+FGF1').

Osteopontin (OPN) expression was significantly reduced during adipogenic differentiation itself by 476-fold (Fig. 7.10 B, 'undiff' vs. 'ctrl'). The administration of FGF1 heightened the expression to 4.60 (1 ng mL^{-1}), 52 (4 ng mL^{-1}), 364 (10 ng mL^{-1}), and 473 (25 ng mL^{-1}). The last fold change was significant and reached the expression level of undifferentiated hBMSCs (Fig. 7.10 B '+FGF1').

Adipogenically converted samples exhibited similar results, although significance could not be achieved due to donor variability. The expression of ANKH declined during the conversion process by 3.66-fold (Fig. 7.11 A, 'ost prediff' vs. 'ctrl'). The supplementation with FGF1 increased expression levels to 2.77 (4 ng mL^{-1}), 6.21 (10 ng mL^{-1}), and 6.08 (25 ng mL^{-1}) (Fig. 7.11 A '+FGF1'). The adipogenic conversion markedly decreased OPN expression by 55-fold (Fig. 7.11 B, 'ost prediff' vs. 'ctrl'). Addition of FGF1 enhanced expression to 2.46 (1 ng mL^{-1}), 5.53 (4 ng mL^{-1}), 54 (10 ng mL^{-1}), and finally 132 (25 ng mL^{-1}) (Fig. 7.11 B '+FGF1').

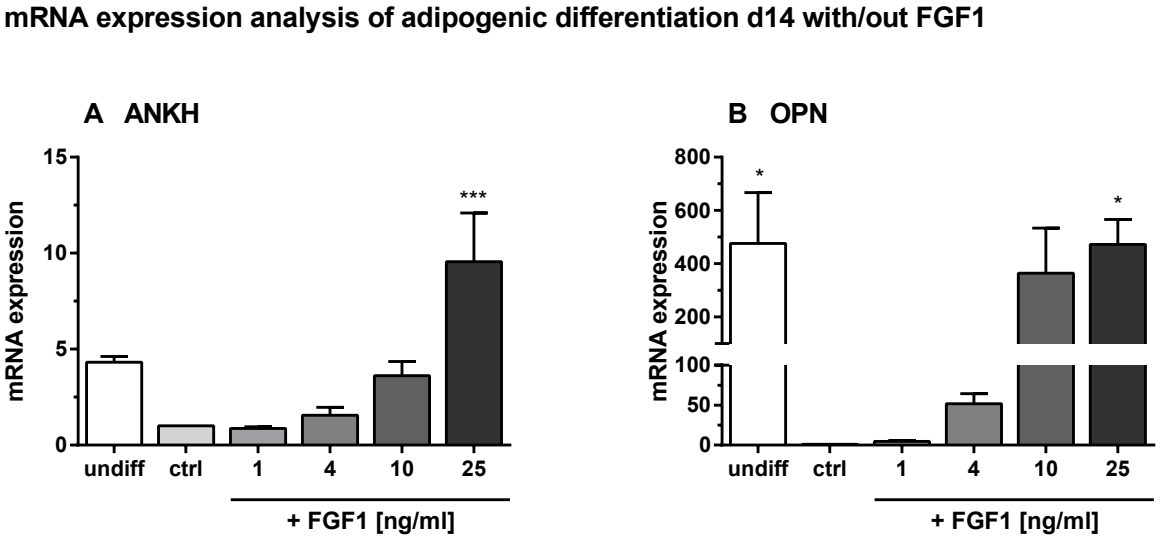

Figure 7.10: FGF1 effects on mRNA expression of mineralization marker genes during adipogenic differentiation on day 14. undiff: hBMSCs incubated in basal medium without differentiation supplements; ctrl: hBMSCs differentiated in adipogenic medium without FGF1; 1 ng mL^{-1}, 4 ng mL^{-1}, 10 ng mL^{-1}, and 25 ng mL^{-1} FGF1: hBMSCs differentiated in adipogenic medium supplemented with the respective FGF1 concentration. For statistical analysis, samples were compared to the differentiation control (ctrl). $\tilde{x} \pm$ SEM; n = 4. * $p \leq 0.05$; *** $p < 0.001$.

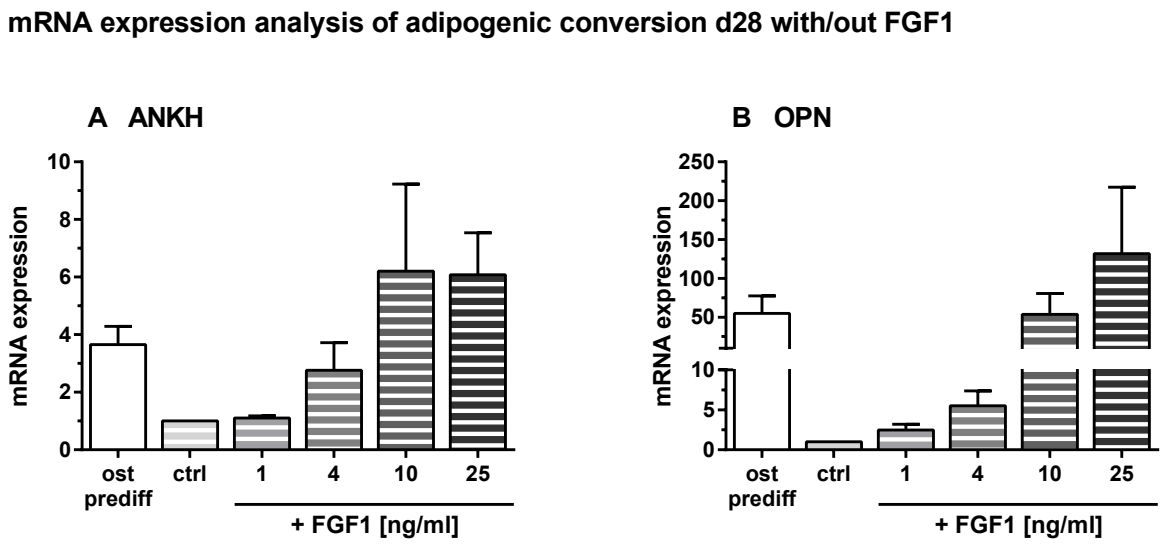

Figure 7.11: FGF1 effects on mRNA expression of mineralization marker genes during adipogenic conversion on day 28. ost prediff: hBMSCs pre-differentiated in osteogenic medium for 14 days without further adipogenic conversion; ctrl: hBMSCs osteogenically pre-differentiated for 14 days, then converted in adipogenic medium without FGF1; 1 ng mL^{-1}, 4 ng mL^{-1}, 10 ng mL^{-1}, and 25 ng mL^{-1} FGF1: hBMSCs osteogenically pre-differentiated for 14 days, then converted in adipogenic medium supplemented with the respective FGF1 concentration. For statistical analysis, samples were compared to the conversion control (ctrl). $\tilde{x} \pm$ SEM; n = 4.

7.3.3 FGF2 increases inhibitory mineralization marker gene expression

In parallel, experiments were performed deploying FGF2 supplementation. The obtained results were similar to the FGF1 outcomes described above. During adipogenic differentiation, the expression of ANKH decreased again about 5.44-fold (Fig. 7.12 A, 'undiff' vs. 'ctrl'). The administration of FGF2 elevated expression rates to 1.67 (10 ng mL^{-1}) and 4.15 (25 ng mL^{-1}), the latter being significant (Fig. 7.12 A '+FGF2'). OPN expression declined significantly during adipogenic differentiation by 194-fold (Fig. 7.12 B, 'undiff' vs. 'ctrl'). The supplementation with FGF2 elevated expression levels again to 1.84 (1 ng mL^{-1}), 6.90 (4 ng mL^{-1}), 38 (10 ng mL^{-1}), and 109 (25 ng mL^{-1}) (Fig. 7.12 B '+FGF2').

After adipogenic conversion, the expression of ANKH was downregulated 4.64-fold (Fig. 7.13 A, 'ost prediff' vs. 'ctrl'). FGF2 administration increased it to 1.27 (4 ng mL^{-1}), 1.90 (10 ng mL^{-1}), and 3.17 (25 ng mL^{-1}) (Fig. 7.13 A '+FGF2'). Meanwhile, OPN expression was reduced about 34-fold by the conversion process (Fig. 7.13 B, 'ost prediff' vs. 'ctrl'). Further FGF2 administration increased expression rates again to 2.33 (10 ng mL^{-1}) and 14 (25 ng mL^{-1}) (Fig. 7.13 B '+FGF2').

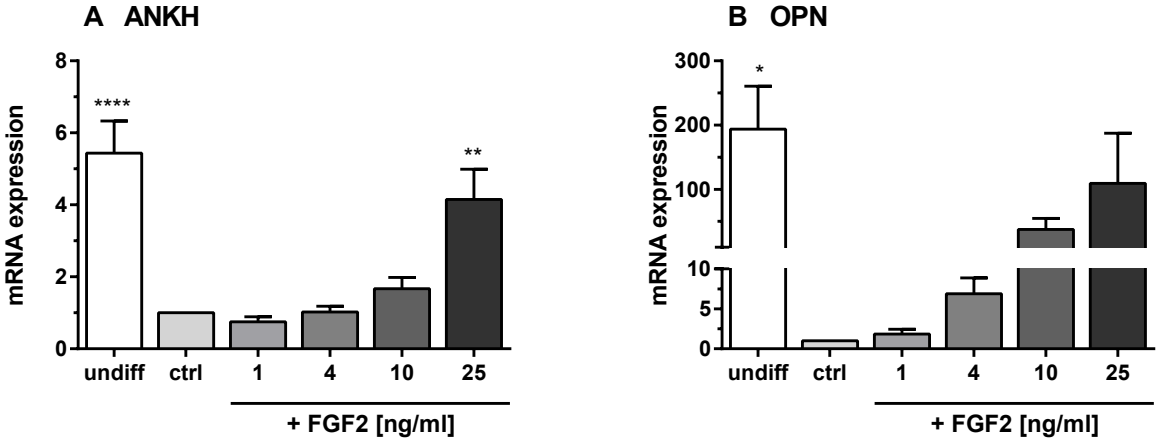

Figure 7.12: FGF2 effects on mRNA expression of mineralization marker genes during adipogenic differentiation on day 14. undiff: hBMSCs incubated in basal medium without differentiation supplements; ctrl: hBMSCs differentiated in adipogenic medium without FGF2; 1 ng mL^{-1}, 4 ng mL^{-1}, 10 ng mL^{-1}, and 25 ng mL^{-1} FGF2: hBMSCs differentiated in adipogenic medium supplemented with the respective FGF2 concentration. For statistical analysis, samples were compared to the differentiation control (ctrl). $\tilde{x} \pm$ SEM; n = 4. * $p \leq 0.05$; ** $p < 0.01$; **** $p < 0.0001$.

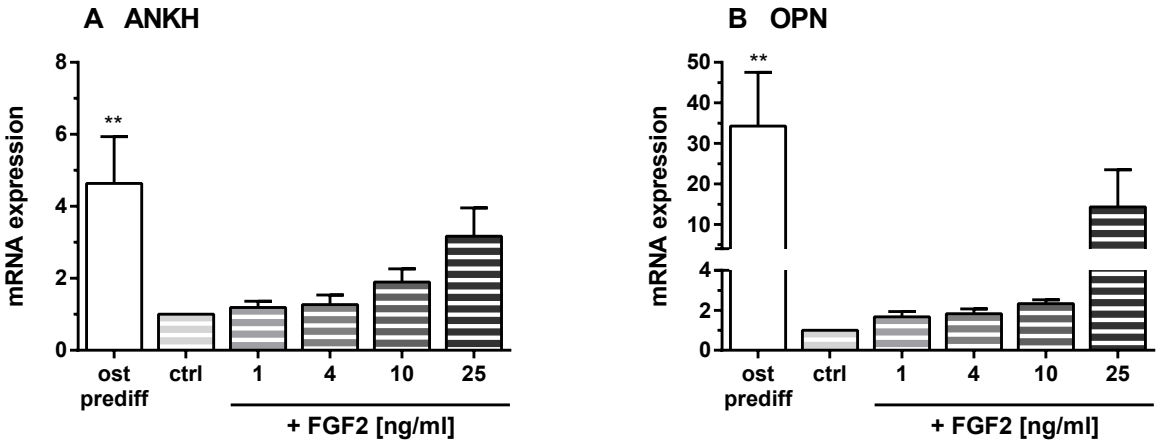

Figure 7.13: FGF2 effects on mRNA expression of mineralization marker genes during adipogenic conversion on day 28. ost prediff: hBMSCs pre-differentiated in osteogenic medium for 14 days without further adipogenic conversion; ctrl: hBMSCs osteogenically pre-differentiated for 14 days, then converted in adipogenic medium without FGF2 for another 14 days; 1 ng mL^{-1}, 4 ng mL^{-1}, 10 ng mL^{-1}, and 25 ng mL^{-1} FGF2: hBMSCs osteogenically pre-differentiated for 14 days, then converted in adipogenic medium supplemented with the respective FGF2 concentration. For statistical analysis, samples were compared to the conversion control (ctrl). $\tilde{x} \pm$ SEM; n = 4. ** $p < 0.01$.

8 FGF1 and FGF2 affect osteogenic differentiation and conversion

In parallel to the experiments performed regarding adipogenesis, the effect of FGF1 and FGF2 on osteogenic differentiation and conversion was investigated. To gain a broad insight into the prevalent processes, we chose different experimental approaches: Firstly, the mineralization of the monolayers' ECM was determined as a reliable readout for the extent of osteogenesis. Secondly, alkaline phosphatase (ALP) mRNA expression and enzyme activity were examined to enlighten the effects on this widely accepted early osteogenic marker. Finally, gene expression analysis for further early and late osteogenic markers as well as those affecting matrix mineralization was performed to investigate underlying changes in differentiation-dependent cell signaling mechanisms.

8.1 Reduction of matrix mineralization

To examine the effect of the culture in the presence of FGF1 and FGF2 on osteogenesis, we analyzed the amount of matrix mineralization on day 14 and day 28 of differentiation as well as on day 28 of conversion. On day 14 and 28 of osteogenic differentiation and conversion, respectively, hBMSCs had formed significant amounts of mineralized matrix. Mineralized spots were observed by phase contrast microscopy (Fig. 8.1 A + B, 'PC') and further highlighted by Alizarin red S (Fig. 8.1 A + B, 'ARS'). The quantifying assay revealed that calcium content was significantly increased by 50- and 73-fold (day 14 and 28 of differentiation) and 49-fold due to conversion when compared to the undifferentiated/adipogenically pre-differentiated controls (Fig. 8.2, A, B, 'undiff' vs. 'ctrl' and C, 'ad prediff' vs. 'ctrl').

The additional supplementation with 25 ng mL^{-1} FGF1 and FGF2 reduced ECM mineralization markedly as seen by Alizarin red S staining (Fig. 8.1 A + B, 'ARS'). Ascending FGF1 concentrations resulted in a concentration-dependent reduction of the calcium content. On day 14 of differentiation, mineralization values decreased to 0.79 (1 ng mL^{-1}), 0.60 (4 ng mL^{-1}), 0.46 (10 ng mL^{-1}), and 0.41 (25 ng mL^{-1}). The two latter values reached high significance (Fig. 8.2 A '+FGF1'). After 28 days of differentiation, the decrease of calcium values was lessened and reached a minimum of 0.56 with 25 ng mL^{-1} (Fig. 8.2 B '+FGF1'). After 28 days of conversion, consisting of 14 days of adipogenic pre-differentiation plus another 14 days of conversion under osteogenic conditions, hBMSCs displayed a highly significant reduction of ECM mineralization. Values declined to 0.42 (1 ng mL^{-1}), 0.32 (4 ng mL^{-1}), 0.27 (1 ng mL^{-1}), and finally 0.21 (25 ng mL^{-1}) (Fig. 8.2 C '+FGF1').

Set-ups regarding FGF2 exhibited similar results. During osteogenic differentiation, calcium contents significantly decreased to 0.56 (10 ng mL^{-1}) and 0.58 (25 ng mL^{-1}) on day 14 (Fig. 8.3 A). On day 28, values displayed a minimum of 0.79 (10 ng mL^{-1}) (Fig. 8.3 B '+FGF2'). However, after osteogenic conversion on day 28, calcium content was reduced to 0.32 (4 ng mL^{-1}) and 0.60 with 10 ng mL^{-1} FGF2 (Fig. 8.3 C '+FGF2').

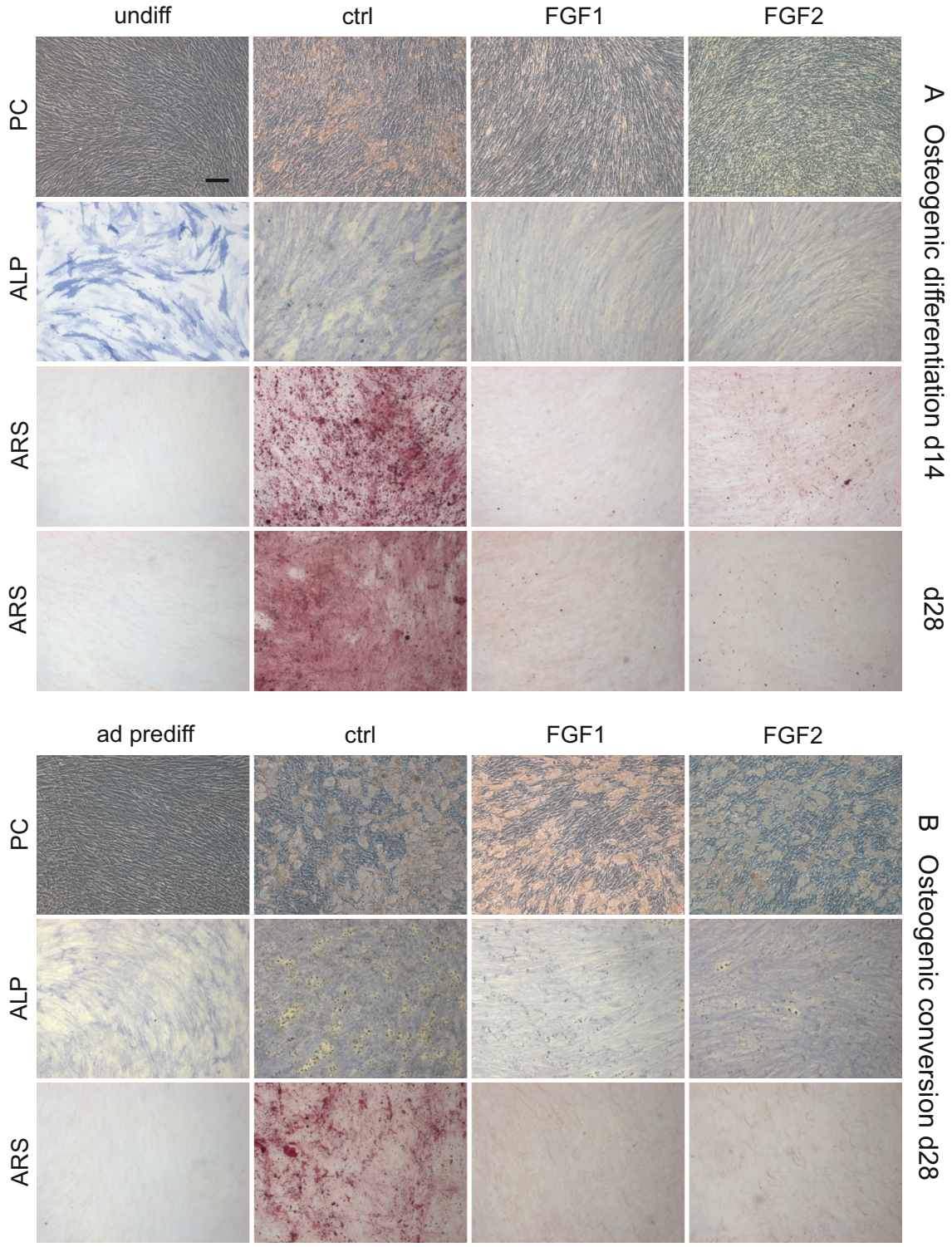

Figure 8.1: Phase contrast microscopy (PC), ALP staining (ALP), and Alizarin red S staining (ARS) after osteogenic differentiation and conversion in the presence of different concentrations of FGF1 and FGF2. Representative donor. undiff: hBMSCs incubated in basal medium without differentiation supplements; ctrl: hBMSCs differentiated or converted in osteogenic medium without FGF1 and FGF2; FGF1 or FGF2: hBMSCs differentiated or converted in osteogenic medium supplemented with 25 ng mL^{-1} FGF1 or FGF2; ad prediff: hBMSCs pre-differentiated in adipogenic medium for 14 days without further osteogenic conversion. Conversion samples were adipogenically pre-differentiated for 14 days, then converted in osteogenic medium for another 14 days. Scale bar represents 100 µm.

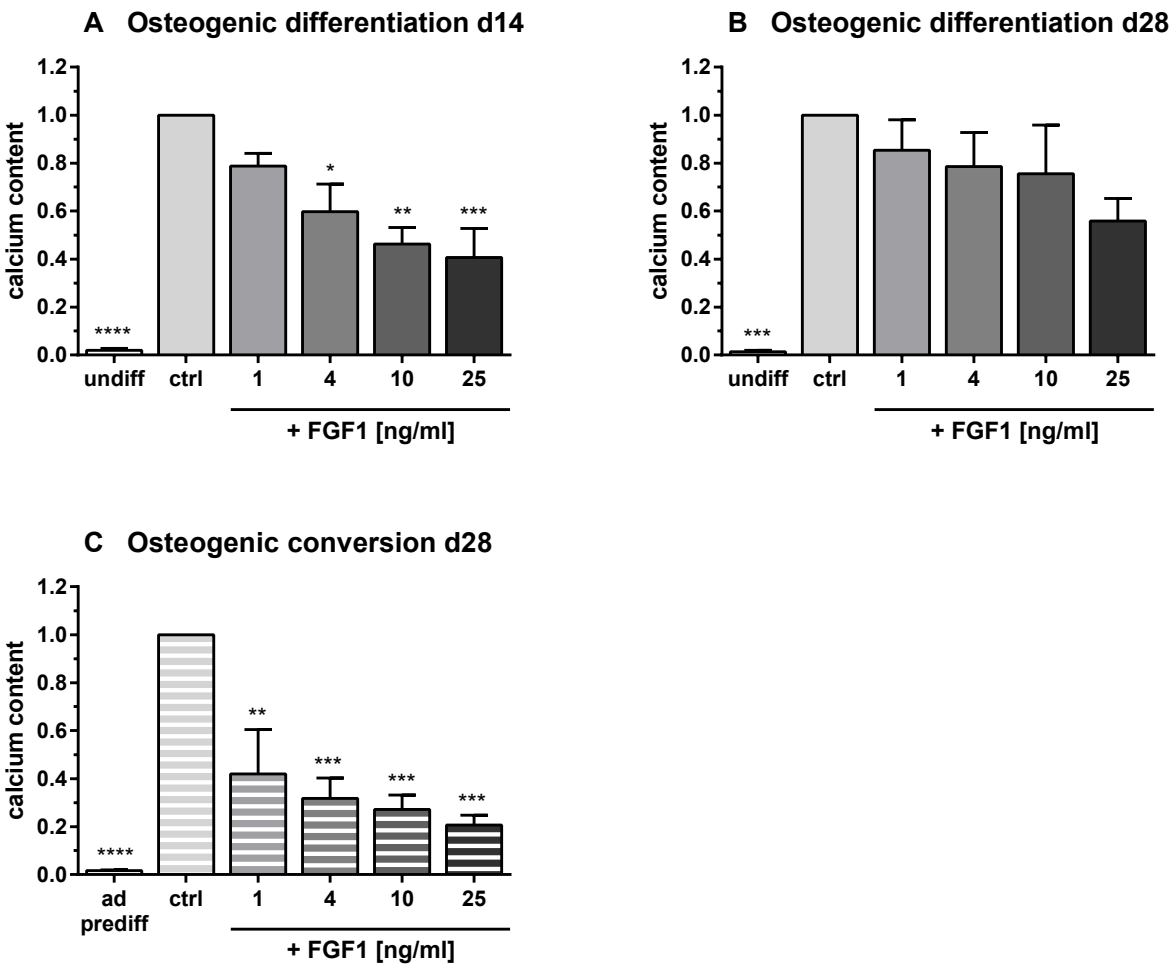

Figure 8.2: Mineralization assay during osteogenic differentiation day 14 (A) and day 28 (B) as well as osteogenic conversion (C) supplemented with different concentrations of FGF1. undiff: hBMSCs incubated in basal medium without differentiation supplements; ctrl: hBMSCs differentiated or converted in osteogenic medium without FGF1; 1 ng mL^{-1}, 4 ng mL^{-1}, 10 ng mL^{-1}, and 25 ng mL^{-1} FGF1: hBMSCs differentiated or converted in osteogenic medium supplemented with the respective FGF1 concentration; ad prediff: hBMSCs pre-differentiated in adipogenic medium for 14 days without further osteogenic conversion. Conversion samples were pre-differentiated in adipogenic medium for 14 days, then converted in osteogenic medium for another 14 days. For statistical analysis, samples were compared to the respective differentiation (ctrl, A, B) or conversion control (ctrl, C). $\tilde{x} \pm$ SEM; n = 3. * $p < 0.05$; ** $p < 0.01$; *** $p < 0.001$; **** $p < 0.0001$.

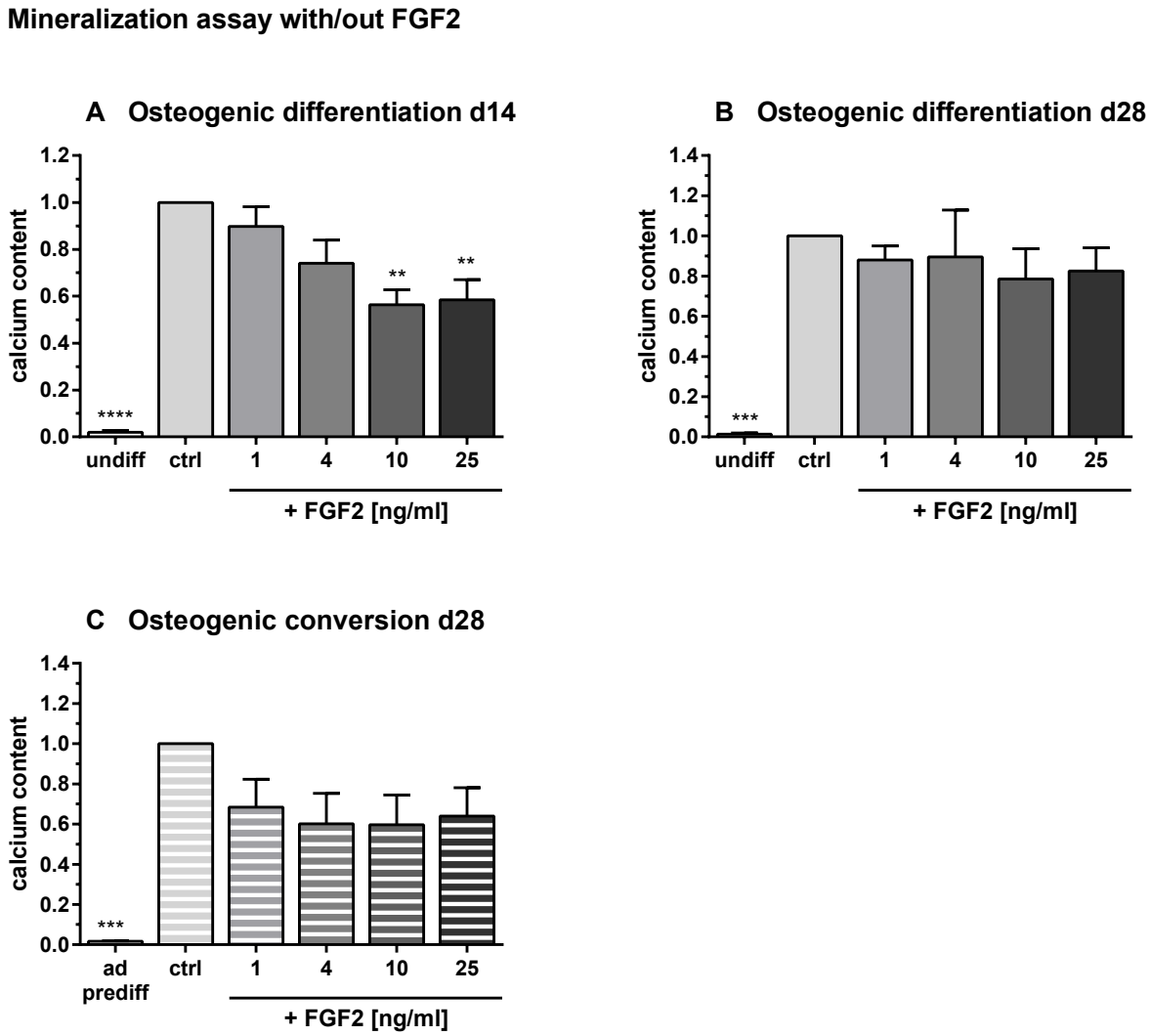

Figure 8.3: Mineralization assay during osteogenic differentiation day 14 (A) and day 28 (B) as well as osteogenic conversion (C) supplemented with different concentrations of FGF2. undiff: hBMSCs incubated in basal medium without differentiation supplements; ctrl: hBMSCs differentiated or converted in osteogenic medium without FGF2; 1 ng mL^{-1}, 4 ng mL^{-1}, 10 ng mL^{-1}, and 25 ng mL^{-1} FGF2: hBMSCs differentiated or converted in osteogenic medium supplemented with the respective FGF1 concentration; ad prediff: hBMSCs pre-differentiated in adipogenic medium for 14 days without further osteogenic conversion. Conversion samples were pre-differentiated in adipogenic medium for 14 days, then converted in osteogenic medium for another 14 days. For statistical analysis, samples were compared to the respective differentiation (ctrl, A, B) or conversion control (ctrl, C). $\tilde{x} \pm$ SEM; n = 3. ** $p < 0.01$; *** $p < 0.001$; **** $p < 0.0001$.

8.2 Gene expression and enzyme activity of ALP

Having found a reducing effect on the mineralization process of the extracellular matrix, we asked whether culture in the presence of FGF1 and FGF2 would also negatively affect ALP mRNA expression and enzyme activity during osteogenic differentiation and conversion. ALP is known to play an important role in the course of mineralization. Therefore, we pursued the corresponding mRNA expression by qPCR at day 7 and 14 for differentiation plus day 21 and 28 for conversion. Furthermore, ALP enzyme activity assays were performed on day 7 of differentiation as well as on day 21 of conversion.

8.2.1 FGF1 downregulates ALPL mRNA expression while only partly decreasing enzyme activity

The mRNA expression of the early osteogenic marker alkaline phosphatase liver, bone, kidney (ALPL) was significantly downregulated by FGF1 administration, while the associated enzyme activity was partly decreased.

The ALPL mRNA expression was significantly upregulated during osteogenic differentiation by 12.64-fold on day 7 and 13.84-fold on day 14 when compared to undifferentiated hBMSCs (Fig. 8.4 A, B, 'undiff' vs. 'ctrl'). The addition of FGF1 decreased ALPL expression. On day 7, values declined to 0.55, 0.35, and 0.36 (4 ng mL^{-1}, 10 ng mL^{-1}, and 25 ng mL^{-1} FGF1) showing high significances (Fig. 8.4 A '+FGF1'). On day 14, values declined to a minimum of 0.27 with 25 ng mL^{-1} FGF1 (Fig. 8.4 B '+FGF1'). The mRNA expression of ALPL was as well significantly upregulated during osteogenic conversion reaching fold changes of 4.76 on day 21 and 5.28 on day 28 in comparison to adipogenically pre-differentiated samples (Fig. 8.4 C, D, 'ad prediff' vs. 'ctrl'). After 21 days of osteogenic conversion, FGF1 administration downregulated ALPL expression highly significantly to 0.62, 0.57, and 0.45 for 4 ng mL^{-1}, 10 ng mL^{-1}, and 25 ng mL^{-1} FGF1 (Fig. 8.4 C '+FGF1'). After 28 days, values were markedly decreased to a minimum of 0.47 (25 ng mL^{-1} FGF1) (Fig. 8.4 D '+FGF1').

The activity of the ALP enzyme was significantly elevated at day 7 of osteogenic differentiation and increased by 4.08-fold when compared to undifferentiated hBMSCs (Fig. 8.5 A, 'undiff' vs. 'ctrl'). Furthermore, ALP enzyme activity was not markedly altered by FGF1 administration (Fig. 8.5 A, '+FGF1'). Besides, osteogenic conversion promoted ALP activity about 3.13-fold in relation to adipogenically pre-differentiated monolayers (Fig. 8.5 B, 'ad prediff' vs. 'ctrl'). During osteogenic conversion at day 21, values were significantly decreased to a minimum of 0.65 with 25 ng mL^{-1} FGF1 (Fig. 8.5 B, '+FGF1'). ALP stainings displayed a similar pattern with elevated colorimetric reaction after 14 days of osteogenic differentiation and 28 days of osteogenic conversion (Fig. 8.1 A + B, 'ALP'). Yet, lipid droplets were not completely dissolved by osteogenic conversion as observed via phase contrast microscopy and ALP staining (where lipid droplets appeared yellowish). Furthermore, FGF1 administration led to a reduced ALP staining.

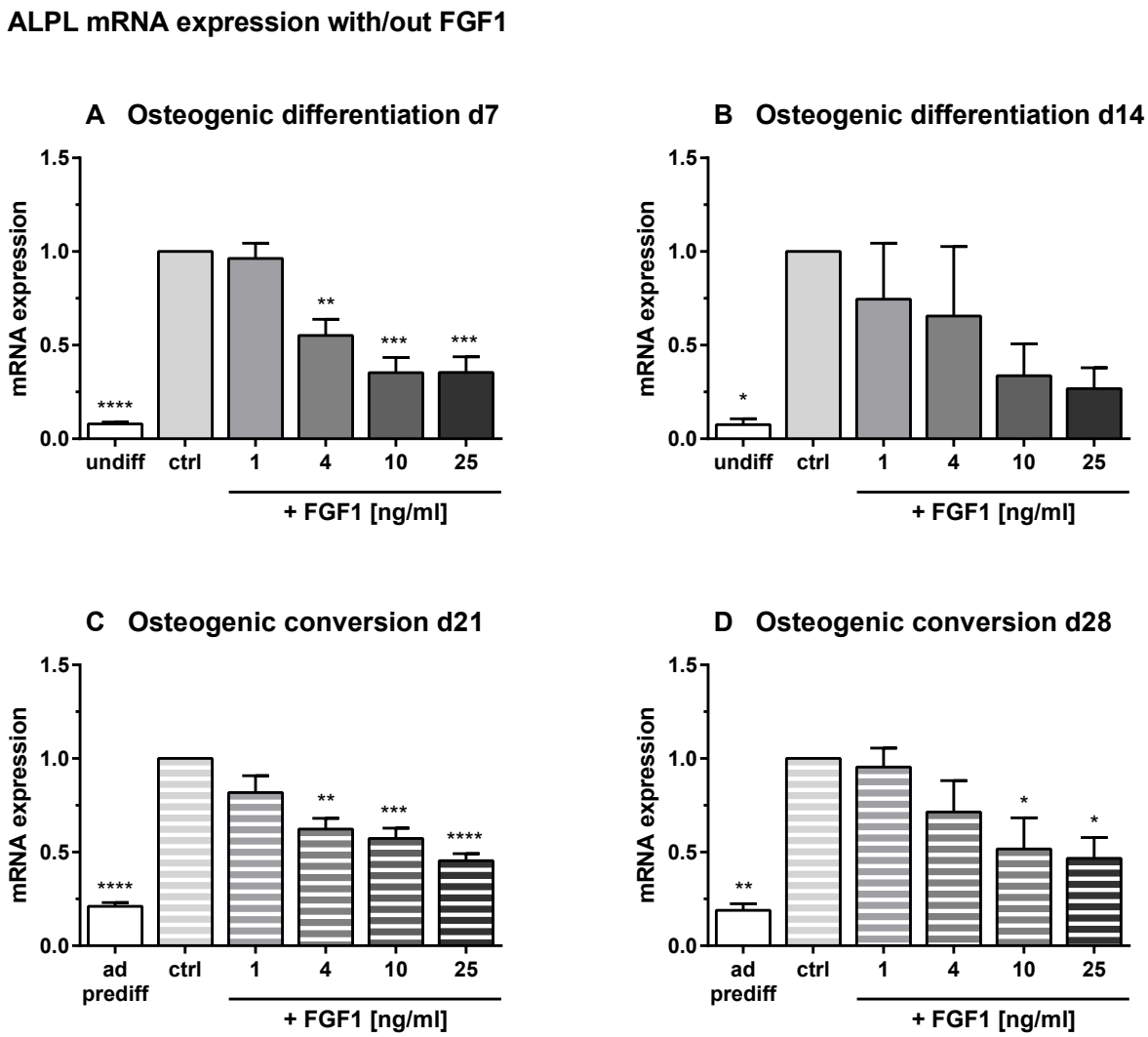

Figure 8.4: Effect of FGF1 on ALPL mRNA expression during osteogenic differentiation (day 7 (A) and 14 (B)) and conversion (day 21 (C) and 28 (D)). undiff: hBMSCs incubated in basal medium without differentiation supplements; ctrl: hBMSCs differentiated or converted in osteogenic medium without FGF1; 1 ng mL^{-1}, 4 ng mL^{-1}, 10 ng mL^{-1}, and 25 ng mL^{-1} FGF1: hBMSCs differentiated or converted in osteogenic medium supplemented with the respective FGF1 concentration; ad prediff: hBMSCs pre-differentiated in adipogenic medium for 14 days without further osteogenic conversion. Conversion samples were pre-differentiated in adipogenic medium for 14 days, then converted in osteogenic medium for another 7 or 14 days. For statistical analysis, samples were compared to the respective differentiation (ctrl, A, B) or conversion control (ctrl, C, D). $\tilde{x} \pm$ SEM; n = 3. * $p < 0.05$; ** $p < 0.01$; *** $p < 0.001$; **** $p < 0.0001$.

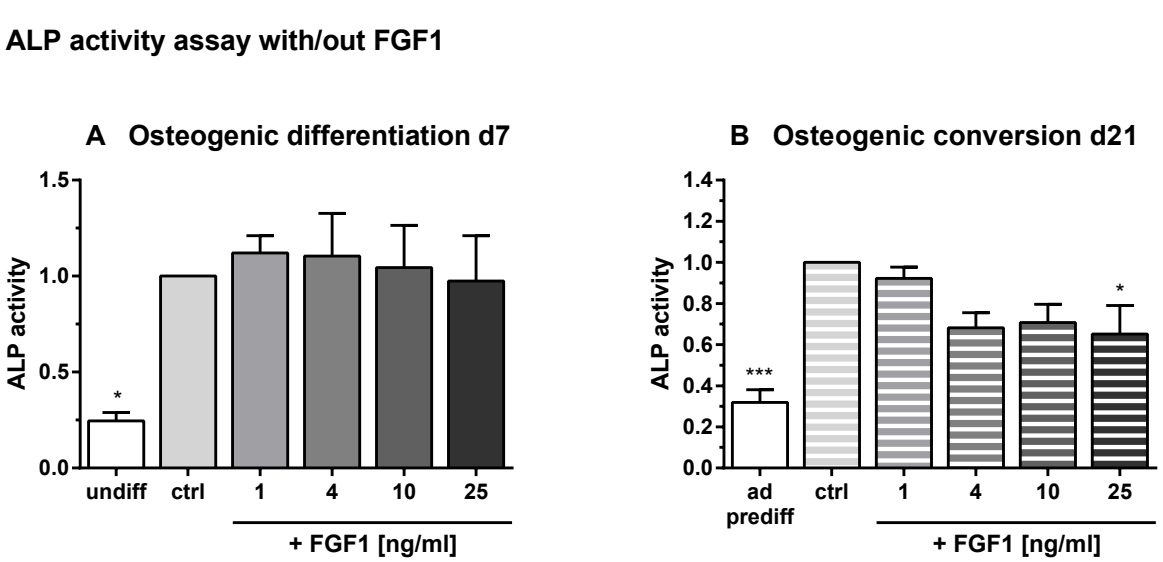

Figure 8.5: ALP activity assay during osteogenic differentiation (A) and conversion (B) supplemented with different concentrations of FGF1. undiff: hBMSCs incubated in basal medium without differentiation supplements; ctrl: hBMSCs differentiated or converted in osteogenic medium without FGF1; 1 ng mL^{-1}, 4 ng mL^{-1}, 10 ng mL^{-1}, and 25 ng mL^{-1} FGF1: hBMSCs differentiated or converted in osteogenic medium additionally supplemented with the respective FGF1 concentration; ad prediff: hBMSCs pre-differentiated in adipogenic medium for 14 days without further osteogenic conversion. Conversion samples were first pre-differentiated in adipogenic medium for 14 days, then converted in osteogenic medium for another 7 days. For statistical analysis, samples were compared to the respective differentiation (ctrl, A) or conversion control (ctrl, B). $\tilde{x} \pm$ SEM; for differentiation samples on day 7: n = 4, for conversion samples on day 21: n = 3. * $p \leq 0.05$; *** $p < 0.001$.

8.2.2 FGF2 markedly decreases ALPL mRNA expression while partly reducing associated enzyme activity

Experiments performed in parallel with FGF2 administration exhibited similar results. ALPL mRNA expression was upregulated via osteogenic differentiation by 1.84 on day 7 and 5.78 on day 14, respectively (Fig. 8.6 A, B, 'undiff' vs. 'ctrl'). The addition of FGF2 led to a marked decrease of ALPL mRNA to values of 0.52 to 0.53 with 4 ng mL^{-1}, 10 ng mL^{-1}, and 25 ng mL^{-1} FGF2 on day 7 (Fig. 8.6 A '+FGF2'). On day 14, ALPL mRNA expression was downregulated to a minimum of 0.42 by 4 ng mL^{-1} FGF2 (Fig. 8.6 B '+FGF2'). The osteogenic conversion resulted in an increase of ALPL expression with fold changes of 2.08 on day 21 and 2.19 on day 28 when compared to adipogenically pre-differentiated hBMSCs (Fig. 8.6 C, D, 'ad prediff' vs. 'ctrl'). On day 21, a marked downregulation was observed due to FGF2 administration with a minimum of 0.58 for the highest concentration (Fig. 8.6 C '+FGF2'). After 28 days of osteogenic conversion, ALPL values declined to 0.44 for 25 ng mL^{-1} FGF2 (Fig. 8.6 D '+FGF2').

Following osteogenic differentiation and conversion, ALP enzyme activity was increased by 5.74 (day 7) and 3.13 (day 21), respectively (Fig. 8.7 A, 'undiff' vs. 'ctrl' and B, 'ad prediff' vs. 'ctrl'). During osteogenic differentiation, ALP activity was not markedly altered by FGF2 addition (Fig. 8.7 A '+FGF2'). However, on day 21 of osteogenic conversion, ALP activity was reduced to 0.64 and 0.75 by 10 ng mL^{-1} and 25 ng mL^{-1} FGF2, respectively (Fig. 8.7 B '+FGF2'). Besides, FGF2 administration led to a reduced ALP staining during differentiation and conversion (Fig. 8.1 A + B, 'ALP').

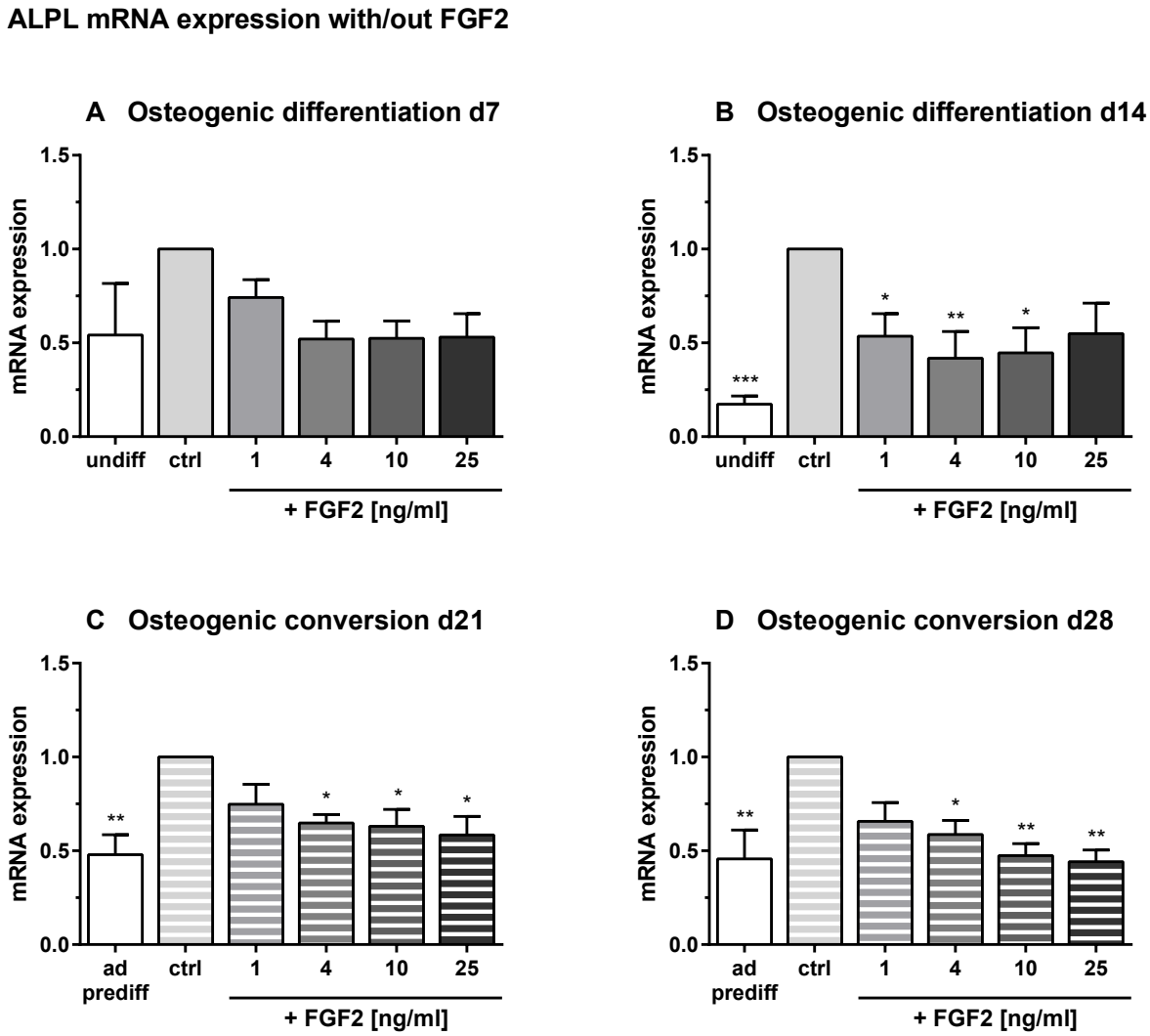

Figure 8.6: Effect of FGF2 on ALPL mRNA expression during osteogenic differentiation (day 7 (A) and 14 (B)) and conversion (day 21 (C) and 28 (D)). undiff: hBMSCs incubated in basal medium without differentiation supplements; ctrl: hBMSCs differentiated or converted in osteogenic medium without FGF2; 1 ng mL^{-1}, 4 ng mL^{-1}, 10 ng mL^{-1}, and 25 ng mL^{-1} FGF2: hBMSCs differentiated or converted in osteogenic medium supplemented with the respective FGF1 concentration; ad prediff: hBMSCs pre-differentiated in adipogenic medium for 14 days without further osteogenic conversion. Conversion samples were pre-differentiated in adipogenic medium for 14 days, then converted in osteogenic medium for another 7 or 14 days. For statistical analysis, samples were compared to the respective differentiation (ctrl, A, B) or conversion control (ctrl, C, D). $\tilde{x} \pm$ SEM; n = 4. * $p < 0.05$; ** $p < 0.01$; *** $p < 0.001$.

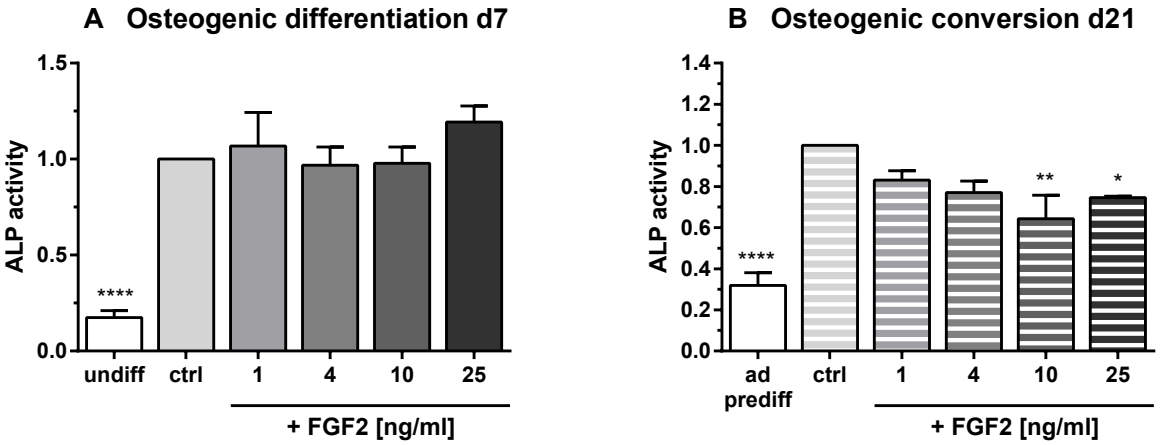

Figure 8.7: ALP activity assay during osteogenic differentiation (A) and conversion (B) supplemented with different concentrations of FGF2. undiff: hBMSCs incubated in basal medium without differentiation supplements; ctrl: hBMSCs differentiated or converted in osteogenic medium without FGF2; 1 ng mL^{-1}, 4 ng mL^{-1}, 10 ng mL^{-1}, and 25 ng mL^{-1} FGF2: hBMSCs differentiated or converted in osteogenic medium supplemented with the respective FGF2 concentration; ad prediff: hBMSCs pre-differentiated in adipogenic medium for 14 days without further osteogenic conversion. Conversion samples were pre-differentiated in adipogenic medium for 14 days, then converted in osteogenic medium for another 7 days. For statistical analysis, samples were compared to the respective differentiation (ctrl, A) or conversion control (ctrl, B). $\tilde{x} \pm$ SEM; n = 4. * $p < 0.05$; ** $p < 0.01$; **** $p < 0.0001$.

8.3 Early osteogenic marker gene expression

The reduction in mineralization induced by the culture in the presence of FGF1 and FGF2 addition prompted us to gain deeper insight into the mRNA expression of different subsets of osteogenic markers in the process of osteogenic differentiation and conversion. To analyze the early osteogenic marker genes RUNX2 and BMP4, hBMSCs were osteogenically differentiated or converted under the addition of different FGF1 and FGF2 concentrations. RNA samples were harvested on day 7 and 14 (differentiation) as well as on day 21 and 28 (conversion) to examine mRNA expression throughout the course of osteogenic differentiation and conversion.

8.3.1 FGF1 downregulates RUNX2 and BMP4 expression

The early master regulator of osteogenesis RUNX2 was in part downregulated by FGF1 addition. A slight, although non-significant downregulation was observed only for the higher FGF1 concentrations on day 7 of osteogenic differentiation (Fig. 8.8 A '+FGF1'). However, on day 14, RUNX2 expression was significantly downregulated in a concentration-dependent manner to a minimum of 0.40 with 25 ng mL^{-1} FGF1 (Fig. 8.8 B '+FGF1').

The osteogenic conversion displayed a similar course. On day 21, RUNX2 expression was downregulated to a minimum of 0.55 (25 ng mL^{-1}) (Fig. 8.8 C '+FGF1'). This decrease reached significance on day 28, showing a relative expression of 0.49 (25 ng mL^{-1}) (Fig. 8.8 D '+FGF1').

The mRNA expression of BMP4 was significantly downregulated by FGF1 on day 7 of osteogenic differentiation to values of 0.53 to 0.49 for 4 ng mL^{-1}, 10 ng mL^{-1}, and 25 ng mL^{-1} FGF1 (Fig. 8.9 A '+FGF1'). During osteogenic conversion, values declined significantly to 0.57 and 0.55 with 4 ng mL^{-1} and 25 ng mL^{-1} (Fig. 8.9 C '+FGF1'). Nevertheless, on day 14 of differentiation as well as on day 28 of conversion, no marked reduction in gene expression could be detected (Fig. 8.9 B, D '+FGF1').

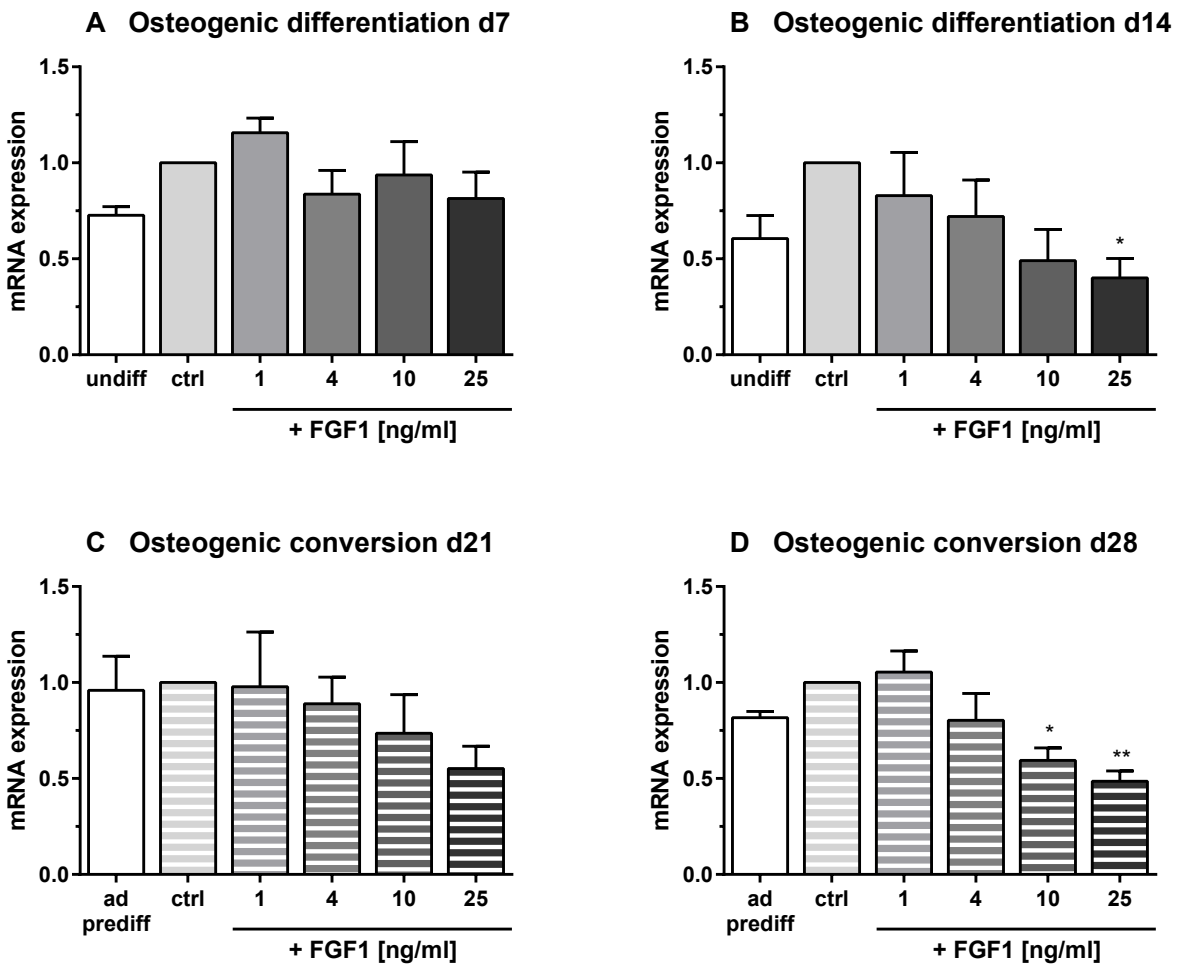

Figure 8.8: Effect of FGF1 on RUNX2 mRNA expression during osteogenic differentiation (day 7 (A) and 14 (B)) and conversion (day 21 (C) and 28 (D)). undiff: hBMSCs incubated in basal medium without differentiation supplements; ctrl: hBMSCs differentiated or converted in osteogenic medium without FGF1; 1 ng mL^{-1}, 4 ng mL^{-1}, 10 ng mL^{-1}, and 25 ng mL^{-1} FGF1: hBMSCs differentiated or converted in osteogenic medium supplemented with the respective FGF1 concentration; ad prediff: hBMSCs pre-differentiated in adipogenic medium for 14 days without further osteogenic conversion. Conversion samples were pre-differentiated in adipogenic medium for 14 days, then converted in osteogenic medium for another 7 or 14 days. For statistical analysis, samples were compared to the respective differentiation (ctrl, A, B) or conversion control (ctrl, C, D). $\tilde{x} \pm$ SEM; n = 4. * $p < 0.05$; ** $p < 0.01$.

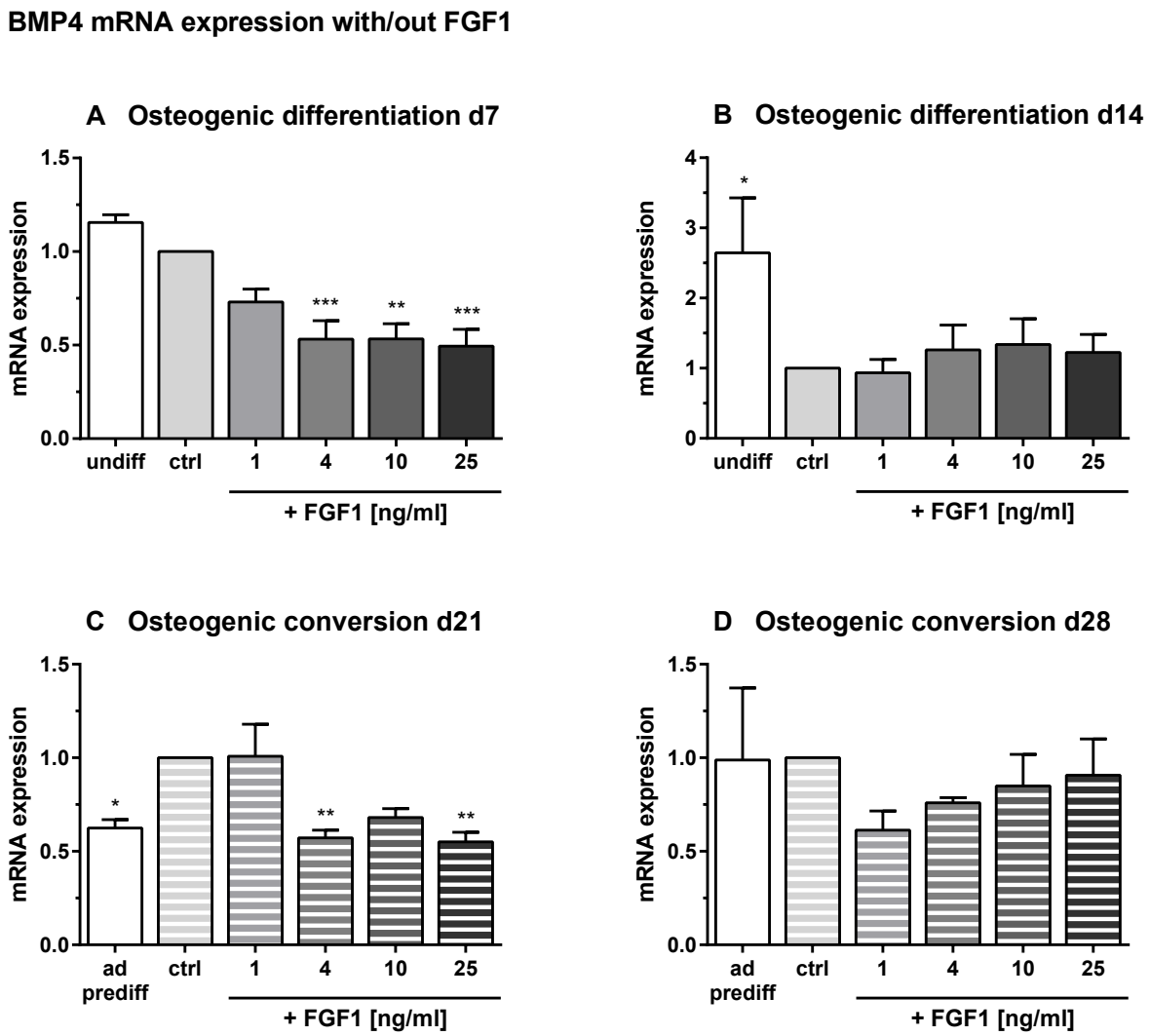

Figure 8.9: Effect of FGF1 on BMP4 mRNA expression during osteogenic differentiation (day 7 (A) and 14 (B)) and conversion (day 21 (C) and 28 (D)). undiff: hBMSCs incubated in basal medium without differentiation supplements; ctrl: hBMSCs differentiated or converted in osteogenic medium without FGF1; 1 ng mL^{-1}, 4 ng mL^{-1}, 10 ng mL^{-1}, and 25 ng mL^{-1} FGF1: hBMSCs differentiated or converted in osteogenic medium supplemented with the respective FGF1 concentration; ad prediff: hBMSCs pre-differentiated in adipogenic medium for 14 days without further osteogenic conversion. Conversion samples were pre-differentiated in adipogenic medium for 14 days, then converted in osteogenic medium for another 7 or 14 days. For statistical analysis, samples were compared to the respective differentiation (ctrl, A, B) or conversion control (ctrl, C, D). $\tilde{x} \pm$ SEM; differentiation samples: n = 4; conversion samples: n = 3. * $p < 0.05$; ** $p < 0.01$; *** $p < 0.001$.

8.3.2 FGF2 reduces RUNX2 and BMP4 expression

The addition of FGF2 exhibited similar results to the observations during FGF1 administration. RUNX2 expression decreased during differentiation and conversion (day 14 and day 28) with significant values of 0.45 and 0.55 for 25 ng mL^{-1} FGF2 (Fig. 8.10 B, D '+FGF2'). Interestingly, an upregulation to a maximum of 2.02 was observed on day 7 of osteogenic differentiation by the lower FGF2 concentrations (Fig. 8.10 A '+FGF2').

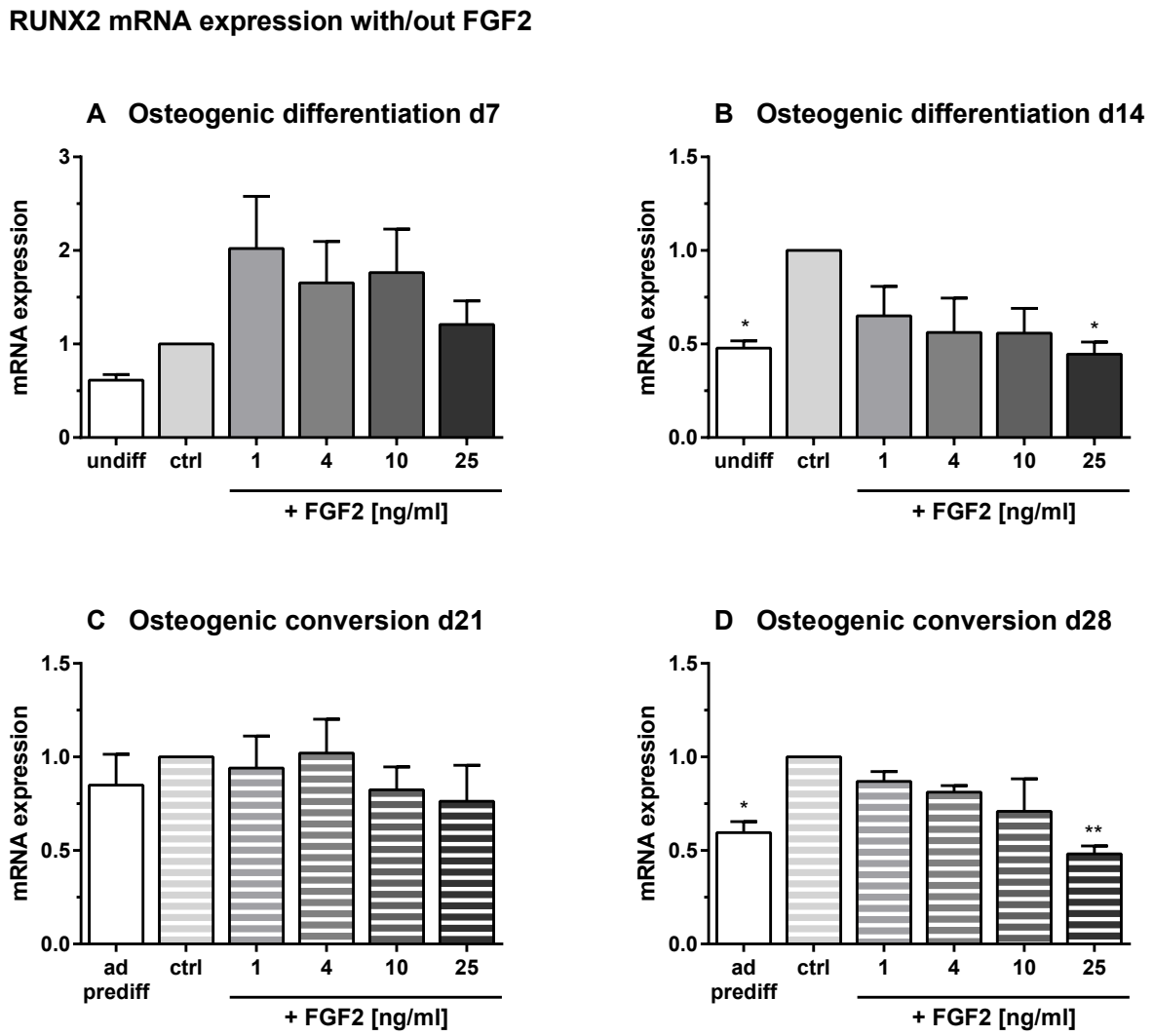

Figure 8.10: Effect of FGF2 on RUNX2 mRNA expression during osteogenic differentiation (day 7 (A) and 14 (B)) and conversion (day 21 (C) and 28 (D)). undiff: hBMSCs incubated in basal medium without differentiation supplements; ctrl: hBMSCs differentiated or converted in osteogenic medium without FGF2; 1 ng mL^{-1}, 4 ng mL^{-1}, 10 ng mL^{-1}, and 25 ng mL^{-1} FGF2: hBMSCs differentiated or converted in osteogenic medium supplemented with the respective FGF2 concentration; ad prediff: hBMSCs pre-differentiated in adipogenic medium for 14 days without further osteogenic conversion. Conversion samples were pre-differentiated in adipogenic medium for 14 days, then converted in osteogenic medium for another 7 or 14 days. For statistical analysis, samples were compared to the respective differentiation (ctrl, A, B) or conversion control (ctrl, C, D). $\tilde{x} \pm$ SEM; n = 4. * $p < 0.05$; ** $p < 0.01$.

The mRNA expression of BMP4 was reduced by FGF2 administration. The downregulation was most pronounced after osteogenic conversion on day 21, declining to 0.44 for 10 ng mL^{-1} (Fig. 8.11 C '+FGF2'). Moreover, values were reduced during later stages of conversion and after 7 days of osteogenic differentiation (Fig. 8.11 A, D '+FGF2').

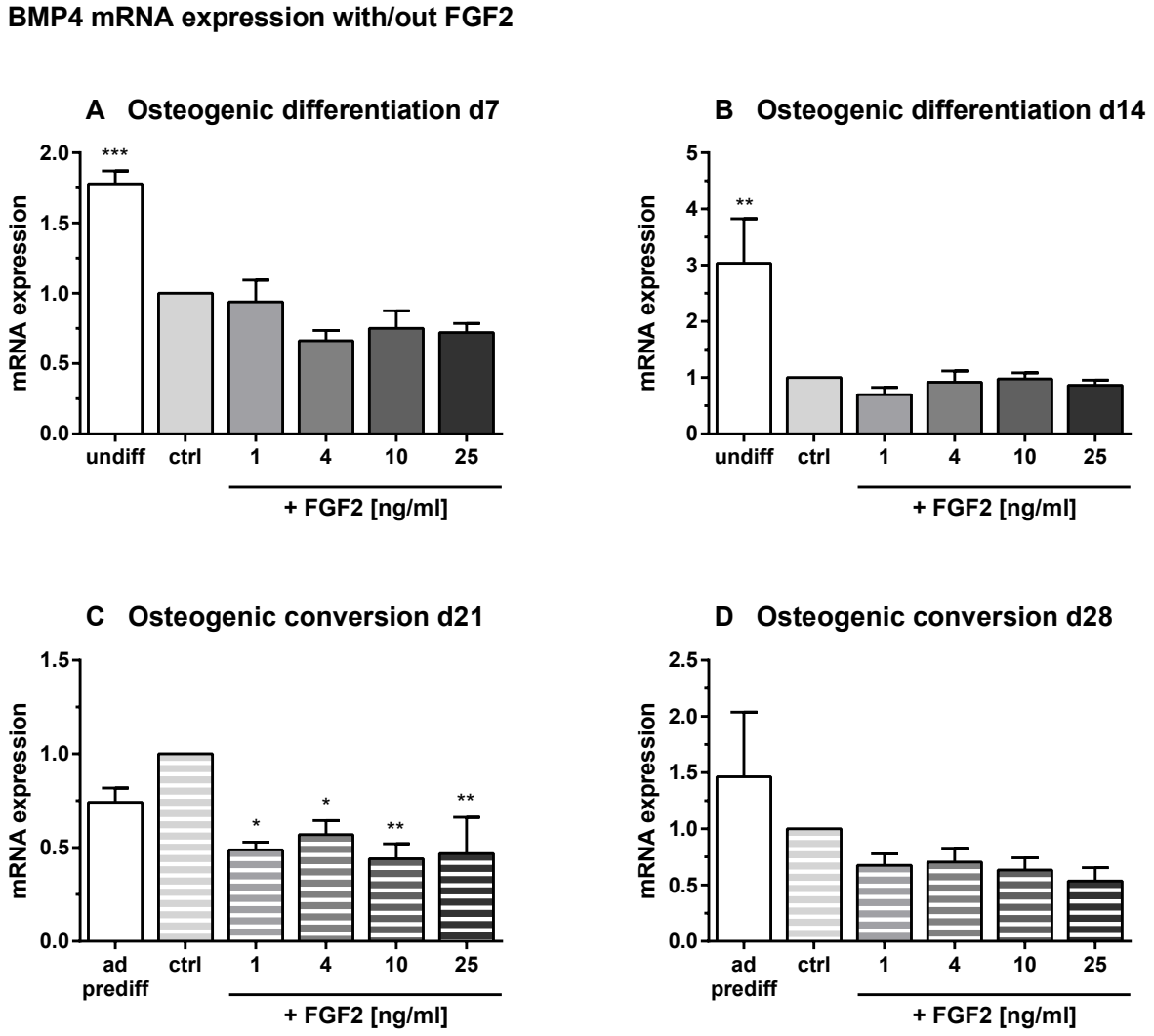

Figure 8.11: Effect of FGF2 on BMP4 mRNA expression during osteogenic differentiation (day 7 (A) and 14 (B)) and conversion (day 21 (C) and 28 (D)). undiff: hBMSCs incubated in basal medium without differentiation supplements; ctrl: hBMSCs differentiated or converted in osteogenic medium without FGF2; 1 ng mL^{-1}, 4 ng mL^{-1}, 10 ng mL^{-1}, and 25 ng mL^{-1} FGF2: hBMSCs differentiated or converted in osteogenic medium supplemented with the respective FGF2 concentration; ad prediff: hBMSCs pre-differentiated in adipogenic medium for 14 days without further osteogenic conversion. Conversion samples were pre-differentiated in adipogenic medium for 14 days, then converted in osteogenic medium for another 7 or 14 days. For statistical analysis, samples were compared to the respective differentiation (ctrl, A, B) or conversion control (ctrl, C, D). $\tilde{x} \pm$ SEM; n = 4, except for conversion on day 21: n = 3. * $p < 0.05$; ** $p < 0.01$; *** $p < 0.001$.

8.4 Later marker genes of osteogenesis

After having analyzed the expression of the early osteogenic markers, we aimed for examining the effects of FGF1 and FGF2 on later osteogenic marker genes responsible for bone matrix formation. Therefore, COL1A1, integrin-binding sialoprotein (IBSP), and OC were investigated during osteogenic differentiation and conversion.

8.4.1 FGF1 strongly downregulates COL1A1 and IBSP expression while mildly augmenting OC expression

The expression of COL1A1 was markedly decreased during the course of osteogenic differentiation and conversion. Intensifying with FGF1 concentration, COL1A1 mRNA expression descended down to 0.09 (day 7 and day 14 of differentiation, day 21 of conversion) for $25\,\mathrm{ng\,mL^{-1}}$, reaching high significances for days 7 and 21 (Fig. 8.12 A, B, C '+FGF1'). Furthermore, COL1A1 expression declined to a minimum of 0.20 on day 28 of conversion with $10\,\mathrm{ng\,mL^{-1}}$ FGF1 (Fig. 8.12 D '+FGF1').

The expression of the later osteogenic marker IBSP was downregulated by FGF1 administration. A marked decrease was observed through all stages of the differentiation and conversion process. After 7 days of osteogenic differentiation, the values declined to 0.16 (with $10\,\mathrm{ng\,mL^{-1}}$ and $25\,\mathrm{ng\,mL^{-1}}$) (Fig. 8.13 A '+FGF1'). On day 14, reductions were highly significant and reached 0.37 ($1\,\mathrm{ng\,mL^{-1}}$), 0.12 ($4\,\mathrm{ng\,mL^{-1}}$), and finally 0.05 (for $10\,\mathrm{ng\,mL^{-1}}$ and $25\,\mathrm{ng\,mL^{-1}}$) (Fig. 8.13 B '+FGF1'). After 21 days of osteogenic conversion, IBSP mRNA expression significantly decreased to 0.22 ($10\,\mathrm{ng\,mL^{-1}}$) and 0.15 ($25\,\mathrm{ng\,mL^{-1}}$) (Fig. 8.13 C '+FGF1'). On day 28, the expression was further reduced to 0.10 ($10\,\mathrm{ng\,mL^{-1}}$) and 0.09 ($25\,\mathrm{ng\,mL^{-1}}$) (Fig. 8.13 D '+FGF1').

The mRNA expression of another late osteogenic marker gene, OC, was not markedly reduced via FGF1 addition. After 7 days of osteogenic differentiation, relative gene expression values slightly declined to 0.49 with $25\,\mathrm{ng\,mL^{-1}}$ but did not reach significance (Fig. 8.14 A '+FGF1'). However, this inhibitory trend was not observed during the other time points. On day 14, OC gene expression increased from 2.3 to 2.6 for $4\,\mathrm{ng\,mL^{-1}}$ to $25\,\mathrm{ng\,mL^{-1}}$ FGF1 (Fig. 8.14 B '+FGF1'). Furthermore, a slight upregulation of OC expression was observed after 21 days of osteogenic conversion with an increase of up to 1.31 with $10\,\mathrm{ng\,mL^{-1}}$ FGF1 (Fig. 8.14 C '+FGF1'). Besides, values were augmented during osteogenic conversion on day 28 from 2.14 up to 2.41 for $4\,\mathrm{ng\,mL^{-1}}$ to $25\,\mathrm{ng\,mL^{-1}}$ (Fig. 8.14 D '+FGF1').

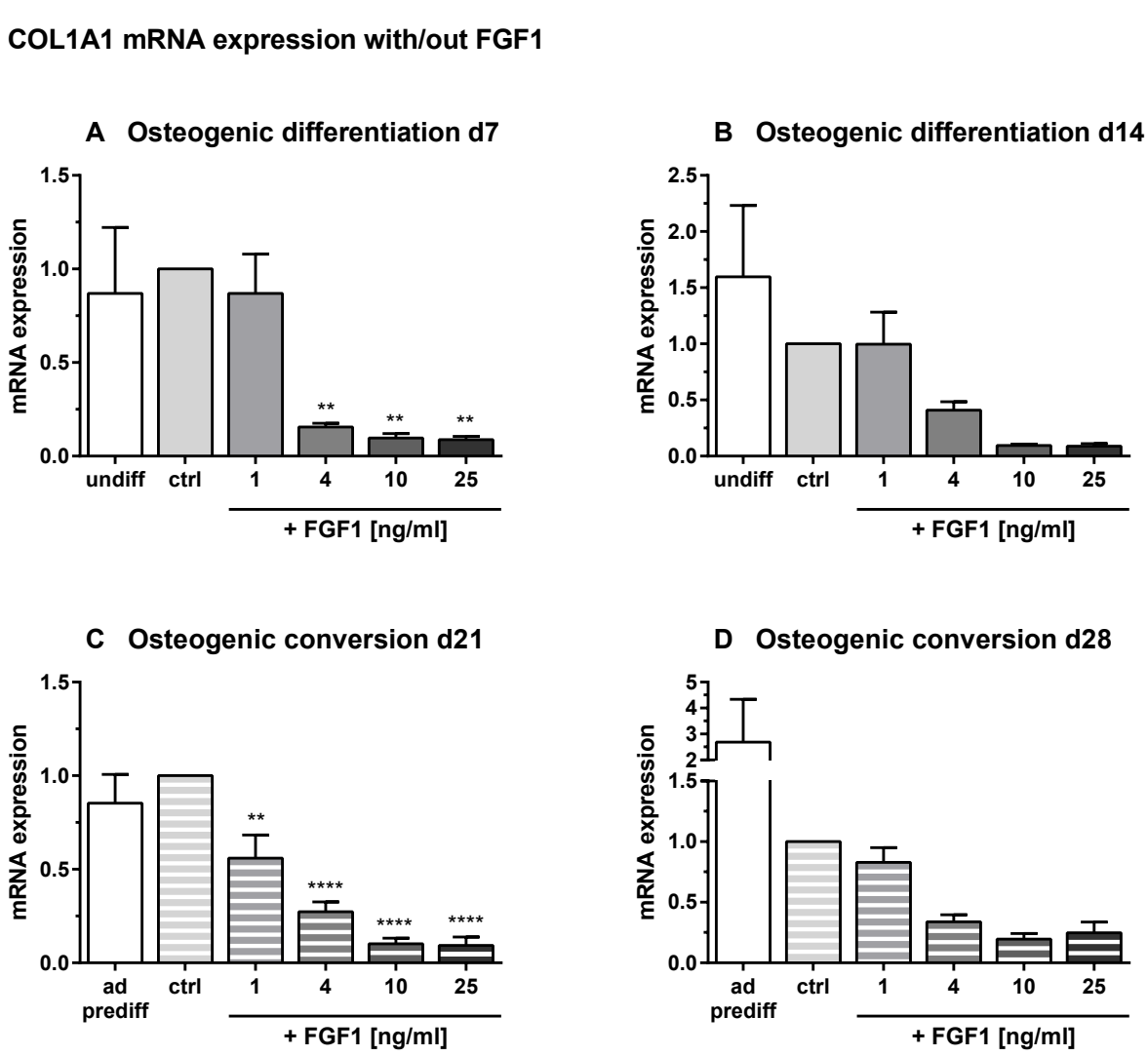

Figure 8.12: Effect of FGF1 on COL1A1 mRNA expression during osteogenic differentiation (day 7 (A) and 14 (B)) and conversion (day 21 (C) and 28 (D)). undiff: hBMSCs incubated in basal medium without differentiation supplements; ctrl: hBMSCs differentiated or converted in osteogenic medium without FGF1; 1 ng mL^{-1}, 4 ng mL^{-1}, 10 ng mL^{-1}, and 25 ng mL^{-1} FGF1: hBMSCs differentiated or converted in osteogenic medium supplemented with the respective FGF1 concentration; ad prediff: hBMSCs pre-differentiated in adipogenic medium for 14 days without further osteogenic conversion. Conversion samples were pre-differentiated in adipogenic medium for 14 days, then converted in osteogenic medium for another 7 or 14 days. For statistical analysis, samples were compared to the respective differentiation (ctrl, A, B) or conversion control (ctrl, C, D). $\tilde{x} \pm$ SEM; n = 4. ** $p < 0.01$; **** $p < 0.0001$.

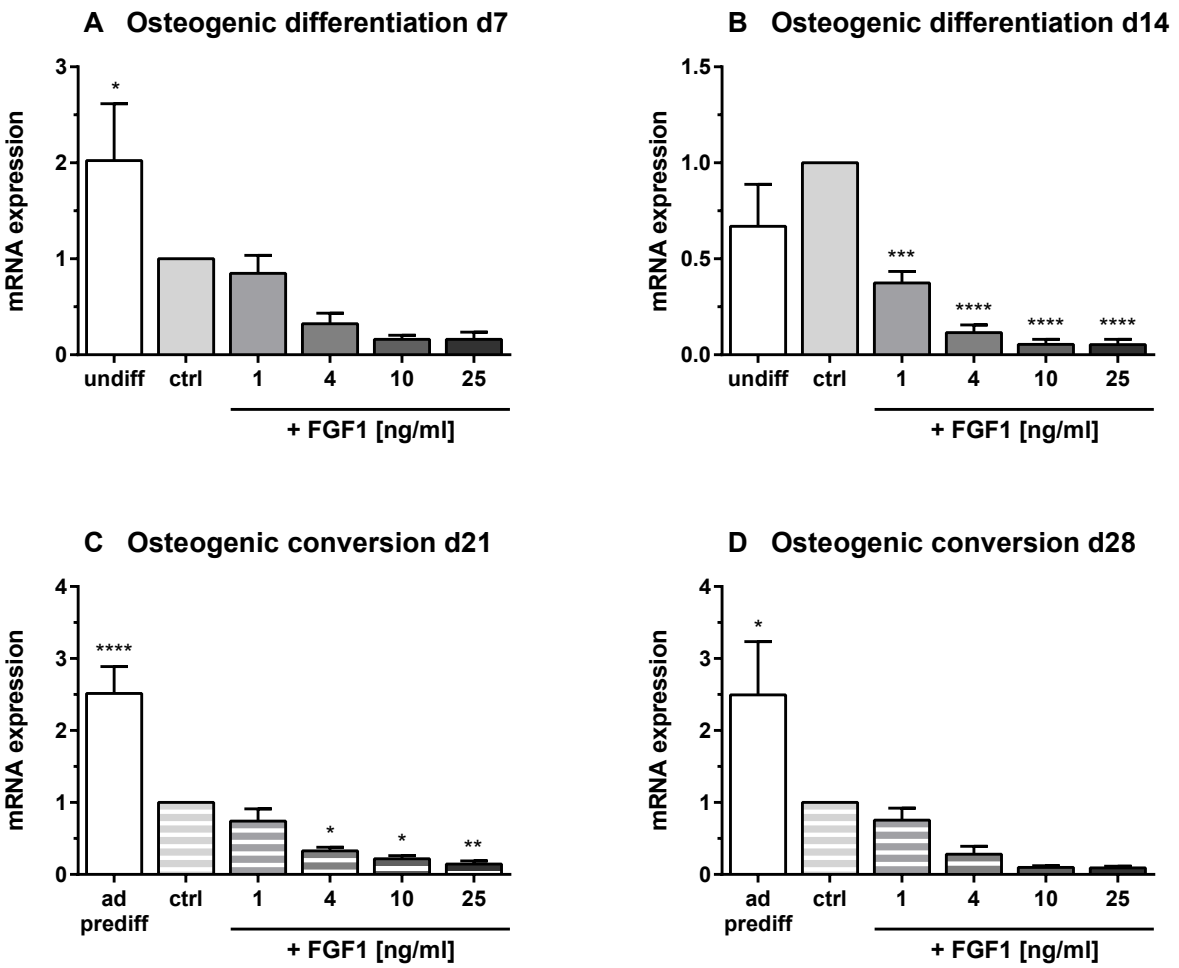

Figure 8.13: Effect of FGF1 on IBSP mRNA expression during osteogenic differentiation (day 7 (A) and 14 (B)) and conversion (day 21 (C) and 28 (D)). undiff: hBMSCs incubated in basal medium without differentiation supplements; ctrl: hBMSCs differentiated or converted in osteogenic medium without FGF1; 1 ng mL^{-1}, 4 ng mL^{-1}, 10 ng mL^{-1}, and 25 ng mL^{-1} FGF1: hBMSCs differentiated or converted in osteogenic medium supplemented with the respective FGF1 concentration; ad prediff: hBMSCs pre-differentiated in adipogenic medium for 14 days without further osteogenic conversion. Conversion samples were pre-differentiated in adipogenic medium for 14 days, then converted in osteogenic medium for another 7 or 14 days . For statistical analysis, samples were compared to the respective differentiation (ctrl, A, B) or conversion control (ctrl, C, D). $\tilde{x} \pm$ SEM; n = 4. * $p < 0.05$; ** $p < 0.01$; *** $p < 0.001$; **** $p < 0.0001$.

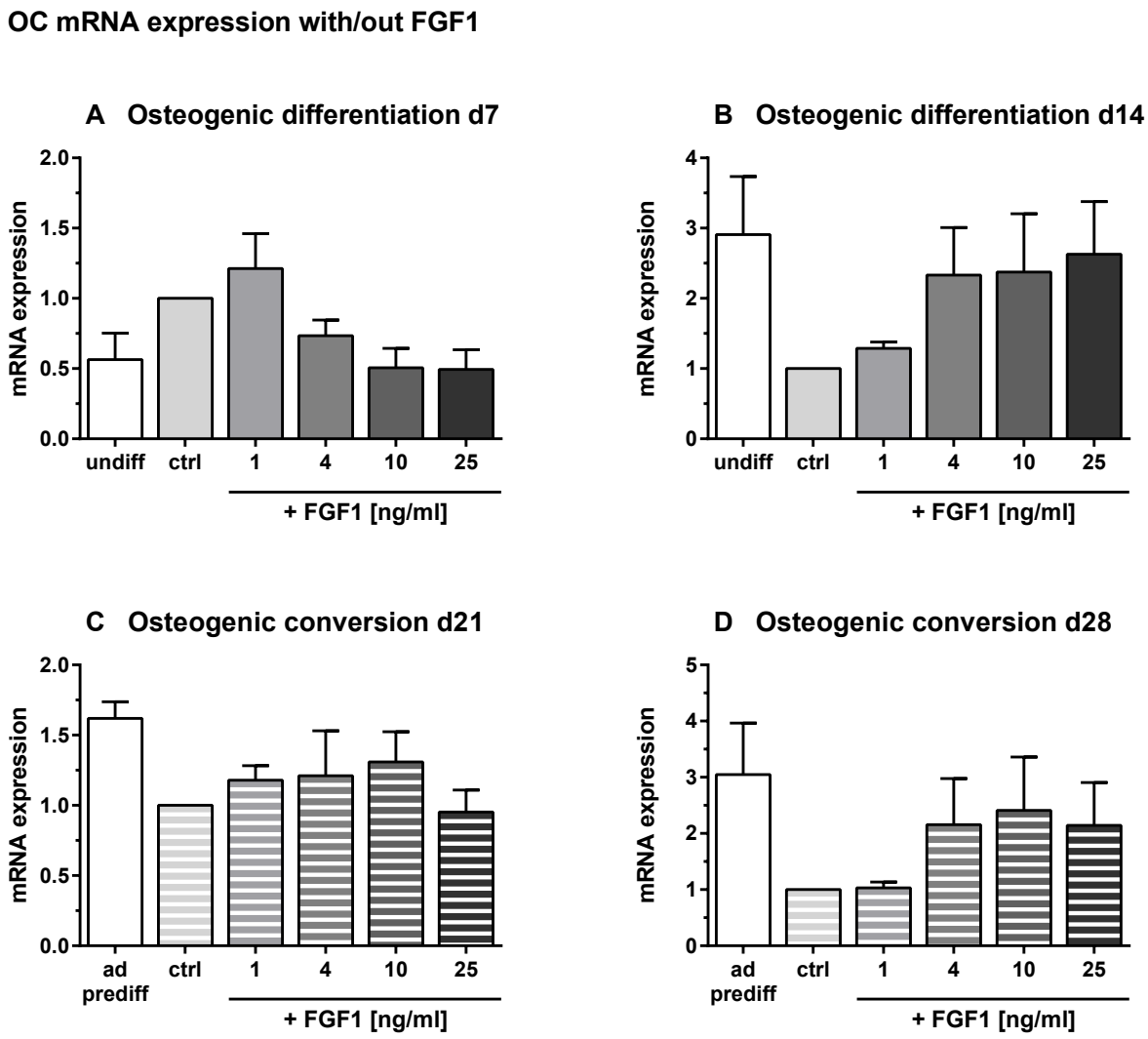

Figure 8.14: Effect of FGF1 on OC mRNA expression during osteogenic differentiation (day 7 (A) and 14 (B)) and conversion (day 21 (C) and 28 (D)). undiff: hBMSCs incubated in basal medium without differentiation supplements; ctrl: hBMSCs differentiated or converted in osteogenic medium without FGF1; 1 ng mL^{-1}, 4 ng mL^{-1}, 10 ng mL^{-1}, and 25 ng mL^{-1} FGF1: hBMSCs differentiated or converted in osteogenic medium supplemented with the respective FGF1 concentration; ad prediff: hBMSCs pre-differentiated in adipogenic medium for 14 days without further osteogenic conversion. Conversion samples were pre-differentiated in adipogenic medium for 14 days, then converted in osteogenic medium for another 7 or 14 days. For statistical analysis, samples were compared to the respective differentiation (ctrl, A, B) or conversion control (ctrl, C, D). $\tilde{x} \pm$ SEM; n = 4.

8.4.2 FGF2 markedly downregulates COL1A1 and IBSP while only slightly upregulating OC

The administration of FGF2 exhibited mostly inhibitory effects on mRNA expression of later osteogenic marker genes. After 7 days of differentiation, relative expression values of COL1A1 highly significantly declined to 0.55, 0.41, and 0.34 by 4 ng mL^{-1}, 10 ng mL^{-1}, and 25 ng mL^{-1} FGF2 (Fig. 8.15 A (Fig. 8.14 D '+FGF2'). On day 14, the values further declined to a minimum of 0.15 with 25 ng mL^{-1} FGF2 (Fig. 8.15 B '+FGF2').

Downregulations during osteogenic conversion on day 21 were highly significant with values of 0.37, 0.29, and 0.27 for 4 ng mL^{-1}, 10 ng mL^{-1}, and 25 ng mL^{-1} (Fig. 8.15 C '+FGF2'). After 28 days, COL1A1 expression declined to 0.23 and 0.18 with 10 ng mL^{-1} and 25 ng mL^{-1} FGF2 (Fig. 8.15 D '+FGF2').

In parallel, the values of relative IBSP mRNA expression decreased. After 7 days of osteogenic differentiation, expression was reduced to 0.18 and 0.07 (10 ng mL^{-1} and 25 ng mL^{-1}) (Fig. 8.16 A '+FGF2'). Moreover, on day 14, relative IBSP values highly significantly declined to 0.41, 0.17, 0.07, and 0.04 for 1 ng mL^{-1}, 4 ng mL^{-1}, 10 ng mL^{-1}, and 25 ng mL^{-1} (Fig. 8.16 B '+FGF2'). During conversion on day 21, IBSP expression decreased from 0.41 to 0.15 down to 0.19 (4 ng mL^{-1}, 10 ng mL^{-1}, and 25 ng mL^{-1} FGF2) (Fig. 8.16 C '+FGF2'). After 28 days, the inhibitory effects increased and the relative expression declined to 0.06 and 0.03 for 10 ng mL^{-1} and 25 ng mL^{-1} FGF2 (Fig. 8.16 D '+FGF2').

In contrast to COL1A1 and IBSP, OC expression was enhanced through FGF2 administration. At the earlier time points of differentiation and conversion (day 7 and 21), OC expression was augmented up to 1.51 and 1.53 by 25 ng mL^{-1} (Fig. 8.17 A, C '+FGF2'). After 14 days of differentiation, values reached 2.37 and 2.31 with 10 ng mL^{-1} and 25 ng mL^{-1} (Fig. 8.17 B '+FGF2'). In addition, OC expression increased to 1.53 and 1.65 for day 28 of conversion (Fig. 8.17 D '+FGF2').

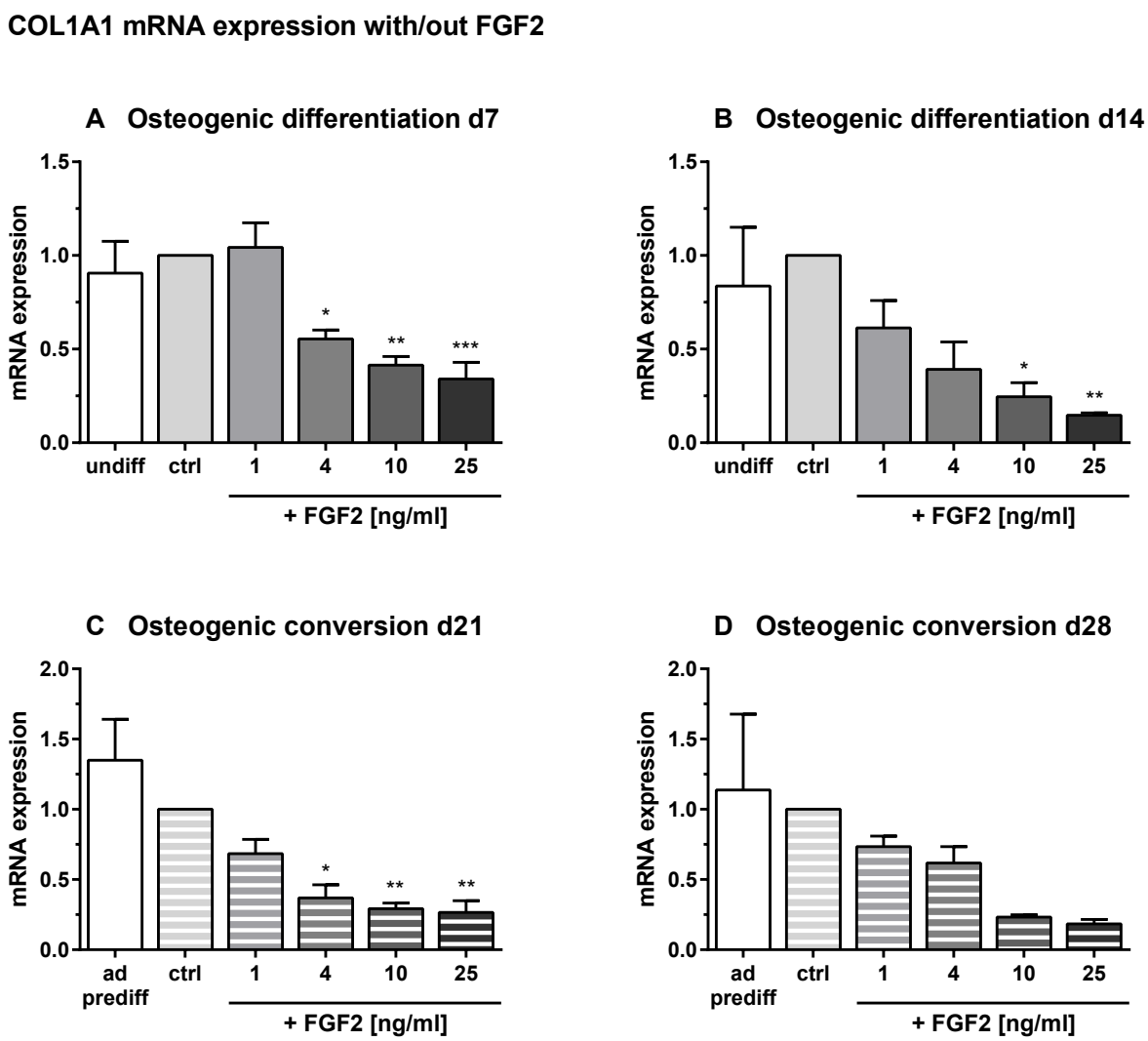

Figure 8.15: Effect of FGF2 on COL1A1 mRNA expression during osteogenic differentiation (day 7 (A) and 14 (B)) and conversion (day 21 (C) and 28 (D)). undiff: hBMSCs incubated in basal medium without differentiation supplements; ctrl: hBMSCs differentiated or converted in osteogenic medium without FGF2; 1 ng mL^{-1}, 4 ng mL^{-1}, 10 ng mL^{-1}, and 25 ng mL^{-1} FGF2: hBMSCs differentiated or converted in osteogenic medium supplemented with the respective FGF2 concentration; ad prediff: hBMSCs pre-differentiated in adipogenic medium for 14 days without further osteogenic conversion. Conversion samples were pre-differentiated in adipogenic medium for 14 days, then converted in osteogenic medium for another 7 or 14 days. For statistical analysis, samples were compared to the respective differentiation (ctrl, A, B) or conversion control (ctrl, C, D). $\tilde{x} \pm$ SEM; n = 4. * $p < 0.05$; ** $p < 0.01$; *** $p < 0.001$.

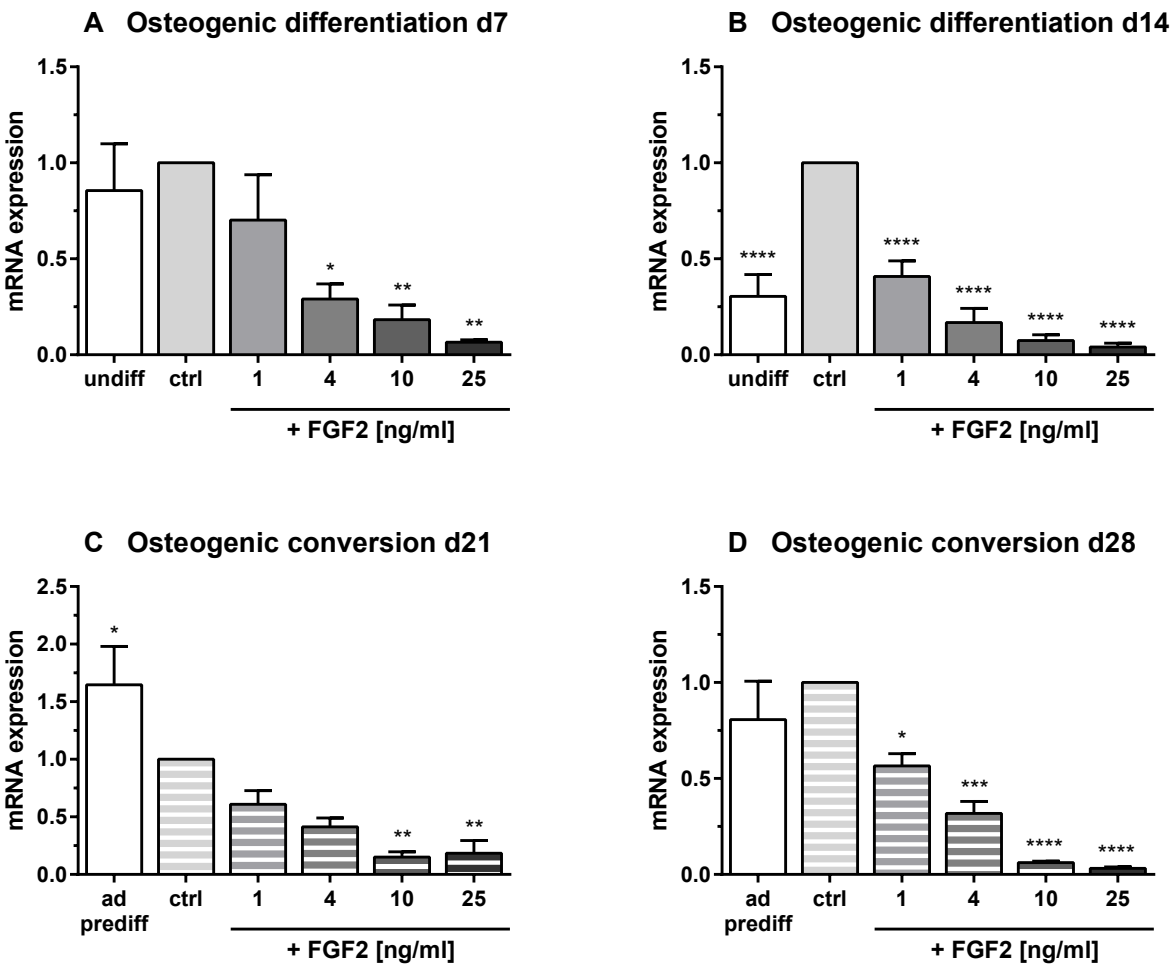

Figure 8.16: Effect of FGF2 on IBSP mRNA expression during osteogenic differentiation (day 7 (A) and 14 (B)) and conversion (day 21 (C) and 28 (D)). undiff: hBMSCs incubated in basal medium without differentiation supplements; ctrl: hBMSCs differentiated or converted in osteogenic medium without FGF2; 1 ng mL^{-1}, 4 ng mL^{-1}, 10 ng mL^{-1}, and 25 ng mL^{-1} FGF2: hBMSCs differentiated or converted in osteogenic medium supplemented with the respective FGF2 concentration; ad prediff: hBMSCs pre-differentiated in adipogenic medium for 14 days without further osteogenic conversion. Conversion samples were pre-differentiated in adipogenic medium for 14 days, then converted in osteogenic medium for another 7 or 14 days. For statistical analysis, samples were compared to the respective differentiation (ctrl, A, B) or conversion control (ctrl, C, D). $\tilde{x} \pm$ SEM; n = 4. * p =< 0.05; ** p < 0.01; *** p < 0.001; **** p < 0.0001.

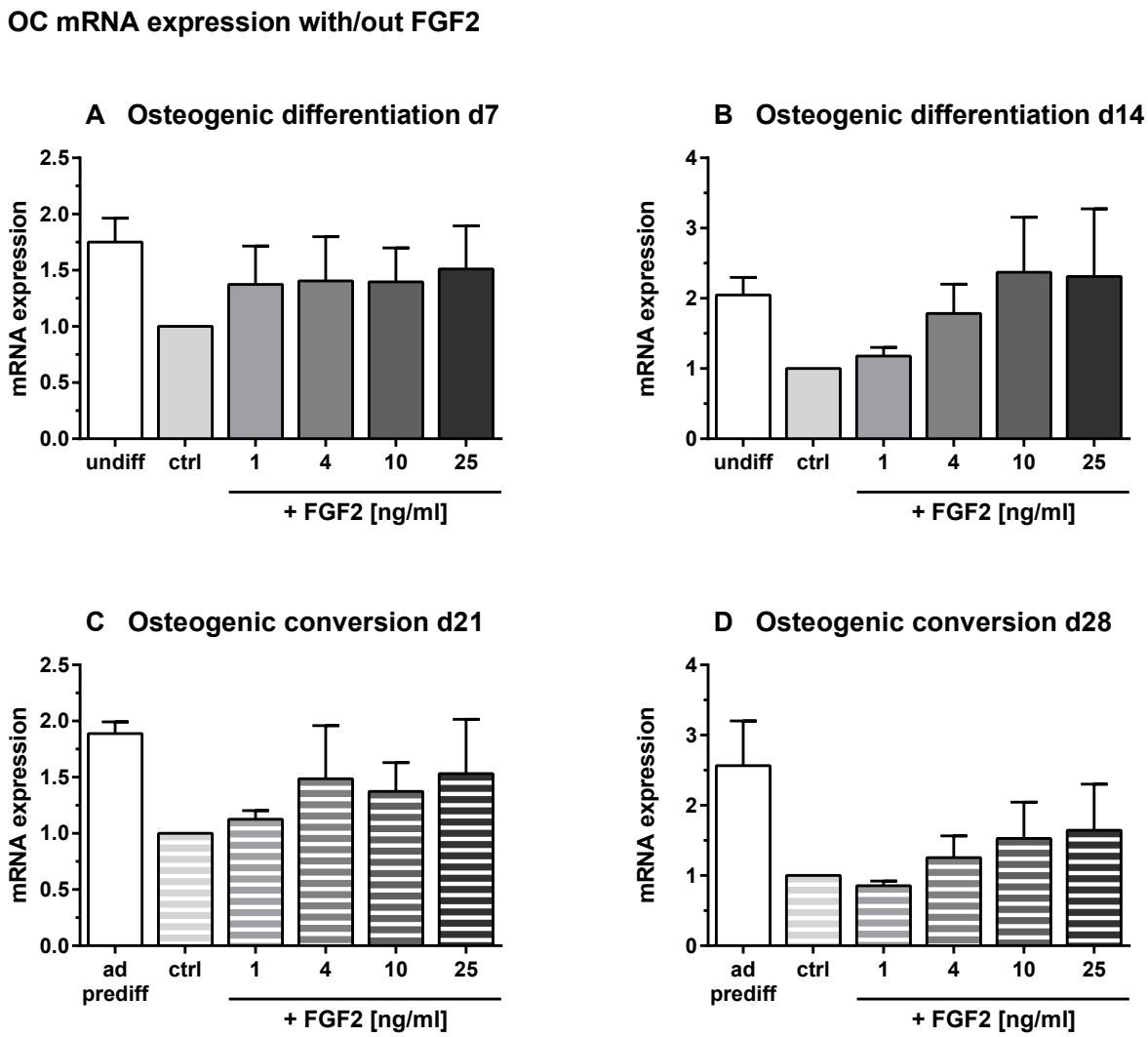

Figure 8.17: Effect of FGF2 on OC mRNA expression during osteogenic differentiation (day 7 (A) and 14 (B)) and conversion (day 21 (C) and 28 (D)). undiff: hBMSCs incubated in basal medium without differentiation supplements; ctrl: hBMSCs differentiated or converted in osteogenic medium without FGF2; 1 ng mL^{-1}, 4 ng mL^{-1}, 10 ng mL^{-1}, and 25 ng mL^{-1} FGF2: hBMSCs differentiated or converted in osteogenic medium supplemented with the respective FGF2 concentration; ad prediff: hBMSCs pre-differentiated in adipogenic medium for 14 days without further osteogenic conversion. Conversion samples were pre-differentiated in adipogenic medium for 14 days, then converted in osteogenic medium for another 7 or 14 days. For statistical analysis, samples were compared to the respective differentiation (ctrl, A, B) or conversion control (ctrl, A, B). $\tilde{x} \pm$ SEM; n = 4.

8.5 Marker genes of mineralization

After investigating the effect of FGF1 and FGF2 on early and late osteogenic markers, we asked whether marker genes regulating the mineralization process were also influenced. We analyzed the genes ANKH, OPN, and ectonucleotide pyrophosphatase/phosphodiesterase 1 (ENPP1) because they are known to affect the ECM mineralization and to inhibit excessive calcification at the same time.

8.5.1 FGF1 markedly upregulates ANKH and OPN expression while decreasing ENPP1 expression

Concerning marker genes controlling the matrix mineralization, the FGF1 administration led to distinct alterations in mRNA expression. The expression of ANKH was upregulated throughout the course of osteogenic differentiation and conversion. After 7 days of differentiation, values increased to 1.90 and 2.09 by 10 ng mL^{-1} and 25 ng mL^{-1} FGF1 (Fig. 8.18 A, 'undiff' vs 'ctrl'). The ANKH expression was further elevated to 1.68 and 2.38 after 14 days of differentiation (Fig. 8.18 B, 'undiff' vs 'ctrl'). Following conversion for 21 days, the expression values of the two highest FGF1 concentrations increased to 1.91 and 2.18 (Fig. 8.18 C '+FGF1'). Reaching significance on day 28, the ANKH expression was enhanced even further to 3.10 and 3.86 by 10 ng mL^{-1} and 25 ng mL^{-1} FGF1 (Fig. 8.18 D '+FGF1').

The ENPP1 expression was as well altered by FGF1 addition in a discontinuous way. After 7 days of osteogenic differentiation, values were slightly augmented to 1.83, 1.53, and 1.75 by 4 ng mL^{-1}, 10 ng mL^{-1}, and 25 ng mL^{-1} FGF1 (Fig. 8.19 A '+FGF1'). However, ENPP1 expression was markedly reduced on day 14 to a minimum of 0.39 by 25 ng mL^{-1} FGF1 (Fig. 8.19 B '+FGF1'). Furthermore, values declined to a minimum of 0.36 by 25 ng mL^{-1} FGF1 on day 21 of osteogenic conversion (Fig. 8.19 C '+FGF1'). On day 28, no obvious alterations were observed, and values ranged between 0.99 (4 ng mL^{-1}) and 1.44 (25 ng mL^{-1}) (Fig. 8.19 D '+FGF1').

On day 7 of osteogenic differentiation, the OPN expression of FGF1 supplemented samples remained on the level of the control (Fig. 8.20 A '+FGF1'). Yet, values augmented to 2.03 by 25 ng mL^{-1} FGF1 on day 14 (Fig. 8.20 B '+FGF1'). After 21 days of osteogenic conversion, OPN expression increased to 1.95 and 2.23 by 10 ng mL^{-1} and 25 ng mL^{-1} FGF1 (Fig. 8.20 C '+FGF1'). On day 28, the upregulation was further enhanced to values of a maximum of 3.94 for 25 ng mL^{-1} FGF1 (Fig. 8.20 D '+FGF1').

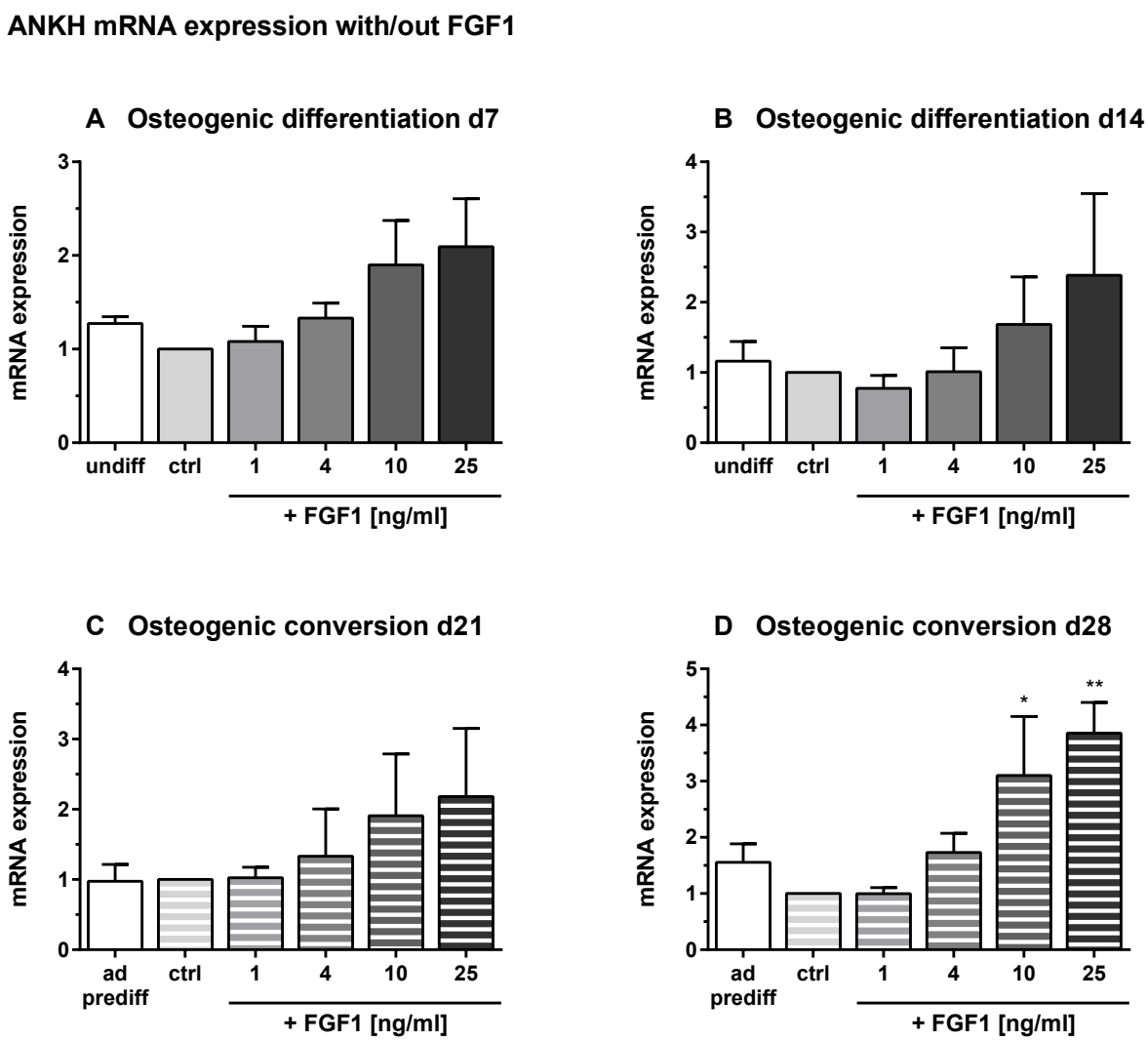

Figure 8.18: Effect of FGF1 on ANKH mRNA expression during osteogenic differentiation (day 7 (A) and 14 (B)) and conversion (day 21 (C) and 28 (D)). undiff: hBMSCs incubated in basal medium without differentiation supplements; ctrl: hBMSCs differentiated or converted in osteogenic medium without FGF1; 1 ng mL^{-1}, 4 ng mL^{-1}, 10 ng mL^{-1}, and 25 ng mL^{-1} FGF1: hBMSCs differentiated or converted in osteogenic medium supplemented with the respective FGF1 concentration; ad prediff: hBMSCs pre-differentiated in adipogenic medium for 14 days without further osteogenic conversion. Conversion samples were pre-differentiated in adipogenic medium for 14 days, then converted in osteogenic medium for another 7 or 14 days. For statistical analysis, samples were compared to the respective differentiation (ctrl, A, B) or conversion control (ctrl, C, D). $\tilde{x} \pm$ SEM; n = 4. * $p < 0.05$; ** $p < 0.01$.

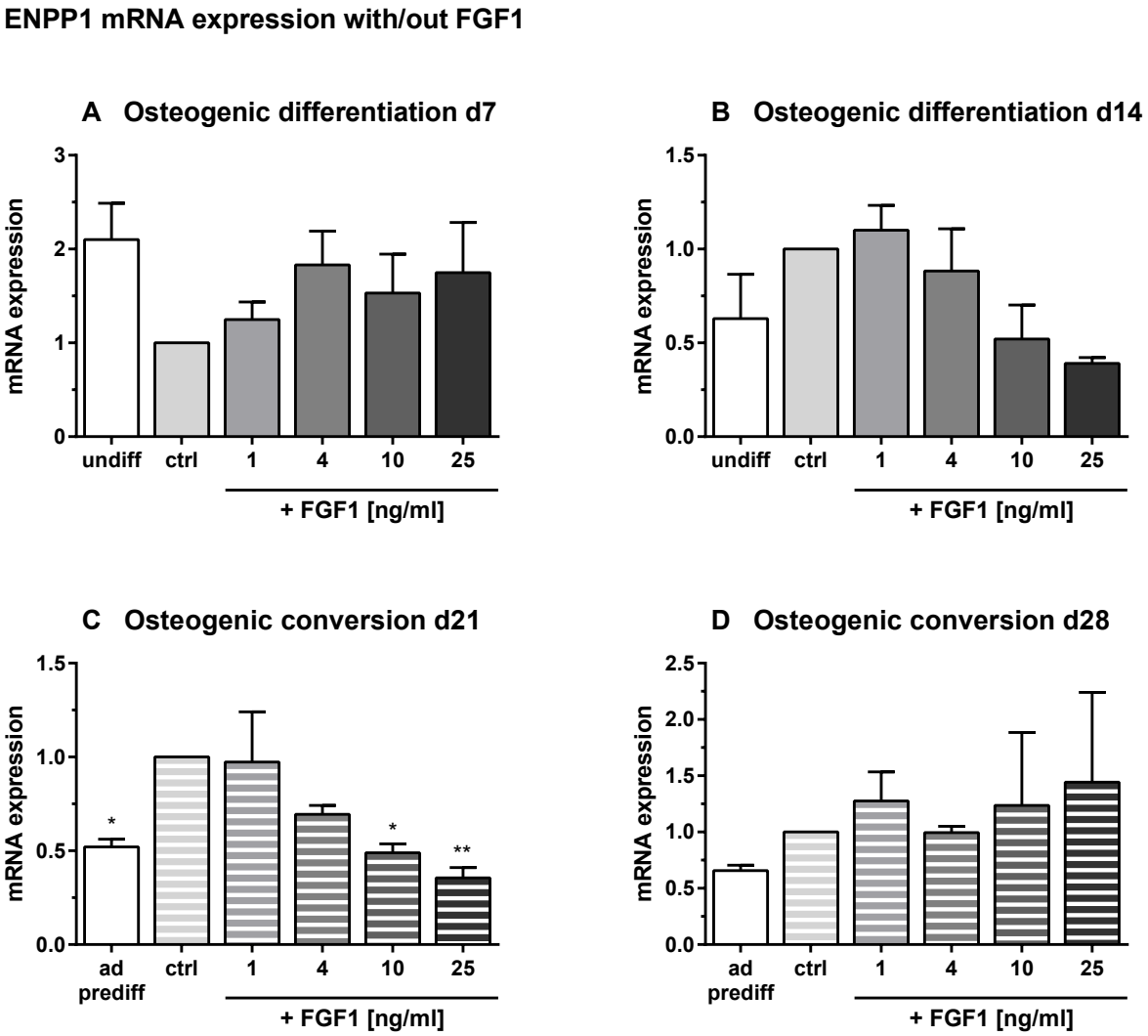

Figure 8.19: Effect of FGF1 on ENPP1 mRNA expression during osteogenic differentiation (day 7 (A) and 14 (B)) and conversion (day 21 (C) and 28 (D)). undiff: hBMSCs incubated in basal medium without differentiation supplements; ctrl: hBMSCs differentiated or converted in osteogenic medium without FGF1; 1 ng mL^{-1}, 4 ng mL^{-1}, 10 ng mL^{-1}, and 25 ng mL^{-1} FGF1: hBMSCs differentiated or converted in osteogenic medium supplemented with the respective FGF1 concentration; ad prediff: hBMSCs pre-differentiated in adipogenic medium for 14 days without further osteogenic conversion. Conversion samples were pre-differentiated in adipogenic medium for 14 days, then converted in osteogenic medium for another 7 or 14 days. For statistical analysis, samples were compared to the respective differentiation (ctrl, A, B) or conversion control (ctrl, C, D). $\tilde{x} \pm$ SEM; n = 3, except for differentiation samples on day 7: n = 4. * $p < 0.05$; ** $p < 0.01$.

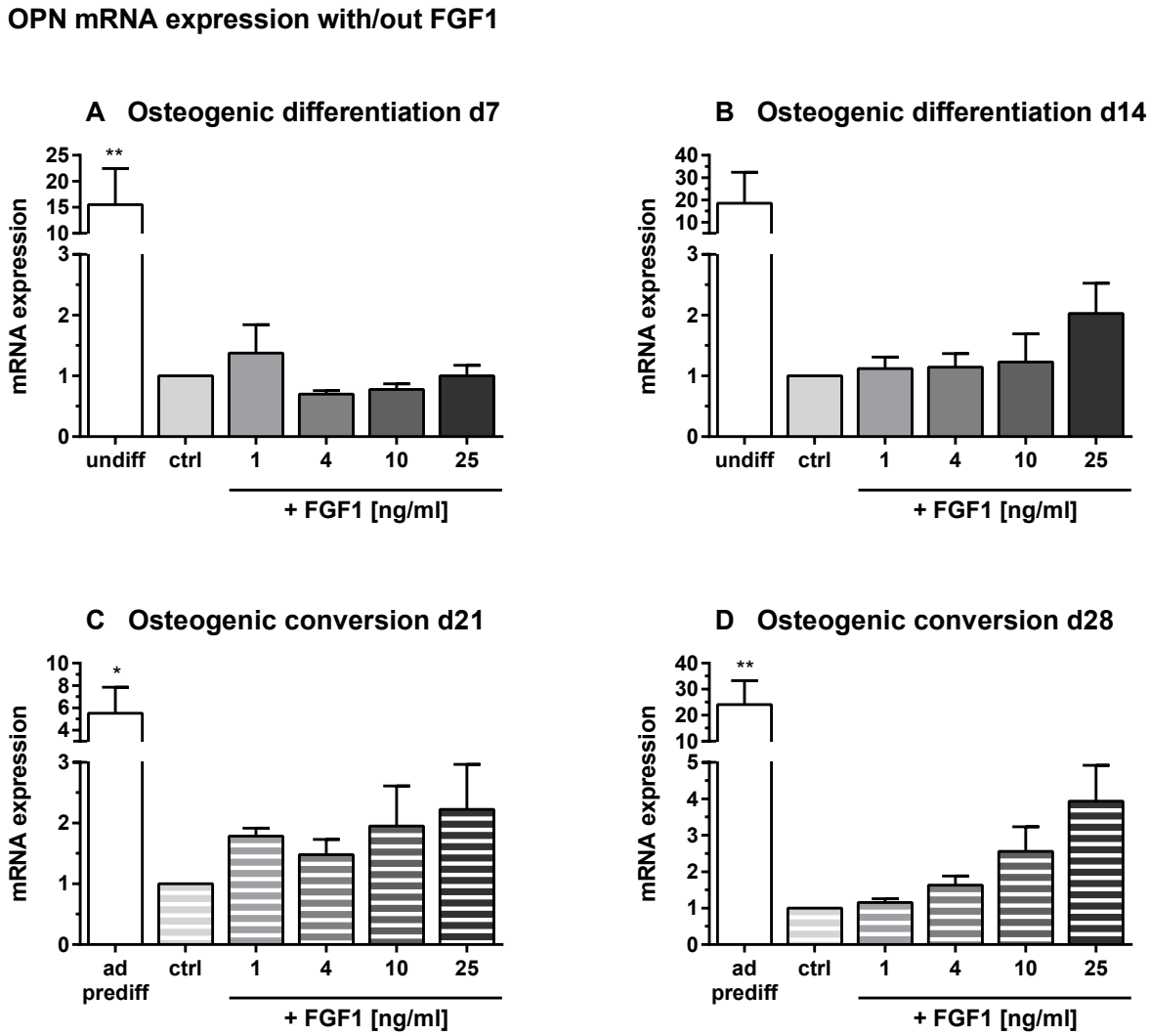

Figure 8.20: Effect of FGF1 on OPN mRNA expression during osteogenic differentiation (day 7 (A) and 14 (B)) and conversion (day 21 (C) and 28 (D)). undiff: hBMSCs incubated in basal medium without differentiation supplements; ctrl: hBMSCs differentiated or converted in osteogenic medium without FGF1; 1 ng mL^{-1}, 4 ng mL^{-1}, 10 ng mL^{-1}, and 25 ng mL^{-1} FGF1: hBMSCs differentiated or converted in osteogenic medium supplemented with the respective FGF1 concentration; ad prediff: hBMSCs pre-differentiated in adipogenic medium for 14 days without further osteogenic conversion. Conversion samples were pre-differentiated in adipogenic medium for 14 days, then converted in osteogenic medium for another 7 or 14 days. For statistical analysis, samples were compared to the respective differentiation (ctrl, A, B) or conversion control (ctrl, C, D). $\tilde{x} \pm$ SEM; n = 4, except for differentiation samples on day 14: n = 3. * $p < 0.05$; ** $p < 0.01$.

8.5.2 FGF2 decreases ENPP1 expression and only slightly affects ANKH and OPN mRNA levels

The mRNA expression of ANKH was slightly increased only by the highest FGF2 concentration of 25 ng mL^{-1}. On day 7 of differentiation, values ranged from 0.44 (4 ng mL^{-1} FGF2) to 1.25 (25 ng mL^{-1}) (Fig. 8.21 A '+FGF2'). After 14 days, ANKH expression varied between 0.56 (4 ng mL^{-1} FGF2) and 1.01 (25 ng mL^{-1}) (Fig. 8.21 B '+FGF2'). Moreover, fold changes augmented to values 1.67 (25 ng mL^{-1} FGF2) after 21 days of conversion (Fig. 8.21 C '+FGF2'). On day 28, ANKH expression reached a maximum of 1.39 (25 ng mL^{-1} FGF2) (Fig. 8.21 D '+FGF2').

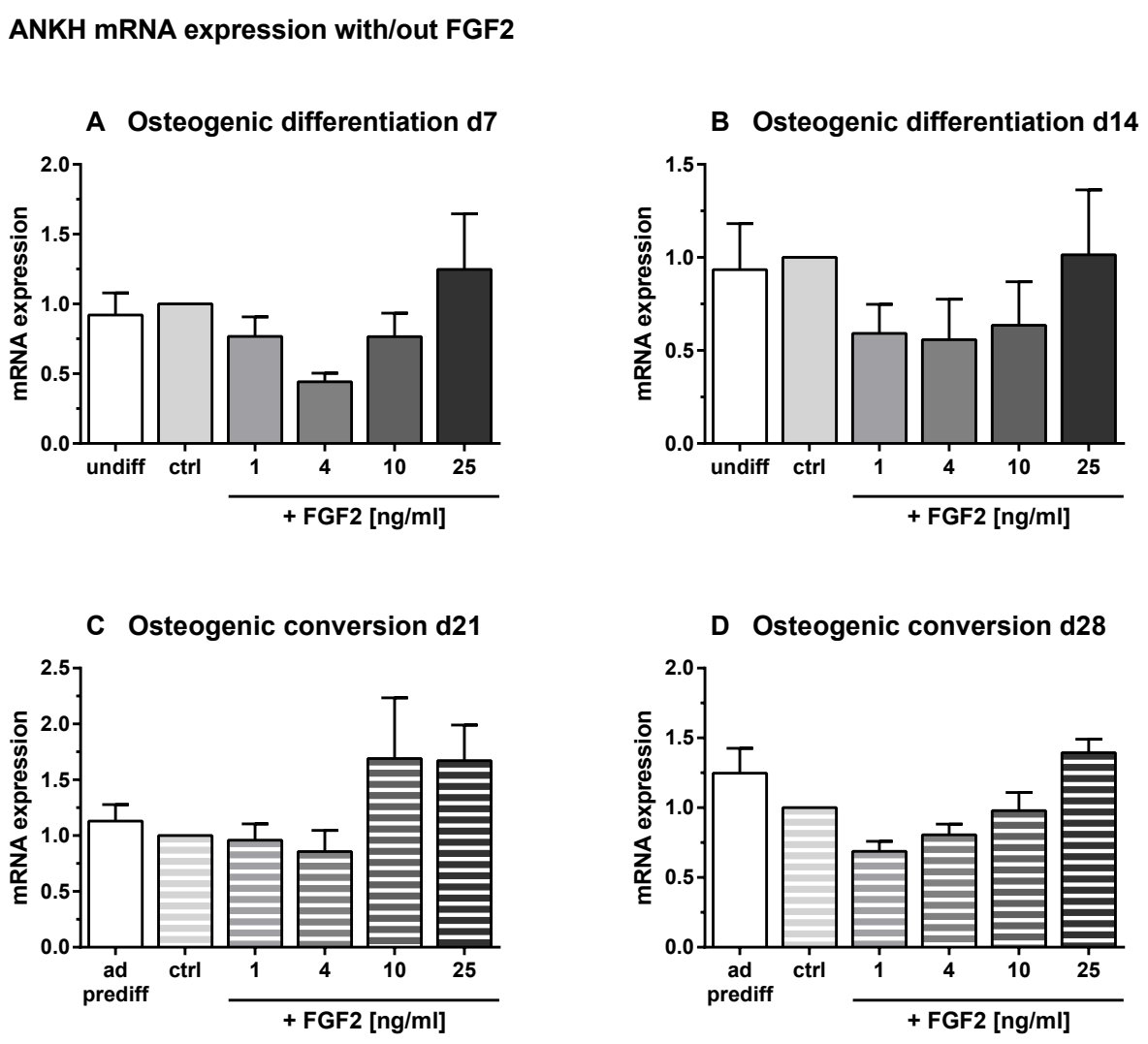

Figure 8.21: Effect of FGF2 on ANKH mRNA expression during osteogenic differentiation (day 7 (A) and 14 (B)) and conversion (day 21 (C) and 28 (D)). undiff: hBMSCs incubated in basal medium without differentiation supplements; ctrl: hBMSCs differentiated or converted in osteogenic medium without FGF2; 1 ng mL^{-1}, 4 ng mL^{-1}, 10 ng mL^{-1}, and 25 ng mL^{-1} FGF2: hBMSCs differentiated or converted in osteogenic medium supplemented with the respective FGF2 concentration; ad prediff: hBMSCs pre-differentiated in adipogenic medium for 14 days without further osteogenic conversion. Conversion samples were pre-differentiated in adipogenic medium for 14 days, then converted in osteogenic medium for another 7 or 14 days. For statistical analysis, samples were compared to the respective differentiation (ctrl, A, B) or conversion control (ctrl, C, D). $\tilde{x} \pm$ SEM; n = 4.

Meanwhile, the expression of ENPP1 was decreased by FGF2. During osteogenic differentiation on day 7, values declined down to 0.45 for 4 ng mL^{-1} FGF2, yet stayed at 0.72 with 25 ng mL^{-1} FGF2 (Fig. 8.22 A '+FGF2'). After 14 days of differentiation, ENPP1 expression decreased further down to 0.42 by 25 ng mL^{-1} FGF2 (Fig. 8.22 B '+FGF2'). Besides, values diminished to 0.47 with 25 ng mL^{-1} FGF2 on day 21 of osteogenic conversion (Fig. 8.22 C '+FGF2') and to 0.54 with 10 ng mL^{-1} and 25 ng mL^{-1} FGF2 (Fig. 8.22 D '+FGF2').

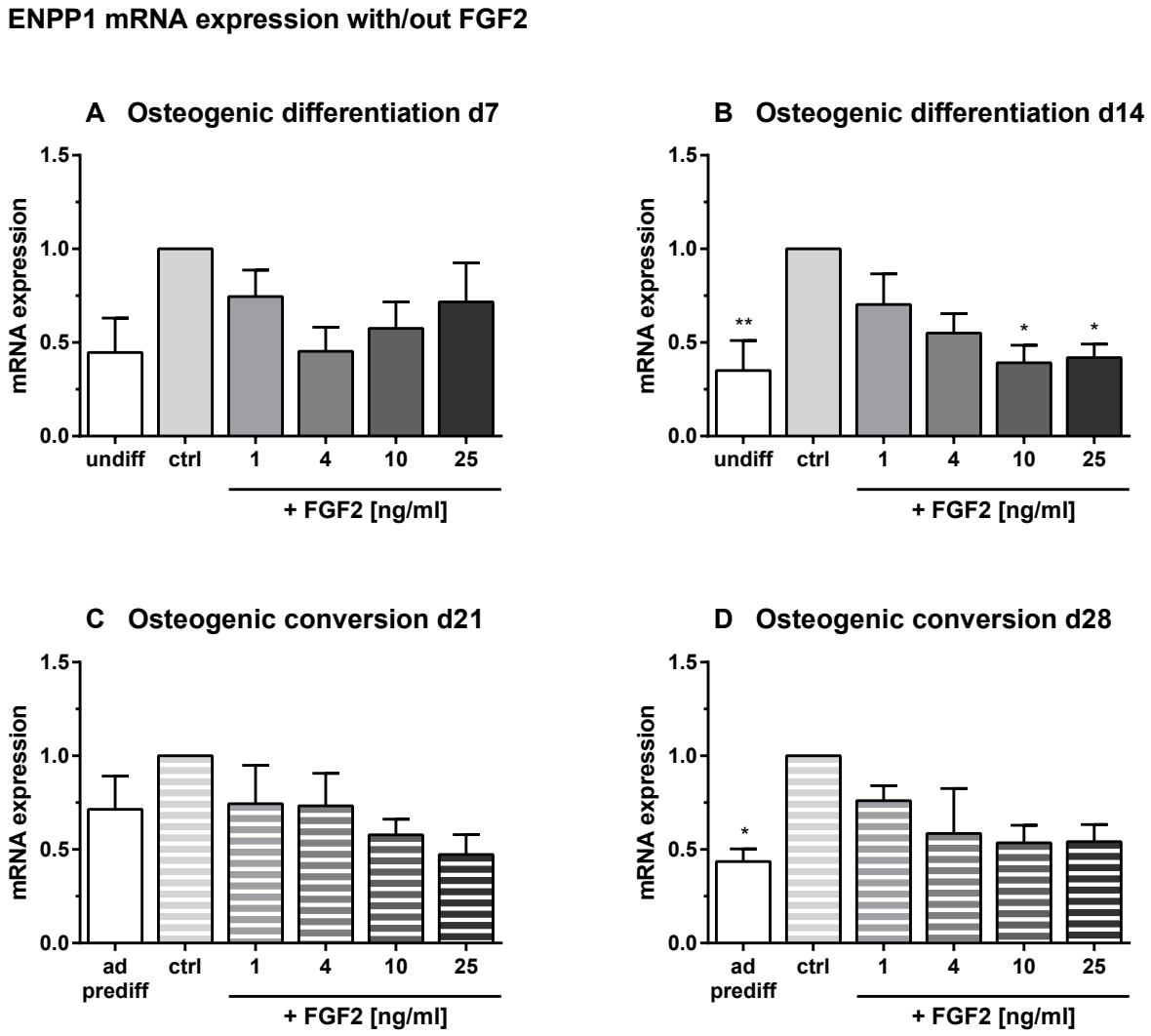

Figure 8.22: Effect of FGF2 on ENPP1 mRNA expression during osteogenic differentiation (day 7 (A) and 14 (B)) and conversion (day 21 (C) and 28 (D)). undiff: hBMSCs incubated in basal medium without differentiation supplements; ctrl: hBMSCs differentiated or converted in osteogenic medium without FGF2; 1 ng mL^{-1}, 4 ng mL^{-1}, 10 ng mL^{-1}, and 25 ng mL^{-1} FGF2: hBMSCs differentiated or converted in osteogenic medium supplemented with the respective FGF2 concentration; ad prediff: hBMSCs pre-differentiated in adipogenic medium for 14 days without further osteogenic conversion. Conversion samples were pre-differentiated in adipogenic medium for 14 days, then converted in osteogenic medium for another 7 or 14 days. For statistical analysis, samples were compared to the respective differentiation (ctrl, A, B) or conversion control (ctrl, C, D). $\tilde{x} \pm$ SEM; n = 3, except for differentiation samples on day 7: n = 4. * $p < 0.05$; ** $p < 0.01$.

The OPN mRNA expression displayed a discontinuous course. On day 7 of osteogenic differentiation, the values of the two highest FGF2 concentrations varied between 0.60 (10 ng mL^{-1}) and 0.75 (25 ng mL^{-1}) (Fig. 8.23 A '+FGF2'). After 14 days, OPN expression slightly decreased to 0.66 with 25 ng mL^{-1} FGF2 (Fig. 8.23 B '+FGF2'). However, on day 21 of osteogenic conversion, values augmented to 1.55 with 10 ng mL^{-1} FGF2, whereas 25 ng mL^{-1} FGF2 exhibited a fold change value of 0.86 (Fig. 8.23 C '+FGF2'). Yet, on day 28, OPN expression declined to 0.57 with 10 ng mL^{-1}, while reaching a value of 0.75 with 25 ng mL^{-1} FGF2 (Fig. 8.23 D '+FGF2').

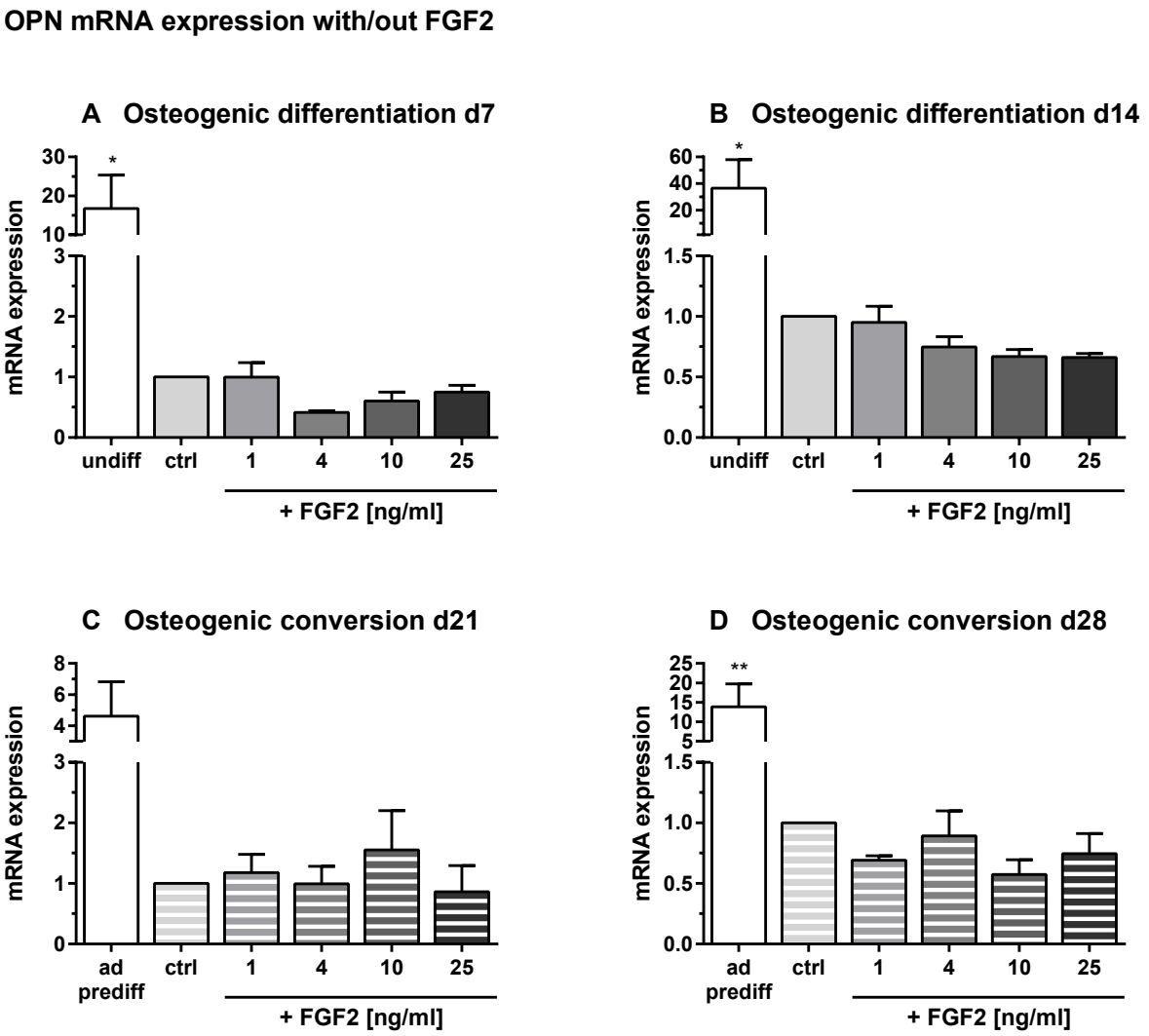

Figure 8.23: Effect of FGF2 on OPN mRNA expression during osteogenic differentiation (day 7 (A) and 14 (B)) and conversion (day 21 (C) and 28 (D)). undiff: hBMSCs incubated in basal medium without differentiation supplements; ctrl: hBMSCs differentiated or converted in osteogenic medium without FGF2; 1 ng mL^{-1}, 4 ng mL^{-1}, 10 ng mL^{-1}, and 25 ng mL^{-1} FGF2: hBMSCs differentiated or converted in osteogenic medium supplemented with the respective FGF1 concentration; ad prediff: hBMSCs pre-differentiated in adipogenic medium for 14 days without further osteogenic conversion. Conversion samples were pre-differentiated in adipogenic medium for 14 days, then converted in osteogenic medium for another 7 or 14 days. For statistical analysis, samples were compared to the respective differentiation (ctrl, A, B) or conversion control (ctrl, C, D). $\tilde{x} \pm$ SEM; n = 4. * $p < 0.05$; ** $p < 0.01$.

8.5.3 OPN protein expression

Knowing that FGF1 upregulates OPN mRNA expression, we wondered if this effect could be pursued on the protein level. Therefore, Western blots for OPN were performed.

The densitometric analysis of the Western blots demonstrated that the OPN protein expression is upregulated during adipogenic as well as osteogenic differentiation compared to undifferentiated hBMSCs (Fig. 8.24, 'undiff' vs 'ctrl'). Notably, the upregulation was higher during adipogenic (5.10-fold) than during osteogenic differentiation (2.57-fold). A further increase of OPN protein via the administration of 25 ng mL^{-1} FGF1 was neither detected in adipogenic nor in osteogenic differentiation. Although the adipogenic values displayed high donor variability (Fig. 8.24 A '+FGF1'), FGF1 addition led to a significant negative regulation of OPN protein expression during osteogenic differentiation (Fig. 8.24 B '+FGF1').

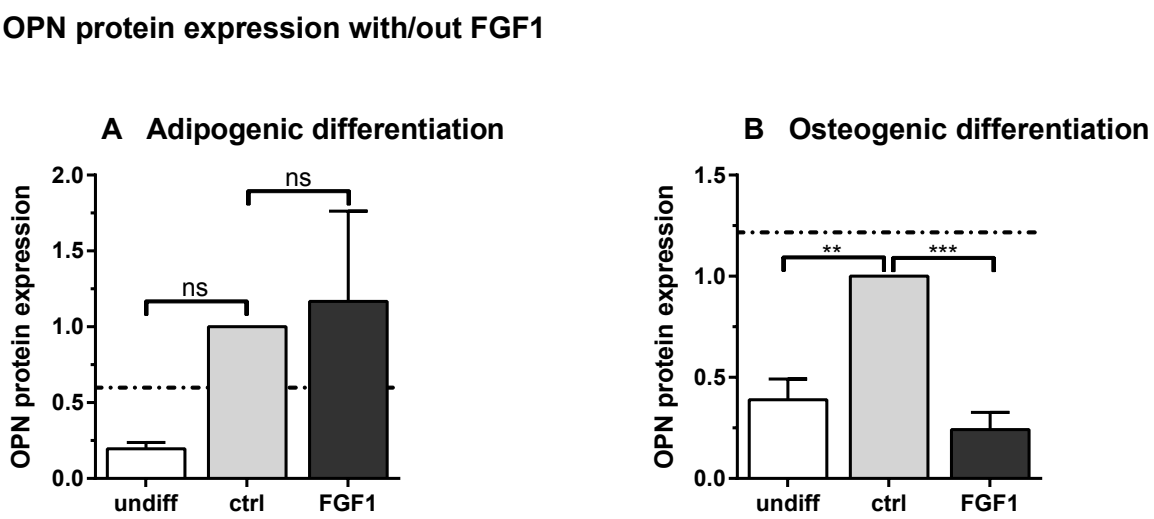

Figure 8.24: Effect of FGF1 on OPN protein expression during adipogenic (A) and osteogenic differentiation (B) on day 14. undiff: hBMSCs incubated in basal medium without differentiation supplements; ctrl: hBMSCs differentiated in adipogenic or osteogenic medium without FGF1; FGF1: hBMSCs differentiated in adipogenic or osteogenic medium supplemented with 25 ng mL^{-1} FGF1. For statistical analysis, values were normalized to β-Actin expression and compared to the respective differentiation control (ctrl). Broken lines indicate the positive control for OPN protein (HeLa cell lysate). $\tilde{x} \pm$ SEM; n = 3. ** $p < 0.01$; *** $p < 0.001$; ns: not significant.

8.5.4 ANKH inhibition does not abolish the anti-mineralizing effect of FGF1

Having observed that the mRNA expression of the inorganic pyrophosphate transport regulator ANKH was upregulated, we wanted to further assess its possible role concerning the reduced mineralization outcome during osteogenic differentiation and conversion. Therefore, we performed differentiation experiments under the addition of the ANKH inhibitor Probenecid. Since the established concentration of 0.25 mmol L^{-1} had no detectable effect, we deployed concentrations of 2 mmol L^{-1} and 10 mmol L^{-1} Probenecid. As the ligand FGF1 was found to be most effective at a concentration of 25 ng mL^{-1} in the previous experiments, all set-ups containing Probenecid were performed with this concentration. To exclude an impact of the inhibitor on the extent of lipid droplet formation or mineralization, one sample was cultured in differentiation medium containing Probenecid without FGF1 ('inh'). Moreover, to overcome effects of the inhibitor solvent NaOH, the differentiation control sample ('ctrl') as well as the FGF1-containing sample ('veh + FGF1') comprised the respective amount of the vehicle NaOH.

The lowest concentration of 0.25 mmol L^{-1} Probenecid did not alter the hBMSCs ability to differentiate into the adipogenic direction when compared to the control cultured in adipogenic medium plus solvent (Fig. 8.25 A, 'ctrl' vs 'inh'). However, the ANKH inhibitor did not diminish the reducing effect of FGF1 on lipid droplet formation, thus the adipogenic phenotype was not rescued by Probenecid ('veh + FGF1' vs 'inh + FGF1'). Similar results were obtained during osteogenic differentiation (Fig. 8.25 B). Here, Probenecid administration led to a slight increase in mineralization compared to the differentiation control ('ctrl' vs 'inh'). Yet, the marked reduction of mineralization caused by FGF1 was not restored by Probenecid addition ('veh + FGF1' vs 'inh + FGF1').

The higher concentration of 2 mmol L^{-1} Probenecid displayed an increased lipid droplet formation during adipogenic differentiation compared to the non-Probenecid-containing control (Fig. 8.25 C, 'ctrl' vs 'inh'). However, there was no alteration in lipid droplet formation concerning both FGF1-containing samples with vehicle and inhibitor ('veh + FGF1' vs 'inh + FGF1'), respectively . Moreover, during osteogenic differentiation, the matrix mineralization was not changed by 2 mmol L^{-1} Probenecid (Fig. 8.25 D, 'ctrl' vs 'inh'). Besides, the ANKH inhibitor did not increase mineralization in combination with FGF1 administration ('veh + FGF1' vs 'inh + FGF1').

The administration of 10 mmol L^{-1} Probenecid to the monolayers markedly declined hBMSC cell viability as could be observed under the light microscope (data not shown). This effect was specifically caused by the ANKH inhibitor itself and not by its solvent NaOH, since the monolayers in the controls remained viable and confluent.

To assess the effects of FGF1 on early time points of hBMSC commitment and differentiation, the involvement of different signaling mediators like receptors and intracellular signaling pathways was investigated as described in the following chapter.

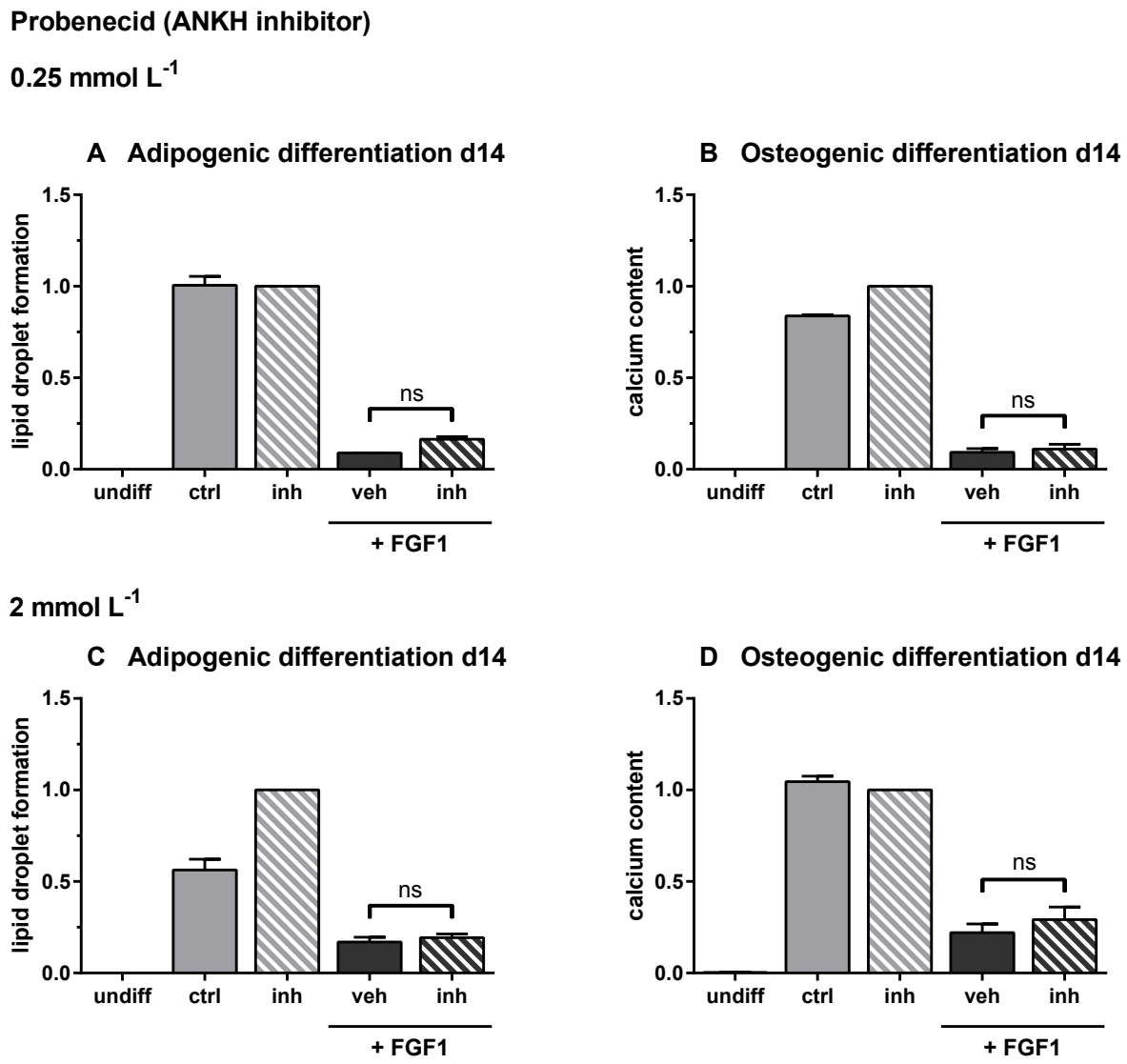

Figure 8.25: Effect of different concentrations of the ANKH inhibitor Probenecid on the FGF1 effects during adipogenic (A, C) and osteogenic differentiation (B, D) on day 14. undiff: hBMSCs incubated in basal medium without differentiation supplements; ctrl: hBMSCs differentiated in adipogenic or osteogenic medium containing the inhibitor solvent NaOH; inh: hBMSCs differentiated in adipogenic or osteogenic medium supplemented with Probenecid; veh + FGF1: hBMSCs differentiated in adipogenic or osteogenic medium containing the inhibitor solvent NaOH (vehicle) plus FGF1; inh + FGF1: hBMSCs differentiated in adipogenic or osteogenic medium supplemented with Probenecid plus FGF1. For statistical analysis, samples were compared to the respective differentiation control containing inhibitor only (inh). $\tilde{x} \pm$ SEM; n = 2. ns: not significant.

9 FGF1 effects are mediated via FGFR1 and ERK1/2 signaling

After having closely investigated the effects of the culture in the presence of FGF1 and FGF2 on the adipogenic and osteogenic differentiation and conversion of primary hBMSCs (see chapter 7 and 8), we aimed at elucidating the underlying signaling mechanism/s. To identify responsible receptors and intracellular signaling pathways, we performed differentiation and conversion experiments under the addition of specific inhibitors.

9.1 Inhibition of FGFR1 rescues the FGF1 phenotype

Previous microarray analyses within our group revealed that the FGF receptors FGFR3 and FGFR4 are not expressed in hBMSCs (Dr. Tatjana Schilling, personal communication, June 10, 2015). To investigate if FGFR1 mediates the signal underlying the FGF1 effects, we performed differentiation and conversion experiments deploying the FGFR1 inhibitor PD166866. Since an FGF1 concentration of $25\,\mathrm{ng\,mL^{-1}}$ was found to be most effective, the following experiments were performed with $25\,\mathrm{ng\,mL^{-1}}$ FGF1. In pre-trials, we figured out that the most effective concentration of PD166866 was $250\,\mathrm{nmol\,L^{-1}}$ for this FGF1 concentration.

As expected, the lipid droplet formation was strongly pronounced during adipogenic differentiation compared to undifferentiated samples (Fig. 9.1 A, 'undiff' vs 'ctrl'), whereas the administration of FGF1 caused a marked reduction of fat droplets ('veh + FGF1'). The addition of the FGFR1 inhibitor PD166866 only to the differentiation cocktail did not alter lipid droplet formation, thus adipogenic differentiation ('inh'). Interestingly, the FGFR1 inhibitor PD166866 totally rescued this FGF1 effect ('inh + FGF1'). The lipid droplet formation was highly significantly increased to the levels of the differentiation ('ctrl') and inhibitor-only controls ('inh').

Following osteogenic differentiation, the ECM mineralization was distinctly enhanced when compared to undifferentiated hBMSCs (Fig. 9.1 B, 'undiff' vs 'ctrl'). In accordance with previous results, FGF1 addition reduced matrix mineralization ('veh + FGF1'). Whereas PD166866 administration only did not alter the mineralization outcome ('inh'), the FGF1 effect was highly significantly rescued by the inhibitor addition ('inh + FGF1'); mineralization values were increased slightly above the levels of the differentiation controls.

After 28 days of adipogenic conversion, lipid droplet formation was explicitly upregulated in comparison to osteogenically pre-differentiated hBMSCs as expected (Fig. 9.1 C, 'ost prediff' vs 'ctrl'). Inhibitor addition to the differentiation medium did not distinctly change adipogenic outcome ('inh'), whereas FGF1 resulted in markedly reduced lipid droplet formation ('veh + FGF1'). The addition of PD166866 together with FGF1 to the differentiation cocktail demonstrated a slight, yet significant increase in lipid outcome, in other words a partial rescue ('inh + FGF1').

During osteogenic conversion, findings resembled those of osteogenic differentiation (Fig. 9.1 D). Mineralization was distinctly increased in the control samples when compared to adipogenically pre-differentiated hBMSCs ('ad prediff' vs 'ctrl'). Furthermore, PD166866 only addition did not change mineralization values ('inh'). Yet, the FGF1 administration markedly reduced the outcome ('veh +

FGF1'). Nevertheless, PD166866 addition to FGF1-containing differentiation cocktail was able to restore mineralization in a highly significant manner ('inh + FGF1').

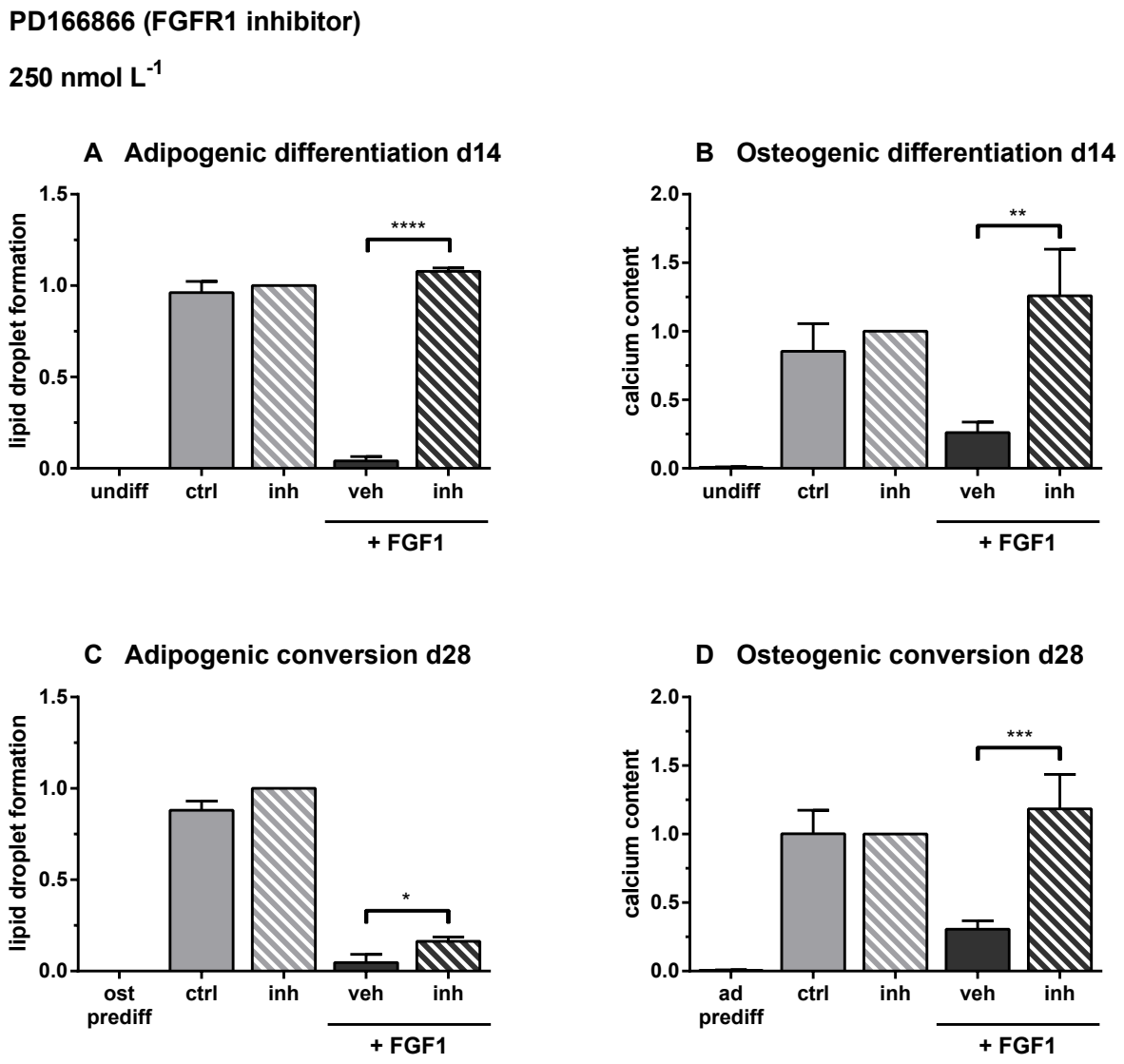

Figure 9.1: Effect of the FGFR1 inhibitor PD166866 on the FGF1 effects during adipogenic (A) and osteogenic differentiation (B) as well as adipogenic (C) and osteogenic conversion (D). undiff: hBMSCs incubated in basal medium without differentiation supplements; ctrl: hBMSCs differentiated or converted in adipogenic or osteogenic differentiation medium without FGF1; inh: hBMSCs differentiated or converted in differentiation medium supplemented with PD166866; veh + FGF1: hBMSCs differentiated or converted in differentiation medium containing the inhibitor solvent DMSO (vehicle) plus FGF1; inh + FGF1: hBMSCs differentiated or converted in differentiation medium supplemented with PD166866 plus FGF1; ost prediff: hBMSCs pre-differentiated in osteogenic medium for 14 days; ad prediff: hBMSCs pre-differentiated in adipogenic medium for 14 days. Conversion samples were pre-differentiated for 14 days, then converted in the respective other medium for another 14 days. For statistical analysis, samples were compared to the respective differentiation/-conversion control containing inhibitor only (inh). $\tilde{x} \pm$ SEM; n = 3 for A; n = 4 for B and C; n = 5 for D. * $p < 0.05$; ** $p < 0.01$; *** $p < 0.001$; **** $p < 0.0001$.

9.2 Gene expression of FGFR1 and FGFR2

Knowing that the FGFR1 inhibitor PD166866 is a potent agent to rescue the effects caused by FGF1, we wanted to gain further insight into the mRNA expression of the FGF receptors FGFR1 and FGFR2.

9.2.1 FGFR1 is more stably expressed than FGFR2 during adipogenic differentiation and conversion

During adipogenic differentiation and conversion, the mRNA expression of FGFR1 was decreased by 0.79 (on day 14) and 0.70 (on day 28) when compared to undifferentiated and osteogenically pre-differentiated hBMSCs (Fig. 9.2 A, 'undiff' vs 'ctrl' and B, 'ost prediff' vs 'ctrl'). Furthermore, FGFR1 expression was downregulated to a minimum of 0.47 with 4 ng mL^{-1} FGF1 compared to the differentiation control (Fig. 9.2 A '+FGF1'). Yet, the administration of 25 ng mL^{-1} FGF1 led only to a slight fold change of 0.75. After 28 days of adipogenic conversion in the presence of FGF1, FGFR1 expression was only slightly altered to values that ranged between 0.69 and 0.78 (10 ng mL^{-1} and 25 ng mL^{-1} FGF1) (Fig. 9.2 B '+FGF1').

Following FGF2 addition, adipogenically differentiated samples exhibited a reduction in FGFR1 expression on day 14; values decreased to 0.46 and 0.56 with 10 ng mL^{-1} and 25 ng mL^{-1} FGF2 (Fig. 9.3 A '+FGF2'). After conversion, the FGFR1 expression only varied from 0.67 to 1.09 for 4 ng mL^{-1} and 25 ng mL^{-1} FGF2 (Fig. 9.3 B '+FGF2').

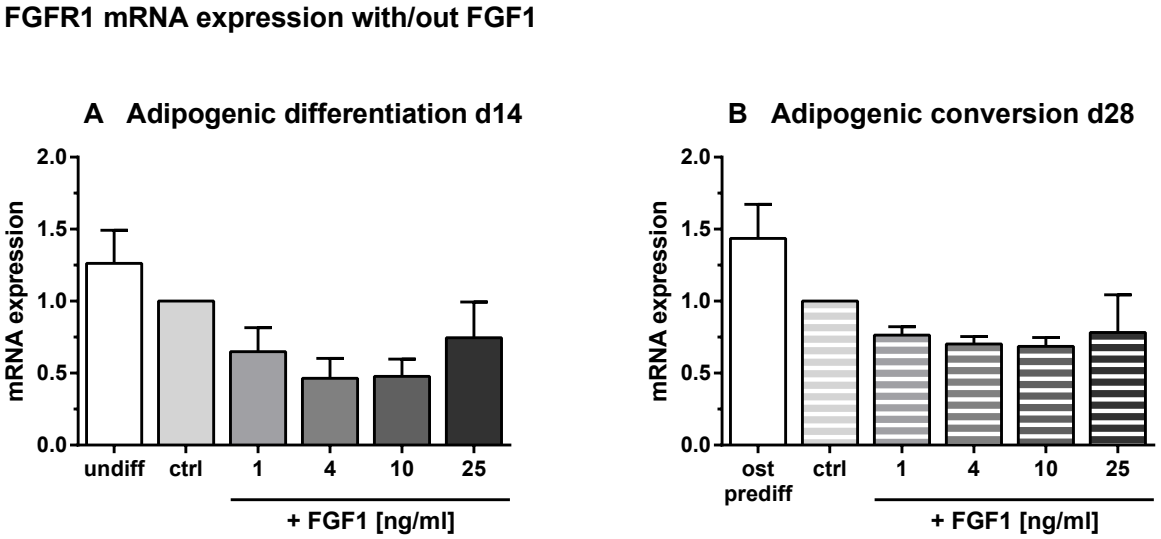

Figure 9.2: Effect of FGF1 on FGFR1 mRNA expression during adipogenic differentiation (A) and conversion (B). undiff: hBMSCs incubated in basal medium without differentiation supplements; ctrl: hBMSCs differentiated or converted in adipogenic medium without FGF1; 1 ng mL^{-1}, 4 ng mL^{-1}, 10 ng mL^{-1}, and 25 ng mL^{-1} FGF1: hBMSCs differentiated or converted in adipogenic medium supplemented with the respective FGF1 concentration; ost prediff: hBMSCs pre-differentiated in osteogenic medium for 14 days without further adipogenic conversion. Conversion samples were pre-differentiated in osteogenic medium for 14 days, then converted in adipogenic medium for another 14 days. For statistical analysis, samples were compared to the respective differentiation (ctrl, A) or conversion control (ctrl, B). $\tilde{x} \pm$ SEM; A: n = 3; B: n = 4.

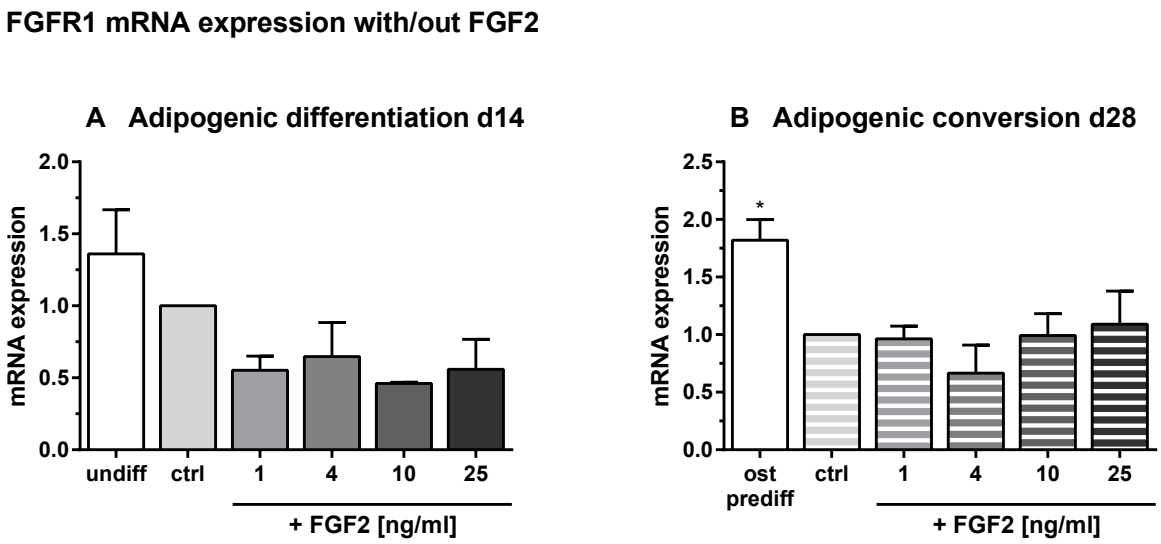

Figure 9.3: Effect of FGF2 on FGFR1 mRNA expression during adipogenic differentiation (A) and conversion (B). undiff: hBMSCs incubated in basal medium without differentiation supplements; ctrl: hBMSCs differentiated or converted in adipogenic medium without FGF2; 1 ng mL^{-1}, 4 ng mL^{-1}, 10 ng mL^{-1}, and 25 ng mL^{-1} FGF2: hBMSCs differentiated or converted in adipogenic medium supplemented with the respective FGF2 concentration; ost prediff: hBMSCs pre-differentiated in osteogenic medium for 14 days without further adipogenic conversion. Conversion samples were pre-differentiated in osteogenic medium for 14 days, then converted in adipogenic medium for another 14 days. For statistical analysis, samples were compared to the respective differentiation (ctrl, A) or conversion control (ctrl, B). $\tilde{x} \pm$ SEM; n = 4. * $p < 0.05$.

The expression of FGFR2 was significantly downregulated during adipogenic differentiation and conversion, respectively. In the FGF1 set-ups, fold changes varied between 0.44 and 0.37 for day 14 and day 28 (Fig. 9.4 A, 'undiff' vs 'ctrl' and B, 'ost prediff' vs 'ctrl'). Similarly, in the FGF2 set-ups, Values significantly declined by 0.47-fold on day 14 and 0.45-fold on day 28 (Fig. 9.5 A, 'undiff' vs 'ctrl' and B, 'ost prediff' vs 'ctrl').

With 14 days of FGF1 addition, the FGFR2 expression notably declined further to a minimum of 0.06 with 25 ng mL^{-1} FGF1 (Fig. 9.4 A '+FGF1'). Following 28 days of adipogenic conversion in the presence of FGF1, FGFR2 mRNA expression was markedly downregulated to 0.13 (25 ng mL^{-1}) (Fig. 9.4 B '+FGF1').

In the set-ups for FGF2 addition, a notable decrease of FGFR2 expression with a minimum value of 0.28 was observed on day 14 (with 25 ng mL^{-1} FGF2) (Fig. 9.5 A '+FGF2'). On day 28 of adipogenic conversion, FGFR2 expression was downregulated to a minimum of 0.36 with 25 ng mL^{-1} FGF2 (Fig. 9.5 B '+FGF2').

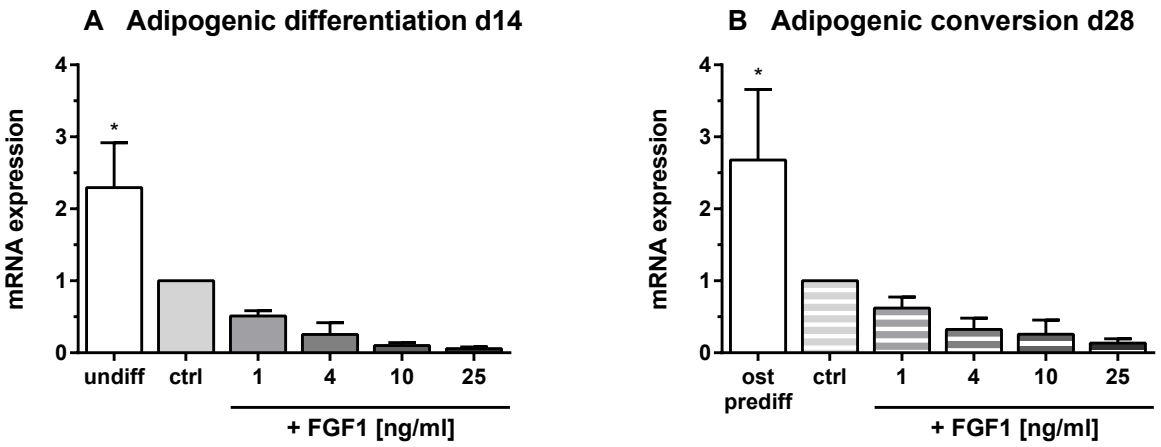

Figure 9.4: Effect of FGF1 on FGFR2 mRNA expression during adipogenic differentiation (A) and conversion (B). undiff: hBMSCs incubated in basal medium without differentiation supplements; ctrl: hBMSCs differentiated or converted in adipogenic medium without FGF1; $1\,\mathrm{ng\,mL^{-1}}$, $4\,\mathrm{ng\,mL^{-1}}$, $10\,\mathrm{ng\,mL^{-1}}$, and $25\,\mathrm{ng\,mL^{-1}}$ FGF1: hBMSCs differentiated or converted in adipogenic medium supplemented with the respective FGF1 concentration; ost prediff: hBMSCs pre-differentiated in osteogenic medium for 14 days without further adipogenic conversion. Conversion samples were pre-differentiated in osteogenic medium for 14 days, then converted in adipogenic medium for another 14 days. For statistical analysis, samples were compared to the respective differentiation (ctrl, A) or conversion control (ctrl, B). $\tilde{x} \pm$ SEM; n = 4, except for differentiation samples on day 14: n = 3. * $p < 0.05$.

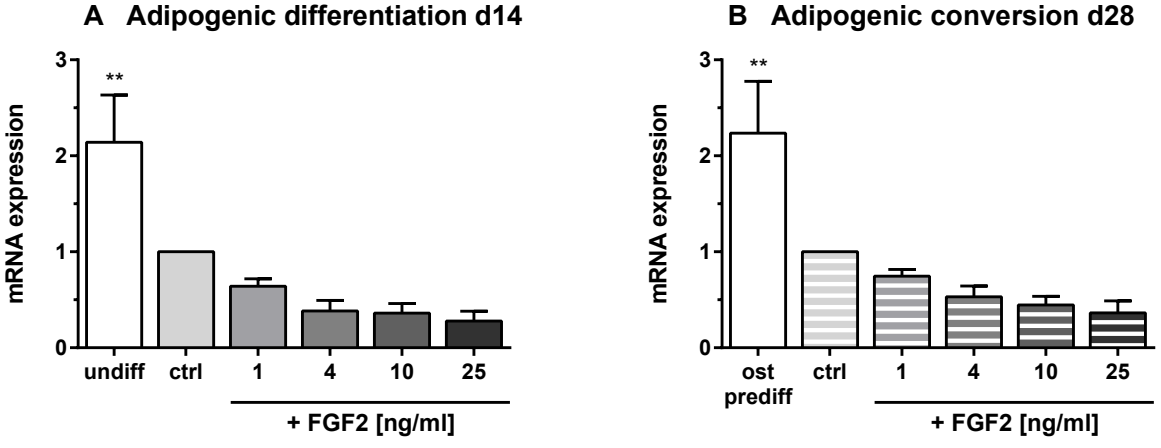

Figure 9.5: Effect of FGF2 on FGFR2 mRNA expression during adipogenic differentiation (A) and conversion (B). undiff: hBMSCs incubated in basal medium without differentiation supplements; ctrl: hBMSCs differentiated or converted in adipogenic medium without FGF2; $1\,\mathrm{ng\,mL^{-1}}$, $4\,\mathrm{ng\,mL^{-1}}$, $10\,\mathrm{ng\,mL^{-1}}$, and $25\,\mathrm{ng\,mL^{-1}}$ FGF2: hBMSCs differentiated or converted in adipogenic medium supplemented with the respective FGF2 concentration; ost prediff: hBMSCs pre-differentiated in osteogenic medium for 14 days without further adipogenic conversion. Conversion samples were pre-differentiated in osteogenic medium for 14 days, then converted in adipogenic medium for another 14 days. For statistical analysis, samples were compared to the respective differentiation (ctrl, A) or conversion control (ctrl, B). $\tilde{x} \pm$ SEM; n = 4. ** $p < 0.01$.

9.2.2 FGFR1 is more steadily expressed than FGFR2 in osteogenic differentiation and conversion

The expression of FGFR1 was not altered during 7 days of osteogenic differentiation (Fig. 9.6 A, 'undiff' vs 'ctrl'). However, values were decreased in the later stages of osteogenic differentiation and during osteogenic conversion to 0.67-fold (day 14), 0.65-fold (day 21), and 0.62-fold (day 28) (Fig. 9.6 B, C, D). The addition of FGF1 resulted in no fold changes on day 7 of differentiation (Fig. 9.6 A '+FGF1'). Yet, FGFR1 expression was declined to 0.71 by 10 ng mL^{-1} FGF1 after 14 days of differentiation (Fig. 9.6 B '+FGF1'). In the course of osteogenic conversion, FGFR1 expression was altered only slightly to values between 0.83 to 1.10 (on day 21) and between 0.83 to 1.07 (on day 28) (Fig. 9.6 C, D '+FGF1').

In the analogous set-ups for FGF2, the expression of FGFR1 stayed the same on day 7 of osteogenic differentiation (Fig. 9.7 A). Yet, we observed a decrease at the later time point (day 14) and during osteogenic conversion; here, values declined to 0.79 (day 14), 0.73 (day 21), and finally 0.65 (day 28) (Fig. 9.7 B, C, D). Whereas no significant decreases were monitored on day 7 of osteogenic differentiation and day 21 plus day 28 of osteogenic conversion, FGFR1 expression was significantly downregulated on day 14 of differentiation to a minimum of 0.45 (4 ng mL^{-1} FGF2) (Fig. 9.7 B '+FGF2'). Nevertheless, values declined to 0.55 by 4 ng mL^{-1} FGF2 on day 21 of osteogenic conversion (Fig. 9.7 C '+FGF2').

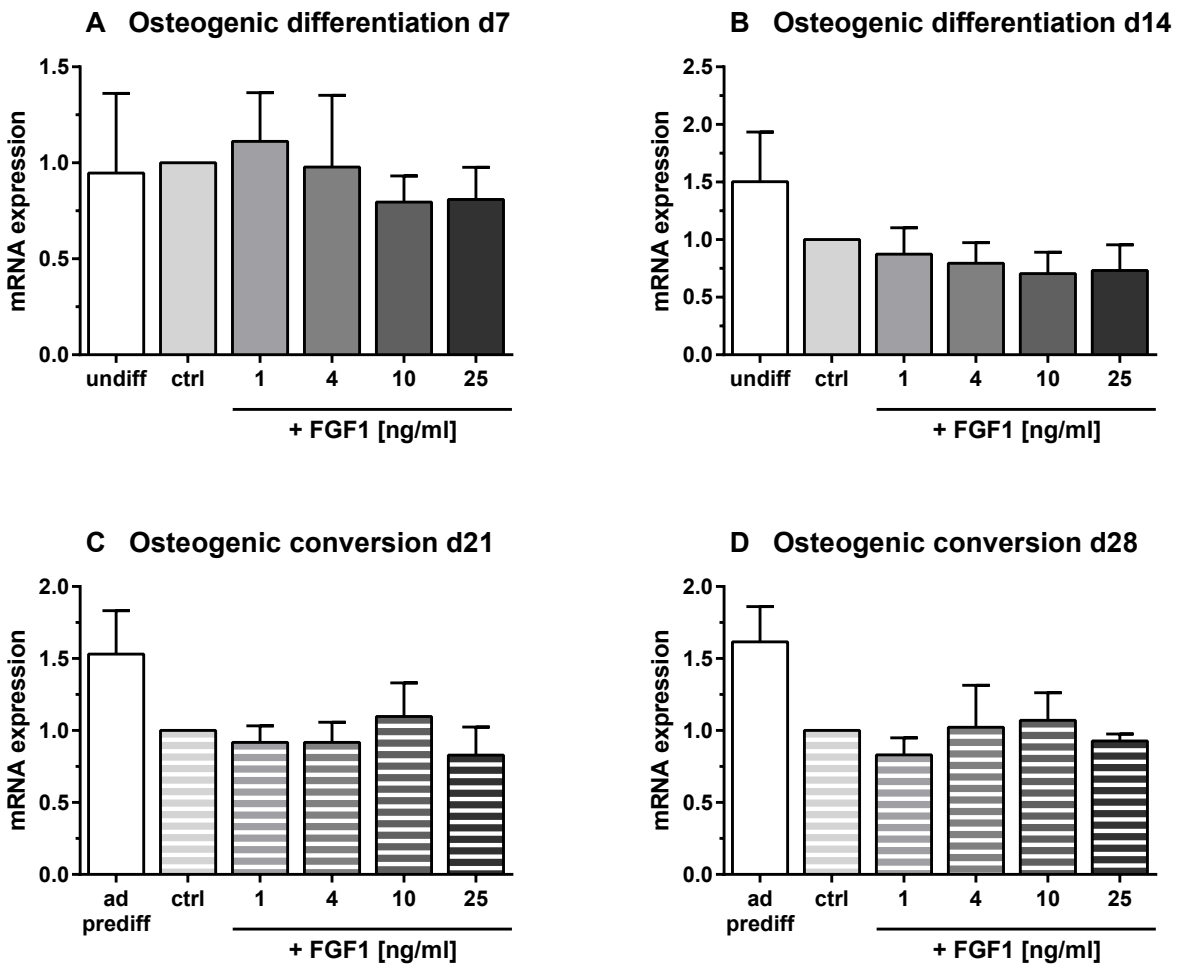

Figure 9.6: Effect of FGF1 on FGFR1 mRNA expression during osteogenic differentiation (day 7 (A) and 14 (B)) and conversion (day 21 (C) and 28 (D)). undiff: hBMSCs incubated in basal medium without differentiation supplements; ctrl: hBMSCs differentiated or converted in osteogenic medium without FGF1; 1 ng mL^{-1}, 4 ng mL^{-1}, 10 ng mL^{-1}, and 25 ng mL^{-1} FGF1: hBMSCs differentiated or converted in osteogenic medium supplemented with the respective FGF1 concentration; ad prediff: hBMSCs pre-differentiated in adipogenic medium for 14 days without further osteogenic conversion. Conversion samples were pre-differentiated in osteogenic medium for 14 days, then converted in adipogenic medium for another 7 or 14 days. For statistical analysis, samples were compared to the respective differentiation (ctrl, A, B) or conversion control (ctrl, C, D). $\tilde{x} \pm$ SEM; n = 4, except for differentiation samples on day 14: n = 3.

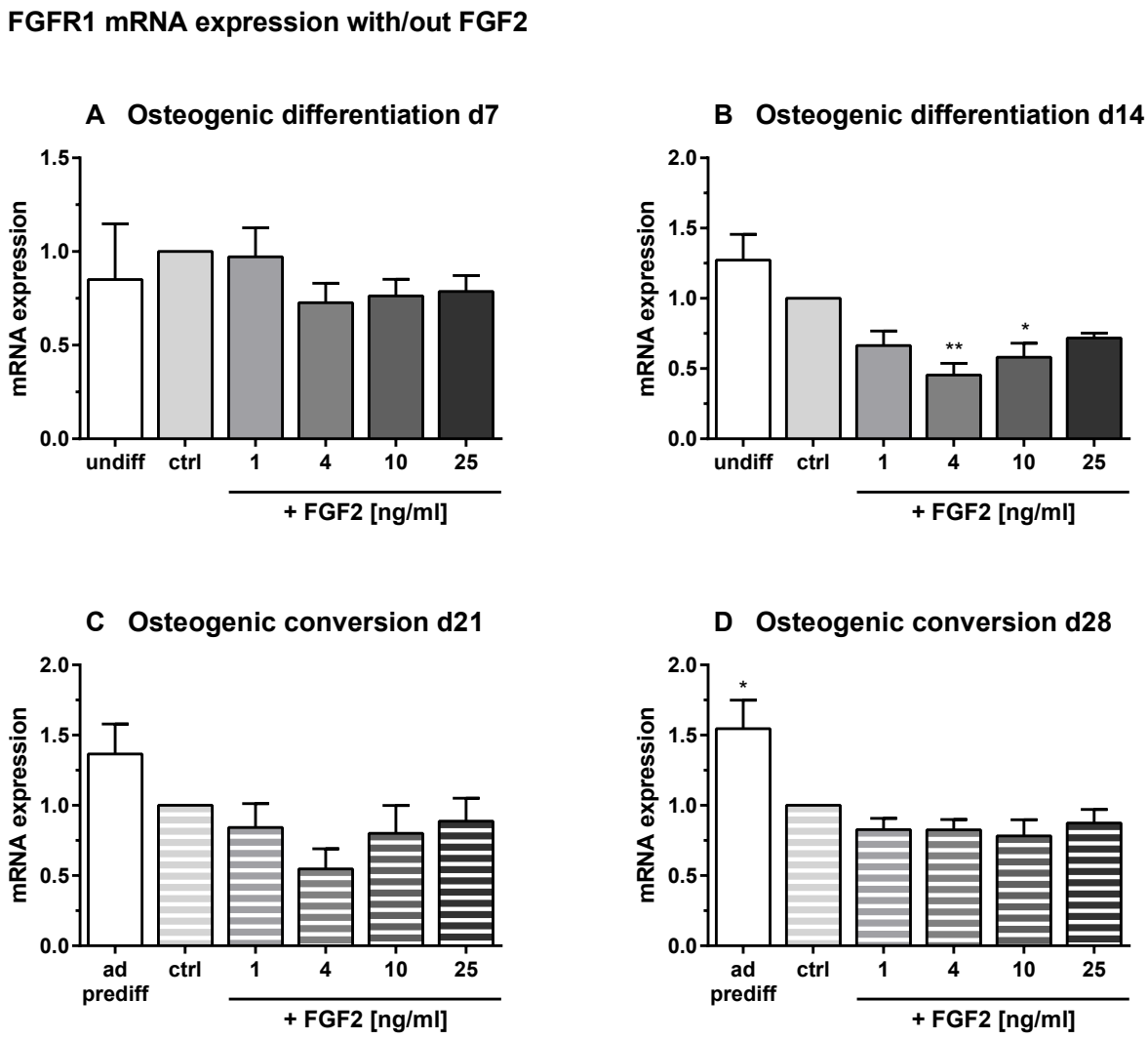

Figure 9.7: Effect of FGF2 on FGFR1 mRNA expression during osteogenic differentiation (day 7 (A) and 14 (B)) and conversion (day 21 (C) and 28 (D)). undiff: hBMSCs incubated in basal medium without differentiation supplements; ctrl: hBMSCs differentiated or converted in osteogenic medium without FGF2; 1 ng mL^{-1}, 4 ng mL^{-1}, 10 ng mL^{-1}, and 25 ng mL^{-1} FGF2: hBMSCs differentiated or converted in osteogenic medium supplemented with the respective FGF2 concentration; ad prediff: hBMSCs pre-differentiated in adipogenic medium for 14 days without further osteogenic conversion. Conversion samples were pre-differentiated in osteogenic medium for 14 days, then converted in adipogenic medium for another 7 or 14 days. For statistical analysis, samples were compared to the respective differentiation (ctrl, A, B) or conversion control (ctrl, C, D). $\tilde{x} \pm$ SEM; n = 4. * $p < 0.05$; ** $p < 0.01$.

Interestingly, the FGFR2 expression was highly significantly downregulated during osteogenic differentiation and conversion. Values were reduced 6.02-fold (day 7), 13.28-fold (day 14), 6.95-fold (day 21), and 13.23-fold (day 28) (Fig. 9.8 A, B, 'undiff' vs 'ctrl' and C, D, 'ad prediff' vs 'ctrl'). Due to FGF1 addition, FGFR2 expression declined even further in a concentration dependent manner. On day 7, values decreased to a minimum of 0.09 by 10 ng mL^{-1} FGF1 (Fig. 9.8 A '+FGF1'). After 14 days of osteogenic differentiation, FGFR2 expression declined to 0.18 with 25 ng mL^{-1} FGF1 (Fig. 9.8 B '+FGF1'). On day 21 of osteogenic conversion, values decreased to a minimum of 0.17 by 25 ng mL^{-1} FGF1 (Fig. 9.8 C '+FGF1'). Furthermore, after 28 days of conversion, FGFR2 expression was downregulated to 0.14 by 25 ng mL^{-1} FGF1 (Fig. 9.8 D '+FGF1').

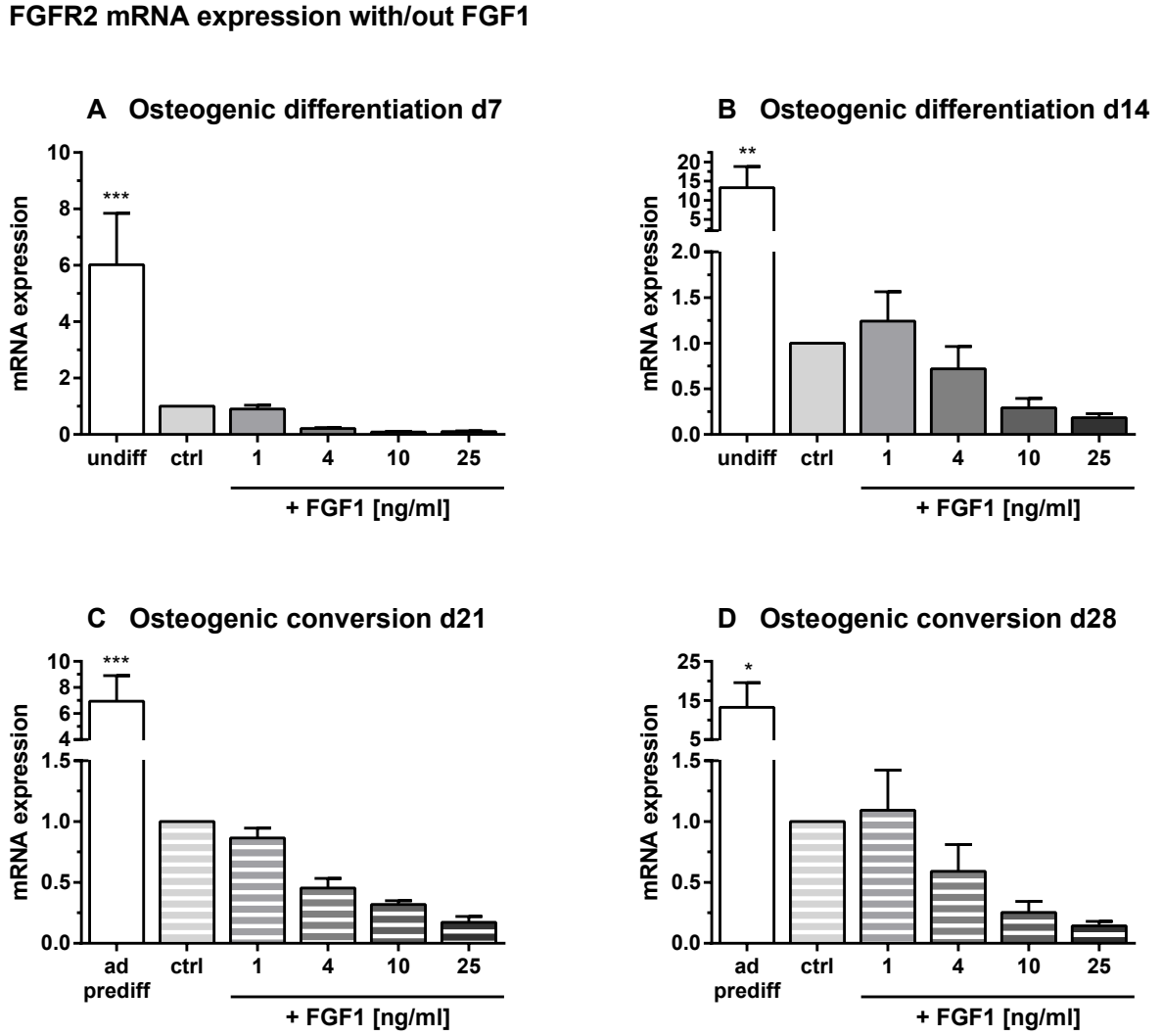

Figure 9.8: Effect of FGF1 on FGFR2 mRNA expression during osteogenic differentiation (day 7 (A) and 14 (B)) and conversion (day 21 (C) and 28 (D)). undiff: hBMSCs incubated in basal medium without differentiation supplements; ctrl: hBMSCs differentiated or converted in osteogenic medium without FGF1; 1 ng mL^{-1}, 4 ng mL^{-1}, 10 ng mL^{-1}, and 25 ng mL^{-1} FGF1: hBMSCs differentiated or converted in osteogenic medium supplemented with the respective FGF2 concentration; ad prediff: hBMSCs pre-differentiated in adipogenic medium for 14 days without further osteogenic conversion. Conversion samples were pre-differentiated in osteogenic medium for 14 days, then converted in adipogenic medium for another 7 or 14 days. For statistical analysis, samples were compared to the respective differentiation (ctrl, A, B) or conversion control (ctrl, C, D). $\tilde{x} \pm$ SEM; n = 4, except for differentiation samples on day 14: n = 3. * $p < 0.05$; ** $p < 0.01$; *** $p < 0.001$.

Concurrently, the mRNA expression of FGFR2 was highly significantly downregulated in the FGF2 set-ups. Values declined 3.75-fold (day 7), 3.15-fold (day 14), 3.51-fold (day 21), and 2.72-fold (day 28) (Fig. 9.9 A, B, 'undiff' vs 'ctrl' and C, D, 'ad prediff' vs 'ctrl'). Following FGF2 addition, the FGFR2 expression decreased further to 0.25 by 25 ng mL^{-1} on day 7 of osteogenic differentiation (Fig. 9.9 A '+FGF2'). On day 14, values were downregulated to a minimum of 0.26 with the same FGF2 concentration (Fig. 9.9 B '+FGF2'). After 21 days of osteogenic conversion, FGFR2 expression decreased to 0.30 with 10 ng mL^{-1} (Fig. 9.9 C '+FGF2'). On day 28, expression declined to a minimum of 0.16 by 25 ng mL^{-1} FGF2 (Fig. 9.9 D '+FGF2').

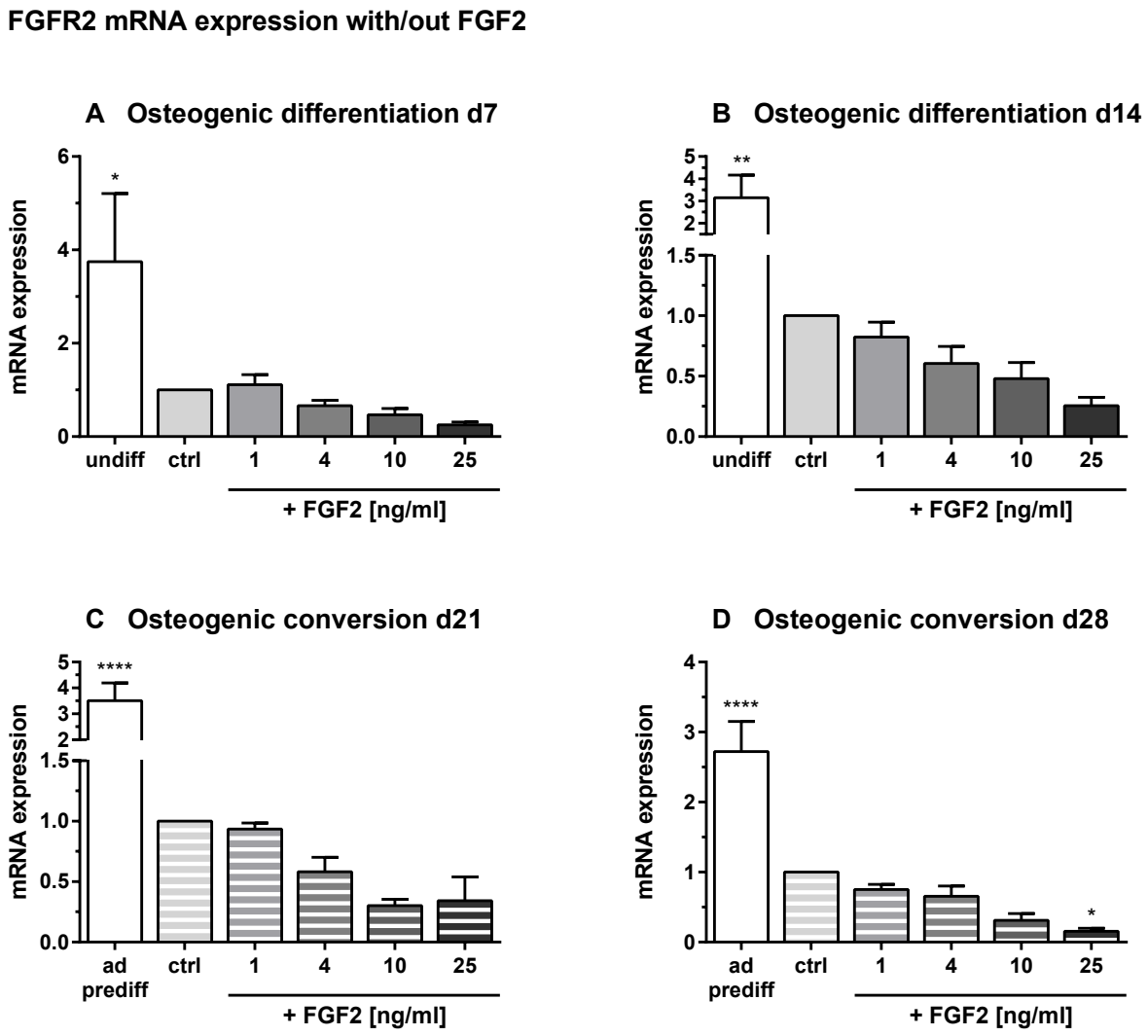

Figure 9.9: Effect of FGF2 on FGFR2 mRNA expression during osteogenic differentiation (day 7 (A) and 14 (B)) and conversion (day 21 (C) and 28 (D)). undiff: hBMSCs incubated in basal medium without differentiation supplements; ctrl: hBMSCs differentiated or converted in osteogenic medium without FGF2; 1 ng mL^{-1}, 4 ng mL^{-1}, 10 ng mL^{-1}, and 25 ng mL^{-1} FGF2: hBMSCs differentiated or converted in osteogenic medium supplemented with the respective FGF1 concentration; ad prediff: hBMSCs pre-differentiated in adipogenic medium for 14 days without further osteogenic conversion. Conversion samples were pre-differentiated in osteogenic medium for 14 days, then converted in adipogenic medium for another 14 days. For statistical analysis, samples were compared to the respective differentiation (ctrl, A, B) or conversion control (ctrl, C, D). $\tilde{x} \pm$ SEM; n = 4. * $p < 0.05$; ** $p < 0.01$; **** $p < 0.0001$.

9.3 PKC, JNK, and p38-MAPK are not responsible for FGF1 signal transduction

Knowing about the signal mediation via the receptor FGFR1, we wondered which downstream signaling pathways are involved in the further intracellular transduction of the FGF1 signal. Based on literature research, we decided to investigate a highly promising group of signaling cascades including the protein kinase C (PKC), c-Jun N-terminal kinase (JNK), p38-mitogen-activated protein kinase (p38-MAPK), and extracellular signal-regulated kinases 1 and 2 (ERK1/2) pathways.

9.3.1 PKC signaling

To investigate whether PKC and its signaling pathway are responsible for the FGF1 signal transduction, adipogenic and osteogenic differentiations under the PKC inhibitor Calphostin C were performed. Since the specific PKC inhibitor Calphostin C affected both, hBMSC viability and differentiation outcomes in preliminary experiments, different inhibitor concentrations were tested to find the optimal concentration. This should be high enough to rescue the FGF1 phenotype while maintaining viable cells and still allowing for differentiation. Differentiation outcome would be strongly affected, if the confluence of hBMSCs was impaired.

The lowest concentration of 50 nmol L^{-1} Calphostin C did not affect the amount of lipid droplet formation or mineralization compared to the respective controls (Fig. 9.10 A, B, 'ctrl' vs 'inh'). Moreover, cell number was not impaired and hBMSCs maintained confluence throughout the experiment. However, no rescue of the FGF1 phenotype was detected neither during adipogenic (Fig. 9.10 A 'inh + FGF1') nor during osteogenic differentiation (Fig. 9.10 B 'inh + FGF1').

Moreover, the Calphostin C concentration of 100 nmol L^{-1} did neither decrease cell number nor affect cell confluence. The adipogenic outcome was not altered when compared to the differentiation control (Fig. 9.10 C, 'ctrl' vs 'inh'). Yet, the formation of lipid droplets was not significantly increased through inhibitor addition to the differentiation medium containing FGF1 ('inh + FGF1'). Although the mineralization during osteogenic differentiation was markedly decreased by 3.75-fold through 100 nmol L^{-1} Calphostin C (Fig. 9.10 D, 'ctrl' vs 'inh'), the lack of a rescuing effect upon FGF1 administration was still detectable ('inh + FGF1').

In addition, the next-highest concentration of 500 nmol L^{-1} Calphostin C exhibited a strongly decreasing effect on lipid droplet formation and mineralization when compared to the differentiation controls (Fig. 9.10 E, F, 'ctrl' vs 'inh'). During adipogenic differentiation, this reduction was donor-dependent and therefore resulted in rather high standard errors of the mean (SEM) (Fig. 9.10 E 'ctrl'). As a consequence, statistical analysis did not reveal a significant rescue of the FGF1 effect. Yet notably, inhibitor addition to the FGF1-containing sample ('inh + FGF1') restored lipid droplet values to the level of the inhibitor-only sample ('inh'), which was beyond the values of the FGF1-containing sample ('inh + FGF1').

Finally, the highest concentration of 1000 nmol L^{-1} Calphostin C resulted in cell death that was pursued by decreasing cell numbers under the light microscope over the differentiation period (data not shown).

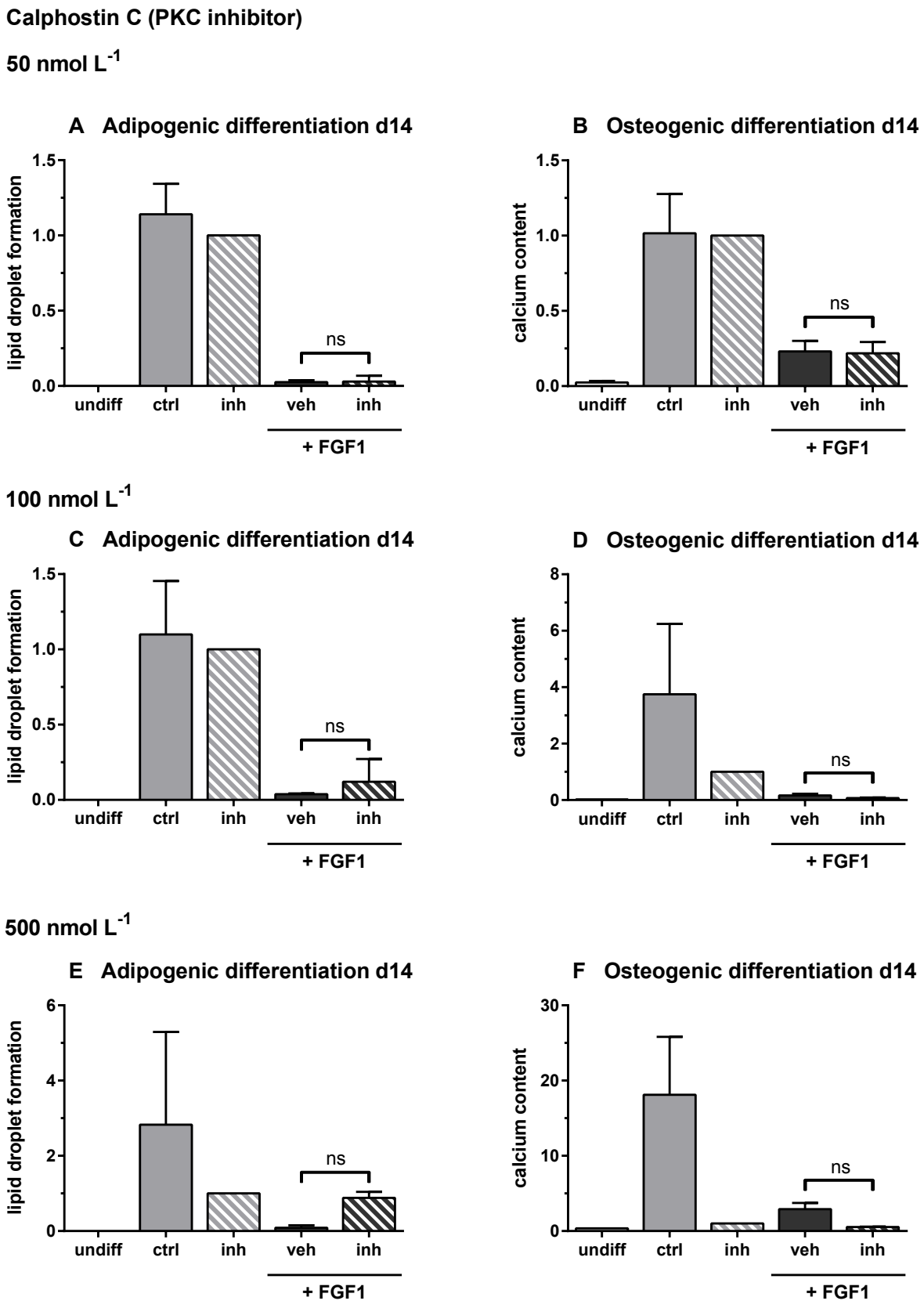

Figure 9.10: Effect of different concentrations of the PKC inhibitor Calphostin C on the FGF1 effects during adipogenic (A, C, E) and osteogenic differentiation (B, D, F). Legend continued on next page.

Figure 9.10: Legend continued from previous page.
undiff: hBMSCs incubated in basal medium without differentiation supplements; ctrl: hBMSCs incubated in adipogenic or osteogenic differentiation medium without FGF1; inh: hBMSCs differentiated in adipogenic or osteogenic medium supplemented with Calphostin C; veh + FGF1: hBMSCs differentiated in adipogenic or osteogenic medium containing the inhibitor solvent DMSO (vehicle) plus FGF1; inh + FGF1: hBMSCs differentiated in adipogenic or osteogenic medium supplemented with Calphostin C plus FGF1. For statistical analysis, samples were compared to the respective differentiation control containing inhibitor only (inh). $\tilde{x} \pm$ SEM; n = 3 for A and B; n = 2 for C-F. ns: not significant.

9.3.2 JNK pathway

In parallel to the PKC cascade, the JNK signaling pathway was tested for its involvement in the mediation of the FGF1 effect. During adipogenic differentiation, the addition of 1 µmol L^{-1} JNK inhibitor SP600125 to the differentiation cocktail led to an increase of lipid droplet formation by 1.70-fold (Fig. 9.11 A, 'ctrl' vs 'inh'). As expected, fat formation was prevented in the sample containing vehicle plus FGF1 ('veh + FGF1'). Interestingly, additional SP600125 supplementation did not result in a rescue, thus an increase in lipid droplet formation ('inh + FGF1').

During osteogenic differentiation, inhibitor addition did not lead to an alteration in mineralization outcome compared to the osteogenic differentiation control (Fig. 9.11 B, 'ctrl' vs 'inh'). The marked reduction in mineralization caused by FGF1 was not rescued by the JNK inhibitor SP600125 ('inh + FGF1').

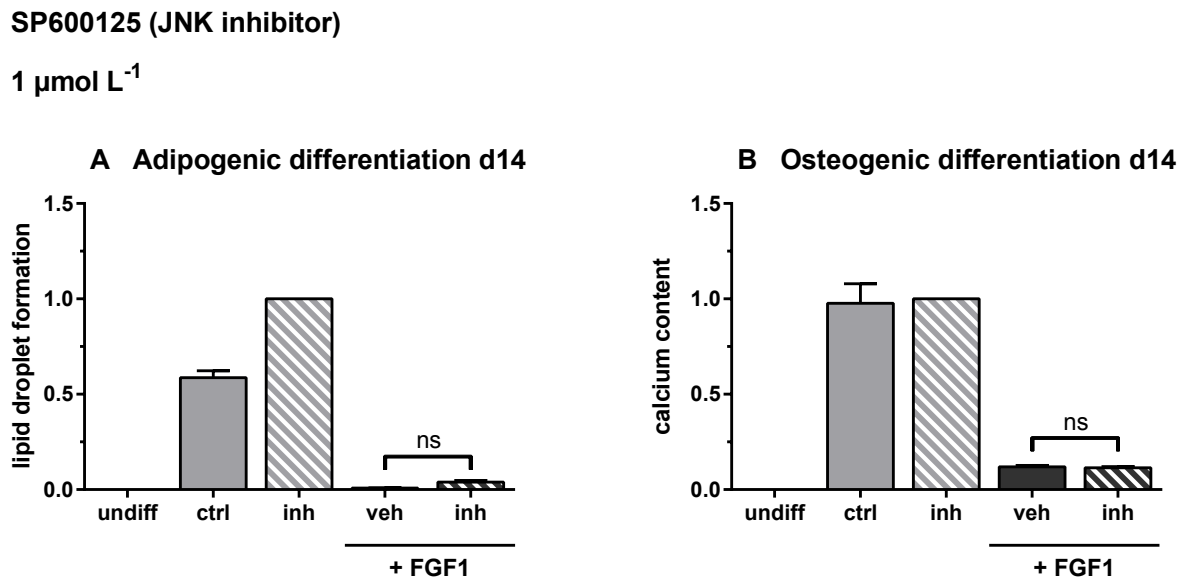

Figure 9.11: Effect of the JNK inhibitor SP600125 on the FGF1 effects during adipogenic (A) and osteogenic differentiation (B). undiff: hBMSCs incubated in basal medium without differentiation supplements; ctrl: hBMSCs differentiated in adipogenic or osteogenic medium without FGF1; inh: hBMSCs differentiated in adipogenic or osteogenic medium supplemented with SP600125; veh + FGF1: hBMSCs differentiated in adipogenic or osteogenic medium containing the inhibitor solvent DMSO (vehicle) plus FGF1; inh + FGF1: hBMSCs differentiated in adipogenic or osteogenic medium supplemented with SP600125 plus FGF1. For statistical analysis, samples were compared to the respective differentiation control containing inhibitor only (inh). $\tilde{x} \pm$ SEM; n = 2. ns: not significant.

9.3.3 p38-MAPK signaling

Besides the PKC and the JNK pathway, we also investigated the p38-MAPK signaling cascade via the specific inhibitor SB203580. After 14 days of adipogenic differentiation, the sample cultured in adipogenic cocktail containing the inhibitor displayed a distinct reduced lipid droplet formation in comparison to the differentiation control by 2.83-fold (Fig. 9.12 A, 'ctrl' vs 'inh'). Even though the sample comprising the vehicle plus FGF1 exhibited even lower lipid droplet amounts ('veh + FGF1'), the addition of the inhibitor SB203580 plus FGF1 to the differentiation medium did not result in a phenotypic rescue but in a further decrease of lipid droplet formation ('inh + FGF1').

The osteogenic differentiation displayed similar results. On day 14, the administration of the inhibitor to the osteogenic medium led to a 0.5-fold reduction in mineralization (Fig. 9.12 B, 'ctrl' vs 'inh'). Nevertheless, the effect of the FGF1 addition was still measurable, and it was not rescued by the addition of SB203580 ('inh + FGF1').

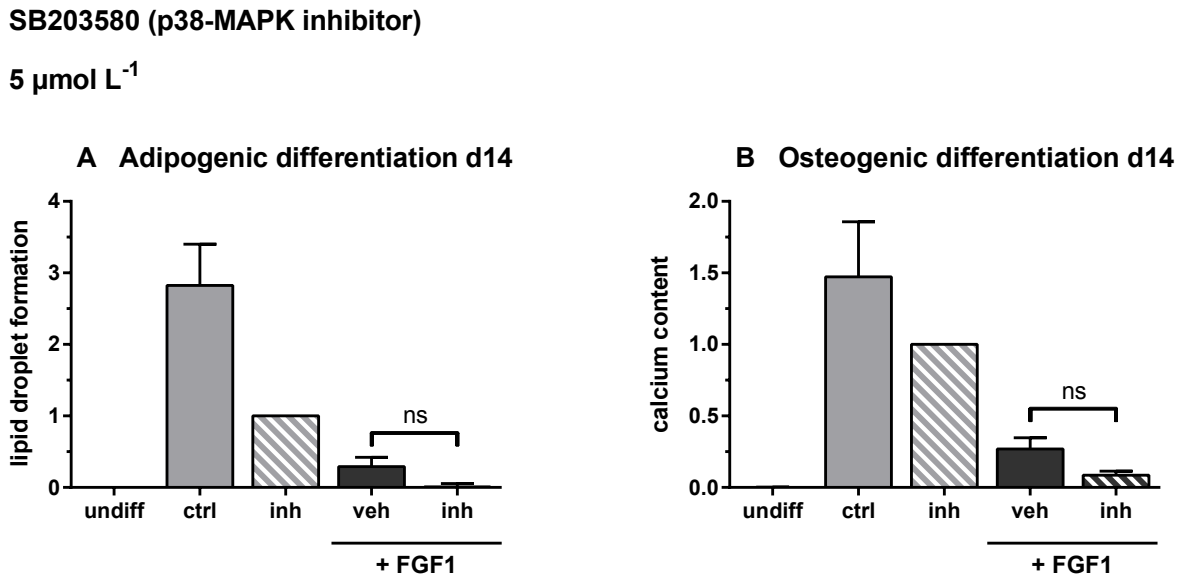

Figure 9.12: Effect of the p38-MAPK inhibitor SB203580 on the FGF1 effects during adipogenic (A) and osteogenic differentiation (B). undiff: hBMSCs incubated in basal medium without differentiation supplements; ctrl: hBMSCs differentiated in adipogenic or osteogenic medium without FGF1; inh: hBMSCs differentiated in adipogenic or osteogenic medium supplemented with SB203580; veh + FGF1: hBMSCs differentiated in adipogenic or osteogenic medium containing the inhibitor solvent DMSO (vehicle) plus FGF1; inh + FGF1: hBMSCs differentiated in adipogenic or osteogenic medium with SB203580 plus FGF1. For statistical analysis, samples were compared to the respective differentiation control containing inhibitor only (inh). $\tilde{x} \pm$ SEM; n = 4. ns: not significant.

9.3.4 p38-MAPK and MEK1/2 pathways

After having found no impact of the p38-MAPK inhibitor SB203580 on the FGF1 effects, we wondered if the the signal could be redirected over alternative MAPKs like ERK1/2, when p38-MAPK is blocked chemically. To double check the dispensability of p38-MAPK for the FGF1 signal transduction, we performed experiments with a combination of the inhibitors SB203580 and U0126. The later inhibits the MAPK/ERK kinases 1 and 2 (MEK1/2), which act directly upstream of ERK1/2 and facilitate its phosphorylation.

After adipogenic differentiation, the administration of the inhibitor combination displayed a marked decrease in lipid droplet formation by 5.85-fold compared to the differentiation control (Fig. 9.13 A, 'ctrl' vs 'inh'). Both inhibitors plus FGF1 ('inh + FGF1') exhibited an even lower formation of lipid droplets than the sample containing the vehicle plus FGF1 ('veh + FGF1'). Following osteogenic differentiation, the inhibitor combination resulted in reduced mineralization by 1.57-fold when added to the differentiation cocktail (Fig. 9.13 B, 'ctrl' vs 'inh'). However, the administration of both inhibitors with FGF1 did not increase mineralization when compared to the FGF1-containing sample ('veh + FGF1' vs 'inh + FGF1').

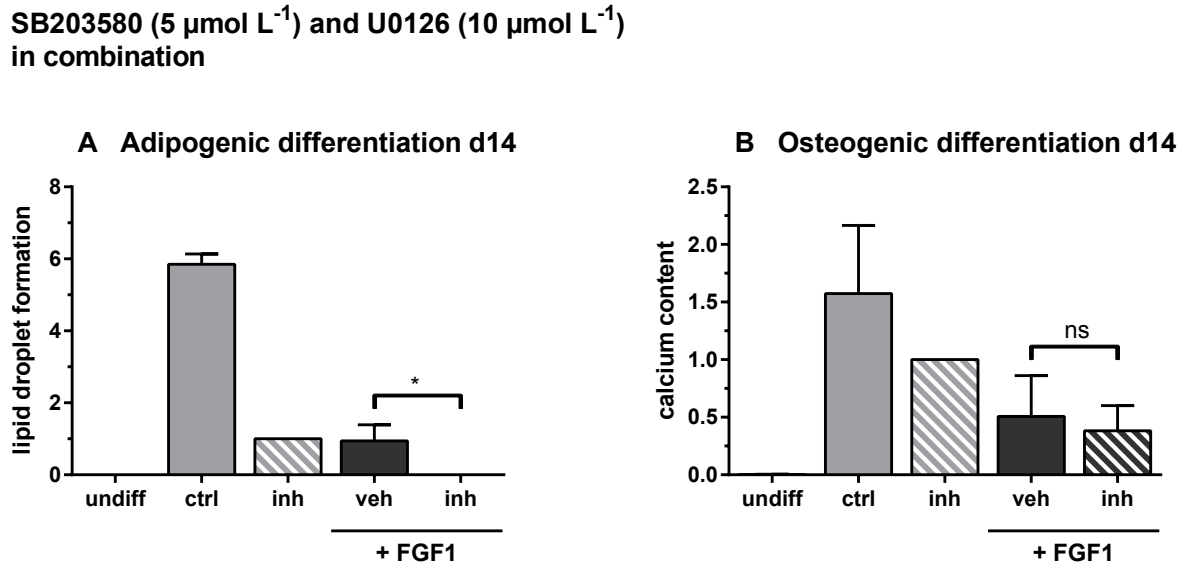

Figure 9.13: Effect of the combination of the p38-MAPK inhibitor SB203580 and the MEK1/2 inhibitor U0126 on the FGF1 effects during adipogenic (A) and osteogenic differentiation (B). undiff: hBMSCs incubated in basal medium without differentiation supplements; ctrl: hBMSCs differentiated in adipogenic or osteogenic medium without FGF1; inh: hBMSCs differentiated in adipogenic or osteogenic medium with both inhibitors; veh + FGF1: hBMSCs differentiated in adipogenic or osteogenic medium containing the inhibitor solvent DMSO (vehicle) plus FGF1; inh + FGF1: hBMSCs differentiated in adipogenic or osteogenic medium supplemented with both inhibitors plus FGF1. For statistical analysis, samples were compared to the respective differentiation control containing inhibitor only (inh). $\tilde{x} \pm$ SEM; n = 2. * $p < 0.05$; ns: not significant.

9.4 ERK1/2 is crucial for FGF1 signal transduction in adipogenic and osteogenic differentiation as well as osteogenic conversion

As neither PKC nor JNK nor p38-MAPK were found to mediate the intracellular signals underlying the FGF1 and FGF2 effects, we were prompted to investigate the ERK1/2 signaling pathway. Therefore, we deployed U0126 as an inhibitor of the MAPK/ERK kinases 1/2 (MEK1/2), which phosphorylate ERK1/2. The inhibitor U0126 was used in an assay-dependent optimum concentration of 10 µmol L^{-1} determined by preliminary experiments. Since this concentration showed slightly adverse effects on differentiation outcome, additional concentrations of 1 µmol L^{-1} and 5 µmol L^{-1}were deployed.

The concentration of 1 µmol L^{-1} neither resulted in a detectable alteration in the adipogenic nor osteogenic differentiation outcome (Fig. 9.14 A, B, 'ctrl' vs 'inh'). During adipogenic differentiation, the FGF1 effects on lipid droplet formation were partly although not significantly rescued (Fig. 9.14 A 'inh + FGF1'). However, during osteogenic differentiation, there was no rescuing effect detected (Fig. 9.14 B 'inh + FGF1').

When a concentration of 5 µmol L^{-1} U0126 was deployed during the differentiation process, adipogenic differentiation was not declined on day 14 (Fig. 9.14 C, 'ctrl' vs 'inh'). Similar to the application of the lower concentration, a slight rescuing effect was observed that did not reach significance ('inh + FGF1'). In contrast to adipogenic differentiation, the osteogenic differentiation of hBMSCs was markedly reduced by 5 µmol L^{-1} U0126 by 4.68-fold (Fig. 9.14 D, 'ctrl' vs 'inh'). The inhibitor addition did not result in a rescue of the FGF1 effect on mineralization ('inh + FGF1').

In contrast to the lower concentrations, 10 µmol L^{-1} U0126 displayed significant rescuing effects during adipogenic and osteogenic differentiation as well as osteogenic conversion. During adipogenic differentiation, the lipid vesicle formation was distinctly reduced through the sole addition of the inhibitor by 1.59-fold (Fig. 9.15 A, 'ctrl' vs 'inh'). The further reduction of the formation of lipid vesicles by FGF1 was significantly overcome by 10 µmol L^{-1} U0126 ('inh + FGF1'). After 14 days of osteogenic differentiation, the inhibitor on its own had a decreasing effect on differentiation outcome and reduced mineralization by 2.36-fold (Fig. 9.15 B, 'ctrl' vs 'inh'). Nevertheless, inhibitor addition to the FGF1-containing set-up resulted in an obvious rescue and mineralization values were significantly increased to the levels of the non-inhibitor-containing control ('inh + FGF1').

After differentiation set-ups had demonstrated the effect of U0126 in an optimum concentration of 10 µmol L^{-1}, conversion experiments were performed with this concentration. Adipogenic conversion was not markedly altered via inhibitor addition only (Fig. 9.15 C, 'ctrl' vs 'inh'). However, only a slight rescuing effect was observed in relation to FGF1 administration that did not reach significance ('inh + FGF1'). After 28 days of osteogenic conversion, the mineralization of the matrix was markedly decreased by 1.75-fold by inhibitor addition only (Fig. 9.15 D, 'ctrl' vs 'inh'). Yet, the reducing effect of FGF1 in mineralization was still detectable and inhibitor addition led to a significant rescue, increasing the values above the level of the inhibitor-only-containing control ('veh + FGF1' vs 'inh + FGF1').

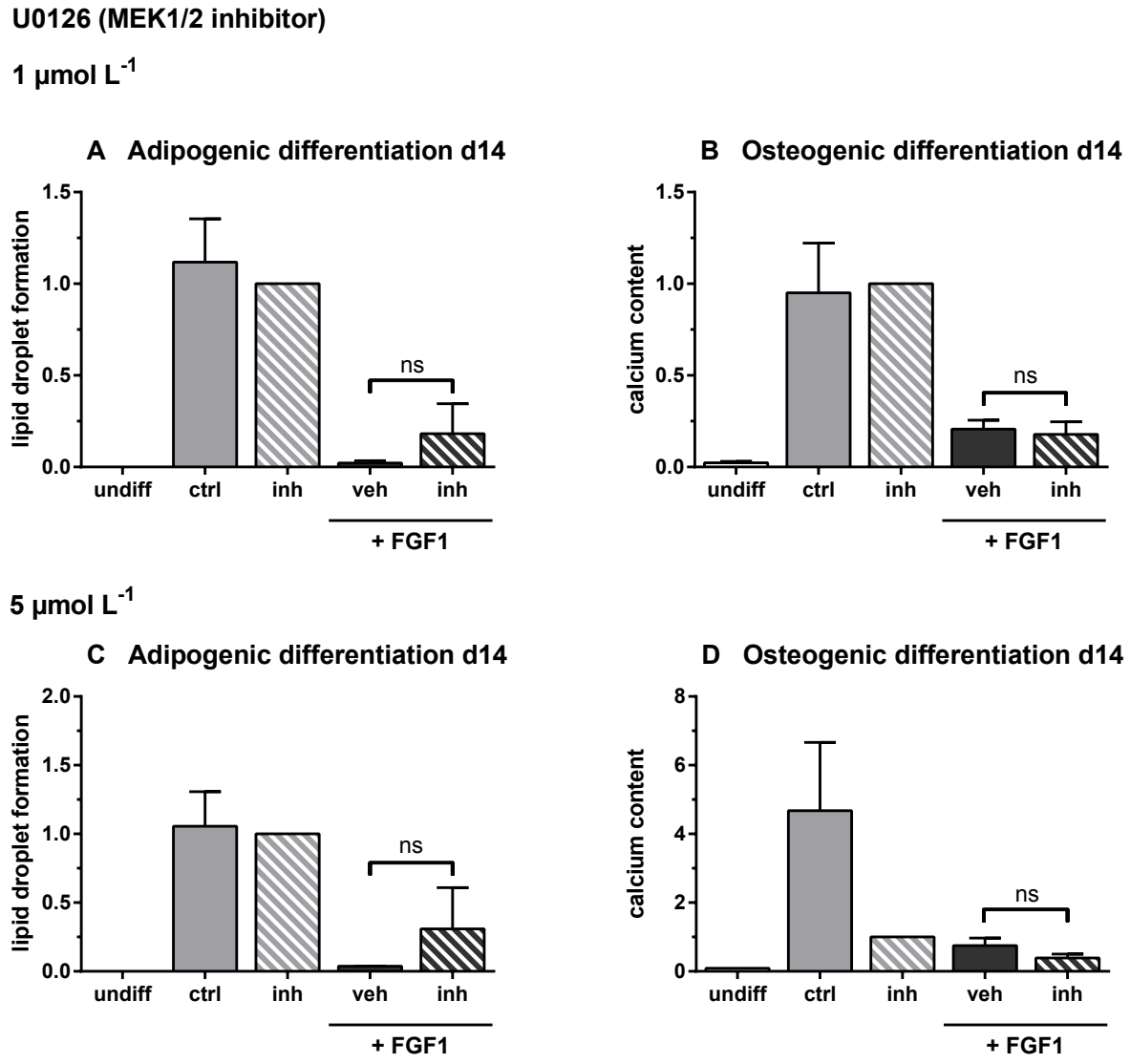

Figure 9.14: Effect of the MEK1/2 inhibitor U0126 (1 µmol L^{-1} and 5 µmol L^{-1}) on the FGF1 effects during adipogenic (A, C) and osteogenic differentiation (B, D). undiff: hBMSCs incubated in basal medium without differentiation supplements; ctrl: hBMSCs differentiated in adipogenic or osteogenic medium without FGF1; inh: hBMSCs differentiated in adipogenic or osteogenic medium supplemented with U0126; veh + FGF1: hBMSCs differentiated in adipogenic or osteogenic medium containing the inhibitor solvent DMSO (vehicle) plus FGF1; inh + FGF1: hBMSCs differentiated in adipogenic or osteogenic medium supplemented with U0126 plus FGF1. For statistical analysis, samples were compared to the respective differentiation control containing inhibitor only (inh). $\tilde{x} \pm$ SEM; n = 3 for A and B; n = 2 for C and D. ns: not significant.

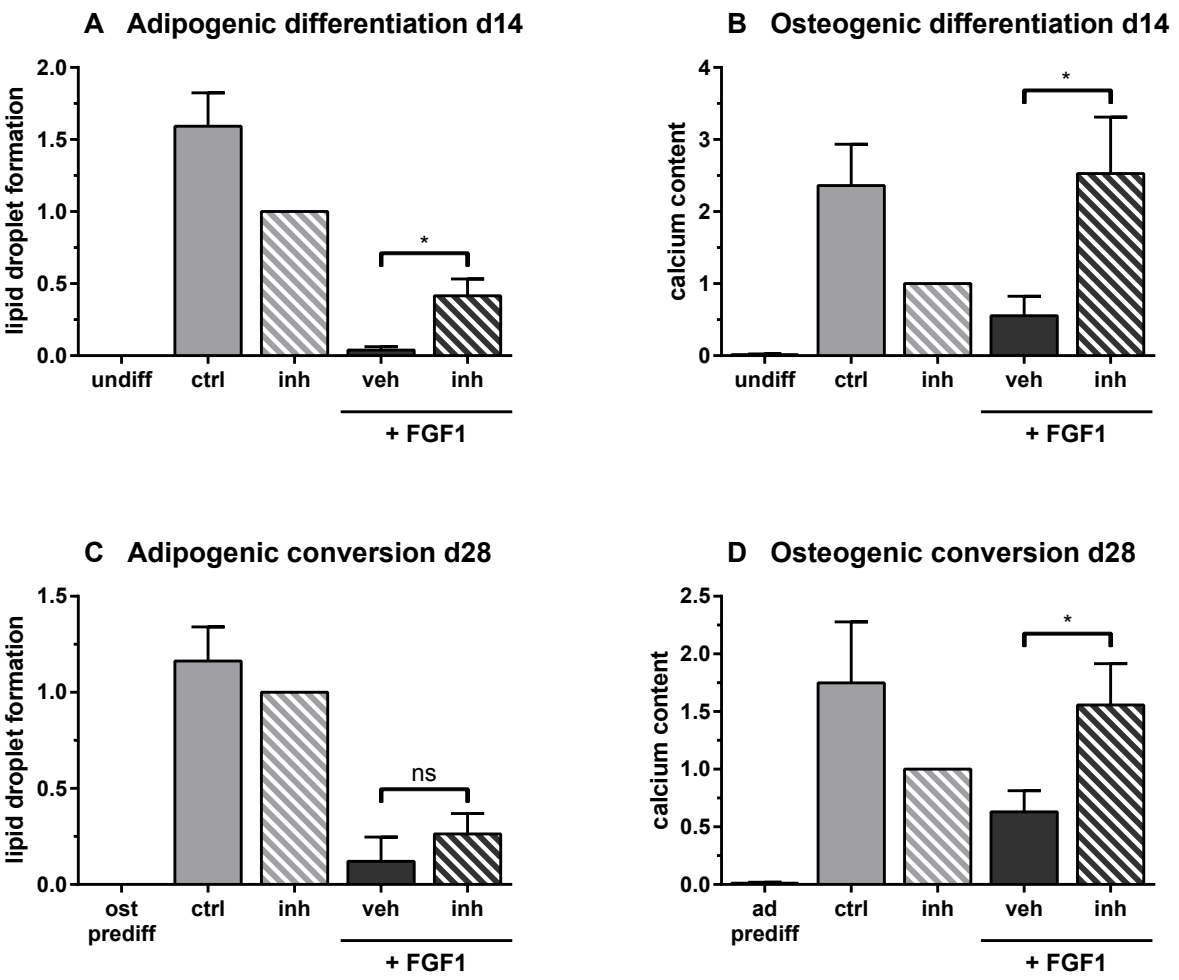

Figure 9.15: Effect of the MEK1/2 inhibitor U0126 (10 µmol L^{-1}) on the FGF1 effects during adipogenic (A) and osteogenic differentiation (B) as well as adipogenic (C) and osteogenic conversion (D). undiff: hBMSCs incubated in basal medium without differentiation supplements; ctrl: hBMSCs differentiated in adipogenic or osteogenic medium without FGF1; inh: hBMSCs differentiated in adipogenic or osteogenic medium supplemented with U0126; veh + FGF1: hBMSCs differentiated in adipogenic or osteogenic medium containing the inhibitor solvent DMSO (vehicle) plus FGF1; inh + FGF1: hBMSCs differentiated in adipogenic or osteogenic medium supplemented with U0126 plus FGF1; ost prediff: hBMSCs pre-differentiated in osteogenic medium for 14 days; ad prediff: hBMSCs pre-differentiated in adipogenic medium for 14 days. Conversion samples were pre-differentiated for 14 days, then converted in the respective other medium for another 14 days. For statistical analysis, samples were compared to the respective differentiation/conversion control containing inhibitor only (inh). $\tilde{x} \pm$ SEM; n = 4 for A and D; n = 4 for B and C. * $p < 0.05$; ns: not significant.

Part IV

Discussion

10 Effect of FGF1 and FGF2 on hBMSC differentiation and conversion

The clinically highly relevant bone disorder osteoporosis is commonly accompanied by an increased accumulation of adipose tissue in the bone marrow, referred to as 'fatty degeneration'[1]. Moreover, the cell number of bone-forming osteoblasts is markedly reduced[2]. Evidence suggests an inverse relationship between the adipogenic and the osteogenic direction of differentiation in primary human bone marrow stromal cells (hBMSCs)[17]. Hence, a pathologically increased adipogenic hBMSC differentiation at the expense of osteogenesis may account for the reduced osteoblast number and the fat accumulation in bone marrow[2]. Aside from this preferential adipogenic differentiation of undifferentiated hBMSCs, the conversion of pre-differentiated osteoblastic cells into the adipogenic lineage (adipogenic conversion) may further contribute to it. Therefore, counteracting and/or reversing adipogenic hBMSC differentiation and conversion might not only reduce the clinical sign of fat accumulation, which is connected to poorer bone quality[22], but as well unclose a supply of osteoblastic cells arising from undifferentiated and adipogenically pre-differentiated hBMSCs.

As reported previously, fibroblast growth factor 1 (FGF1) was inversely regulated during adipogenic and osteogenic conversion processes, while FGF2 was downregulated during adipogenic conversion[46]. Both FGFs were scored as promising regulators of conversion processes, which might activate signaling pathway(s) favoring osteogenesis over adipogenesis in bone marrow precursor cells. Therefore, downstream molecules might represent a pharmaceutical target for a novel approach for osteoporosis therapy and/or prevention. Literature has reported contradictory results regarding the effects of FGF1 and FGF2 on adipogenesis and osteogenesis and especially studies deploying primary hBMSCs are scarce. To the best of our knowledge, our study is the first to thoroughly describe the impact of FGF1 and FGF2 on both adipogenic and osteogenic lineage decisions and conversion processes of primary hBMSCs in parallel.

The three key aims presented in chapter 4 will be addressed as follows: [1] The effects on adipogenesis will be discussed in chapter 11, divided into differentiation (11.1 and 11.2) and conversion (11.3). The results on osteogenesis will be discussed in chapter 12, including mineralization (12.1), alterations in marker gene expression (12.2, 12.3, and 12.4), and a special focus on conversion (12.5). [2] Underlying signaling pathways will be discussed in 11.4 and 12.6 and the events during differentiation and conversion will be summarized in 11.5 and 12.7 for adipogenesis and osteogenesis, respectively. [3] Finally, conclusions with regard to exercising control over the adipogenic and osteogenic differentiation and conversion processes of hBMSCs will be drawn in chapter 13.

11 Impact of FGF1 and FGF2 on the adipogenesis of hBMSCs

The investigation of the effect of FGF1 and FGF2 on the adipogenic differentiation and conversion of hBMSCs was carried out by culture in the presence of different FGF concentrations during the differentiation/conversion period in our *in vitro* model. To examine the extend of the adipogenic outcome after differentiation and conversion, several readouts on the histological and transcriptional level were combined. The quantification of intracellular lipid formation was established and served as a reliable indicator for adipogenesis occurring *in vitro*. Moreover, gene expression analysis of different adipogenic marker genes revealed underlying transcriptional mechanisms. Peroxisome proliferator-activated receptor $\gamma 2$ (PPAR$\gamma 2$) depicts the master regulator of adipogenic commitment and differentiation[28]. Moreover, it inhibits osteogenic differentiation[151,152] by downregulating osteogenic marker genes[153] thereby representing a possible tool for lineage switching. The CCAAT/enhancer binding protein α (C/EBPα) constitutes another early key marker driving the onset of adipogenic differentiation. PPAR$\gamma 2$ and C/EBPα create a positive feedback loop by activating each others promoter regions[31]. In addition, they activate key factors involved in lipogenesis like fatty acid binding protein 4 (FABP4) and lipoprotein lipase (LPL).

11.1 Inhibition of adipogenic differentiation by FGF1

Our results from Oil red O staining and lipid droplet assay clearly depict that culture in the presence of FGF1 completely inhibited the formation of lipid droplets during adipogenic differentiation (Fig. 7.2 A). Moreover, FGF1 addition resulted in a highly significant reduction of early (PPAR$\gamma 2$ and C/EBPα) as well as late (FABP4 and LPL) adipogenic marker gene expression (Fig. 7.4). The highest concentration of $25\,\mathrm{ng\,mL^{-1}}$ FGF1 decreased values completely or at least nearly complete to the levels of undifferentiated hBMSCs. In summary, the results displayed a high reproducibility over the different donors.

These anti-adipogenic observations stand in striking contrast to the work of Hutley and colleagues, who reported that FGF1 promoted adipogenesis in mesenchymal precursors isolated from adipose tissue, referred to as human pre-adipocytes (hPAs)[154]. The adipogenic markers triacylglycerol accumulation and glycerinaldehyde-3-phosphate dehydrogenase (GAPDH) activity were distinctly increased following FGF1 addition. Furthermore, the pharmacological inhibition of FGF1 signaling at multiple steps suppressed pre-adipocyte replication and differentiation[154]. Taken together, FGF1 seemed to perform a priming effect on the hPAs during their proliferative stage, which was characterized by an increased expression of the adipogenic marker PPARγ before the induction of differentiation, signifying an increased commitment of hPAs to the adipogenic linage. Interestingly, the murine pre-adipocyte cell line 3T3-L1, a broadly used model for adipogenesis, did not display an increased differentiation potential following FGF1 treatment. But since the authors found FGF1 to be endogenously expressed in 3T3-L1 cells, which are known for their highly efficient adipogenic differentiation potential, they suggested FGF1 to be a key human adipogenic factor.

However, in these studies the major adipogenic effect of FGF1 occurred during the proliferative stage of development. Therefore, it might mainly be a cause of an increased cell number of pre-adipocytes since FGFs are known to act as proliferative factors. Moreover, the increased confluence of the cells

in vitro itself might have further supported the adipogenic differentiation because, as known from experimental experience, differentiation processes work best in confluent monolayers. Nevertheless, the platelet-derived growth factor (PDGF), showing a comparable mitogenic potential to FGF1, failed to increase the adipogenic differentiation potential of hPAs[155]. Subsequently, Widberg and colleagues confirmed that FGF1 was priming pre-adipocytes for adipose differentiation during their proliferation.

When comparing these previous studies reporting a pro-adipogenic effect of FGF1 to my current study proving an anti-adipogenic effect, the origin of deployed cells has to be considered. Whereas the aforementioned studies of Hutley and Widberg *et al.* were carried out with precursor cells isolated from adipose tissue, my study is based on stromal precursors from bone marrow. It is likely that the cells referred to as hPAs were in a different stage of commitment/differentiation when deployed in the experiments: The hPAs might already have been primed towards adipogenesis before the start of the experiments, meaning before FGF1 administration. In contrast, the hBMSCs deployed in my study might have been 'unprimed' or – regarding their bone marrow origin – they might rather be primed towards osteogenesis than adipogenesis. In conclusion, the use of mesenchymal precursor cells from different body sites is likely to be the cause of the opposing study outcome.

Additional evidence drawn from the literature supports this conclusion. Firstly, Newell and colleagues, who published a pro-adipogenic impact of FGF1 like the above mentioned studies, used hPAs as well. They reported an increased expression of adipocyte markers during differentiation under FGF1 administration[156]. Moreover, hPAs differentiated in the presence of FGF1 were more insulin responsive and secreted increased levels of the adipocyte marker adiponectin, further underlining an increase in adipogenesis. Secondly, FGF1 was found to enhance adipogenic differentiation of 3T3-L1 pre-adipocytes[157]. Thirdly, a dual-stage delivery of FGF1 and bone morphogenetic protein 4 (BMP4) via a three-dimensional (3D) hydrogel significantly elevated lipid accumulation in human adipose-derived stromal cells (hASCs) when compared to a simultaneous delivery[158]. Greenwood-Goodwin *et al.* concluded that the dual-stage release of FGF1 and BMP4 within 3D micro-environments promoted the *in vitro* differentiation of mature adipocytes and referred to FGF1 as a 'pro-adipogenic' factor[158]. Nevertheless, the supporting effect of FGF1 on adipogenic differentiation is again likely to be a result of the cells' adipose origin and commitment preceding FGF1 addition.

However, our finding of an inhibiting effect on adipogenic differentiation is further supported by *in vivo* data. When challenged with a high fat diet (HFD), FGF1 knockout mice ($FGF1^{-/-}$) developed an aggressive diabetic phenotype linked with an aberrant expansion of adipose tissue[159]. This is remarkable since $FGF1^{-/-}$ mice do not show a specific phenotype under standard laboratory conditions. Interestingly, HFD resulted in a marked induction of FGF1 expression restricted to adipose tissue, which was regulated by PPARγ acting via an evolutionary conserved promoter situated at the PPARγ response element within the FGF1 gene. Hence, FGF1 seems to play an important role in adipogenic differentiation of precursor cells and adipose tissue expansion by preventing excessive adipogenesis. It has to be taken into account that there are different kinds of adipose tissue present in the body, which are distinctly characterized by e.g. localization, morphology, and function and which might be affected differently by FGF signaling.

Based on current literature and our results, we conclude that the effect of FGF1 on adipogenic differentiation is dependent on the tissue origin of the deployed precursor cells and their commitment and differentiation status. Although pro-adipogenic effects were shown and well described for mesenchymal precursors derived from adipose tissue, the stromal cells of bone marrow origin in our study clearly displayed anti-adipogenic reactions when FGF1 was administered throughout the course of

differentiation and conversion. This underlines the importance of deploying an appropriate *in vitro* model based on mesenchymal precursors of bone marrow origin to properly investigate the effect of FGF1 on the preferential adipogenesis that likely plays a role in osteoporosis. Furthermore, the comparison to current literature hints at a tissue or site-specific effect that results in adipogenic inhibition limited to mesenchymal precursors of the bone marrow but not other mesenchymal tissues like adipose tissue. A site-specific effect of FGF1 and its downstream target molecules would be advantageous for a therapeutic approach to avoid side-effects in e.g. fat storages of the body.

11.2 Reduction of adipogenic differentiation by FGF2

When discussing the impact of FGF1 on adipogenesis, the effects of FGF2 have to be considered in parallel. The previous studies in our group displayed that FGF2 was regulated similarly as FGF1 during osteogenic conversion, thereby hinting at a comparable impact on adipogenic and osteogenic fate decisions[46]. Moreover, FGF2 resembles FGF1 in protein structure and both growth factors signal via the same receptors FGFR1-4[66]. Concurrently, we hypothesized that the culture in the presence of FGF2 would exert similar effects in our *in vitro* model of differentiation and conversion as FGF1. In the current study, FGF2 distinctly reduced lipid droplet formation and downregulated the expression of all four examined adipogenic marker genes in a highly significant and clearly concentration-dependent way (Fig. 7.3 A, 7.6). The highest concentration of 25 ng mL^{-1} proved to be the most effective. Yet, the expression levels of FGF2-supplemented samples did not recede to the basal level of undifferentiated or osteogenically pre-differentiated hBMSCs as did those supplemented with FGF1.

Although FGF2 acted nearly identical to FGF1, the latter displayed a more pronounced effect on adipogenic inhibition. This may be caused by the additional supplementation with heparin in all FGF1 set-ups although other differences like e.g. receptor-ligand affinity can not be excluded. Heparin is a negatively charged and highly sulfated glucosaminoglycan known to interact with a multitude of proteins including growth factors, chemokines, cytokines, enzymes, extracellular matrix proteins, lipoproteins, and hormone receptors[160–165]. More importantly, heparin and heparan sulfates coordinate the binding of canonical FGFs like FGF1 and FGF2 to their receptor, thereby most probably controlling FGF signaling[66]. Albeit, in current literature FGF2 is mainly deployed without the addition of heparin, whereas experiments covering FGF1 commonly include heparin supplementation. Therefore, in order to achieve comparable results, we focused on experimental set-ups featuring heparin only for FGF1 approaches. In conclusion, different outcomes for FGF1 and -2 may be caused by heparin addition and the effects of FGF1 and FGF2 ought not to be compared to each other directly.

In line with our findings, Roncari *et al.* found that FGF2 significantly inhibited adipose differentiation of perirenal pre-adipocytes from rats cultured *in vitro*[166]. Inhibition became almost complete at the higher concentrations of up to 63 nmol L^{-1}. Similarly, FGF2 inhibited the differentiation of human pre-adipocytes while stimulating their replication[167]. Moreover, FGF2 prevented the adipose differentiation of 3T3-L1 pre-adipocytes[157]. Also consistent with our findings, FGF2 treatment of human adipocyte precursor cells caused a significantly reduced activity of the adipose marker GAPDH with concentrations ranging from 10 ng mL^{-1} to 100 ng mL^{-1}[168]. FGF2 addition to the primary culture of newly developed fat cells also decreased their GAPDH activity. Similarly, FGF2 reverted the full adipogenic differentiation of the murine adipose cell line TA1 at a concentration of 10 ng mL^{-1}[169].

In addition to exogenous FGF2 administration, the endogenous FGF2 expression seems to be negatively affected by adipogenic differentiation as well. Differentiated pre-adipocytes revealed a de-

creased FGF2 mRNA and protein expression compared to undifferentiated pre-adipocytes[167]. Likewise, a high-molecular weight form of FGF2 was initially strongly expressed in hPAs, but expression decreased markedly 6-9 days after induction of differentiation directly coinciding with the first appearance of visible lipid droplets within the cells[170]. Interestingly, Hutley and colleagues, who reported the pro-adipogenic effect of FGF1 administration on adipogenic differentiation of hPAs (see 11.1), finally linked their observations to an endogenous downregulation of FGF2[171]. The supplementation of exogenous FGF1 reduced endogenous FGF2 mRNA and protein expression by approx. 80%. Similarly, siRNA knockdown of FGF2 increased adipogenic marker gene expression of PPARγ, GAPDH, and adiponectin, thereby pointing again at a negative correlation between FGF2 and adipogenesis. These results highlight the complexity of the paracrine interplay between FGFs within human adipose tissue.

In contrast to my study and those mentioned before, some studies reported pro-adipogenic effects of FGF2. During different phases of cell culture, FGF2 supplementation led to a strongly enhanced adipogenesis of mesenchymal stem cells (MSCs) isolated from bone marrow of Sprague Dawley rats[172]. The PPARγ2 mRNA expression was upregulated prior to adipogenic induction and the responsiveness of MSCs towards the PPARγ ligand troglitazone was strongly increased. Moreover, Kakudo and colleagues reported that FGF2 significantly enhanced the adipogenic differentiation of human adipose-derived stem cells (hASCs) from abdominal subcutaneous fat; the mRNA expression of PPARγ2 was upregulated when receiving FGF2 before the induction of adipogenesis[173]. It should be considered that in our system, in contrast to the study by Kakudo *et al.*, FGF2 administration only started after the proliferation phase together with the induction of differentiation.

In summary, the role of FGF2 on adipogenesis is controversial in literature, since both positive and negative effects have been reported. When administered only during the proliferation phase before adipogenic induction, a positive impact on adipogenesis was observed, which was similar to the outcome of studies on FGF1 discussed in 11.1. Our opposing observation of an anti-adipogenic effect are in line with earlier findings in several cell types, where FGF2 was administered during the differentiation phase. In conclusion, this outcome highlights the influence of the time point and duration of the treatment. Moreover, the results hint at a reprogramming event that might 'homogenize' the commitment state of the heterogeneous population of adipogenic and mesenchymal precursor cells to an early phase. When administered during proliferation, as described in several publications, this homogenization seems to increase the cells' response to the following stimuli of adipogenic induction. This is also supported by the paper of Neubauer *et al.*, where pre-treatment with FGF2 for 3 days in the proliferative phase prior to differentiation induction increased the adipogenic outcome in hMSCs in comparison to the non-pre-treated control[172]. However, when a pre-treatment was performed on confluent hBMSCs monolayers for 3 days prior to the start of adipogenic differentiation during the current project, we observed a significant decrease of the adipogenic outcome to 60% (data not shown). These findings further highlight the influence of the cell confluence and the impact of the proliferative vs. post-proliferative state, respectively.

11.3 Impact on adipogenic conversion

After examining the effect of FGF1 and FGF2 on adipogenic differentiation, we were prompted to gain deeper insight into the lineage switching of pre-differentiated osteoblastic cells into adipocytes, termed adipogenic conversion. Conversion (then referred to as 'transdifferentiation') was defined by Song *et al.* as one cell type being committed to and progressing along a specific developmental lineage

switching into another cell type of a different lineage through genetic reprogramming[23]. Firstly, after the induction of adipogenic conversion by a medium switch from osteogenic to adipogenic medium, my results distinctly showed an upregulation of early (PPARγ2 and C/EBPα) and late (FABP4 and LPL) adipogenic marker genes (Fig. 7.5). This upregulation was highly significant and reproducible through all donors, reaching two- to three-digit and even four- to five-digit increases for early and late adipogenic markers, respectively.

Secondly, lipid droplet accumulation increased significantly within the cells (Fig. 7.2). Finally, several sets of osteogenic markers were obviously downregulated by adipogenic conversion itself, covering the early genes runt-related transcription factor 2 (RUNX2) and BMP4, the markers of osteoblastic maturation collagen 1 A1 (COL1A1) and osteocalcin (OC) (Fig. 7.8, 7.9), and the mineralization markers ANKH inorganic pyrophosphate transport regulator (ANKH) and osteopontin (OPN) (Fig. 7.11, Fig. 7.13). The conversion of hBMSCs was previously established in our lab and has been characterized so far by semi-quantitative PCR with the downregulation of the osteogenic markers alkaline phosphatase (ALP) and OC and the upregulation of PPARγ2 and LPL, accompanied by the histologically detected accumulation of lipid droplets[24]. The current study was the first to apply quantitative measurements for transcriptional and histological alterations including qPCR and lipid droplet assay. Thereby, it more precisely characterized our system of adipogenic conversion in hBMSC-derived osteoblastic cells and, hence, strengthened its impact.

Apart from our approach, conversion events from the osteogenic to the adipogenic lineage were described before. Most interestingly and in line with our findings, fully differentiated hMSC-derived osteoblasts showing increased ALP enzyme activity and matrix mineralization were found to be still capable to change fate into adipocytes displaying lipid droplet formation and LPL gene expression *in vitro* by Song and colleagues[23]. This was especially remarkable because it had been widely accepted that as differentiation progresses, the multiple differentiation potentials of mesenchymal cells gradually became more restricted, such that terminally committed osteoblasts would be unable to differentiate into other cell types.

However, the concept of conversion was challenged by critical considerations regarding the heterogeneous nature of primary hMSC populations. Accordingly, 'contaminating' progenitor cells might be present in the starting cell population that could be non-responsive to osteogenic induction while being responsive to adipogenic induction. In consequence, when the culture environment was switched, these progenitors would appear to be 'converted'. For this reason, the observed conversion phenomenon was validated by starting with a homogeneous population of osteogenic cells whose differentiation status was experimentally ascertained[23]. hMSCs were transfected with a green fluorescent protein (GFP)-expression vector driven by the OC promoter and GFP-positive cells were selected by fluorescence activated cell sorting (FACS) after 15 days of osteogenic differentiation. When seeded in high dilution in adipogenic medium, approx. 40% of these osteoblastic cells were still capable of adipogenic conversion on the single cell level. Regarding the difficult experimental conditions aggravating hMSC viability and differentiation, e.g. vector transfection, cell sorting, and single cell culture, these data convincingly proved the capacity of pre-differentiated hMSCs to be converted into another mesenchymal lineage.

Apart from the work of Song *et al.*, Foo and colleagues reported that the human fetal osteoblastic cell line hFOB 1.19 displayed intracellular lipid accumulation accompanied by the downregulation of bone cell markers when cultured in the presence of the estrogen receptor blocker Fulvestrant[35]. This, again, indicates a conversion of committed or differentiated osteoblastic cells towards the adipogenic

lineage. In addition, MSC-derived committed osteoblastic cells upregulated the adipogenic markers LPL and leptin while downregulating OC mRNA expression when co-cultured with adipocytes *in vitro*[36]. Thus, MSC-derived adipocytes seemed to be able to initiate the osteoblasts to convert into the adipogenic phenotype. Furthermore, the thiazolidinedione pioglitazone, a prescription drug used for the treatment of diabetes mellitus type 2, promoted the adipogenic conversion of BMSCs from rat *in vitro*[37]. The study also displayed that lipid droplets appeared earlier in cells that were osteogenically pre-differentiated for only 5 days than in those being pre-differentiated for 14 days; this hints at a necessary de-differentiation period preceding the second differentiation or 'conversion' step. In contrast, several isoflavones were found to inhibit the adipogenic conversion of murine MSC-derived osteoblastic cells[33]. Taken together, these publications highlight that osteoblastic cells are capable of reprogramming events towards the adipogenic lineage and that such conversions can be initiated or blocked by distinct substances.

In line, my findings clearly exhibit that FGF1 as well as FGF2 inhibited the conversion of osteogenically pre-differentiated hBMSCs by preventing the adipogenic lineage switch. The upregulation of the adipogenic marker genes usually taking place with adipogenic conversion was blocked with high significance (Fig. 7.5, 7.7). Similarly, the formation of lipid droplets was inhibited (Fig 7.2 B, 7.3 B). The result that both FGF1 and FGF2 strongly prevented the adipogenic conversion of osteogenically pre-differentiated cells is in accordance with the previous findings from microarray analysis[46], where FGF1 and FGF2 were scored as two of the most promising candidates for initiating lineage switching from the adipocytic to the osteoblastic lineage.

Interestingly, FGF2 was shown before to possibly promote lineage switching towards osteogenesis at the expense of adipogenesis in mice by Xiao *et al.*[116]. Here, the FGF2 knockout ($FGF2^{-/-}$) mice had a greater accumulation of bone marrow fat in long bones than wild type littermates. Additionally, $FGF2^{-/-}$ BMSCs displayed a reduced ALP activity and mineralization but a marked increase of adipocyte cell number and adipogenic marker gene expression (PPARγ2 and FABP4) when cultured in the respective differentiation medium *in vitro*. Treatment with exogenous FGF2 blocked adipocyte formation and increased ALP activity. However, in contrast to these findings, ALP mRNA expression was not augmented by FGF2 or FGF1 administration in our study (data not shown). Also the osteogenic master regulator RUNX2 and further osteogenic markers like BMP4, COL1A1, and OC were not markedly regulated via FGF addition to the adipogenic conversion set-ups (Fig. 7.8, 7.9).

Yet, like the study of Xiao an coworkers, our results also highlight the role of PPARγ2, which was significantly downregulated during adipogenic conversion by FGF1 and FGF2. This adipogenic master regulator was found to critically influence the lineage decision between adipogenesis and osteogenesis in mesenchyme-derived cells in recent studies. After lentiviral knockdown of PPARγ expression in the murine bone marrow of the femur *in vivo*, adipocyte cell number and adipogenic markers significantly decreased, whereas the amount of osteoblasts was enhanced and osteoclast cell number was reduced[174]. Meanwhile, trabecular micro-architecture was significantly increased. In addition, the suppression of the PPARγ transactivation of target genes by i.e. non-canonical Wnt signaling promoted osteoblast differentiation[19]. Furthermore, it was repeatedly demonstrated that PPARγ ligands promoted the adipogenic differentiation of bone marrow stromal cells while inhibiting their osteogenesis[175–179]. They did not only activate PPARγ but also suppressed RUNX2 gene expression and activity[177]. Moreover, the antidiabetic drug Rosiglitazone, a potent PPARγ ligand, increased the volume of bone marrow adipose tissue while reducing bone mineral density and trabecular bone area[179]. Even more interestingly, the critical role of PPARγ in the balance and commitment of adipogenesis and osteoblastogenesis was shown using transgenic mice[20]. Homozygous $PPAR\gamma^{-/-}$ embryonic stem

cells failed to differentiate into adipocytes while spontaneously differentiating into osteoblasts, which was restored by PPARγ gene reintroduction. Furthermore, heterozygous PPAR$\gamma^{+/-}$ mice displayed higher bone mass than wild type littermates; this difference became more prominent with aging. In addition, PPARγ haploinsufficiency stimulated increased osteoblastogenesis of bone marrow progenitors *in vitro*. To conclude, the marked downregulation of PPARγ2 expression by FGF1 and FGF2 might represent a vital prerequisite for the lineage switching towards osteoblastogenesis.

Apart from affecting adipogenic marker gene expression, FGF1 and FGF2 also upregulated the osteogenic markers of mineralization ANKH and OPN. Values even exceeded the expression levels of osteogenically pre-differentiated samples for 25 ng mL^{-1} FGF1 (Fig. 7.11, 7.13). Similarly, ANKH and OPN mRNA expression was also upregulated during adipogenic differentiation when FGF1 and FGF2 were added (Fig. 7.10, 7.12). ANKH plays an important role in matrix mineralization during osteogenesis; by regulating the transport of inorganic pyrophosphate, it is capable of inhibiting bone mineral formation[180]. Moreover, ANKH function might exert a negative effect on adipogenesis since its chemical inhibition increased adipogenic differentiation (Fig. 8.25 C). Yet, ANKH inhibition was not able to revert the effects of FGF1 on adipogenesis (Fig. 8.25 C).

OPN is as well able to inhibit matrix mineralization yet represents one of the proteins forming the osteoid[180]. Interestingly, a role of OPN in the lineage decision between adipogenic and osteogenic differentiation of mouse MSCs was described before[38]. Blocking OPN function promoted adipogenic and inhibited osteogenic differentiation. Re-expression of OPN in OPN$^{-/-}$ MSCs restored a normal balance between adipogenesis and osteogenesis. Furthermore, OPN was shown to inhibit the C/EBP signaling pathway, which is crucial for the onset of adipogenesis, through the OPN receptor integrin $\alpha v/\beta 1$. In consistence with these *in vitro* results, OPN$^{-/-}$ mice had a higher fat to total body weight ratio than wildtype littermates. In conclusion, the upregulation of OPN by FGF1 and FGF2 in our hBMSC *in vitro* system could be a probable cause or at least a promoter of the inhibition of adipogenesis by blocking C/EBP signaling and thereby inhibiting the onset of adipogenesis.

Taken together, our *in vitro* model of adipogenic conversion was further characterized by deploying quantifying measurements for the first time. An enlarged set of adipogenic marker genes was shown to be upregulated while lipid droplet formation increased. Meanwhile, the expression of a broadened number of osteogenic markers like RUNX2, BMP4, COL1A1, and OC decreased by adipogenic conversion itself. Moreover, our results displayed that FGF1 and FGF2 were potent factors to diminish the conversion of osteoblastic cells into the adipogenic fate. This could be mediated via the downregulation of PPARγ2, omitting its shift of lineage decisions towards adipogenesis at the expense of osteogenesis. Likewise, OPN upregulation by FGF1 and FGF2 may further relocate the balance of differentiation by blocking adipogenic onset via the integrin-C/EBP-axis. However, a direct positive or supportive effect of FGF1 and FGF2 on the expression of marker genes concerning osteogenic induction, like RUNX2, BMP4, and ALP, as well as osteoblastic maturation, like COL1A1, IBSP, OC, could not be experimentally verified during adipogenesis. Also, the increased expression of the osteogenic markers OPN and ANKH must be interpreted carefully since they might rather be related to an inhibitory or reducing impact concerning bone mineral formation than to an osteogenic lineage switching itself. Given however that FGF1 and FGF2 seem to be able to 'homogenize' the state of commitment and differentiation, enhance the proliferation of mesenchymal precursors, and may optimize the adipogenic and osteogenic potential (when given in the proliferative phase), their application during hBMSC expansion in tissue engineering procedures might be considered.

11.4 Signaling pathways mediating the anti-adipogenic effect

The fact that FGF1 and FGF2 exerted similar effects on adipogenesis indicated that underlying signaling processes were mediated via the same FGF receptor. The more pronounced effects of FGF1 were most probably a result of the additional supplementation with heparin that coordinated and stabilized the binding to the FGF receptor. Consequently, experiments concerning underlying signaling pathways focused on FGF1 with the most efficient concentration of $25\,\mathrm{ng\,mL^{-1}}$. Knowing from preceding microarray analyses within our group that hBMSCs only expressed FGFR1 and FGFR2 (Dr. Tatjana Schilling, personal communication, June 10, 2015), experiments with the potent FGFR1 inhibitor PD166866[181] were performed in order to find the responsible receptor. If FGFR1 was the responsible receptor, PD166866 addition would rescue the phenotype of suppressed lipid formation.

My results clearly showed that the FGFR1 inhibitor PD166866 was a potent agent to rescue the effects caused by FGF1 during adipogenic differentiation (Fig. 9.1 A). Yet, PD166866 might as well affect other receptors apart from FGFR1 including FGFR2 or other members of the receptor tyrosine kinase family. However, the rather stable expression of FGFR1 during the whole course of adipogenic differentiation and conversion further indicated that the described signal was predominantly mediated via FGFR1 (Fig. 9.2, 9.3). In contrast, FGFR2 was markedly downregulated (Fig. 9.4, 9.5). In addition to the inhibitor experiments, differentiation set-ups were performed after deploying small hairpin RNAs (shRNAs) to knockdown the gene expression of either FGFR1 or FGFR2; they also pointed at FGFR1 to be the responsible receptor (data not shown). Since alternative splicing was shown to give rise to the FGFR1 isoform IIIc in mesenchymal lineages[76–79], we suggest that this receptor variant could be mainly responsible for the FGF1 signal transduction in our system.

Interestingly, the importance of the FGFR1 has been highlighted before by other studies. The FGF1 effects on adipogenic differentiation found by Widberg *et al.* were dependent upon signal transduction by FGFR1[155]. Moreover, a decrease in FGFR1 expression preceded the significant reduction of FGF2 expression during adipogenic differentiation of hPAs[170]. These transcriptional changes coincided with the first appearance of visible lipid droplet formation within the cells clearly pointing at the crucial role of FGF signaling via FGFR1 for adipogenesis. In summary, we conclude that the FGFR1 is the receptor mainly responsible for mediating the observed anti-adipogenic FGF effects in our study.

However, the rescuing effect of the inhibitor PD166866 was only partial during adipogenic conversion (Fig. 9.1 C). This coincides with a more decreased FGFR1 expression during adipogenic conversion compared to differentiation (Fig. 9.2, 9.3, A vs. B), suggesting that the FGF1 signal might be redirected at least in part over an alternative signaling route under this condition. Moreover, the FGFR3 and FGFR4 were previously shown to be not expressed in hBMSCs by microarray analyses. Taken together, we cannot finally answer the question which receptor might be additionally responsible for FGF signal mediation during adipogenic conversion so far.

Knowing about the responsible receptor at the cell surface, we asked which intracellular downstream signaling cascades were involved. Therefore, distinctive pathways were chosen based on recent literature and targeted with selective chemical inhibitors. The different concentrations of the protein kinase C (PKC) inhibitor Calphostin C did not significantly rescue the FGF1 phenotype (Fig. 9.10 A, C, E). However, the highest concentration of $500\,\mathrm{nmol\,L^{-1}}$ markedly decreased adipogenic differentiation itself, so that a slight rescuing effect on adipogenic inhibition by FGF1 could not be foreclosed (Fig. 9.10 E). Nevertheless, if PKC would play a major role in mediating the anti-adipogenic FGF function, a rescuing effect should be observable even at lower Calphostin C levels (Fig. 9.10 A, C). PKC is a member

of the serine/threonine protein kinase family playing important roles in the control of various cellular functions and its involvement in adipogenesis has been reported in other *in vitro* systems so far. It is activated via phospholipase C (PLC) γ and its subsequent hydrolysis into inositol triphosphate (IP3) and diacylglycerol[48,90].

When PKCη[182] and PKCϵ[183] were ectopically expressed in the multipotent murine embryonic fibroblast cell line NIH-3T3, these cells could be induced to undergo adipocyte differentiation in response to adipogenic culture conditions. Furthermore, PKCϵ protein expression increased during the course of terminal differentiation in committed 3T3-F442A murine pre-adipocytes and was co-localized with C/EBPβ, one of the transcription factors critically involved in the initiation of adipogenesis[183]. In addition, treatment with PKC inhibitors suppressed the adipogenesis of 3T3-L1 pre-adipocytes[184]. Taken together, literature demonstrated a crucial role for PKC signaling in both adipogenic commitment and pre-adipocyte terminal differentiation. Although PKC did not mediate the anti-adipogenic FGF effect in our system, my results clearly confirmed that PKC signaling plays a vital role in the adipogenic differentiation of primary hBMSCs among other signaling cascades.

Experiments concerning c-Jun N-terminal kinase (JNK) signaling clearly revealed that this pathway was not responsible for the transduction of the FGF signal either (Fig. 9.11 A). Yet, the sole addition of the JNK inhibitor SP600125 to the adipogenic medium promoted differentiation itself. The JNK is a downstream effector of the Ras/MAPK pathway, together with i.e. the p38-mitogen activated protein kinase (p38-MAPK), and the extracellular signal-regulated kinase (ERK)[48,88]. My results are in agreement with earlier findings reporting a negative link towards adipogenesis. JNK seemed to mediate a shift in lineage decisions towards osteogenesis at the expense of adipogenesis[185]; when investigating the effect of the widely used bisphosphonate Alendronate, SP600125 addition would block Alendronate's pro-osteogenic regulation of BMSC differentiation . Hence, my findings further underline this negative correlation between JNK signaling and adipogenic differentiation.

When examining the p38-MAPK pathway, no reverting effect on the anti-adipogenic FGF function was found (Fig. 9.12 A). Nevertheless, adipogenic outcome itself was decreased by the p38-MAPK inhibitor SB203580. However, when the MAPK p38 is chemically blocked by SB203580, it might be possible that the signal transduction is redirected over an alternative MAPK signaling route like ERK1/2 and their upstream kinases MAPK/ERK kinases 1 and 2 (MEK1/2). As a consequence, no phenotypic rescue of the FGF1 effects could be observed, eventually, and the involvement of p38-MAPK would be concealed. Thus, in literature, set-ups including inhibitors for these two pathways exist in combination, even though they are scarce. For this reason, experiments with SB203580 and the MEK1/2 inhibitor U0126 were performed in combination, which showed no rescue of the FGF effect, but strongly decreased adipogenic differentiation itself (Fig. 9.13 A). Hence, an involvement of the p38-MAPK hidden by an alternative signaling route via MEK1/2 was excluded. Consistent with our findings, suppressing effects on adipogenesis through the combined treatment with SB203580 and U0126 were described earlier in hMSCs[186]. Furthermore, our results give additional evidence that p38 and MEK1/2 play a crucial supporting role in hBMSC adipogenesis.

Considering the negative outcome of PKC, JNK, and p38-MAPK inhibitor experiments, the involvement of ERK1/2 signaling was investigated. The present data clearly displayed that the ERK1/2 pathway was crucial for the intracellular transduction of the FGF1 signal that lead to the negative effects on adipogenic hBMSC differentiation (Fig. 9.15 A). In contrast, the impact of inhibitor addition during adipogenic conversion was not significant (Fig. 9.15 C) suggesting that an alternative signaling pathway was underlying the marked anti-adipogenic effects of FGF1 and FGF2 during conversion. This

might be linked to the only partial involvement of the FGFR1 during adipogenic conversion discussed above (Fig. 9.1 C).

In accordance with our findings on differentiation, FGFs are known and potent activators of the MEK/ERK pathway[55]. More intriguingly, a negative connection between ERK activation and adipogenic differentiation has been demonstrated before. Kim and colleagues revealed that ERK phosphorylation facilitates the well studied inhibition of adipogenesis by the pre-adipocyte factor 1 (Pref-1)[187]. By activating ERK, Pref-1 prevented the induction of PPARγ2 gene expression. Similarly, we observed the inhibition of PPARγ2 by FGF1 and FGF2 in our study, which points at a mutual pathway for the prevention of adipogenic differentiation. Moreover, ERK phosphorylation was involved in the effect of sodium butyrate that promoted MSC lineage decisions in favor of osteogenesis while suppressing adipogenesis[188]. In line with our findings, JNK and p38 cascades were not responsible. Another parallel was a marked decrease in PPARγ2 expression.

Even more interesting, ERK facilitated the induction of the transcriptional co-activator with PDZ-binding motif (TAZ) during FGF2 administration in the murine multipotent mesenchymal cell line C3H10T1/2[189]. TAZ is known to inhibit adipocyte differentiation while promoting osteogenesis in MSCs[190]. Its nuclear localization was increased by FGF2, enabling the interaction with RUNX2 to activate RUNX2-mediated gene transcription[189]. Thus, FGF1 and FGF2 might prevent adipogenic differentiation and conversion by inducing TAZ via the ERK1/2 signaling cascade in our system. However, the previous microarray analysis did not reveal alterations of TAZ expression during conversion itself (Dr. T. Schilling, personal communication).

In contrast to these studies, a rapid but transient ERK activation during the initial phase of adipogenic induction seemed to be necessary for adipogenic differentiation in 3T3-L1 pre-adipocytes[191,192]. This is in accordance with our findings of a reduced adipogenic differentiation capacity under U0126 administration (Fig. 9.15 A). Interestingly, even during the initial phase of adipogenic differentiation, FGF1 and FGF2 were found to prolong and induce robust ERK phosphorylation[156,191]. This might account for the pro-adipogenic effects of FGF1 on pre-adipocyte differentiation, however, the effect on bone marrow precursors was clearly anti-adipogenic. In summary, our study plainly depicts that ERK1/2 signaling facilitates the observed effects of FGF1 on adipogenic differentiation. This underlines literature evidence that prolonged ERK activation suppresses adipogenic differentiation and might be able to shift lineage decisions towards osteogenesis.

11.5 Summary adipogenic differentiation and conversion

Taken together, the culture in the presence of FGF1 and FGF2 strongly prevented adipogenic differentiation and adipogenic conversion of osteogenically pre-differentiated cells. These findings are in line with earlier studies describing an anti-adipogenic effect when FGF1 and FGF2 were given during the phase of cell differentiation but not proliferation. The FGF effects preventing adipogenic differentiation were transduced via the FGFR1 and intracellularly mediated by the MEK1/2 and ERK1/2 signaling cascade (Fig. 11.1). An impact of PKC, JNK, and p38-MAPK on FGF signal transduction was excluded, even though these pathways affected adipogenic hBMSC differentiation itself in a positive (PKC and p38) or negative manner (JNK). In contrast to differentiation, adipogenic conversion displayed a markedly decreased involvement of the FGFR1, which might be connected to the involvement of an alternative intracellular signaling pathway since ERK1/2 was not involved in FGF1 signal transduction.

Especially the strong downregulation of the adipogenic key transcription factor PPARγ2 is likely to be the crucial factor in adipogenic prevention by FGF1 and FGF2. As shown in current studies, this downregulation also holds the possibility for a lineage switching towards osteogenesis[19,20,151–153,174,177], yet does not necessarily include it[193]. In line with recent literature, PPARγ2 induction was inhibited by ERK activation (Fig. 11.1). Moreover, the expression of the early marker C/EBPα was inhibited by FGF addition. Hence, the positive feedback loop between PPARγ2 and C/EBPα, which normally drives adipogenesis[31], could not be installed. Furthermore, the anti-adipogenic transcription factor TAZ might as well be induced through ERK activation as was described in murine C3H10T1/2 cells[189]. In consequence, these processes led to a diminished FABP4 and LPL transcription as well as lipid formation and finally to a strong inhibition of adipogenesis and adipogenic lineage switching of pre-differentiated osteoblastic cells. However, the administration of FGF1 and FGF2 did not seem to be able to initiate osteogenesis when given during adipogenic differentiation and conversion since several key osteogenic marker genes were not induced. The effects on osteogenic differentiation and conversion will be discussed in the following chapter.

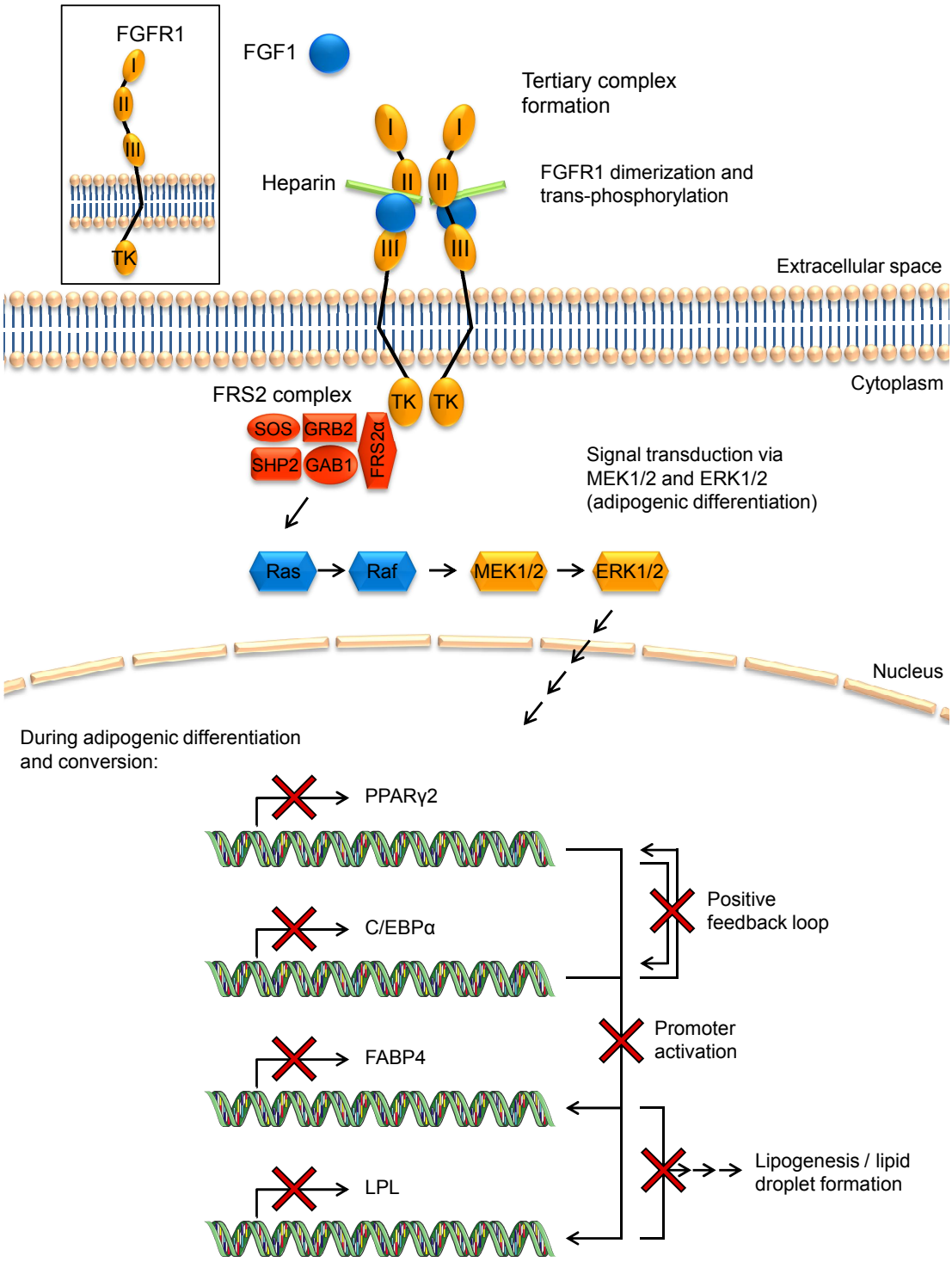

Figure 11.1: FGF1 signal transduction during adipogenic differentiation and conversion. The inhibiting effect on adipogenic differentiation is mediated via the FGF receptor (FGFR) 1. Upon ligand binding, the tertiary complex is formed from two FGF, two FGFR1, and two heparin molecules. This leads to FGFR1 dimerization and trans-phosphorylation of tyrosine residues. Subsequently, the adaptor protein FGFR substrate (FRS) 2α is phosphorylated and recruits the FRS2 complex.
Legend continued on next page.

Figure 11.1: Legend continued from previous page.
The signal is further transduced via the MEK1/2 and ERK1/2 pathway, which are probably activated via Ras/MAPK signaling. Signal transduction during adipogenic conversion seems to be only partly mediated by FGFR1 while being intracellularly transduced by an alternative signaling route. Nevertheless, the culture in the presence of FGF1/2 results in specific alterations of adipogenic gene expression with strong inhibition of PPARγ2, C/EBPα, FABP4, and LPL during both adipogenic differentiation and conversion. Like this, the early adipogenic markers PPARγ2 and C/EBPα are not able to create the positive feedback loop that normally drives the onset of adipogenesis. Moreover, the subsequent promoter activation of later adipogenic marker genes is diminished. Consequently, lipogenesis and lipid droplet formation are prevented. Figure in part adapted from Servier Medical Art (`http://www.servier.com/Powerpoint-image-bank`).

12 Impact of FGF1 and FGF2 on the osteogenesis of hBMSCs

Considering the anti-adipogenic effect on hBMSC differentiation and conversion on the one hand, we asked whether the culture in the presence of FGF1 and FGF2 would provide a positive, supporting effect on osteogenesis on the other hand. Both lineages descend from the same mesenchymal precursor cells and scientific evidence suggests an inverse relationship between these two cell fates[17]. Finding a signaling molecule or cascade to favor osteogenesis at the expense of adipogenesis could aid in reverting the fat accumulation in bone marrow. Moreover, adipogenically pre-differentiated cells might be used as a source for cells of the osteoblastic lineage to overcome the decreased osteoblast cell number during osteoporosis and aging. However, although adipogenesis of hBMSCs was strongly prevented by FGF1 and FGF2, the findings of our study clearly displayed a suppressing effect on osteogenic outcome.

12.1 Reduction of the ECM mineralization

The extend of osteogenic differentiation was determined by several read-outs. The mineralization of the extracellular matrix (ECM) formed by the osteoblasts is one of the most reliable, especially *in vitro*. Therefore, the calcium quantification assay was introduced, which directly represents the formation of the bone mineral hydroxyapatite $Ca_{10}(PO_4)_6(OH)_2$, which makes up to 60% of bone (with bone matrix proteins and water each constituting another 20%)[3]. Mineralization is initiated via matrix vesicles secreted by osteoblasts, which contain membrane-associated ALP and PHOSPHO-1, a cytosolic phosphatase with specificity for phosphoethanolamine and phosphocholine[6]. These two enzymes mainly facilitate the mineralization process. The major role of ALP is to hydrolyze the mineralization inhibitor inorganic pyrophosphate (PP_i) to enable mineral precipitation and growth[6,180,194]. Besides, this cleavage generates inorganic phosphate (P_i) that is needed for hydroxyapatite formation[195,196]. Subsequently, ALP acts as a center for calcium and phosphate deposition leading to the nucleation and growth of hydroxyapatite crystals[197].

When analyzing the mineralization of the ECM during osteogenic differentiation and conversion, the most interesting finding was a significant reduction by the addition of FGF1 and to a lesser extent FGF2 (Fig. 8.2, 8.3). This reduction became smaller when differentiation proceeded from day 14 to day 28 (Fig. 8.2, 8.3, A, B), hinting at a delaying effect. In addition, also the Alizarin red S stainings displayed a marked reduction in mineralization by FGF1 and FGF2 culture (Fig. 8.1 A, B, 'ARS'), yet mineralization discrepancies increased with time, here (A 'd14' vs. 'd28'). Apart from decreased mineralization, ALPL mRNA expression was significantly repressed (Fig. 8.4, 8.6). Likewise, ALP enzyme activity was diminished in conversion samples on day 21 by FGF1 and FGF2 (Fig. 8.5 B, 8.7 B). Although a decrease of ALP activity on day 7 of osteogenic differentiation was not observed (Fig. 8.5 A, 8.7 A), histological ALP stainings performed on day 14 displayed a visually reduced enzyme activity (Fig. 8.1 A, 'ALP') suggesting that the decrease in enzyme activity followed the transcriptional downregulation with a delay of several days, thereby being more prominent at the endpoint of differentiation/conversion.

The smaller effects of FGF2 compared to FGF1 were most likely in part caused by the additional supplementation of heparin with FGF1, yet other distinctions like e.g. a different ligand-receptor affinity

can not be excluded. As explained in the previous section 11.2, heparin acts as a co-factor for FGFR binding and activation[49]. Yet, current literature usually did not include its addition in experiments featuring FGF2 since it is contained in FCS. However, missing heparin addition might account for the reduced effect of FGF2 in our set-ups.

In line with my findings, matrix mineralization and ALP expression were also blocked when primary and immortalized OB1 murine osteoblasts were induced to undergo osteogenic differentiation under the administration of $10\,ng\,mL^{-1}$ FGF1 and heparin *in vitro*[124]. Similar results were found in rat fetal osteoblasts[198]. Moreover, FGF2 significantly inhibited ALPL gene expression in the murine osteoblast precursor cell line MC3T3-E1[125] and in primary murine osteoblasts[126]. In agreement, $50\,ng\,mL^{-1}$ FGF2 markedly reduced the differentiation and mineralization of the human osteoblast-like osteosarcoma cell line Saos-2, displayed by a downregulation of ALPL mRNA expression as well as a decrease of bone nodule formation[118]. Furthermore, the ALP enzyme activity and the *in vitro* mineralization capacity of the matrix vesicles were markedly inhibited.

Similarly, the treatment with $50\,ng\,mL^{-1}$ FGF2 over 28 days of osteogenic differentiation markedly decreased matrix mineralization and ALP activity in human calvarial osteoblastic cells[122]. In accordance, the inhibition of FGF receptors in hMSCs enhanced matrix calcification and the expression and activity of ALP induced by BMP2 addition[127]. Likewise, anti-osteogenic effects were also reported in primary human osteoblasts, where $10\,ng\,mL^{-1}$ FGF2 reduced the expression of ALP and further osteoblastic markers *in vitro*[128]. Comparably to the current study, osteoblasts were isolated from femoral trabecular bone tissue from the hip joint or knee.

Unlike these studies demonstrating an inhibition of osteogenic differentiation by FGF1 and FGF2, others reported a promoting effect of FGF2. Treatment with FGF2 induced ALP mRNA expression in hBMSC from rib[110] and increased ALP activity[111] and ALP protein levels in hMSCs under osteogenic culture conditions[112]. Besides, murine MSCs treated with FGF2 for two passages (followed by FGF9 treatment during the third passage) displayed an increased mineralization *in vitro* and were more successful in forming new bone *in vivo* when transplanted in immunodeficient mice[113]. Likewise, FGF2 co-treatment increased the mineralization of cell cultures from elderly mouse and human bone when compared to BMP2 administration alone[114]. Moreover, FGF2 administration promoted calcium deposition in marrow MSCs[115].

However, it is apparent that all of these studies started FGF2 administration already during the proliferative phase. In contrast, in my experimental set-up FGFs were only administered in the course of differentiation that followed proliferation. Thus, the described pro-osteogenic effects were most probably a result of an increased proliferation of osteoblastic precursor cells as suggested by the aforementioned findings of Walsh, Kizhner, and Tang *et al.*[110,113,198]. In our current study, this effect was precluded by the distinct experimental set-up, where hBMSCs were grown to post-confluence before initiating osteogenic differentiation and FGF addition. Therefore, our data clearly depict that FGF1 and FGF2 reduce and arrest the osteogenic differentiation and mineralization of post-confluent hBMSCs. In conclusion, the comparison of my results with current literature suggests that the effects of FGF2 and FGF1 on osteogenic differentiation are dependent on the time point of supplementation, like during the adipogenic differentiation process.

Taken together, the causal link between the addition of FGF1 and FGF2 and a reduced mineralization under osteogenic conditions was reported before in murine and human osteoblastic cell lines. Our findings demonstrated that this link also applies to primary hBMSCs. It was connected to the significant downregulation of ALPL expression and reduction of enzyme activity. Since ALP is known to

cleave the mineralization inhibitor PP_i into P_i, the substrate of hydroxyapatite, these data suggest that the decreased mineralization resulted from increased extracellular PP_i levels inhibiting hydroxyapatite formation. To further unravel the underlying mechanisms, the expression of additional correlating marker genes were investigated.

12.2 Upregulation of markers inhibiting ECM mineralization

Bone mineralization is not only linked to mRNA expression and enzyme activity of ALP but also strongly connected to the function of the ectonucleotide pyrophosphatase/phosphodiesterase 1 (ENPP1), the multiple-pass transmembrane protein inorganic pyrophosphate transport regulator ANKH, and the secreted phosphoprotein OPN. In short, these factors ectoplasmically synthesize PP_i (ENPP1) and regulate its transport into the extracellular space (ANKH). Here, the mineralization inhibitor PP_i is cleaved by the ALP enzyme into P_i, one of the substrates for the inorganic bone matrix component hydroxyapatite. Whereas ALP activity and the presence of P_i facilitate and promote hydroxyapatite formation, the presence of PP_i and OPN in the extracellular space inhibit it[180,199]. At the same time however, OPN is one of the main organic components of bone matrix and acts as a linking and structural protein in bone tissue.

When analyzing the mRNA expression levels of ANKH, ENPP1, and OPN using qPCR, we found distinct alterations. ANKH expression was markedly upregulated by FGF1 addition with significant fold-changes on day 28 of osteogenic conversion (Fig. 8.18). FGF2 administration led to only slight upregulations with the highest concentration of $25\,ng\,mL^{-1}$ (Fig. 8.21). OPN was slightly upregulated by FGF1 on the later time points of differentiation and conversion (Fig. 8.20). Examining OPN protein expression using whole cell lysates could not confirm the increased expression (Fig. 8.24). Most likely, the small upregulations observed on the transcriptional level did not result in an increase of protein that could be detected by Western blotting. Yet, the performance of this analysis was based on previous results from a subset of donors, where FGF1 administration led to more pronounced OPN upregulations. This suggests that this effect occurs donor-dependently. Another reason could be that this phospho-protein was not detected in the cell lysates because it was secreted into the extracellular space immediately after its synthesis. In addition, the expression of ENPP1 was downregulated via FGF1 mainly on day 14 of osteogenic differentiation and on day 21 of conversion, where it reached significance (Fig. 8.19). FGF2 addition resulted in a slight downregulation of ENPP1 reaching significance for day 14 of differentiation (Fig. 8.22).

In agreement with my results, the work of Hatch *et al.* linked the inhibition of mineralization and the downregulation of ALP expression by FGF2 to the upregulation of ANK, the homologous gene of ANKH in mouse, on the mRNA and protein level[200–203]. Here, $50\,ng\,mL^{-1}$ FGF2 was administered to the murine pre-osteoblast cell line MC3T3-E1[200–202] and murine primary pre-osteoblast cultures[203]. Likewise, $10\,ng\,mL^{-1}$ FGF2 upregulated ANK mRNA expression in the murine osteocyte cell line MLO-Y4 under mineralizing culture conditions[204]. Moreover, when treated with $10\,ng\,mL^{-1}$ FGF1 plus $5\,IU\,mL^{-1}$ heparin or $10\,ng\,mL^{-1}$ FGF2 alone, the mRNA and protein expression of human ANKH and its murine counterpart ANK were induced in human fibroblasts and the mouse embryonic fibroblast cell line NIH-3T3[205].

Apart from the ANKH upregulation, expressional increases of OPN after FGF administration were described earlier as well. The mRNA and protein expression of OPN was upregulated by FGF1 treatment in rat aortic smooth muscle cells, hinting at a connection to the pathological mineralization dur-

ing atherosclerosis[206]. Similarly, OPN expression was increased by FGF1 administration in parallel to osteogenic culture conditions in rat fetal osteoblasts[198]. Also, FGF2 promoted OPN transcription by 16.7-fold in Saos-2 cells[207]. As shown by the study of Harmey *et al.*, OPN levels were increased in knockout mice deficient of ALP expression[180]. Moreover, elevated PP_i levels lead to upregulated OPN expression in wildtype murine osteoblasts. Since the PP_i levels in our system are likely to be increased because of the reduced cleavage by ALP enzyme, this might be the reason underlying the OPN upregulation.

Whereas my findings clearly depicted an ENPP1 downregulation, literature reported the upregulation of ENPP1 due to FGF1 and FGF2 administration. FGF1 and FGF2 treatment of the osteoblast-like sarcoma cell lines Saos-2 and U2OS in a concentration of $10\,ng\,mL^{-1}$ induced ENPP1 expression and activity[208]. Meanwhile, ALP activity was downregulated in accordance with my results. In addition, FGF2 stimulated ENPP1 expression in murine pre-osteoblasts isolated from calvaria[209]. Interestingly, when initially investigating the kinase ENPP1, Oda and colleagues co-purified it with the FGF1 receptor and revealed that it responds to FGF1 stimulation[210]. In sharp contrast to my findings, also the studies of Hatch and Kyono mentioned above connected the FGF-driven upregulation of ANKH to significant increases in ENPP1 expression[200–204]. However, the ENPP1 upregulation peaked after 12 h and 24 h and displayed a subsequent decrease, which was already marked after 48 h. This highlights that there may be fundamental differences between acute regulatory effects of FGFs on direct target genes and long-term effects depending on a program proceeding over days, following permanent FGF stimulation. Interestingly, wildtype murine osteoblasts treated with PP_i showed a decrease in ENPP1 expression in line with my findings[180].

To sum up, the phenotype of reduced mineralization and downregulated ALPL levels was expanded by distinctive regulations of mineralization marker genes. As ANKH transports PP_i into the extracellular space, the ANKH upregulation could further contribute to the elevated PP_i levels. Yet, our finding that pharmacological inhibition of ANKH by Probenecid did not rescue the reduced mineralization phenotype strongly contradicts this hypothesis (Fig. 8.25 B, D). An intriguing explanation is that the downregulation of ENPP1, the PP_i producing enzyme, could override the effects of ANKH upregulation concerning extracellular PP_i levels. Besides, it was described that ENPP1 is capable of exhibiting phosphatase activity only in the case of reduced ALPL expression and ALP deficiency, respectively, thereby partly substituting ALP function[6]. Yet, since both ALP and ENPP1 are downregulated in our system, this back-up cannot be installed.

Apart from downregulated ALP expression, the upregulation of OPN probably further impeded hydroxyapatite formation and mineralization in the respective donors; this can be concluded from the knockout experiments by Millán and co-workers, where the hypo-mineralization of the skeleton observed in ALP knockout mice was shown to arise from the combined inhibitory effects of PP_i and OPN[180]. Moreover, we hypothesized if FGF1 and FGF2 would probably alter osteogenic differentiation not only at the relatively late stage of ECM mineralization but also at an earlier time point during ECM formation and osteogenic commitment . To analyze these earlier stages of osteogenic differentiation, the gene expression changes of further osteogenic markers were examined.

12.3 Downregulation of osteogenic markers for ECM formation

Before the process of matrix mineralization can take place, the ECM is build by osteoblastic cells, then surrounds and progressively entraps them while it hardens by calcium deposition[3]. In bone

tissue, the ECM constitutes of two main components, the inorganic and the organic one. Hydroxyapatite forms the inorganic part of the bone, meanwhile, the organic part of bone comprises several collagenous and non-collagenous proteins. COL1A1 is the main organic component. After being secreted by osteoblasts, it builds fibrils, along which the hydroxyapatite crystals form[197]. Beyond that, the integrin-binding sialoprotein (IBSP) is one of the major structural non-collagenous proteins and has been implicated in the nucleation of hydroxyapatite. Moreover, OC is another structural non-collagenous protein secreted by osteoblasts. As high OC protein levels are well correlated with increased bone mineral density (BMD), it is used as a preliminary bio-marker for bone formation.

The organic components of the ECM represent later markers of osteogenic differentiation. Their mRNA expression was monitored throughout osteogenic differentiation and conversion in the presence of FGF1 and FGF2. The mRNA expression of OC was downregulated for day 7 of osteogenic differentiation by FGF1 and depicted slight upregulations in FGF-containing samples for later time points (Fig. 8.14, 8.17). Regarding FGF effects on OC expression, literature provides multifaceted results. On the one hand, a downregulation accompanied by inhibited matrix formation due to FGF1 administration was reported in rat fetal osteoblasts[198]. FGF2 also decreased OC expression among other osteogenic marker genes in MC3T3-E1 osteoblast-like cells[125]. On the other hand, upregulating effects of FGF2 have been reported in the presence of Forskolin[211] and in relation to Runx2 protein acetylation[212] in MC3T3-E1 cells as well as in marrow MSCs[115]. It has to be considered that these studies administered FGF2 during the proliferative culture phase unlike the current study. The results of Debiais displayed a transient OC downregulation suggesting that the effects of FGF2 are stage-specific and may change throughout the course of osteogenic differentiation[122]. Likewise, our findings on OC regulation display a tendency towards a stage-specific, yet mild reduction of this organic ECM component followed by a slight upregulation in later time points.

When examining the mRNA expression of the other two organic matrix components COL1A1 and IBSP, the effects of FGF1 and FGF2 were strongly inhibiting throughout all stages of osteogenic differentiation and conversion. While the COL1A1 decrease was more significant at day 7 and 21 (Fig. 8.12, 8.15), IBSP downregulation was more pronounced during the later stages of differentiation and conversion (Fig. 8.13, 8.16). In accordance with my results, FGF2 was found to completely inhibit the expression of COL1A1 and osteogenic differentiation in primary murine bone cells[126]. Likewise, a COL1A1 downregulation via FGF2 was also found in MC3T3-E1 osteoblast-like cells[125], the Saos-2 cell line[118], and in human osteoblastic cells isolated from the calvaria[122]. Although some studies reported a positive connection between FGF2 administration and IBSP expression[213–216], the study of Biver and colleagues confirmed a negative effect on the transcription of IBSP among other osteogenic markers. In consistency with my results, inhibition of FGF receptors enhanced IBSP expression when experiments were performed with post-confluent hMSCs[127].

Taken together, FGF1 and FGF2 strongly reduce the expression of the organic ECM components COL1A1 and IBSP in hBMSCs, thereby significantly impeding the process of matrix formation. Moreover, OC is regulated time-dependently and to a markedly smaller extent than the other two markers of ECM formation. Thus in total, osteoid formation is strongly impeded by the culture in the presence of FGF1 and FGF2.

12.4 Downregulation of markers initiating osteogenic commitment

Since both ECM formation and mineralization were affected by FGF1 and FGF2 administration, we asked whether the initial phase of osteogenic commitment and differentiation was altered as well. Therefore, we analyzed early key marker gene expression of osteogenic differentiation. The transcription factor Runx2 is a master regulator of osteoblast differentiation[29,30]. This nuclear protein contains a Runt DNA-binding domain and acts as a scaffold for nucleic acids and regulatory factors involved in skeletal gene expression. Like this, it regulates the transcription of COL1, ALP, OPN, and OC[217,218]. In addition, the BMP family is part of the transforming growth factor-β (TGF-β) superfamily. BMPs are crucial transcription factors required for skeletal development and the maintenance of adult bone homeostasis inducing osteoblast commitment and differentiation[219]. Furthermore, BMP signaling induces the expression of RUNX2 and BMPs, thereby creating a positive feedback loop[220]. Interestingly, the early osteogenic markers RUNX2 and BMP4 were both markedly downregulated in the current study by the administration of FGF1 and FGF2, especially with the highest concentration of 25 ng mL^{-1} (Fig. 8.8, 8.9, 8.10, 8.11). .

Although some studies reported a promoting effect of FGF2 on the mRNA expression of RUNX2[111], their experimental set-up differed sharply from the current study. In these studies, FGF2 was administered during the proliferative phase that preceded the phase of osteogenic differentiation. The effects were similar as described in section 12.1, and upregulated RUNX2 transcription was connected to an increased osteogenic differentiation. Besides, it was stated that FGF2 phosphorylated and thereby activated Runx2 on the protein level in MC3T3-E1 pre-osteoblastic cells[212]. Yet, the authors did not state if FGF2 was given after reaching confluence like in my study.

However, studies that examined an FGF administration during the differentiation phase alone (equaling my experimental set-up) reported a negative effect on RUNX2 expression and a reduced osteogenic differentiation in accordance with my results. Liu *et al.* published the downregulation of RUNX2 among other osteogenic markers in Saos-2 cells after FGF2 administration[118]. Apart from this, FGF2 was shown to decrease the protein levels of TAZ, which acts as a co-activator of RUNX2 and promotes osteogenic differentiation[221]. Moreover, as post-translational modification play an important role in the regulation of Runx2 protein function, the lack of changes in RUNX2 expression during the earlier phases of osteogenic differentiation and conversion does not necessarily exclude changes in Runx2 signaling. It has to be taken into account that, in contrast to other studies deploying FGFs at the proliferative state where it might have enhanced the proliferation of osteoblastic progenitors, the cell proliferation could not be increased in our study since experiments were performed with post-confluent cells.

In parallel to RUNX2, literature provides evidence for a positive effect of FGF2 on the expression of BMP2[128,222] and BMP receptors (BMPRs)-1A and -2[44], only when FGF2 was administered during the expansive phase of cell culture. Similar to my findings, FGF2 was found to significantly reduce gene expression of BMP2 in MC3T3-E1 osteoblast-like cells[125]. Moreover, BMP4 transcription was downregulated by FGF2 in rat osteoblast cells[223]. Furthermore, Biver and colleagues discovered a strongly inhibiting effect of FGF2 on the mRNA expression of BMP2 and BMP4 as well as on the corresponding receptors BMPR-1A, BMPR-1B, and BMPR-2 during the osteogenic differentiation of bone marrow-derived hMSCs[224]. FGF2 also blocked BMPR-1B gene expression, which is normally induced in the presence of retinoic acid in murine adipose-derived stem cells (mASCs)[141]. In agreement, the upregulation of the BMP9 receptors activin A receptor type I and type II (ALK1 and ALK2) was inhibited by FGF2 in MSCs[225]. Here, exogenous expression of ALK1 and ALK2 restored osteogenic differenti-

ation[225]; likewise, constitutive expression of BMPR-1B counteracted the inhibitory effects of FGF2 on osteogenic differentiation in mASCs[141]. Together with my data, these studies indicate a crucial role of BMP signaling in the implementation of the anti-osteogenic effect of FGF2.

Taken together, our data display that the administration of FGF1 and FGF2 during osteogenic differentiation and conversion affected every stage from the initial osteogenic commitment, subsequent differentiation, and maturation. In short, ECM mineralization was diminished due to the reduction of the ALP while the mineralization inhibitors ANKH and OPN were upregulated. Moreover, genes encoding the organic components of the bone matrix COL1A1 and IBSP were markedly downregulated. Finally and most intriguing, already the earliest stage of osteogenic commitment was impeded by FGF administration, so that RUNX2 and BMP4 expression was markedly reduced. Thereby, the positive feedback loop between these transcription factors was likely impeded and the activation of downstream promoters was impaired. Moreover, TAZ expression might be reduced as well as shown for MC3T3-E1 cells[221]. To sum up, despite the strong inhibiting effect on adipogenic differentiation and conversion, both growth factors turned out to also suppress the osteogenic outcome of hBMSCs. Therefore, we conclude that FGF1 and FGF2 might entrap hBMSCs in a stage prior to commitment and differentiation. However, the impact on the osteogenic conversion of pre-differentiated adipocytes also should be taken into account.

12.5 Impact on osteogenic conversion

When examining the effects of osteogenic conversion, we found several alterations on the transcriptional and functional level. Most importantly, the matrix mineralization and ALP activity were highly significantly increased when osteogenic converted samples were compared to adipogenic pre-differentiated cells (Fig. 8.2, 8.5). These data clearly confirmed that the switch towards the osteogenic fate has successfully taken place. However and similar to earlier results, lipid droplets did not vanish completely during the osteogenic conversion process, indicating that not every single cell followed the path of de-differentiation and lineage switching. Yet, transcriptional alterations further supported the implementation of osteogenic conversion. ALP mRNA expression was highly significantly upregulated (Fig. 8.4 C, D). RUNX2 and BMP4 transcription was increased as well through osteogenic conversion, mostly on day 28 and day 21, respectively (Fig. 8.8, 8.9, C, D). Meanwhile, the transcription of OC and OPN was downregulated (Fig. 8.14, 8.20, C, D), whereas ENPP1 expression was promoted (Fig. 8.19 C, D).

The concept of osteogenic conversion has been highlighted by several studies and it is intensely discussed as means to alter the balance between adipogenesis and osteogenesis for the benefit of related diseases like osteoporosis[23,24,34,40–43,46,226,227]. The experimental set-up was established and described in our lab by Schilling *et al.* first[24], based on the work of Song and Tuan[23]. In line with my findings, the strong upregulation of the osteoblast marker ALP was reported then[24]. Nevertheless, OC expression was also increased in contrast to my results[23,24]. However, a conversion period of three or four weeks was used in these set-ups, strongly differing from my experiments deploying a conversion period of only two weeks. One plausible explanation is that the transcription of the late osteogenic marker OC, which is involved in the maturation of osteoblasts into osteocytes, was not yet activated at this early time point.

The transcriptional upregulation of RUNX2 was an important result of the current study since it had not been described in our *in vitro* system so far. Interestingly, RUNX2 was shown to be sufficient

to induce the osteogenic fate change of 3T3-L1 pre-adipocytes[41]. Following the forced expression of exogenous RUNX2 using a retroviral vector, pre-adipocytes displayed increased ALP activity and osteogenic marker gene expression as well as a low-level mineralization. Meanwhile the expression of adipogenic markers decreased. Besides, several studies described the upregulation of RUNX2 expression during osteogenic conversion of pre-differentiated adipocytic cells in consistency with my results[34,40,42]. Taken together, these data suggest that RUNX2 plays an essential role in the induction of the osteogenic conversion of adipocytic cells in bone marrow.

Moreover, the important role of BMP signaling was emphasized in other studies before. The overexpression of BMP receptors in 3T3-F442 pre-adipocytes suppressed further adipogenic differentiation[226]. Yet, the conversion towards the osteogenic fate was induced and matrix formation as well as mineralization occurred under retinoic acid administration. Besides, 3T3-L1 pre-adipocytes could be converted directly into osteoblastic cells when the BMP2 gene was rendered responsive to Wnt3a via drug-induced epigenetic modifications[43]. Apart from BMP2, also the ALP gene had to be made responsive to Wnt3a, which was shown to only stimulate osteoblast differentiation in cells with an intrinsic osteogenic potential before[228]. Further studies described the upregulation of ALP expression during osteogenic conversion[34,40,41] while an enhanced ALP activity was reported only by Oki *et al.*[40]. These data underline my findings of increased BMP4 and ALP expression accompanied by enhanced ALP activity and further support the central role of BMP signaling in osteogenic conversion.

Taken together, our *in vitro* system was successfully investigated and described concerning a broadened range of expressional markers during osteogenic conversion. Most importantly, the significance of our system was strengthened by the finding of an enhanced ALP activity and significantly increased matrix mineralization. In addition, our results were the first to report the upregulation of ENPP1 expression during osteogenic conversion. Moreover, our data highlighted the important role of RUNX2 and BMP signaling during osteogenic conversion of adipogenically pre-differentiated hBMSCs.

After having investigated the alterations of osteogenic markers taking place through osteogenic conversion itself, we wanted to address the question if FGF1 and/or FGF2 administration could promote this process. As FGF1 and FGF2 strongly inhibited adipogenic differentiation and conversion (see chapter 7) and since FGF1 was reciprocally regulated during the onset of adipogenic and osteogenic conversion (being upregulated during the osteogenic one)[46], we hypothesized that these growth factors might shift the balance between adipogenesis and osteogenesis in favor of osteogenesis. Therefore, FGF1 and FGF2 were added to the osteogenic conversion of adipogenically pre-differentiated hBMSCs when the medium was switched from adipogenic to osteogenic medium until the end of conversion on day 28.

Interestingly, FGF1 and FGF2 did not promote the osteogenic fate change but reduced it, so that results of conversion were similar to those of osteogenic differentiation. The matrix mineralization and ALP activity were decreased by FGF1 and FGF2 administration (Fig. 8.2 C, 8.3 C, 8.5 B, 8.7 B). In line, the osteogenic marker genes RUNX2, BMP4, ALP, and ENPP1 that were upregulated by the osteogenic conversion as described above were downregulated by FGF1 and FGF2, reaching or approaching the levels of the non-converted samples (Fig. 8.8, 8.10, 8.9, 8.11, 8.4, 8.6, 8.19, 8.22, C, D).

To our knowledge, there have been no studies so far investigating the effects of FGF1 or FGF2 in a set-up where adipogenically pre-differentiated cells were subjected to osteogenic conversion. However, the study of Xiao *et al.* found a connection between FGF2 deficiency, reduced osteogenesis and increased marrow adiposity[116]. In the knockout ($FGF2^{-/-}$) mice, BMD was decreased and a greater accumulation of marrow fat was found in long bones. Additionally, $FGF2^{-/-}$ BMSCs cultured *in vitro*

displayed reduced ALP activity and mineralization whereas adipogenic marker genes were upregulated. Unlike my findings, these results would suggest a positive impact of FGF2 on lineage decisions of mesenchymal precursors of the bone marrow towards osteogenesis at the expense of adipogenesis. Yet, systemic side effects in the knockout mice could not be excluded and the described observations might not be a direct effect of FGF2 absence. However, when confluent hBMSC-derived adipocytes were directly subdued to osteogenic conversion, the effects of FGFs were clearly anti-osteogenic.

Taken together, FGF1 and FGF2 clearly downregulated the central regulators of osteogenic conversion RUNX2, BMP4, and ALP. This resulted in a strong decrease of ALP activity and matrix mineralization. These findings further support our conclusion that FGF1 and FGF2 might entrap hBMSCs in a stage prior to commitment and differentiation.

12.6 Signaling pathways mediating the anti-osteogenic effect

In parallel to adipogenic differentiation and conversion, inhibitor experiments were also carried out for osteogenic set-ups deploying the same highly selective chemical inhibitors. The FGFR1 inhibitor PD166866 completely rescued the negative effects of FGF1 on ECM mineralization during osteogenic differentiation and conversion with high significance (Fig. 9.1 B, D). This suggested that FGFR1 was the responsible receptor for signal transduction of the anti-osteogenic effect. Moreover, FGFR1 expression was only slightly downregulated during osteogenic differentiation and conversion (Fig. 9.6, 9.7) while FGFR2 was strongly downregulated (Fig. 9.8, 9.9). Additionally, FGFR2 downregulation was further negatively enhanced by FGF1 and FGF2 administration (Fig. 9.8, 9.9). These transcriptional data also indicated that FGFR1 and not FGFR2 was crucial for signal mediation.

In line with my findings, FGFR1 was also found responsible for signal mediation when FGF1 was administered to rat aortic smooth muscle cells *in vitro*, where the subsequent upregulation of OPN mRNA and protein was attenuated by PD166866[206]. Moreover, the isoforms of FGFR2 were downregulated during osteogenic differentiation in mASCs[141]. In similar, FGFR2 was reported to be expressed in proliferating osteo-progenitor cells in the fetal mouse cranial suture but was downregulated when osteogenic differentiation was initiated[229]. Furthermore, the onset of differentiation was connected to FGFR1 upregulation but this was reduced after differentiation proceeded, which is again in direct agreement with my results.

As several studies indicated, FGFR1 and FGFR2 may have distinct roles concerning the differentiation and proliferation of osteogenic cells, respectively. The conditional FGFR1 deletion in murine osteochondro-progenitor cells increased cell proliferation while it delayed osteogenic differentiation (as shown by the examination of osteogenic marker genes) and matrix mineralization[230]. Yet, FGFR1 inactivation accelerated differentiation and mineralization in differentiated osteoblasts. Moreover, FGFR1 deficiency *in vivo*, either in progenitor cells or in differentiated osteoblasts, resulted in increased bone mass in adult mice, suggesting that signaling through FGFR1 negatively controls osteoblast maturation and bone formation *in vivo*[230]. Furthermore, FGFR1 signaling in osteoblasts might be necessary to maintain the balance between bone formation and remodeling through a direct effect on the maturation of osteoblasts[230].

In marked contrast, the activating FGFR2 mutations causing craniosynostosis in humans were shown to promote osteoblast differentiation via the upregulation of RUNX2 and osteogenic marker genes[95,139]. The concept that constitutive activation of FGFR2 promotes osteoblast gene expression and bone formation is further supported by recent studies featuring FGFR2 mutations in murine[231,232] and human

osteoblasts[233,234]. Furthermore, the conditional inactivation of FGFR2 in mice caused a reduced bone density, a severely decreased proliferation of osteo-progenitor cells, and abnormal function of mature osteoblasts[235]. Besides, the onset of ossification was delayed in Fgfr2c/ null mice[236]. In addition, FGFR2 activity promoted osteogenic differentiation of murine mesenchymal C3H10T1/2 cells[237].

In summary, these studies indicate that FGFR1 is responsible for the initiation of the osteogenic differentiation yet negatively regulates the later differentiation state. Conversely, FGFR2 positively controls osteoblast proliferation and bone formation. Taking into account our results, we conclude that FGFR1 is a key player of osteogenic differentiation in hBMSCs. Our findings display that its activation via FGF1 (and most likely FGF2) negatively controls osteoblast differentiation of bone marrow precursor cells as well as subsequent maturation and mineralization. Likewise, the osteogenic conversion of adipogenic cells is impeded. The positive effects of FGF2 administration on bone formation reported by other studies[105–108,116] might probably be a result of FGFR2 activation, leading to increased proliferation of osteoblast progenitors and thereby indirectly promoting osteoblast differentiation. An increase of the osteogenic differentiation capacity via generating a higher pool of osteo-progenitors might not have been possible in our set-up since experiments were carried out with post-confluent monolayers. Thus, FGF1 and FGF2 administration led to an increased FGFR1 activation and subsequent signaling resulted in reduced osteogenic differentiation. Moreover, it seems likely that the 'mesenchymal' subtype of the FGFR1, isoform IIIc, is mainly responsible for signal transduction[76–79].

Besides the responsible receptor, we deployed different inhibitors to investigate the crucial intracellular signaling cascades. The different concentrations of Calphostin C did not rescue the negative FGF1 effect on mineralization (Fig. 9.10 B, D, F). Hence, the PKC signaling cascade had no major role in the intracellular mediation of the FGF1 signal in our system. Interestingly, the results of Lee *et al.* suggested that PKC signaling might be a critical control point for the balance between osteogenesis and adipogenesis[238]. When chemically inhibiting or genetically ablating PKCδ in hBMSCs, osteogenic differentiation was significantly decreased while the adipogenic outcome was induced meanwhile.

However, this connection could not be verified in our system. Although the osteogenic differentiation was reduced by PKC inhibitor addition, the adipogenic outcome was not increased. Besides, PKC was responsible for the FGF2-induced RUNX2 expression in MC3T3-E1 pre-osteoblastic cells[237,239,240]. Again, PKCδ seemed to be one of the key isoforms involved. In addition to the transcriptional upregulation of RUNX2, DNA-binding and transcriptional activity of the Runx2 protein were increased. In contrast to PKC, MAPK inhibitors had no effect. These results suggest that the pro-osteogenic effect of FGF2 that led to increased RUNX2 expression and was most probably mediated via FGFR2 (see above) is further transduced by PKC signaling, i.e. PCKδ. In sharp contrast, the opposing anti-osteogenic effect described in the current study were not transduced via the PKC signaling cascade.

Moreover, JNK signaling was not responsible for the transduction of the FGF1 effects either. The pharmacological inhibitor SP600125 did not alter the osteogenic outcome (Fig. 9.11 B). In contrast to our findings, the JNK signaling pathway was found to be responsible for the anti-osteogenic effects mediated by TAZ downregulation caused by FGF2 administration in the osteoblast-like MC3T3-E1 cell line[221]. As described previously, the TAZ functions as co-activator of RUNX2 and co-repressor of PPARγ, thereby inducing osteoblast differentiation of mesenchymal precursor cells. The inhibiting effect of FGF2 on bone mineralization and the TAZ reduction was blocked by a stress-activated protein kinase (SAPK)/JNK-specific inhibitor in this study. Yet, the anti-osteogenic effects of the current study based on primary human BMSCs were clearly mediated by an alternative pathway pointing at the signaling complexity of FGF1 and FGF2.

Furthermore, the experiments with the inhibitor SB203580 displayed that the p38-MAPK signaling pathway also did not transduce the FGF1 effects on osteogenic differentiation (Fig. 9.12 B). Additionally, our findings excluded that an involvement of the p38-MAPK was hidden by an alternative signaling route via MEK1/2 and ERK1/2 (Fig. 9.13 B). Yet, the experiments using the MEK1/2 inhibitor U0126 alone clearly displayed that the ERK1/2 pathway is crucial for the intracellular transduction of the FGF1 signal that leads to the negative effects on osteogenic hBMSC differentiation and conversion (Fig. 9.15 B, D).

Recent literature has repeatedly highlighted the involvement of the ERK1/2 pathway in FGF/FGFR signaling in the course of osteogenesis before, both during pro- and anti-osteogenic effects. Interestingly, ERK1/2 activation by FGF2 was reported to be essential for promoting the cell proliferation in osteoblast precursor cells[241]. Moreover, when Xiao *et al.* described that FGF2 stimulated RUNX2 expression in MC3T3-E1 pre-osteoblastic cells and mouse BMSCs, they found that this induction was transduced via ERK1/2 phosphorylation[212]. Accordingly, ERK-MAP kinase was phosphorylated by activating FGFR2 mutations and resulted in increased transcriptional activity of Runx2, followed by enhanced osteogenic marker gene expression, as shown in transgenic mice and a human craniosynostosis patient[231,233]. In line, activating FGFR2 mutations promoted osteogenic differentiation in mesenchymal cells via ERK1/2 signaling[237]. Taken together, the ERK1/2 signaling cascade may probably transduce the pro-osteogenic effect of FGF2 that is linked to the activation of the FGFR2. However, apart from this positive impact on bone formation that contradicts our findings, literature also provides evidence for a connection between ERK1/2 and the anti-osteogenic effects of FGFs on osteogenesis. Such connections may, however, be different *in vitro* and *in vivo*, given that e.g. mechanical strain and fluid flow further induce ERK1/2 phosphorylation and consecutive osteogenic differentiation[242,243]. Hence, it might be possible that FGF1/2 signaling prepares the cells for rapid osteogenic commitment and differentiation under appropriate conditions such as mechanical strain.

In agreement with my findings, FGF1 administration stimulated OPN mRNA and protein expression in rat aortic smooth muscle cells[206]. This transcriptional alteration was transduced via MEK/MAP kinases. Moreover, FGF2 stimulated the expression of the osteocyte-specific marker dentin matrix acidic phospho-protein 1 (DMP1) while ERK1/2 inhibition or ablation blocked both basal DMP1 expression and its FGF2-induced induction[204]. In line, FGF2 administration inhibited the osteogenic differentiation of stem cells from human exfoliated deciduous teeth via ERK signaling[244]. Similarly, FGF1 inhibited osteoblast differentiation via activating ERK1/2 signaling in the osteoblastic cell lines OB1 and OB5 as well as in primary mouse calvarial osteoblasts[245]. Interestingly, the ERK1/2 activation by FGF2 treatment led to the inhibition of Wnt/β-catenin signaling, which probably caused the osteogenic differentiation deficiency[244], whereas phosphoinositide 3-kinase (PI3K)-Akt signaling, which was involved in promoting osteoblast differentiation, was induced by Wnt signals and itself increased the levels of stabilized β-catenin[245]. These results hint at an involvement of the Wnt/β-catenin pathway also in our system. Near identical with our results, FGF2 inhibited the osteoblastic differentiation of hBMSCs as well as the upregulation of BMPs and BMPR via the ERK1/2 signaling cascade[224].

To sum up, several studies described the involvement of ERK1/2 signaling in the anti-osteogenic effects of FGF1 and FGF2. Our results verified this finding for primary hBMSCs and clearly connected it to the activation of FGFR1. Besides, the contribution of ERK1/2 to the pro-osteogenic effects caused by FGFR2 activating mutations highlights the complexity of underlying signaling pathways. Moreover, it has to be taken into account that the ERK1/2 activation might be time-dependent since an inhibition of ERK1/2 by FGF2 has been reported in murine MSCs[246].

12.7 Summary osteogenic differentiation and conversion

Taken together, the culture in the presence of FGF1 and FGF2 reduced the osteogenic differentiation of trabecular hBMSCs as well as the osteogenic conversion of adipogenically pre-differentiated cells. Interestingly, all stages of osteogenesis were impeded, starting at the initiation of commitment with downregulated expression of the osteogenic master transcription factor RUNX2 (Fig. 12.1). Its positive feedback loop with BMP4 was further impaired by the additional downregulation of this early osteogenic key marker. Most probably, these effects led to the downregulation of the downstream markers ALP and COL1A1, thereby strongly impeding ECM formation, as COL1A1 is the major matrix protein, and ECM mineralization, since ALP is known to drive hydroxyapatite formation through the cleavage of the mineralization inhibitor PP_i.

Furthermore, the expression of IBSP, another organic matrix component, was markedly downregulated, whereas OC was upregulated only slightly and time-dependently. Moreover, factors known to negatively control ECM mineralization either by enhancing extracellular PP_i levels (ANKH) or by inhibiting hydroxyapatite formation (OPN) were upregulated. OPN upregulation seemed to be rather donor-dependently. Yet, as inhibitor experiments with Probenecid revealed, the negative effects of ANKH upregulation seemed to be overridden by a decreased expression of ENPP1, which is responsible for PP_i production.

The effects of FGF1 were transduced via FGFR1 and intracellularly mediated via ERK1/2 signaling, as were the anti-adipogenic effects described before. Our results underlined that FGFR1 negatively controls osteoblast differentiation of precursor cells as well as subsequent maturation and mineralization. This is in line with recent literature indicating that the pro-osteogenic effects of FGF2 are mediated via the activation of the alternative receptor FGFR2. In contrast, FGFR1 was suggested to exhibit negative effects on osteogenic differentiation[97], which was confirmed by our findings. The activation of ERK1/2 signaling was described to impede osteogenic differentiation before and may involve inactivation of Wnt/β-catenin signaling as reported for stem cells from human exfoliated deciduous teeth[244]. In conclusion, FGF1 and FGF2 did not support osteogenic lineage decisions or fate switching in our study. They rather entrapped trabecular hBMSCs in a pre-committed state since already the very earliest markers of commitment and/or differentiation like RUNX2 and PPARγ2 for osteogenic and adipogenic commitment, respectively, were downregulated. Additionally, the fact that pharmacological inhibition of ANKH PP_i transport activity could not rescue the anti-mineralizing phenotype further supports an early phase impairment of osteogenic differentiation that impedes the following steps of osteogenesis.

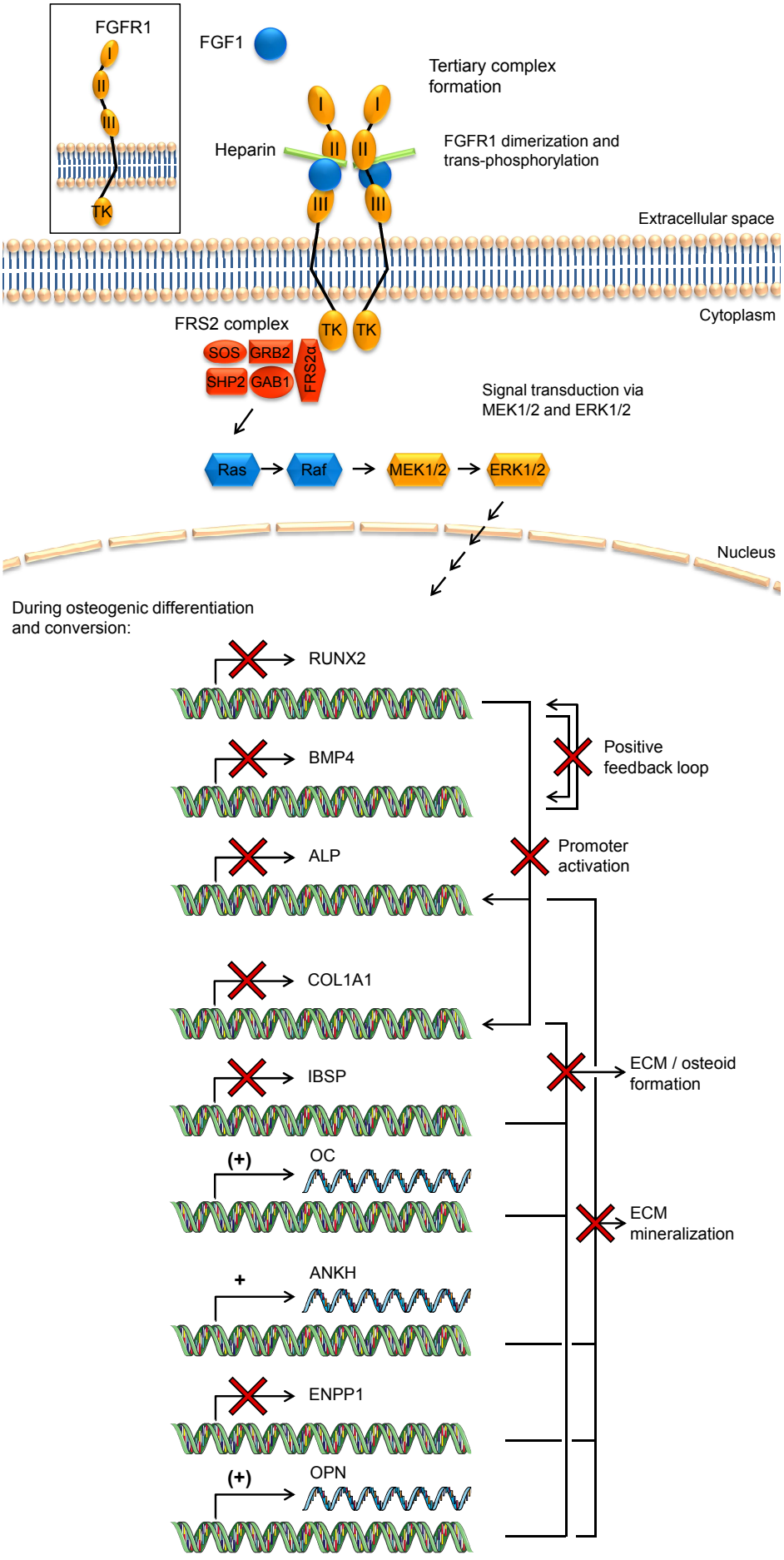
FGFR1
I
II
III
TK
FGF1
Tertiary complex formation
Heparin
FGFR1 dimerization and trans-phosphorylation
Extracellular space
Cytoplasm
FRS2 complex
SOS
GRB2
SHP2
GAB1
FRS2α
TK
TK
Signal transduction via MEK1/2 and ERK1/2
Ras
Raf
MEK1/2
ERK1/2
Nucleus
During osteogenic differentiation and conversion:
RUNX2
BMP4
Positive feedback loop
ALP
Promoter activation
COL1A1
IBSP
ECM / osteoid formation
(+)
OC
ECM mineralization
+
ANKH
ENPP1
(+)
OPN

Figure 12.1: FGF1 signal transduction during osteogenic differentiation and conversion. The reducing effect on osteogenesis is mediated via the FGF receptor (FGFR) 1. Upon ligand binding, two FGFR1, two FGF1, and two heparin molecules form the tertiary complex leading to FGFR1 dimerization and trans-phosphorylation of tyrosine residues. In consequence, the adaptor protein FGFR substrate (FRS) 2α is phosphorylated and recruits the FRS2 complex. The signal is further transduced via the MEK1/2 and ERK1/2 pathway, which are probably activated via Ras/MAPK signaling. This results in specific alterations of osteogenic gene expression with downregulation of the master transcription factor RUNX2 and the early osteogenic markers BMP4 and ALP. This impedes the positive feedback loop between RUNX2 and BMP4. In addition, the promoter activation of ALP and COL1A1 via Runx2 is diminished and ALP is markedly downregulated in consequence. Moreover, the expression of the bone matrix proteins COL1A1 and IBSP is downregulated, impeding the formation of ECM and osteoid. OC is slightly upregulated in a time-dependent way. ANKH expression is increased, but its effect on ECM mineralization by probably increasing extracellular levels of the mineralization inhibitor PP_i seems to be overridden by the decreased ENPP1 transcription. The mildly increased OPN expression may further contribute to decreased ECM mineralization. Figure in part adapted from Servier Medical Art (`http://www.servier.com/Powerpoint-image-bank`).

13 Conclusions

When evaluating the results with regard to exercising control on the inverse adipogenic and osteogenic processes, we conclude from the current study that neither FGF1 nor its subfamily member FGF2 were able to shift hBMSC differentiation or conversion in favor of osteogenesis. They rather inhibited adipogenic and osteogenic differentiation and conversion completely (adipogenic) or at least in part (osteogenic). In consequence, the benefit for a potential osteoporosis therapy and prevention, which would be based on preventing the preferential adipogenic differentiation and on increasing osteoblastogenesis at the costs of adipogenesis, would be limited. The downstream targets of FGF signaling like FGFR1, ERK1/2, and others could not represent a pharmaceutical target for active hBMSC lineage shifting towards osteogenesis.

However, our study clearly displayed that FGF1 and FGF2 as well as the elucidated downstream signaling molecules were involved in the highly effective inhibition of the adipogenesis of undifferentiated trabecular hBMSCs and pre-differentiated osteoblastic cells. Hence, these agents could be applied to potently prevent unwanted adipogenesis *in vitro*. Moreover, if there may be a stabilizing effect that both synchronizes and enhances incoming early and late osteogenic signals remains to be demonstrated. In addition, our results might aid in finding a pharmacological control point to eliminate the increased adipogenic differentiation and conversion as potential cause of fat accumulation and decreased osteoblastogenesis in bone marrow during aging and especially osteoporosis.

Since the earliest genes of adipogenic as well as osteogenic commitment and differentiation were markedly downregulated by FGF1 and FGF2, we conclude that hBMSCs were entrapped in a state prior to commitment. As hBMSCs depict a tool for tissue engineering approaches, these agents could be deployed *in vitro* to enrich for and maintain a population of osteoblastic progenitor cells at a defined stage prior to differentiation.

14 Perspectives

The current study clearly demonstrated the prevention of adipogenic as well as the reduction of osteogenic differentiation and conversion processes and elucidated underlying signaling mechanisms. The signaling pathway/s underlying the anti-adipogenic effect of FGF1 and FGF2 on adipogenic conversion could be further investigated by performing additional experiments deploying chemical inhibitors. In addition, the connection of the obtained results to the field of Wnt/β-catenin signaling would be of interest. It is well known that the activation of Wnt/β-catenin is crucial for osteoblastic differentiation[32]. Therefore, we would hypothesize that FGF1 and FGF2 might inhibit Wnt signaling, either by downregulating drivers like Wnt5a or by upregulating pathway inhibitors like members of the dickkopf (DKK) protein family or the soluble frizzled-related protein 1 (SFRP1). Since qPCR primers for different members of the Wnt pathway were established during my thesis, it would be feasible to examine the course of Wnt protein and inhibitor expression throughout osteogenic differentiation and conversion.

Moreover, the impact of exogenous FGF1 and FGF2 administration on the endogenously expressed amounts of these growth factors could be examined. Previously, Hutley and colleagues found a connection between FGF1 addition and a diminished FGF2 mRNA and protein expression that was crucial for the observed FGF1 effects on adipogenic hPA differentiation[171]. Hence, the investigation of the exogenous expression of FGF1 and FGF2 during adipogenesis and also osteogenesis in our system could reveal similar impacts, giving insight into the paracrine interplay of FGF signaling. This would be of particular interest since such connections have not been described for osteogenic differentiation, yet.

Apart from the canonical FGF1 and FGF2, it would be of particular interest to broaden the scope of the study towards hormonal FGFs like FGF23 and its co-receptor Klotho. FGF23 is secreted mostly be mature osteoblasts and osteocytes and is known to regulate the systemic mineral metabolism by inhibiting renal tubular phosphate reabsorption and suppressing circulating vitamin D3 and PTH levels[49]. FGF23 was shown to signal via FGFR1(IIIc) after this canonical FGF receptor was directly converted into the FGF23 receptor by Klotho, which is expressed in the distal tubules of the kidney[247]. Linking and expanding our findings towards this hormonal FGF might be of special clinical interest since elevated serum levels of FGF23 were found in patients with the chronic kidney disease-mineral and bone disorder (CKD-MBD)[248]. This disorder increases the risk of fractures by weakening and thinning of the bone and is a common problem in people with kidney disease affecting almost all patients receiving dialysis[249]. Serum FGF23 concentrations were shown to predict mortality not only among patients receiving dialysis but also among pre-dialysis CKD patients[248]. In addition, they may play a critical role in the bone metabolism in these patients via systemic as well as direct effects on mineralization[250].

Interestingly, an impact of FGF23 on lineage fate determination has been shown before in BMSCs from Klotho deficient mice[251]. Klotho$^{-/-}$ BMSCs developed fewer osteoblastic but more adipocytic colonies than wildtype cells, which stands in line with earlier findings linking Klotho mutations to aging and bone loss[252,253]. In murine C3H10T1/2 cells, Klotho was weakly expressed and FGF23 affected the lineage decision dose-dependently[251]. Moreover, a combination of FGF23 and Klotho reduced the osteogenic differentiation of MC3T3-E1 cells including matrix mineralization, ALP activity, and osteogenic markers[254]. Similar to my results, these effects were mediated via the FGFR1 and MEK/ERK signaling. Furthermore, an interplay between the canonical and hormonal FGFs has been established since FGF23 upregulation increased the gene expression of FGF1 and FGF2[255] and FGF23 promoter

activity was stimulated by FGF1 and FGF2[256]. In addition, Klotho specifies FGFR1(IIIc) for FGF23 binding, hence impeding the interaction and subsequent signal transduction of this receptor with other ligands like canonical FGFs. Further analysis could reveal a new connection between FGF23-Klotho-FGFR1(IIIc) signaling and the FGF1/2-FGFR1-ERK1/2 axis elucidated in the current study, thereby linking the hormonal FGF23 to the described effects on adipogenic and osteogenic hBMSC differentiation and conversion.

Bibliography

[1] Mattias Lorentzon and Steven R Cummings. Osteoporosis: the evolution of a diagnosis. *Journal of Internal Medicine*, 277(6):650–661, April 2015. ISSN 09546820. doi: 10.1111/joim.12369.

[2] P. J . Marie. Osteoporosis: a disease of bone formation. *Medicographia*, 32(1):10–17, 2010. URL `http://www.medicographia.com/2010/07/osteoporosis-a-disease-of-bone-formation/`.

[3] Julie C Crockett, Michael J Rogers, Fraser P Coxon, Lynne J Hocking, and Miep H Helfrich. Bone remodelling at a glance. *Journal of cell science*, 124(Pt 7):991–998, 2011. ISSN 0021-9533. doi: 10.1242/jcs.063032.

[4] Steven L Teitelbaum. Osteoclasts: what do they do and how do they do it? *The American journal of pathology*, 170(2):427–435, February 2007. ISSN 00029440. doi: 10.2353/ajpath.2007.060834.

[5] Gerard Karsenty, Henry M Kronenberg, and Carmine Settembre. Genetic control of bone formation. *Annual review of cell and developmental biology*, 25:629–648, January 2009. ISSN 1081-0706. doi: 10.1146/annurev.cellbio.042308.113308.

[6] Manisha C Yadav, Ana Maria Sper Simão, Sonoko Narisawa, Carmen Huesa, Marc D McKee, Colin Farquharson, and José Luis Millán. Loss of skeletal mineralization by the simultaneous ablation of PHOSPHO1 and alkaline phosphatase function: A unified model of the mechanisms of initiation of skeletal calcification. *Journal of Bone and Mineral Research*, 26(2):286–297, February 2011. ISSN 08840431. doi: 10.1002/jbmr.195.

[7] Lynda F Bonewald and Mark L Johnson. Osteocytes, mechanosensing and Wnt signaling. *Bone*, 42(4):606–615, May 2008. ISSN 87563282. doi: 10.1016/j.bone.2007.12.224.

[8] V Everts, J M Delaissé, W Korper, D C Jansen, W Tigchelaar-Gutter, P Saftig, and W Beertsen. The bone lining cell: its role in cleaning Howship's lacunae and initiating bone formation. *Journal of bone and mineral research : the official journal of the American Society for Bone and Mineral Research*, 17(1):77–90, January 2002. ISSN 0884-0431. doi: 10.1359/jbmr.2002.17.1.77.

[9] Thomas Levin Andersen, Teis Esben Sondergaard, Katarzyna Ewa Skorzynska, Frederik Dagnaes-Hansen, Trine Lindhardt Plesner, Ellen Margrethe Hauge, Torben Plesner, and Jean-Marie Delaisse. A physical mechanism for coupling bone resorption and formation in adult human bone. *The American journal of pathology*, 174(1):239–247, January 2009. ISSN 00029440. doi: 10.2353/ajpath.2009.080627.

[10] P. J. Marie, M. C. de Vernejoul, D. Connes, and M. Hott. Decreased DNA synthesis by cultured osteoblastic cells in eugonadal osteoporotic men with defective bone formation. *Journal of Clinical Investigation*, 88(4):1167–1172, 1991. ISSN 00219738. doi: 10.1172/JCI115418.

[11] Ilaria Bellantuono, Abdullah Aldahmash, and Moustapha Kassem. Aging of marrow stromal (skeletal) stem cells and their contribution to age-related bone loss. *Biochimica et Biophysica Acta - Molecular Basis of Disease*, 1792(4):364–370, 2009. ISSN 09254439. doi: 10.1016/j.bbadis.2009.01.008.

[12] P Meunier, J Aaron, C Edouard, and G Vignon. Osteoporosis and the replacement of cell populations of the marrow by adipose tissue. A quantitative study of 84 iliac bone biopsies. *Clinical orthopaedics and related research*, 80:147–154, October 1971. ISSN 0009-921X.

[13] R Burkhardt, G Kettner, W Böhm, M Schmidmeier, R Schlag, B Frisch, B Mallmann, W Eisenmenger, and T Gilg. Changes in trabecular bone, hematopoiesis and bone marrow vessels in aplastic anemia, primary osteoporosis, and old age: a comparative histomorphometric study. *Bone*, 8(3):157–164, 1987. ISSN 87563282. doi: 10.1016/8756-3282(87)90015-9.

[14] J N Beresford, J H Bennett, C Devlin, P S Leboy, and M E Owen. Evidence for an inverse relationship between the differentiation of adipocytic and osteogenic cells in rat marrow stromal cell cultures. *Journal of cell science*, 102 (Pt 2:341–351, June 1992. ISSN 01696009. doi: 10.1016/0169-6009(92)92129-E.

[15] K H Koo, R Dussault, P Kaplan, R Kim, I O Ahn, J Christopher, H R Song, and G J Wang. Age-related marrow conversion in the proximal metaphysis of the femur: evaluation with T1-weighted MR imaging. *Radiology*, 206(3):745–748, 1998. ISSN 00338419.

[16] Liming Pei and Peter Tontonoz. Fat's loss is bone's gain. *Journal of Clinical Investigation*, 113(6):805–806, 2004. ISSN 00219738. doi: 10.1172/JCI200421311.

[17] Mark E Nuttall and Jeffrey M Gimble. Controlling the balance between osteoblastogenesis and adipogenesis and the consequent therapeutic implications. *Current Opinion in Pharmacology*, 4 (3):290–294, June 2004. ISSN 14714892. doi: 10.1016/j.coph.2004.03.002.

[18] Jeffrey M Gimble, Sanjin Zvonic, Z Elizabeth Floyd, Moustapha Kassem, and Mark E Nuttall. Playing with bone and fat. *Journal of Cellular Biochemistry*, 98(2):251–266, 2006. ISSN 07302312. doi: 10.1002/jcb.20777.

[19] Ichiro Takada, Alexander P Kouzmenko, and Shigeaki Kato. Molecular switching of osteoblastogenesis versus adipogenesis: implications for targeted therapies. *Expert opinion on therapeutic targets*, 13(5):593–603, May 2009. ISSN 1472-8222. doi: 10.1517/14728220902915310.

[20] Toru Akune, Shinsuke Ohba, Satoru Kamekura, Masayuki Yamaguchi, Ung Il Chung, Naoto Kubota, Yasuo Terauchi, Yoshifumi Harada, Yoshiaki Azuma, Kozo Nakamura, Takashi Kadowaki, and Hiroshi Kawaguchi. PPARgamma insufficiency enhances osteogenesis through osteoblast formation from bone marrow progenitors. *Journal of Clinical Investigation*, 113(6):846–855, 2004. ISSN 00219738. doi: 10.1172/JCI200419900.

[21] Clifford J Rosen and Mary L Bouxsein. Mechanisms of disease: is osteoporosis the obesity of bone? *Nature clinical practice. Rheumatology*, 2(1):35–43, 2006. ISSN 1745-8382. doi: 10.1038/ncprheum0070.

[22] Ann V Schwartz. Marrow Fat and Bone: Review of Clinical Findings. *Frontiers in Endocrinology*, 6:40, January 2015. ISSN 1664-2392. doi: 10.3389/fendo.2015.00040.

[23] Lin Song and Rocky S Tuan. Transdifferentiation potential of human mesenchymal stem cells derived from bone marrow. *The FASEB journal : official publication of the Federation of American Societies for Experimental Biology*, 18(9):980–982, 2004. ISSN 1530-6860. doi: 10.1096/fj.03-1100fje.

[24] Tatjana Schilling, Ulrich Nöth, Ludger Klein-Hitpass, Franz Jakob, and Norbert Schütze. Plasticity in adipogenesis and osteogenesis of human mesenchymal stem cells. *Molecular and Cellular Endocrinology*, 271(1-2):1–17, 2007. ISSN 03037207. doi: 10.1016/j.mce.2007.03.004.

[25] M F Pittenger, A M Mackay, S C Beck, R K Jaiswal, R Douglas, J D Mosca, M A Moorman, D W Simonetti, S Craig, and D R Marshak. Multilineage potential of adult human mesenchymal stem

cells. *Science (New York, N.Y.)*, 284(5411):143–147, 1999. ISSN 0036-8075. doi: 10.1126/science.284.5411.143.

[26] S Wakitani, T Saito, and A I Caplan. Myogenic cells derived from rat bone marrow mesenchymal stem cells exposed to 5-azacytidine. *Muscle & nerve*, 18(12):1417–1426, December 1995. ISSN 0148-639X. doi: 10.1002/mus.880181212.

[27] A I Caplan. Mesenchymal stem cells. *Journal of orthopaedic research : official publication of the Orthopaedic Research Society*, 9(5):641–650, 1991. ISSN 0736-0266. doi: 10.1002/jor.1100090504.

[28] Julie R Jones, Cordelia Barrick, Kyoung-Ah Kim, Jill Lindner, Bertrand Blondeau, Yuka Fujimoto, Masakazu Shiota, Robert A Kesterson, Barbara B Kahn, and Mark A Magnuson. Deletion of PPARgamma in adipose tissues of mice protects against high fat diet-induced obesity and insulin resistance. *Proceedings of the National Academy of Sciences of the United States of America*, 102(17):6207–6212, 2005. ISSN 0027-8424. doi: 10.1073/pnas.0306743102.

[29] F Otto, A P Thornell, T Crompton, A Denzel, K C Gilmour, I R Rosewell, G W Stamp, R S Beddington, S Mundlos, B R Olsen, P B Selby, and M J Owen. Cbfa1, a candidate gene for cleidocranial dysplasia syndrome, is essential for osteoblast differentiation and bone development. *Cell*, 89(5):765–771, May 1997. ISSN 00928674. doi: 10.1016/S0092-8674(00)80259-7.

[30] T Komori, H Yagi, S Nomura, A Yamaguchi, K Sasaki, K Deguchi, Y Shimizu, R T Bronson, Y H Gao, M Inada, M Sato, R Okamoto, Y Kitamura, S Yoshiki, and T Kishimoto. Targeted disruption of Cbfa1 results in a complete lack of bone formation owing to maturational arrest of osteoblasts. *Cell*, 89(5):755–764, May 1997. ISSN 00928674. doi: 10.1016/S0092-8674(00)80258-5.

[31] Christopher E Lowe, Stephen O'Rahilly, and Justin J Rochford. Adipogenesis at a glance. *Journal of cell science*, 124(Pt 16):2681–2686, August 2011. ISSN 0021-9533. doi: 10.1242/jcs.101741.

[32] David J J de Gorter and Peter ten Dijke. Signal transduction cascades controlling osteoblast differentiation. In Clifford J. Rosen, Roger Bouillon, Juliet E. Compston, and Vicki Rosen, editors, *Primer on the Metabolic Bone Diseases and Disorders of Mineral Metabolism*, chapter 2, pages 15–24. Wiley, 8th edition, 2014. ISBN 978-1-1184-5388-9. URL `http://eu.wiley.com/WileyCDA/WileyTitle/productCd-1118453883.html`.

[33] Xiaofeng Li, Peng Liu, Wenzhong Liu, Peter Maye, Jianghong Zhang, Yazhou Zhang, Marja Hurley, Caiying Guo, Adele Boskey, Le Sun, Stephen E Harris, David W Rowe, Hua Zhu Ke, and Dianqing Wu. Dkk2 has a role in terminal osteoblast differentiation and mineralized matrix formation. *Nature genetics*, 37(9):945–952, 2005. ISSN 1061-4036. doi: 10.1038/ng1614.

[34] Ruth Z Birk, Liat Abramovitch-Gottlib, Iris Margalit, Moran Aviv, Efrat Forti, Shimona Geresh, and Razi Vago. Conversion of adipogenic to osteogenic phenotype using crystalline porous biomatrices of marine origin. *Tissue engineering*, 12(1):21–31, January 2006. ISSN 1076-3279. doi: 10.1089/ten.2006.12.ft-11.

[35] Clara Foo, Soenke Frey, Hong Hyun Yang, Rene Zellweger, and Luis Filgueira. Downregulation of beta-catenin and transdifferentiation of human osteoblasts to adipocytes under estrogen deficiency. *Gynecological endocrinology : the official journal of the International Society of Gynecological Endocrinology*, 23(9):535–540, September 2007. ISSN 0951-3590. doi: 10.1080/09513590701556483.

[36] Aline Clabaut, Séverine Delplace, Christophe Chauveau, Pierre Hardouin, and Odile Broux. Human osteoblasts derived from mesenchymal stem cells express adipogenic markers upon

coculture with bone marrow adipocytes. *Differentiation*, 80(1):40–45, July 2010. ISSN 03014681. doi: 10.1016/j.diff.2010.04.004.

[37] Linfang Wang, Lihua Li, Haibo Gao, and Yuming Li. Effect of pioglitazone on transdifferentiation of preosteoblasts from rat bone mesenchymal stem cells into adipocytes. *Journal of Huazhong University of Science and Technology - Medical Science*, 32(4):530–533, August 2012. ISSN 16720733. doi: 10.1007/s11596-012-0091-x.

[38] Yaqian Chen, Yang Yang, and Yi Man. Age and Site Should Be Considered When Investigating the Effect of Growth Factors on Human Bone-Derived Cells. *The Journals of Gerontology Series A: Biological Sciences and Medical Sciences*, 69(9):1094–1095, September 2014. ISSN 1079-5006. doi: 10.1093/gerona/glu107.

[39] Bo Gao, Liu Yang, and Zhuo-Jing Luo. Transdifferentiation between bone and fat on bone metabolism. *International journal of clinical and experimental pathology*, 7(5):1834–41, January 2014. ISSN 1936-2625.

[40] Yoshinao Oki, Saiko Watanabe, Tuyoshi Endo, and Koichiro Kano. Mature adipocyte-derived dedifferentiated fat cells can trans-differentiate into osteoblasts in vitro and in vivo only by all-trans retinoic acid. *Cell structure and function*, 33(2):211–222, January 2008. ISSN 0386-7196. doi: 10.1247/csf.08038.

[41] Tomihisa Takahashi. Overexpression of Runx2 and MKP-1 stimulates transdifferentiation of 3T3-L1 preadipocytes into bone-forming osteoblasts in vitro. *Calcified Tissue International*, 88(4): 336–347, April 2011. ISSN 0171967X. doi: 10.1007/s00223-011-9461-9.

[42] Mujib Ullah, Michael Sittinger, and Jochen Ringe. Transdifferentiation of adipogenically differentiated cells into osteogenically or chondrogenically differentiated cells: Phenotype switching via dedifferentiation. *International Journal of Biochemistry and Cell Biology*, 46(1):124–137, November 2014. ISSN 13572725. doi: 10.1016/j.biocel.2013.11.010.

[43] Young Dan Cho, Won Joon Yoon, Woo Jin Kim, Kyung Mi Woo, Jeong Hwa Baek, Gene Lee, Young Ku, Andre J. Van Wijnen, and Hyun Mo Ryoo. Epigenetic modifications and canonical wingless/int-1 class (WNT) signaling enable trans-differentiation of nonosteogenic cells into osteoblasts. *Journal of Biological Chemistry*, 289(29):20120–20128, July 2014. ISSN 1083351X. doi: 10.1074/jbc.M114.558064.

[44] Jun-Beom Park. Effects of the combination of dexamethasone and fibroblast growth factor2 on differentiation of osteoprecursor cells. *Molecular Medicine Reports*, 9(2):659–62, February 2013. ISSN 1791-2997. doi: 10.3892/mmr.2013.1811.

[45] Agnes D Berendsen and Bjorn R Olsen. Osteoblast-adipocyte lineage plasticity in tissue development, maintenance and pathology. *Cellular and Molecular Life Sciences*, 71(3):493–497, February 2014. ISSN 1420682X. doi: 10.1007/s00018-013-1440-z.

[46] Tatjana Schilling, Robert Küffner, Ludger Klein-Hitpass, Ralf Zimmer, Franz Jakob, and Norbert Schütze. Microarray analyses of transdifferentiated mesenchymal stem cells. *Journal of Cellular Biochemistry*, 103(2):413–433, 2008. ISSN 07302312. doi: 10.1002/jcb.21415.

[47] D M Ornitz and N Itoh. Fibroblast growth factors. *Genome biology*, 2(3):REVIEWS3005, 2001. ISSN 1465-6914. doi: 10.1186/gb-2001-2-3-reviews3005.

[48] Chad M Teven, Evan M Farina, Jane Rivas, and Russell R Reid. Fibroblast growth factor (FGF) signaling in development and skeletal diseases. *Genes & Diseases*, 1(2):199–213, December 2014. ISSN 23523042. doi: 10.1016/j.gendis.2014.09.005.

[49] David M Ornitz and Nobuyuki Itoh. The Fibroblast Growth Factor signaling pathway. *Wiley Interdisciplinary Reviews: Developmental Biology*, 4(3):n/a–n/a, May 2015. ISSN 17597684. doi: 10.1002/wdev.176.

[50] Makoto Kuro-o. Endocrine FGFs and Klothos: emerging concepts. *Trends in Endocrinology and Metabolism*, 19(7):239–245, 2008. ISSN 10432760. doi: 10.1016/j.tem.2008.06.002.

[51] Nobuyuki Itoh. Hormone-like (endocrine) Fgfs: Their evolutionary history and roles in development, metabolism, and disease. *Cell and Tissue Research*, 342(1):1–11, 2010. ISSN 0302766X. doi: 10.1007/s00441-010-1024-2.

[52] Yun Chau Long and Alexei Kharitonenkov. Hormone-like fibroblast growth factors and metabolic regulation. *Biochimica et biophysica acta*, 1812(7):791–795, 2011. ISSN 0006-3002. doi: 10.1016/j.bbadis.2011.04.002.

[53] Matthew J. Potthoff, Steven A. Kliewer, and David J. Mangelsdorf. Endocrine fibroblast growth factors 15/19 and 21: From feast to famine. *Genes and Development*, 26(4):312–324, 2012. ISSN 08909369. doi: 10.1101/gad.184788.111.

[54] Ming Chang Hu, Kazuhiro Shiizaki, Makoto Kuro-o, and Orson W Moe. Fibroblast growth factor 23 and Klotho: physiology and pathophysiology of an endocrine network of mineral metabolism. *Annual review of physiology*, 75:503–33, 2013. ISSN 1545-1585. doi: 10.1146/annurev-physiol-030212-183727.

[55] C J Powers, S W McLeskey, and A Wellstein. Fibroblast growth factors, their receptors and signaling. *Endocrine-Related Cancer*, 7(3):165–197, September 2000. ISSN 13510088. doi: 10.1677/erc.0.0070165.

[56] V P Eswarakumar, I Lax, and J Schlessinger. Cellular signaling by fibroblast growth factor receptors. *Cytokine and Growth Factor Reviews*, 16(2 SPEC. ISS.):139–149, 2005. ISSN 13596101. doi: 10.1016/j.cytogfr.2005.01.001.

[57] Andrew Beenken and Moosa Mohammadi. The FGF family: biology, pathophysiology and therapy. *Nature reviews. Drug discovery*, 8(3):235–253, 2009. ISSN 1474-1776. doi: 10.1038/nrd2792.

[58] Alexei Kharitonenkov. FGFs and metabolism. *Current Opinion in Pharmacology*, 9(6):805–810, 2009. ISSN 14714892. doi: 10.1016/j.coph.2009.07.001.

[59] Ralph T. Böttcher and Christof Niehrs. Fibroblast growth factor signaling during early vertebrate development. *Endocrine Reviews*, 26(1):63–77, 2005. ISSN 0163769X. doi: 10.1210/er.2003-0040.

[60] Bernard Thisse and Christine Thisse. Functions and regulations of fibroblast growth factor signaling during embryonic development. *Developmental Biology*, 287(2):390–402, 2005. ISSN 00121606. doi: 10.1016/j.ydbio.2005.09.011.

[61] D M Ornitz, A Yayon, J G Flanagan, C M Svahn, E Levi, and P Leder. Heparin is required for cell-free binding of basic fibroblast growth factor to a soluble receptor and for mitogenesis in

whole cells. *Molecular and cellular biology*, 12(1):240–247, 1992. ISSN 0270-7306. doi: 10.1128/mcb.12.1.240.

[62] David M Ornitz and Nobuyuki Itoh. Fibroblast growth factors. *Genome biology*, 2(3): REVIEWS3005, 2001. ISSN 1465-6914. doi: 10.1186/gb-2001-2-3-reviews3005.

[63] Stephane Sarrazin, William C. Lamanna, and Jeffrey D. Esko. Heparan sulfate proteoglycans. *Cold Spring Harbor Perspectives in Biology*, 3(7):1–33, 2011. ISSN 19430264. doi: 10.1101/cshperspect.a004952.

[64] A C Rapraeger, A Krufka, and B B Olwin. Requirement of heparan sulfate for bFGF-mediated fibroblast growth and myoblast differentiation. *Science (New York, N.Y.)*, 252(5013):1705–1708, 1991. ISSN 0036-8075. doi: 10.1126/science.1646484.

[65] A Yayon, M Klagsbrun, J D Esko, P Leder, and D M Ornitz. Cell surface, heparin-like molecules are required for binding of basic fibroblast growth factor to its high affinity receptor. *Cell*, 64(4): 841–848, 1991. ISSN 00928674. doi: 10.1016/0092-8674(91)90512-W.

[66] Rebecca A. Jackson, Victor Nurcombe, and Simon M. Cool. Coordinated fibroblast growth factor and heparan sulfate regulation of osteogenesis. *Gene*, 379(1-2):79–91, 2006. ISSN 03781119. doi: 10.1016/j.gene.2006.04.028.

[67] Isao Matsuo and Chiharu Kimura-Yoshida. Extracellular modulation of Fibroblast Growth Factor signaling through heparan sulfate proteoglycans in mammalian development. *Current Opinion in Genetics and Development*, 23(4):399–407, 2013. ISSN 1879-0380. doi: 10.1016/j.gde.2013.02.004.

[68] Stacey J Coleman, Charo Bruce, Athina-Myrto Chioni, Hemant M Kocher, and Richard P Grose. The ins and outs of fibroblast growth factor receptor signalling. *Clinical science (London, England : 1979)*, 127(4):217–31, August 2014. ISSN 1470-8736. doi: 10.1042/CS20140100.

[69] J C Coutts and J T Gallagher. Receptors for fibroblast growth factors. *Immunology and cell biology*, 73(6):584–589, 1995. ISSN 0818-9641. doi: 10.1038/icb.1995.92.

[70] M R Passos-Bueno, W R Wilcox, E W Jabs, A L Sertié, L G Alonso, and H Kitoh. Clinical spectrum of fibroblast growth factor receptor mutations. *Human Mutation*, 14(2):115–125, January 1999. ISSN 10597794. doi: 10.1002/(SICI)1098-1004(1999)14:2⟨115::AID-HUMU3⟩3.0.CO;2-2.

[71] T Miki, D P Bottaro, T P Fleming, C L Smith, W H Burgess, A M Chan, and S A Aaronson. Determination of ligand-binding specificity by alternative splicing: two distinct growth factor receptors encoded by a single gene. *Proceedings of the National Academy of Sciences of the United States of America*, 89(1):246–250, 1992. ISSN 0027-8424. doi: 10.1073/pnas.89.1.246.

[72] Arasu T Chellaiah, Donald G McEwen, Sabine Werner, Jingsong Xu, and David M Ornitz. Fibroblast growth factor receptor (FGFR) 3. *The Journal of Biological Chemistry*, 269(15):11620–11627, 1994.

[73] M C Naski and D M Ornitz. FGF signaling in skeletal development. *Frontiers in bioscience: a journal and virtual library*, 3:d781–d794, 1998. ISSN 1093-4715; 1093-4715. doi: 10.1080/15513819809168795.

[74] David M Ornitz, Jingsong Xu, Jennifer S Colvin, Donald G McEwen, Craig A MacArthur, François Coulier, Guangxia Gao, and Mitchell Goldfarb. Receptor specificity of the fibroblast

growth factor family. *Journal of Biological Chemistry*, 271(25):15292–15297, 1996. ISSN 00219258. doi: 10.1074/jbc.271.25.15292.

[75] T Miki, T P Fleming, D P Bottaro, J S Rubin, D Ron, and S A Aaronson. Expression cDNA cloning of the KGF receptor by creation of a transforming autocrine loop. *Science (New York, N.Y.)*, 251 (4989):72–75, 1991. ISSN 0036-8075. doi: 10.1126/science.1846048.

[76] G Yan, Y Fukabori, G McBride, S Nikolaropolous, and W L McKeehan. Exon switching and activation of stromal and embryonic fibroblast growth factor (FGF)-FGF receptor genes in prostate epithelial cells accompany stromal independence and malignancy. *Molecular and cellular biology*, 13(8):4513–4522, August 1993. ISSN 0270-7306. doi: 10.1128/MCB.13.8.4513.Updated.

[77] E Gilbert, F Del Gatto, P Champion-Arnaud, M C Gesnel, and R Breathnach. Control of BEK and K-SAM splice sites in alternative splicing of the fibroblast growth factor receptor 2 pre-mRNA. *Molecular and cellular biology*, 13(9):5461–5468, 1993. ISSN 02707306.

[78] A Avivi, A Yayon, and D Givol. A novel form of FGF receptor-3 using an alternative exon in the immunoglobulin domain III. *FEBS letters*, 330(3):249–252, September 1993. ISSN 00145793. doi: 10.1016/0014-5793(93)80882-U.

[79] Emmanuel Scotet and Elisabeth Houssaint. The choice between alternative IIIb and IIIc exons of the FGFR-3 gene is not strictly tissue-specific. *Biochimica et Biophysica Acta - Gene Structure and Expression*, 1264(2):238–242, November 1995. ISSN 01674781. doi: 10.1016/0167-4781(95)00156-B.

[80] A Orr-Urtreger, M T Bedford, M S Do, L Eisenbach, and P Lonai. Developmental expression of the alpha receptor for platelet-derived growth factor, which is deleted in the embryonic lethal Patch mutation. *Development (Cambridge, England)*, 115(1):289–303, 1992. ISSN 0950-1991.

[81] J Schlessinger, A N Plotnikov, O A Ibrahimi, A V Eliseenkova, B K Yeh, A Yayon, R J Linhardt, and M Mohammadi. Crystal structure of a ternary FGF-FGFR-heparin complex reveals a dual role for heparin in FGFR binding and dimerization. *Molecular cell*, 6(3):743–750, 2000. ISSN 10972765. doi: 10.1016/S1097-2765(00)00073-3.

[82] Jø rgen Wesche, Kaisa Haglund, and Ellen Margrethe Haugsten. Fibroblast growth factors and their receptors in cancer. *The Biochemical journal*, 437(2):199–213, 2011. ISSN 1470-8728. doi: 10.1042/BJ20101603.

[83] M Mohammadi, I Dikic, A Sorokin, W H Burgess, M Jaye, and J Schlessinger. Identification of six novel autophosphorylation sites on fibroblast growth factor receptor 1 and elucidation of their importance in receptor activation and signal transduction. *Molecular and cellular biology*, 16 (3):977–989, 1996. ISSN 0270-7306.

[84] M Mohammadi, A M Honegger, D Rotin, R Fischer, F Bellot, W Li, C A Dionne, M Jaye, M Rubinstein, and J Schlessinger. A tyrosine-phosphorylated carboxy-terminal peptide of the fibroblast growth factor receptor (Flg) is a binding site for the SH2 domain of phospholipase C-gamma 1. *Molecular and cellular biology*, 11(10):5068–5078, 1991. ISSN 0270-7306. doi: 10.1128/MCB.11.10.5068.Updated.

[85] Andy Wong, Betty Lamothe, Arnold Lee, Joseph Schlessinger, and Irit Lax. FRS2 alpha attenuates FGF receptor signaling by Grb2-mediated recruitment of the ubiquitin ligase Cbl. *Proceed-*

ings of the National Academy of Sciences of the United States of America, 99(10):6684–6689, 2002. ISSN 0027-8424. doi: 10.1073/pnas.052138899.

[86] Irit Lax, Andy Wong, Betty Lamothe, Arnold Lee, Adam Frost, Jessica Hawes, and Joseph Schlessinger. The docking protein FRS2α controls a MAP kinase-mediated negative feedback mechanism for signaling by FGF receptors. *Molecular Cell*, 10(4):709–719, 2002. ISSN 10972765. doi: 10.1016/S1097-2765(02)00689-5.

[87] Karel Dorey and Enrique Amaya. FGF signalling: diverse roles during early vertebrate embryogenesis. *Development (Cambridge, England)*, 137(22):3731–3742, 2010. ISSN 0950-1991. doi: 10.1242/dev.037689.

[88] D Shao and M A Lazar. Modulating nuclear receptor function: May the phos be with you. *Journal of Clinical Investigation*, 103(12):1617–1618, June 1999. ISSN 00219738. doi: 10.1172/JCI7421.

[89] Lisa Dailey, Davide Ambrosetti, Alka Mansukhani, and Claudio Basilico. Mechanisms underlying differential responses to FGF signaling. *Cytokine & growth factor reviews*, 16(2):233–247, April 2005. ISSN 13596101. doi: 10.1016/j.cytogfr.2005.01.007.

[90] Ye-Rang Yun, Jong Eun Won, Eunyi Jeon, Sujin Lee, Wonmo Kang, Hyejin Jo, Jun-Hyeog Jang, Ueon Sang Shin, and Hae-Won Kim. Fibroblast growth factors: biology, function, and application for tissue regeneration. *Journal of tissue engineering*, 2010:218142, 2010. ISSN 2041-7314. doi: 10.4061/2010/218142.

[91] Pamela A. Maher. Nuclear translocation of fibroblast growth factor (FGF) receptors in response to FGF-2. *Journal of Cell Biology*, 134(2):529–536, 1996. ISSN 00219525. doi: 10.1083/jcb.134.2.529.

[92] J F Reilly and P A Maher. Importin beta-mediated nuclear import of fibroblast growth factor receptor: role in cell proliferation. *The Journal of cell biology*, 152(6):1307–1312, 2001. ISSN 0021-9525.

[93] Michal K Stachowiak, Xiaohong Fang, Jason M Myers, Star M Dunham, Ronald Berezney, Pamela A Maher, and Ewa K Stachowiak. Integrative Nuclear FGFR1 Signaling (INFS) as a Part of a Universal "Feed-Forward-And-Gate" Signaling Module That Controls Cell Growth and Differentiation. *Journal of Cellular Biochemistry*, 90(4):662–691, November 2003. ISSN 07302312. doi: 10.1002/jcb.10606.

[94] David M Bryant and Jennifer L Stow. Nuclear translocation of cell-surface receptors: Lessons from fibroblast growth factor. *Traffic*, 6(10):947–954, October 2005. ISSN 13989219. doi: 10.1111/j.1600-0854.2005.00332.x.

[95] David M Ornitz and Pierre J Marie. FGF signaling pathways in endochondral and intramembranous bone development and human genetic disease. *Genes & development*, 16(12):1446–1465, June 2002. ISSN 0890-9369. doi: 10.1101/gad.990702.

[96] P. J. Marie. Fibroblast growth factor signaling controlling osteoblast differentiation. *Gene*, 316 (1-2):23–32, 2003. ISSN 03781119. doi: 10.1016/S0378-1119(03)00748-0.

[97] Pierre J Marie. Fibroblast growth factor signaling controlling bone formation: An update. *Gene*, 498(1):1–4, 2012. ISSN 03781119. doi: 10.1016/j.gene.2012.01.086.

[98] Yurong Fei and Marja M. Hurley. Role of fibroblast growth factor 2 and wnt signaling in anabolic

effects of parathyroid hormone on bone formation. *Journal of Cellular Physiology*, 227(11):3539–3545, 2012. ISSN 00219541. doi: 10.1002/jcp.24075.

[99] Hiroshi Kawaguchi. Bone fracture and the healing mechanisms. Fibroblast growth factor-2 and fracture healing. *Clinical calcium*, 19(5):653–659, 2009. ISSN 0917-5857. doi: CliCa0905653659.

[100] Yuichiro Takei, Tomoko Minamizaki, and Yuji Yoshiko. Functional Diversity of Fibroblast Growth Factors in Bone Formation. *International Journal of Endocrinology*, 2015:1–12, January 2015. ISSN 1687-8337. doi: 10.1155/2015/729352.

[101] H Nagai, R Tsukuda, and H Mayahara. Effects of basic fibroblast growth factor (bFGF) on bone formation in growing rats. *Bone*, 16(3):367–373, 1995. ISSN 87563282. doi: 10.1016/8756-3282(94)00049-2.

[102] C R Dunstan, R Boyce, B F Boyce, I R Garrett, E Izbicka, W H Burgess, and G R Mundy. Systemic administration of acidic fibroblast growth factor (FGF-1) prevents bone loss and increases new bone formation in ovariectomized rats. *Journal of bone and mineral research : the official journal of the American Society for Bone and Mineral Research*, 14(6):953–959, 1999. ISSN 08840431. doi: 10.1359/jbmr.1999.14.6.953.

[103] H. Okazaki, T. Kurokawa, K. Nakamura, T. Matsushita, K. Mamada, and H. Kawaguchi. Stimulation of bone formation by recombinant fibroblast growth factor-2 in callotasis bone lengthening of rabbits. *Calcified Tissue International*, 64(6):542–546, 1999. ISSN 0171967X. doi: 10.1007/s002239900646.

[104] J Ignacio Aguirre, Martha E Leal, Mercedes F Rivera, Sally M Vanegas, Marda Jorgensen, and Thomas J Wronski. Effects of basic fibroblast growth factor and a prostaglandin E2 receptor subtype 4 agonist on osteoblastogenesis and adipogenesis in aged ovariectomized rats. *Journal of bone and mineral research : the official journal of the American Society for Bone and Mineral Research*, 22(6):877–88, June 2007. ISSN 0884-0431. doi: 10.1359/jbmr.070313.

[105] Takahiro Naganawa, Liping Xiao, J D Coffin, Thomas Doetschman, Maria Giovanna Sabbieti, Dimitrios Agas, and Marja M Hurley. Reduced expression and function of bone morphogenetic protein-2 in bones of Fgf2 null mice. *Journal of Cellular Biochemistry*, 103(6):1975–1988, April 2008. ISSN 07302312. doi: 10.1002/jcb.21589.

[106] M M Hurley, Y Okada, L Xiao, Y Tanaka, M Ito, N Okimoto, T Nakamura, C J Rosen, T Doetschman, and J D Coffin. Impaired bone anabolic response to parathyroid hormone in Fgf2-/- and Fgf2+/- mice. *Biochemical and Biophysical Research Communications*, 341(4):989–994, March 2006. ISSN 0006291X. doi: 10.1016/j.bbrc.2006.01.044.

[107] Maria Giovanna Sabbieti, Dimitrios Agas, Liping Xiao, Luigi Marchetti, J Douglas Coffin, Thomas Doetschman, and Marja M Hurley. Endogenous FGF-2 is critically important in PTH anabolic effects on bone. *Journal of Cellular Physiology*, 219(1):143–151, April 2009. ISSN 00219541. doi: 10.1002/jcp.21661.

[108] A Montero, Y Okada, M Tomita, M Ito, H Tsurukami, T Nakamura, T Doetschman, J D Coffin, and M M Hurley. Disruption of the fibroblast growth factor-2 gene results in decreased bone mass and bone formation. *The Journal of clinical investigation*, 105(8):1085–1093, 2000. ISSN 0021-9738. doi: 10.1172/JCI8641.

[109] T. Naganawa, L. Xiao, E. Abogunde, T. Sobue, I. Kalajzic, M. Sabbieti, D. Agas, and M. M.

Hurley. In vivo and in vitro comparison of the effects of FGF-2 null and haplo-insufficiency on bone formation in mice. *Biochemical and Biophysical Research Communications*, 339(2):490–498, 2006. ISSN 0006291X. doi: 10.1016/j.bbrc.2005.10.215.

[110] S Walsh, C Jefferiss, K Stewart, G R Jordan, J Screen, and J N Beresford. Expression of the developmental markers STRO-1 and alkaline phosphatase in cultures of human marrow stromal cells: Regulation by fibroblast growth factor (FGF)-2 and relationship to the expression of FGF receptors 1-4. *Bone*, 27(2):185–195, 2000. ISSN 87563282. doi: 10.1016/S8756-3282(00)00319-7.

[111] Mi Ran Byun, A. Rum Kim, Jun Ha Hwang, Kyung Min Kim, Eun Sook Hwang, and Jeong Ho Hong. FGF2 stimulates osteogenic differentiation through ERK induced TAZ expression. *Bone*, 58:72–80, 2014. ISSN 87563282. doi: 10.1016/j.bone.2013.09.024.

[112] Tomomi Ito, Rumi Sawada, Yoko Fujiwara, and Toshie Tsuchiya. FGF-2 increases osteogenic and chondrogenic differentiation potentials of human mesenchymal stem cells by inactivation of TGF-beta signaling. *Cytotechnology*, 56(1):1–7, January 2008. ISSN 09209069. doi: 10.1007/s10616-007-9092-1.

[113] T. Kizhner, D. Ben-David, E. Rom, A. Yayon, and E. Livne. Effects of FGF2 and FGF9 on osteogenic differentiation of bone marrow-derived progenitors. *In Vitro Cellular and Developmental Biology - Animal*, 47(4):294–301, 2011. ISSN 10712690. doi: 10.1007/s11626-011-9390-y.

[114] Liisa T Kuhn, Guomin Ou, Lyndon Charles, Marja M Hurley, Craig M Rodner, and Gloria Gronowicz. Fibroblast growth factor-2 and bone morphogenetic protein-2 have a synergistic stimulatory effect on bone formation in cell cultures from elderly mouse and human bone. *The journals of gerontology. Series A, Biological sciences and medical sciences*, 68(10):1170–80, October 2013. ISSN 1758-535X. doi: 10.1093/gerona/glt018.

[115] K Hanada, J E Dennis, and A I Caplan. Stimulatory effects of basic fibroblast growth factor and bone morphogenetic protein-2 on osteogenic differentiation of rat bone marrow-derived mesenchymal stem cells. *Journal of bone and mineral research : the official journal of the American Society for Bone and Mineral Research*, 12(10):1606–1614, October 1997. ISSN 0884-0431. doi: 10.1359/jbmr.1997.12.10.1606.

[116] Liping Xiao, Takanori Sobue, Alycia Esliger, Mark S. Kronenberg, J. Douglas Coffin, Thomas Doetschman, and Marja M. Hurley. Disruption of the Fgf2 gene activates the adipogenic and suppresses the osteogenic program in mesenchymal marrow stromal stem cells. *Bone*, 47(2):360–370, 2010. ISSN 87563282. doi: 10.1016/j.bone.2010.05.021.

[117] J D Coffin, R Z Florkiewicz, J Neumann, T Mort-Hopkins, G W Dorn, P Lightfoot, R German, P N Howles, A Kier, and B A O'Toole. Abnormal bone growth and selective translational regulation in basic fibroblast growth factor (FGF-2) transgenic mice. *Molecular biology of the cell*, 6(12):1861–1873, December 1995. ISSN 1059-1524.

[118] Chao Liu, Yazhou Cui, Jing Luan, Xiaoyan Zhou, Zhenxing Liu, and Jinxiang Han. Fibroblast growth factor-2 inhibits mineralization of osteoblast-like Saos-2 cells by inhibiting the functioning of matrix vesicles. *Drug Discoveries and Therapeutics*, 8(1):42–47, February 2014. ISSN 1881784X. doi: 10.5582/ddt.8.42.

[119] H Nagai, R Tsukuda, and H Mayahara. Effects of basic fibroblast growth factor (bFGF) on bone

formation in growing rats. *Bone*, 16(3):367–373, 1995. ISSN 87563282. doi: 10.1016/8756-3282(94)00049-2.

[120] S. B. Rodan, G. Wesolowski, K. Yoon, and G. A. Rodan. Opposing effects of fibroblast growth factor and pertussis toxin on alkaline phosphatase, osteopontin, osteocalcin, and type I collagen mRNA levels in ROS 17/2.8 cells. *Journal of Biological Chemistry*, 264(33):19934–19941, 1989. ISSN 00219258.

[121] M M Hurley, C Abreu, J R Harrison, A C Lichtler, L G Raisz, and B E Kream. Basic fibroblast growth factor inhibits type I collagen gene expression in osteoblastic MC3T3-E1 cells. *The Journal of biological chemistry*, 268(8):5588–5593, 1993. ISSN 0021-9258.

[122] F Debiais, M Hott, A M Graulet, and P J Marie. The effects of fibroblast growth factor-2 on human neonatal calvaria osteoblastic cells are differentiation stage specific. *Journal of bone and mineral research : the official journal of the American Society for Bone and Mineral Research*, 13(4):645–654, April 1998. ISSN 0884-0431. doi: 10.1359/jbmr.1998.13.4.645.

[123] Ali Fakhry, Chootima Ratisoontorn, Charulatha Vedhachalam, Imad Salhab, Eiki Koyama, Phoeby Leboy, Maurizio Pacifici, Richard E. Kirschner, and Hyun Duck Nah. Effects of FGF-2/-9 in calvarial bone cell cultures: Differentiation stage-dependent mitogenic effect, inverse regulation of BMP-2 and noggin, and enhancement of osteogenic potential. *Bone*, 36(2):254–266, 2005. ISSN 87563282. doi: 10.1016/j.bone.2004.10.003.

[124] Alka Mansukhani, Paola Bellosta, Malika Sahni, and Claudio Basilico. Signaling by fibroblast growth factors (FGF) and fibroblast growth factor receptor 2 (FGFR2)-activating mutations blocks mineralization and induces apoptosis in osteoblasts. *Journal of Cell Biology*, 149(6):1297–1308, 2000. ISSN 00219525. doi: 10.1083/jcb.149.6.1297.

[125] Millie Hughes-Fulford and Chai-Fei Li. The role of FGF-2 and BMP-2 in regulation of gene induction, cell proliferation and mineralization. *Journal of orthopaedic surgery and research*, 6(1):8, January 2011. ISSN 1749-799X. doi: 10.1186/1749-799X-6-8.

[126] I. Kalajzic, Z. Kalajzic, M. M. Hurley, A. C. Lichtler, and David W. Rowe. Stage specific inhibition of osteoblast lineage differentiation by FGF2 and noggin. *Journal of Cellular Biochemistry*, 88(6):1168–1176, April 2003. ISSN 07302312. doi: 10.1002/jcb.10459.

[127] Emmanuel Biver, Cyril Thouverey, David Magne, and Joseph Caverzasio. Crosstalk between tyrosine kinase receptors, GSK3 and BMP2 signaling during osteoblastic differentiation of human mesenchymal stem cells. *Molecular and Cellular Endocrinology*, 382(1):120–130, January 2014. ISSN 03037207. doi: 10.1016/j.mce.2013.09.018.

[128] A Robubi, C Berger, M Schmid, K R Huber, A Engel, and W Krugluger. Gene expression profiles induced by growth factors in in vitro cultured osteoblasts. *Bone and Joint Research*, 3(7):236–240, July 2014. ISSN 2046-3758. doi: 10.1302/2046-3758.37.2000231.

[129] P Rutland, L J Pulleyn, W Reardon, M Baraitser, R Hayward, B Jones, S Malcolm, R M Winter, M Oldridge, and S F Slaney. Identical mutations in the FGFR2 gene cause both Pfeiffer and Crouzon syndrome phenotypes. *Nature genetics*, 9(2):173–176, 1995. ISSN 1061-4036. doi: 10.1038/ng0295-173.

[130] U Schell, A Hehr, G J Feldman, N H Robin, E H Zackai, C de Die-Smulders, D H Viskochil, J M

Stewart, G Wolff, and H Ohashi. Mutations in FGFR1 and FGFR2 cause familial and sporadic Pfeiffer syndrome. *Human molecular genetics*, 4(3):323–328, 1995. ISSN 0964-6906.

[131] E W Jabs, X Li, A F Scott, G Meyers, W Chen, M Eccles, J I Mao, L R Charnas, C E Jackson, and M Jaye. Jackson-Weiss and Crouzon syndromes are allelic with mutations in fibroblast growth factor receptor 2. *Nature genetics*, 8(3):275–279, 1994. ISSN 1061-4036. doi: 10.1038/ng1194-275.

[132] W J Park, G A Meyers, X Li, C Theda, D Day, S J Orlow, M C Jones, and E W Jabs. Novel FGFR2 mutations in Crouzon and Jackson-Weiss syndromes show allelic heterogeneity and phenotypic variability. *Human molecular genetics*, 4(7):1229–1233, 1995. ISSN 0964-6906.

[133] W Reardon, R M Winter, P Rutland, L J Pulleyn, B M Jones, and S Malcolm. Mutations in the fibroblast growth factor receptor 2 gene cause Crouzon syndrome. *Nature genetics*, 8(1):98–103, 1994.

[134] M Oldridge, A O Wilkie, S F Slaney, M D Poole, L J Pulleyn, P Rutland, A D Hockley, M J Wake, J H Goldin, and R M Winter. Mutations in the third immunoglobulin domain of the fibroblast growth factor receptor-2 gene in Crouzon syndrome. *Human molecular genetics*, 4(6):1077–1082, 1995. ISSN 0964-6906.

[135] Daniela Steinberger, John B Mulliken, and Ulrich Müller. Crouzon syndrome: Previously unrecognized deletion, duplication, and point mutation within FGFR2 gene. *Human Mutation*, 8(4):386–390, January 1996. ISSN 10597794. doi: 10.1002/(SICI)1098-1004(1996)8:4⟨386::AID-HUMU18⟩3.0.CO;2-Z.

[136] Omar A. Ibrahimi, Fuming Zhang, Anna V. Eliseenkova, Robert J. Linhardt, and Moosa Mohammadi. Proline to arginine mutations in FGF receptors 1 and 3 result in Pfeiffer and Muenke craniosynostosis syndromes through enhancement of FGF binding affinity. *Human Molecular Genetics*, 13(1):69–78, 2004. ISSN 09646906. doi: 10.1093/hmg/ddh011.

[137] Elisabeth Lajeunie, Solange Heuertz, Vincent El Ghouzzi, Jelena Martinovic, Dominique Renier, Martine Le Merrer, and Jacky Bonaventure. Mutation screening in patients with syndromic craniosynostoses indicates that a limited number of recurrent FGFR2 mutations accounts for severe forms of Pfeiffer syndrome. *European journal of human genetics : EJHG*, 14(3):289–298, 2006. ISSN 1018-4813. doi: 10.1038/sj.ejhg.5201558.

[138] G A Meyers, D Day, R Goldberg, D L Daentl, K A Przylepa, L J Abrams, J M Graham, M Feingold, J B Moeschler, E Rawnsley, A F Scott, and E W Jabs. FGFR2 exon IIIa and IIIc mutations in Crouzon, Jackson-Weiss, and Pfeiffer syndromes: evidence for missense changes, insertions, and a deletion due to alternative RNA splicing. *American journal of human genetics*, 58(3):491–498, 1996. ISSN 0002-9297.

[139] P J Marie, J D Coffin, and M M Hurley. FGF and FGFR signaling in chondrodysplasias and craniosynostosis. *Journal of Cellular Biochemistry*, 96(5):888–896, December 2005. ISSN 07302312. doi: 10.1002/jcb.20582.

[140] Rita Shiang, Leslie M Thompson, Ya Zhen Zhu, Deanna M Church, Thomas J Fielder, Maureen Bocian, Sara T Winokur, and John J Wasmuth. Mutations in the transmembrane domain of FGFR3 cause the most common genetic form of dwarfism, achondroplasia. *Cell*, 78(2):335–342, July 1994. ISSN 00928674. doi: 10.1016/0092-8674(94)90302-6.

[141] Natalina Quarto, Derrick C. Wan, and Michael T. Longaker. Molecular mechanisms of FGF-2 inhibitory activity in the osteogenic context of mouse adipose-derived stem cells (mASCs). *Bone*, 42(6):1040–1052, 2008. ISSN 87563282. doi: 10.1016/j.bone.2008.01.026.

[142] A O Wilkie, S F Slaney, M Oldridge, M D Poole, G J Ashworth, A D Hockley, R D Hayward, D J David, L J Pulleyn, and P Rutland. Apert syndrome results from localized mutations of FGFR2 and is allelic with Crouzon syndrome. *Nature genetics*, 9(2):165–172, February 1995. ISSN 1061-4036. doi: 10.1038/ng0295-165.

[143] Ulrich Nöth, Anna M. Osyczka, Richard Tuli, Noreen J. Hickok, Keith G. Danielson, and Rocky S. Tuan. Multilineage mesenchymal differentiation potential of human trabecular bone-derived cells. *Journal of Orthopaedic Research*, 20(5):1060–1069, 2002. ISSN 07360266. doi: 10.1016/S0736-0266(02)00018-9.

[144] S E Haynesworth, J Goshima, V M Goldberg, and A I Caplan. Characterization of cells with osteogenic potential from human marrow. *Bone*, 13(1):81–88, 1992. ISSN 8756-3282. doi: 10.1016/8756-3282(92)90364-3.

[145] Neelam Jaiswal, Stephen E Haynesworth, Arnold I Caplan, and Scott P Bruder. Osteogenic differentiation of purified, culture-expanded human mesenchymal stem cells in vitro. *Journal of Cellular Biochemistry*, 64(2):295–312, 1997. ISSN 07302312. doi: 10.1002/(SICI)1097-4644(199702)64:2⟨295::AID-JCB12⟩3.0.CO;2-I.

[146] Yu Ming Li, Tatjana Schilling, Peggy Benisch, Sabine Zeck, Jutta Meissner-Weigl, Doris Schneider, Catarina Limbert, Jochen Seufert, Moustapha Kassem, Norbert Schütze, Franz Jakob, and Regina Ebert. Effects of high glucose on mesenchymal stem cell proliferation and differentiation. *Biochemical and Biophysical Research Communications*, 363(1):209–215, 2007. ISSN 0006291X. doi: 10.1016/j.bbrc.2007.08.161.

[147] Chongben Zhang, Yingke He, Mitsuhara Okutsu, Lai Chun Ong, Yi Jin, Lin Zheng, Pierce Chow, Sidney Yu, Mei Zhang, and Zhen Yan. Autophagy is involved in adipogenic differentiation by repressesing proteasome-dependent PPARγ2 degradation. *American journal of physiology. Endocrinology and metabolism*, 305(4):E530–9, 2013. ISSN 1522-1555. doi: 10.1152/ajpendo.00640.2012.

[148] Michael W Pfaffl, Graham W Horgan, and Leo Dempfle. Relative expression software tool (REST) for group-wise comparison and statistical analysis of relative expression results in real-time PCR. *Nucleic acids research*, 30(9):e36, May 2002. ISSN 13624962. doi: 10.1093/nar/30.9.e36.

[149] Jo Vandesompele, Katleen De Preter, Filip Pattyn, Bruce Poppe, Nadine Van Roy, Anne De Paepe, and Frank Speleman. Accurate normalization of real-time quantitative RT-PCR data by geometric averaging of multiple internal control genes. *Genome biology*, 3(7):RESEARCH0034, June 2002. ISSN 1465-6914. doi: 10.1186/gb-2002-3-7-research0034.

[150] Andreas Untergasser, Ioana Cutcutache, Triinu Koressaar, Jian Ye, Brant C. Faircloth, Maido Remm, and Steven G. Rozen. Primer3-new capabilities and interfaces. *Nucleic Acids Research*, 40 (15):e115, August 2012. ISSN 03051048. doi: 10.1093/nar/gks596.

[151] Cecilia Granéli, Camilla Karlsson, Helena Brisby, Anders Lindahl, and Peter Thomsen. The effects of PPAR-γ inhibition on gene expression and the progression of induced osteogenic dif-

ferentiation of human mesenchymal stem cells. *Connective Tissue Research*, 55(4):262–274, August 2014. ISSN 0300-8207. doi: 10.3109/03008207.2014.910198.

[152] Jiashing Yu, Yuan Kun Tu, Yueh Bih Tang, and Nai Chen Cheng. Stemness and transdifferentiation of adipose-derived stem cells using l-ascorbic acid 2-phosphate-induced cell sheet formation. *Biomaterials*, 35(11):3516–3526, April 2014. ISSN 01429612. doi: 10.1016/j.biomaterials.2014.01.015.

[153] Mon-Juan Lee, Hui-Ting Chen, Mei-Ling Ho, Chung-Hwan Chen, Shu-Chun Chuang, Sung-Cheng Huang, Yin-Chih Fu, Gwo-Jaw Wang, Lin Kang, and Je-Ken Chang. PPARγ silencing enhances osteogenic differentiation of human adipose-derived mesenchymal stem cells. *Journal of cellular and molecular medicine*, 17(9):1188–93, 2013. ISSN 1582-4934. doi: 10.1111/jcmm.12098.

[154] Louise Hutley, Wenda Shurety, Felicity Newell, Ross McGeary, Nicole Pelton, Jennifer Grant, Adrian Herington, Donald Cameron, Jon Whitehead, and Johannes Prins. Fibroblast growth factor 1: A key regulator of human adipogenesis. *Diabetes*, 53(12):3097–3106, December 2004. ISSN 00121797. doi: 10.2337/diabetes.53.12.3097.

[155] C H Widberg, F S Newell, a W Bachmann, S N Ramnoruth, M C Spelta, J P Whitehead, L J Hutley, and J B Prins. Fibroblast growth factor receptor 1 is a key regulator of early adipogenic events in human preadipocytes. *American journal of physiology. Endocrinology and metabolism*, 296 (1):E121–E131, January 2009. ISSN 0193-1849. doi: 10.1152/ajpendo.90602.2008.

[156] Felicity S Newell, Hua Su, Hans Tornqvist, Jonathan P Whitehead, Johannes B Prins, and Louise J Hutley. Characterization of the transcriptional and functional effects of fibroblast growth factor-1 on human preadipocyte differentiation. *The FASEB journal : official publication of the Federation of American Societies for Experimental Biology*, 20(14):2615–2617, December 2006. ISSN 15306860. doi: 10.1096/fj.05-5710fje.

[157] H I Krieger-Brauer and H Kather. Antagonistic effects of different members of the fibroblast and platelet-derived growth factor families on adipose conversion and NADPH-dependent H2O2 generation in 3T3 L1-cells. *The Biochemical journal*, 307 (Pt 2:549–556, April 1995. ISSN 0264-6021.

[158] Midori Greenwood-Goodwin, Eric S Teasley, and Sarah C Heilshorn. Dual-stage growth factor release within 3D protein-engineered hydrogel niches promotes adipogenesis. *Biomaterials Science*, 2(11):1627–1639, November 2014. ISSN 2047-4830. doi: 10.1039/C4BM00142G.

[159] Johan W. Jonker, Jae Myoung Suh, Annette R. Atkins, Maryam Ahmadian, Pingping Li, Jamie Whyte, Mingxiao He, Henry Juguilon, Yun-Qiang Yin, Colin T. Phillips, Ruth T. Yu, Jerrold M. Olefsky, Robert R. Henry, Michael Downes, and Ronald M. Evans. A PPARγFGF1 axis is required for adaptive adipose remodelling and metabolic homeostasis. *Nature*, 485(7398):391–394, 2012. ISSN 0028-0836. doi: 10.1038/nature10998.A.

[160] Sheng Xiong, Ling Zhang, and Qing-Yu He. Fractionation of proteins by heparin chromatography. *Methods in molecular biology (Clifton, N.J.)*, 424:213–221, 2008. ISSN 1064-3745. doi: 10.1007/978-1-60327-064-9_18.

[161] Ishan Capila and Robert J Linhardt. Heparin - Protein interactions. *Angewandte Chemie - International Edition*, 41(3):390–412, 2002. ISSN 14337851. doi: 10.1002/1521-3773(20020201)41:3⟨390::AID-ANIE390⟩3.0.CO;2-B.

[162] Jeffrey D Esko and Robert J Linhardt. Chapter 35 Proteins that Bind Sulfated Glycosaminoglycans. *Essentials of Glycobiology*, pages 1–12, 2009.

[163] Ulf Lindahl and Jin ping Li. Chapter 3 Interactions Between Heparan Sulfate and Proteins-Design and Functional Implications. *International Review of Cell and Molecular Biology*, 276(C): 105–159, 2009. ISSN 19376448. doi: 10.1016/S1937-6448(09)76003-4.

[164] Alessandro Ori, Mark C Wilkinson, and David G Fernig. A systems biology approach for the investigation of the heparin/heparan sulfate interactome. *Journal of Biological Chemistry*, 286(22): 19892–19904, 2011. ISSN 00219258. doi: 10.1074/jbc.M111.228114.

[165] Franck Peysselon and Sylvie Ricard-Blum. Heparin-protein interactions: From affinity and kinetics to biological roles. Application to an interaction network regulating angiogenesis. *Matrix Biology*, 35:73–81, November 2014. ISSN 15691802. doi: 10.1016/j.matbio.2013.11.001.

[166] D A Roncari and P E Le Blanc. Inhibition of rat perirenal preadipocyte differentiation. *Biochemistry and cell biology = Biochimie et biologie cellulaire*, 68(1):238–242, 1990. ISSN 0829-8211. doi: 10.1139/o90-032.

[167] K Teichert-Kuliszewska, B S Hamilton, M Deitel, and D A Roncari. Decreasing expression of a gene encoding a protein related to basic fibroblast growth factor during differentiation of human preadipocytes. *Biochemistry and cell biology = Biochimie et biologie cellulaire*, 72(1-2):54–57, January 1993. ISSN 0829-8211.

[168] H Hauner, K Röhrig, and T Petruschke. Effects of epidermal growth factor (EGF), platelet-derived growth factor (PDGF) and fibroblast growth factor (FGF) on human adipocyte development and function. *European journal of clinical investigation*, 25(2):90–96, February 1995. ISSN 0014-2972.

[169] M Navre and G M Ringold. Differential effects of fibroblast growth factor and tumor promoters on the initiation and maintenance of adipocyte differentiation. *The Journal of cell biology*, 109(4 Pt 1):1857–1863, 1989. ISSN 0021-9525.

[170] Nayan G Patel, Sudhesh Kumar, and Margaret C Eggo. Essential role of fibroblast growth factor signaling in preadipoctye differentiation. *The Journal of clinical endocrinology and metabolism*, 90 (2):1226–1232, February 2005. ISSN 0021-972X. doi: 10.1210/jc.2004-1309.

[171] Louise J. Hutley, Felicity S. Newell, Yu Hee Kim, Xiao Luo, Charlotte H. Widberg, Wenda Shurety, Johannes B. Prins, and Jonathan P. Whitehead. A putative role for endogenous FGF-2 in FGF-1 mediated differentiation of human preadipocytes. *Molecular and Cellular Endocrinology*, 339(1-2):165–171, 2011. ISSN 03037207. doi: 10.1016/j.mce.2011.04.012.

[172] Markus Neubauer, Claudia Fischbach, Petra Bauer-Kreisel, Esther Lieb, Michael Hacker, Joerg Tessmar, Michaela B Schulz, Achim Goepferich, and Torsten Blunk. Basic fibroblast growth factor enhances PPARgamma ligand-induced adipogenesis of mesenchymal stem cells. *FEBS Letters*, 577(1-2):277–283, 2004. ISSN 00145793. doi: 10.1016/j.febslet.2004.10.020.

[173] Natsuko Kakudo, Ayuko Shimotsuma, and Kenji Kusumoto. Fibroblast growth factor-2 stimulates adipogenic differentiation of human adipose-derived stem cells. *Biochemical and Biophysical Research Communications*, 359(2):239–244, 2007. ISSN 0006291X. doi: 10.1016/j.bbrc.2007.05.070.

[174] Aaron W James, Jia Shen, Kevork Khadarian, Shen Pang, Greg Chung, Raghav Goyal, Greg Asa-

trian, Omar Velasco, Jung Kim, Xinli Zhang, Kang Ting, and Chia Soo. Lentiviral Delivery of PPARγ shRNA Alters the Balance of Osteogenesis and Adipogenesis, Improving Bone Microarchitecture. *Tissue Engineering Part A*, 20(19-20):2699–2710, October 2014. ISSN 1937-3341. doi: 10.1089/ten.tea.2013.0736.

[175] J M Gimble, C E Robinson, X Wu, and K A Kelly. The function of adipocytes in the bone marrow stroma: An update. *Bone*, 19(5):421–428, November 1996. ISSN 87563282. doi: 10.1016/S8756-3282(96)00258-X.

[176] Beata Lecka-Czernik, Igor Gubrij, Elena J Moerman, Oumitana Kajkenova, David A Lipschitz, Stavros C Manolagas, and Robert L Jilka. Inhibition of Osf2/Cbfa1 expression and terminal osteoblast differentiation by PPARγ2. *Journal of Cellular Biochemistry*, 74(3):357–371, 1999. ISSN 07302312. doi: 10.1002/(SICI)1097-4644(19990901)74:3⟨357::AID-JCB5⟩3.0.CO;2-7.

[177] Beata Lecka-Czernik, Elena J Moerman, David F Grant, Jürgen M Lehmann, Stavros C Manolagas, and Robert L Jilka. Divergent effects of selective peroxisome proliferator-activated receptor-gamma 2 ligands on adipocyte versus osteoblast differentiation. *Endocrinology*, 143(6):2376–2384, 2002. ISSN 0013-7227. doi: 10.1210/endo.143.6.8834.

[178] L Tornvig, Li Mosekilde, J Justesen, E Falk, and M Kassem. Troglitazone treatment increases bone marrow adipose tissue volume but does not affect trabecular bone volume in mice. *Calcified Tissue International*, 69(1):46–50, 2001. ISSN 0171967X. doi: 10.1007/s002230020018.

[179] S O Rzonca, L J Suva, D Gaddy, D C Montague, and B Lecka-Czernik. Bone Is a Target for the Antidiabetic Compound Rosiglitazone. *Endocrinology*, 145(1):401–406, 2004. ISSN 00137227. doi: 10.1210/en.2003-0746.

[180] Dympna Harmey, Lovisa Hessle, Sonoko Narisawa, Kristen A Johnson, Robert Terkeltaub, and José Luis Millán. Concerted regulation of inorganic pyrophosphate and osteopontin by akp2, enpp1, and ank: an integrated model of the pathogenesis of mineralization disorders. *The American journal of pathology*, 164(4):1199–1209, April 2004. ISSN 0002-9440. doi: 10.1016/S0002-9440(10)63208-7.

[181] R L Panek, G H Lu, T K Dahring, B L Batley, C Connolly, J M Hamby, and K J Brown. In vitro biological characterization and antiangiogenic effects of PD 166866, a selective inhibitor of the FGF-1 receptor tyrosine kinase. *The Journal of pharmacology and experimental therapeutics*, 286(1):569–577, July 1998. ISSN 0022-3565.

[182] E Livneh, T Shimon, E Bechor, Y Doki, I Schieren, and I B Weinstein. Linking protein kinase C to the cell cycle: ectopic expression of PKC eta in NIH3T3 cells alters the expression of cyclins and Cdk inhibitors and induces adipogenesis. *Oncogene*, 12(7):1545–1555, April 1996. ISSN 09509232.

[183] P R Webb, C Doyle, and N G Anderson. Protein kinase C-epsilon promotes adipogenic commitment and is essential for terminal differentiation of 3T3-F442A preadipocytes. *Cellular and Molecular Life Sciences*, 60(7):1504–1512, July 2003. ISSN 1420682X. doi: 10.1007/s00018-003-2337-z.

[184] Yiran Zhou, Dongmei Wang, Fuqiang Li, Jian Shi, and Jianguo Song. Different roles of protein kinase C-βI and -δ in the regulation of adipocyte differentiation. *The International Journal of Biochemistry & Cell Biology*, 38(12):2151–2163, January 2006. ISSN 13572725. doi: 10.1016/j.biocel.2006.06.009.

[185] Lingjie Fu, Tingting Tang, Yanying Miao, Shuhong Zhang, Zhihu Qu, and Kerong Dai. Stimulation of osteogenic differentiation and inhibition of adipogenic differentiation in bone marrow stromal cells by alendronate via ERK and JNK activation. *Bone*, 43(1):40–47, July 2008. ISSN 87563282. doi: 10.1016/j.bone.2008.03.008.

[186] Baiyao Xu, Yang Ju, and Guanbin Song. Role of p38, ERK1/2, focal adhesion kinase, RhoA/ROCK and cytoskeleton in the adipogenesis of human mesenchymal stem cells. *Journal of Bioscience and Bioengineering*, 117(5):624–631, May 2014. ISSN 13474421. doi: 10.1016/j.jbiosc.2013.10.018.

[187] Kyung-Ah Kim, Jung-Hyun Kim, Yuhui Wang, and Hei Sook Sul. Pref-1 (preadipocyte factor 1) activates the MEK/extracellular signal-regulated kinase pathway to inhibit adipocyte differentiation. *Molecular and cellular biology*, 27(6):2294–2308, March 2007. ISSN 0270-7306. doi: 10.1128/MCB.02207-06.

[188] Tain Hsiung Chen, Wei Ming Chen, Ke Hsun Hsu, Cheng Deng Kuo, and Shih Chieh Hung. Sodium butyrate activates ERK to regulate differentiation of mesenchymal stem cells. *Biochemical and Biophysical Research Communications*, 355(4):913–918, April 2007. ISSN 0006291X. doi: 10.1016/j.bbrc.2007.02.057.

[189] Mi Ran Byun, A. Rum Kim, Jun Ha Hwang, Kyung Min Kim, Eun Sook Hwang, and Jeong Ho Hong. FGF2 stimulates osteogenic differentiation through ERK induced TAZ expression. *Bone*, 58:72–80, 2014. ISSN 87563282. doi: 10.1016/j.bone.2013.09.024.

[190] Jeong-Ho Hong, Eun Sook Hwang, Michael T McManus, Adam Amsterdam, Yu Tian, Ralitsa Kalmukova, Elisabetta Mueller, Thomas Benjamin, Bruce M Spiegelman, Phillip A Sharp, Nancy Hopkins, and Michael B Yaffe. TAZ, a transcriptional modulator of mesenchymal stem cell differentiation. *Science (New York, N.Y.)*, 309(5737):1074–1078, 2005. ISSN 0036-8075. doi: 10.1126/science.1110955.

[191] Deepanwita Prusty, Bae-Hang Park, Kathryn E Davis, and Stephen R Farmer. Activation of MEK/ERK signaling promotes adipogenesis by enhancing peroxisome proliferator-activated receptor gamma (PPARgamma) and C/EBPalpha gene expression during the differentiation of 3T3-L1 preadipocytes. *The Journal of biological chemistry*, 277(48):46226–46232, November 2002. ISSN 00219258. doi: 10.1074/jbc.M207776200.

[192] Elisabetta Donzelli, Caterina Lucchini, Elisa Ballarini, Arianna Scuteri, Fabrizio Carini, Giovanni Tredici, and Mariarosaria Miloso. ERK1 and ERK2 are involved in recruitment and maturation of human mesenchymal stem cells induced to adipogenic differentiation. *Journal of Molecular Cell Biology*, 3(2):123–131, January 2011. ISSN 16742788. doi: 10.1093/jmcb/mjq050.

[193] Wei Hua Yu, Fu Gui Li, Xiao Yong Chen, Jian Tao Li, Yan Heng Wu, Li Hua Huang, Zhen Wang, Panlong Li, Tao Wang, Bruce T Lahn, and Andy Peng Xiang. PPARgamma suppression inhibits adipogenesis but does not promote osteogenesis of human mesenchymal stem cells. *International Journal of Biochemistry and Cell Biology*, 44(2):377–384, February 2012. ISSN 13572725. doi: 10.1016/j.biocel.2011.11.013.

[194] H Clarke Anderson, Joseph B Sipe, Lovisa Hessle, Rama Dhanyamraju, Elisa Atti, Nancy P Camacho, and José Luis Millán. Impaired calcification around matrix vesicles of growth plate and bone in alkaline phosphatase-deficient mice. *The American journal of pathology*, 164(3):841–847, 2004. ISSN 0002-9440. doi: 10.1016/S0002-9440(10)63172-0.

[195] R J Majeska and R E Wuthier. Studies on matrix vesicles isolated from chick epiphyseal cartilage. Association of pyrophosphatase and ATPase activities with alkaline phosphatase. *Biochimica et biophysica acta*, 391(1):51–60, 1975. ISSN 00052744. doi: 10.1016/0005-2744(75)90151-5.

[196] M D Fallon, M P Whyte, and S L Teitelbaum. Stereospecific inhibition of alkaline phosphatase by L-tetramisole prevents in vitro cartilage calcification. *Laboratory investigation; a journal of technical methods and pathology*, 43(6):489–494, 1980. ISSN 00236837.

[197] Julie C Crockett, Michael J Rogers, Fraser P Coxon, Lynne J Hocking, and Miep H Helfrich. Bone remodelling at a glance. *Journal of cell science*, 124(Pt 7):991–998, April 2011. ISSN 0021-9533. doi: 10.1242/jcs.063032.

[198] Kam Tsun Tang, Casey Capparelli, Janet L. Stein, Gary S Stein, Jane B Lian, Anna C Huber, Lewis E Braverman, and William J DeVito. Acidic fibroblast growth factor inhibits osteoblast differentiation in vitro: Altered expression of collagenase, cell growth-related, and mineralization-associated genes. *Journal of Cellular Biochemistry*, 61(1):152–166, April 1996. ISSN 07302312. doi: 10.1002/(SICI)1097-4644(19960401)61:1⟨152::AID-JCB16⟩3.0.CO;2-Q.

[199] Hideo Orimo. The mechanism of mineralization and the role of alkaline phosphatase in health and disease. *Journal of Nihon Medical School = Nihon Ika Daigaku zasshi*, 77(1):4–12, February 2010. ISSN 1345-4676. doi: 10.1272/jnms.77.4.

[200] Nan E Hatch, Francisco Nociti, Erica Swanson, Mark Bothwell, and Martha Somerman. FGF2 alters expression of the pyrophosphate/phosphate regulating proteins, PC-1, ANK and TNAP, in the calvarial osteoblastic cell line, MC3T3E1(C4). *Connective tissue research*, 46(4-5):184–192, January 2005. ISSN 0300-8207. doi: 10.1080/03008200500237203.

[201] Nan E. Hatch. Potential role of PC-1 expression and pyrophosphate elaboration in the molecular etiology of the FGFR- associated craniosynostosis syndromes. *Orthodontics and Craniofacial Research*, 10(2):53–58, 2007. ISSN 16016335. doi: 10.1111/j.1601-6343.2007.00387.x.

[202] Nan E. Hatch and Renny T. Franceschi. Osteoblast differentiation stage-specific expression of the pyrophosphate-generating enzyme PC-1. *Cells Tissues Organs*, 189:65–69, 2008. ISSN 14226405. doi: 10.1159/000151375.

[203] Nan E Hatch and Renny T Franceschi. Osteoblast differentiation stage-specific expression of the pyrophosphate-generating enzyme PC-1. *Cells Tissues Organs*, 189(1-4):65–69, January 2008. ISSN 14226405. doi: 10.1159/000151375.

[204] Ai Kyono, Nanthawan Avishai, Zhufeng Ouyang, Gary E Landreth, and Shunichi Murakami. FGF and ERK signaling coordinately regulate mineralizationrelated genes and play essential roles in osteocyte differentiation. *Journal of Bone and Mineral Metabolism*, 30(1):19–30, January 2012. ISSN 09148779. doi: 10.1007/s00774-011-0288-2.

[205] Yan Guo, Debbie K W Hsu, Sheau Line Y Feng, Christine M Richards, and Jeffrey A Winkles. Polypeptide growth factors and phorbol ester induce progressive ankylosis (Ank) gene expression in murine and human fibroblasts. *Journal of Cellular Biochemistry*, 84(1):27–38, January 2001. ISSN 07302312. doi: 10.1002/jcb.1263.

[206] Guohong Li. Fibroblast Growth Factor Receptor-1 Signaling Induces Osteopontin Expression and Vascular Smooth Muscle Cell-Dependent Adventitial Fibroblast Migration In Vitro. *Circulation*, 106(7):854–859, August 2002. ISSN 00097322. doi: 10.1161/01.CIR.0000024113.26985.CC.

[207] Yohei Nakayama, Li Yang, Hideki Takai, Hirotoshi Kaneko, Yoshimitsu Abiko, and Yorimasa Ogata. Fibroblast growth factor 2 and forskolin induce mineralization-associated genes in two kinds of osteoblast-like cells. *Journal of Oral Science*, 54(3):251–259, September 2012. ISSN 1343-4934. doi: 10.2334/josnusd.54.251.

[208] J L Solan, L J Deftos, J W Goding, and R A Terkeltaub. Expression of the nucleoside triphosphate pyrophosphohydrolase PC-1 is induced by basic fibroblast growth factor (bFGF) and modulated by activation of the protein kinase A and C pathways in osteoblast-like osteosarcoma cells. *Journal of bone and mineral research : the official journal of the American Society for Bone and Mineral Research*, 11(2):183–192, 1996. ISSN 08840431. doi: 10.1002/jbmr.5650110207.

[209] Yan Li, Jin Liu, Mark Hudson, Sungsu Kim, and Nan E. Hatch. FGF2 promotes Msx2 stimulated PC-1 expression via Frs2/MAPK signaling. *Journal of Cellular Biochemistry*, 111(5):1346–1358, 2010. ISSN 07302312. doi: 10.1002/jcb.22861.

[210] Y Oda, M D Kuo, S S Huang, and J S Huang. The plasma cell membrane glycoprotein, PC-1, is a threonine-specific protein kinase stimulated by acidic fibroblast growth factor. *The Journal of biological chemistry*, 266(25):16791–16795, September 1991. ISSN 0021-9258.

[211] J. M. Boudreaux and D. a. Towler. Synergistic induction of osteocalcin gene expression. Identification of a bipartite element conferring fibroblast growth factor 2 and cyclic AMP responsiveness in the rat osteocalcin promoter. *Journal of Biological Chemistry*, 271(13):7508–7515, 1996. ISSN 00219258. doi: 10.1074/jbc.271.13.7508.

[212] Guozhi Xiao, Di Jiang, Rajaram Gopalakrishnan, and Renny T Franceschi. Fibroblast growth factor 2 induction of the osteocalcin gene requires MAPK activity and phosphorylation of the osteoblast transcription factor, Cbfa1/Runx2. *Journal of Biological Chemistry*, 277(39):36181–36187, September 2002. ISSN 00219258. doi: 10.1074/jbc.M206057200.

[213] Emi Shimizu, Youhei Nakayama, Yu Nakajima, Naoko Kato, Hideki Takai, Dong Soon Kim, Masato Arai, Ryoichiro Saito, Jaro Sodek, and Yorimasa Ogata. Fibroblast growth factor 2 and cyclic AMP synergistically regulate bone sialoprotein gene expression. *Bone*, 39(1):42–52, July 2006. ISSN 87563282. doi: 10.1016/j.bone.2005.12.011.

[214] Emi Shimizu-Sasaki, Muneyoshi Yamazaki, Shunsuke Furuyama, Hiroshi Sugiya, Jaro Sodek, and Yorimasa Ogata. Identification of a Novel Response Element in the Rat Bone Sialoprotein (BSP) Gene Promoter that Mediates Constitutive and Fibroblast Growth Factor 2-induced Expression of BSP. *Journal of Biological Chemistry*, 276(8):5459–5466, February 2001. ISSN 00219258. doi: 10.1074/jbc.M008971200.

[215] Emi Shimizu-Sasaki, Muneyoshi Yamazaki, Shunsuke Furuyama, Hiroshi Sugiya, Jaro Sodek, and Yorimasa Ogata. Identification of FGF2-response element in the rat bone sialoprotein gene promoter. *Connective tissue research*, 44 Suppl 1:103–108, January 2003. ISSN 0300-8207. doi: 10.1080/03008200390152179.

[216] Liming Zhou and Yorimasa Ogata. Transcriptional regulation of the human bone sialoprotein gene by fibroblast growth factor 2. *Journal of oral science*, 55(1):63–70, 2013. ISSN 1880-4926.

[217] Hideyuki Harada, Shuzo Tagashira, Masanori Fujiwara, Shinji Ogawa, Takashi Katsumata, Akira Yamaguchi, Toshihisa Komori, and Masashi Nakatsuka. Cbfa1 isoforms exert functional

differences in osteoblast differentiation. *Journal of Biological Chemistry*, 274(11):6972–6978, March 1999. ISSN 00219258. doi: 10.1074/jbc.274.11.6972.

[218] Britt Kern, Jianhe Shen, Michael Starbuck, and Gerard Karsenty. Cbfa1 Contributes to the Osteoblast-specific Expression of type I collagen Genes. *Journal of Biological Chemistry*, 276(10): 7101–7107, 2001. ISSN 00219258. doi: 10.1074/jbc.M006215200.

[219] Di Chen, Ming Zhao, and Gregory R Mundy. Bone morphogenetic proteins. *Growth factors (Chur, Switzerland)*, 22(4):233–241, 2004. ISSN 0897-7194. doi: 10.1080/08977190412331279890.

[220] K S Lee, H J Kim, Q L Li, X Z Chi, C Ueta, T Komori, J M Wozney, E G Kim, J Y Choi, H M Ryoo, and S C Bae. Runx2 is a common target of transforming growth factor beta1 and bone morphogenetic protein 2, and cooperation between Runx2 and Smad5 induces osteoblast-specific gene expression in the pluripotent mesenchymal precursor cell line C2C12. *Molecular and cellular biology*, 20(23):8783–8792, December 2000. ISSN 0270-7306. doi: 10.1128/MCB.20.23.8783-8792.2000.

[221] Homare Eda, Katsuhiko Aoki, Keishi Marumo, Katsuyuki Fujii, and Kiyoshi Ohkawa. FGF-2 signaling induces downregulation of TAZ protein in osteoblastic MC3T3-E1 cells. *Biochemical and Biophysical Research Communications*, 366(2):471–475, February 2008. ISSN 0006291X. doi: 10.1016/j.bbrc.2007.11.140.

[222] Oliver Frank, Manuel Heim, Marcel Jakob, Andrea Barbero, Dirk Schäfer, Igor Bendik, Walter Dick, Michael Heberer, and Ivan Martin. Real-time quantitative RT-PCR analysis of human bone marrow stromal cells during osteogenic differentiation in vitro. *Journal of Cellular Biochemistry*, 85(4):737–746, April 2002. ISSN 07302312. doi: 10.1002/jcb.10174.

[223] Renata C. Pereira, Sheila Rydziel, and Ernesto Canalis. Bone morphogenetic protein-4 regulates its own expression in cultured osteoblasts. *Journal of Cellular Physiology*, 182(2):239–246, 2000. ISSN 00219541. doi: 10.1002/(SICI)1097-4652(200002)182:2⟨239::AID-JCP13⟩3.0.CO;2-W.

[224] Emmanuel Biver, Anne-Sophie Soubrier, Cyril Thouverey, Bernard Cortet, Odile Broux, Joseph Caverzasio, and Pierre Hardouin. Fibroblast growth factor 2 inhibits up-regulation of bone morphogenic proteins and their receptors during osteoblastic differentiation of human mesenchymal stem cells. *Biochemical and Biophysical Research Communications*, 427(4):737–742, 2012. ISSN 0006291X. doi: 10.1016/j.bbrc.2012.09.129.

[225] Tao Song, Wenjuan Wang, Jing Xu, Dan Zhao, Qian Dong, Li Li, Xue Yang, Xinglian Duan, Yiwen Liang, Yan Xiao, Jin Wang, Juanwen He, Ming Tang, Jian Wang, and Jinyong Luo. Fibroblast growth factor 2 inhibits bone morphogenetic protein 9-induced osteogenic differentiation of mesenchymal stem cells by repressing Smads signaling and subsequently reducing Smads dependent up-regulation of ALK1 and ALK2. *The international journal of biochemistry & cell biology*, 45(8):1639–46, August 2013. ISSN 1878-5875. doi: 10.1016/j.biocel.2013.05.005.

[226] Jeremy Skillington, Lisa Choy, and Rik Derynck. Bone morphogenetic protein and retinoic acid signaling cooperate to induce osteoblast differentiation of preadipocytes. *Journal of Cell Biology*, 159(1):135–146, October 2002. ISSN 00219525. doi: 10.1083/jcb.200204060.

[227] Mujib Ullah, Stefan Stich, Michael Notter, Jan Eucker, Michael Sittinger, and Jochen Ringe. Transdifferentiation of mesenchymal stem cells-derived adipogenic-differentiated cells into osteogenic- or chondrogenic-differentiated cells proceeds via dedifferentiation and have a cor-

relation with cell cycle arresting and driving genes. *Differentiation*, 85(3):78–90, February 2013. ISSN 03014681. doi: 10.1016/j.diff.2013.02.001.

[228] Young Dan Cho, Woo Jin Kim, Won Joon Yoon, Kyung Mi Woo, Jeong Hwa Baek, Gene Lee, Gwan Shik Kim, and Hyun Mo Ryoo. Wnt3a stimulates Mepe, Matrix extracellular phosphoglycoprotein, expression directly by the activation of the canonical Wnt signaling pathway and indirectly through the stimulation of autocrine Bmp-2 expression. *Journal of Cellular Physiology*, 227(6):2287–2296, June 2012. ISSN 00219541. doi: 10.1002/jcp.24038.

[229] S Iseki, A O Wilkie, and G M Morriss-Kay. Fgfr1 and Fgfr2 have distinct differentiation- and proliferation-related roles in the developing mouse skull vault. *Development (Cambridge, England)*, 126(24):5611–5620, 1999. ISSN 0950-1991.

[230] Anne L. Jacob, Craig Smith, Juha Partanen, and David M. Ornitz. Fibroblast growth factor receptor 1 signaling in the osteo-chondrogenic cell lineage regulates sequential steps of osteoblast maturation. *Developmental Biology*, 296(2):315–328, 2006. ISSN 00121606. doi: 10.1016/j.ydbio.2006.05.031.

[231] Hiroyuki Suzuki, Naoto Suda, Momotoshi Shiga, Yukiho Kobayashi, Masataka Nakamura, Sachiko Iseki, and Keiji Moriyama. Apert syndrome mutant FGFR2 and its soluble form reciprocally alter osteogenesis of primary calvarial osteoblasts. *Journal of Cellular Physiology*, 227 (9):3267–3277, September 2012. ISSN 00219541. doi: 10.1002/jcp.24021.

[232] Yukiho Tanimoto, Masahiko Yokozeki, Kenji Hiura, Kazuya Matsumoto, Hideki Nakanishi, Toshio Matsumoto, Pierre J Marie, and Keiji Moriyama. A soluble form of fibroblast growth factor receptor 2 (FGFR2) with S252W mutation acts as an efficient inhibitor for the enhanced osteoblastic differentiation caused by FGFR2 activation in Apert syndrome. *Journal of Biological Chemistry*, 279(44):45926–45934, October 2004. ISSN 00219258. doi: 10.1074/jbc.M404824200.

[233] Jounghyen Park, Ok Jin Park, Won Joon Yoon, Hyun Jung Kim, Kang Young Choi, Tae Joon Cho, and Hyun Mo Ryoo. Functional characterization of a novel FGFR2 mutation, E731K, in craniosynostosis. *Journal of Cellular Biochemistry*, 113(2):457–464, February 2012. ISSN 07302312. doi: 10.1002/jcb.23368.

[234] Roberto D Fanganiello, Andréa L Sertié, Eduardo M Reis, Erika Yeh, Nélio AJ Oliveira, Daniela F Bueno, Irina Kerkis, Nivaldo Alonso, Sérgio Cavalheiro, Hamilton Matsushita, Renato Freitas, Sergio Verjovski-Almeida, and Maria Rita Passos-Bueno. Apert p.Ser252Trp Mutation in FGFR2 Alters Osteogenic Potential and Gene Expression of Cranial Periosteal Cells. *Molecular Medicine*, 13(7-8):422–442, 2007. ISSN 10761551. doi: 10.2119/2007-00027.Fanganiello.

[235] Kai Yu, Jingsong Xu, Zhonghao Liu, Drazen Sosic, Jiansu Shao, Eric N Olson, Dwight A Towler, and David M Ornitz. Conditional inactivation of FGF receptor 2 reveals an essential role for FGF signaling in the regulation of osteoblast function and bone growth. *Development (Cambridge, England)*, 130(13):3063–3074, 2003. ISSN 0950-1991. doi: 10.1242/dev.00491.

[236] Vereragavan P Eswarakumar, Efrat Monsonego-Ornan, Mark Pines, Ileana Antonopoulou, Gillian M Morriss-Kay, and Peter Lonai. The IIIc alternative of Fgfr2 is a positive regulator of bone formation. *Development (Cambridge, England)*, 129(16):3783–3793, 2002. ISSN 0950-1991.

[237] Hichem Miraoui, Karim Oudina, Hervé Petite, Yukiho Tanimoto, Keiji Moriyama, and Pierre J. Marie. Fibroblast growth factor receptor 2 promotes osteogenic differentiation in mesenchymal

cells via ERK1/2 and protein kinase C signaling. *The Journal of biological chemistry*, 284(8):4897–4904, December 2009. ISSN 0021-9258. doi: 10.1074/jbc.M805432200.

[238] Sooho Lee, Hee-Yeon Cho, Hang Bui, and Dongchul Kang. The osteogenic or adipogenic lineage commitment of human mesenchymal stem cells is determined by protein kinase C delta. *BMC Cell Biology*, 15(1):42, November 2014. ISSN 1471-2121. doi: 10.1186/s12860-014-0042-4.

[239] Hyun Jung Kim, Jung Hwan Kim, Suk Chul Bae, Je Yong Choi, Hyun Jung Kim, and Hyun Mo Ryoo. The protein kinase C pathway plays a central role in the fibroblast growth factor-stimulated expression and transactivation activity of Runx2. *Journal of Biological Chemistry*, 278 (1):319–326, January 2003. ISSN 00219258. doi: 10.1074/jbc.M203750200.

[240] Byung Gyu Kim, Hyun Jung Kim, Hye Jeong Park, Youn Jeong Kim, Won Joon Yoon, Seung Jin Lee, Hyun Mo Ryoo, and Je Yoel Cho. Runx2 phosphorylation induced by fibroblast growth factor-2/protein kinase C pathways. *Proteomics*, 6(4):1166–1174, February 2006. ISSN 16159853. doi: 10.1002/pmic.200500289.

[241] Kyung-Min Choi, Young-Kwon Seo, Hee-Hoon Yoon, Kye-Yong Song, Soon-Yong Kwon, Hwa-Sung Lee, and Jung-Keug Park. Effect of ascorbic acid on bone marrow-derived mesenchymal stem cell proliferation and differentiation. *Journal of bioscience and bioengineering*, 105(6):586–594, 2008. ISSN 13891723. doi: 10.1263/jbb.105.586.

[242] Donald F Ward, Roman M Salasznyk, Robert F Klees, Julianne Backiel, Phaedra Agius, Kristin Bennett, Adele Boskey, and George E Plopper. Mechanical strain enhances extracellular matrix-induced gene focusing and promotes osteogenic differentiation of human mesenchymal stem cells through an extracellular-related kinase-dependent pathway. *Stem cells and development*, 16 (3):467–480, 2007. ISSN 1547-3287. doi: 10.1089/scd.2007.0034.

[243] Peng Zhang, Yuqiong Wu, Zonglai Jiang, Lingyong Jiang, and Bing Fang. Osteogenic response of mesenchymal stem cells to continuous mechanical strain is dependent on ERK1/2-Runx2 signaling. *International Journal of Molecular Medicine*, 29(6):1083–1089, 2012. ISSN 11073756. doi: 10.3892/ijmm.2012.934.

[244] B Li, C Qu, C. Chen, Y Liu, K Akiyama, R Yang, F Chen, Y Zhao, and S Shi. Basic fibroblast growth factor inhibits osteogenic differentiation of stem cells from human exfoliated deciduous teeth through ERK signaling. *Oral Diseases*, 18(3):285–292, April 2012. ISSN 1354523X. doi: 10.1111/j.1601-0825.2011.01878.x.

[245] Angela Raucci, Paola Bellosta, Roberta Grassi, Claudio Basilico, and Alka Mansukhani. Osteoblast proliferation or differentiation is regulated by relative strengths of opposing signaling pathways. *Journal of Cellular Physiology*, 215(2):442–451, 2008. ISSN 00219541. doi: 10.1002/jcp.21323.

[246] Wen-Tzu Lai, Veena Krishnappa, and Donald G Phinney. Fibroblast growth factor 2 (Fgf2) inhibits differentiation of mesenchymal stem cells by inducing Twist2 and Spry4, blocking extracellular regulated kinase activation, and altering Fgf receptor expression levels. *Stem cells*, 29(7): 1102–1111, July 2011. ISSN 1549-4918. doi: 10.1002/stem.661.

[247] Itaru Urakawa, Yuji Yamazaki, Takashi Shimada, Kousuke Iijima, Hisashi Hasegawa, Katsuya Okawa, Toshiro Fujita, Seiji Fukumoto, and Takeyoshi Yamashita. Klotho converts canonical

FGF receptor into a specific receptor for FGF23. *Nature*, 444(7120):770–774, December 2006. ISSN 0028-0836. doi: 10.1038/nature05315.

[248] Kosaku Nitta, Nobuo Nagano, and Ken Tsuchiya. Fibroblast Growth Factor 23/Klotho Axis in Chronic Kidney Disease. *Nephron Clinical Practice*, 128(1-2):1–10, January 2014. ISSN 1660-2110. doi: 10.1159/000365787.

[249] Keitaro Yokoyama. Chronic Kidney Disease-Mineral and Bone Disorder (CKD-MBD). *Tokyo Jikeikai Medical Journal*, 128(6):241–246, 2013. ISSN 03759172. doi: 10.3724/SP.J.1008.2013.00899.

[250] Yu-Chen Guo and Quan Yuan. Fibroblast growth factor 23 and bone mineralisation. *International Journal of Oral Science*, 7(1):8–13, January 2015. ISSN 1674-2818. doi: 10.1038/ijos.2015.1.

[251] Yan Li, Xu He, Hannes Olauson, Tobias E Larsson, and Urban Lindgren. FGF23 affects the lineage fate determination of mesenchymal stem cells. *Calcified Tissue International*, 93(6):556–564, December 2013. ISSN 0171967X. doi: 10.1007/s00223-013-9795-6.

[252] M Kuro-o, Y Matsumura, H Aizawa, H Kawaguchi, T Suga, T Utsugi, Y Ohyama, M Kurabayashi, T Kaname, E Kume, H Iwasaki, A Iida, T Shiraki-Iida, S Nishikawa, R Nagai, and Y I Nabeshima. Mutation of the mouse klotho gene leads to a syndrome resembling ageing. *Nature*, 390(6655):45–51, 1997. ISSN 0028-0836. doi: 10.1038/36285.

[253] Hiroaki Masuda, Hirotaka Chikuda, Tatsuo Suga, Hiroshi Kawaguchi, and Makoto Kuro-o. Regulation of multiple ageing-like phenotypes by inducible klotho gene expression in klotho mutant mice. *Mechanisms of Ageing and Development*, 126(12):1274–1283, December 2005. ISSN 00476374. doi: 10.1016/j.mad.2005.07.007.

[254] V. Shalhoub, S. C. Ward, B. Sun, J. Stevens, L. Renshaw, N. Hawkins, and W. G. Richards. Fibroblast growth factor 23 (FGF23) and alpha-klotho stimulate osteoblastic MC3T3.E1 cell proliferation and inhibit mineralization. *Calcified Tissue International*, 89(2):140–150, 2011. ISSN 0171967X. doi: 10.1007/s00223-011-9501-5.

[255] Kazuaki Miyagawa, Miwa Yamazaki, Masanobu Kawai, Jin Nishino, Takao Koshimizu, Yasuhisa Ohata, Kanako Tachikawa, Yuko Mikuni-Takagaki, Mikihiko Kogo, Keiichi Ozono, and Toshimi Michigami. Dysregulated gene expression in the primary osteoblasts and osteocytes isolated from hypophosphatemic Hyp mice. *PLoS ONE*, 9(4):e93840, January 2014. ISSN 19326203. doi: 10.1371/journal.pone.0093840.

[256] Shiguang Liu, Wen Tang, Jianwen Fang, Jinyu Ren, Hua Li, Zhousheng Xiao, and L D Quarles. Novel regulators of Fgf23 expression and mineralization in Hyp bone. *Molecular endocrinology (Baltimore, Md.)*, 23(9):1505–1518, September 2009. ISSN 1944-9917. doi: 10.1210/me.2009-0085.

Part V

Appendix

List of Figures

List of Tables

List of Abbreviations

Table 14.1: Abbreviations and symbols used in this thesis

3D	three-dimensional
3T3-F442A	murine pre-adipocyte cell line
3T3-L1	murine pre-adipocyte cell line, common model for adipogenesis
ad prediff	adipogenically pre-differentiated
Akt	protein kinase B (PKB) alias Akt
ALP	alkaline phosphatase (corresponding protein to the ALPL gene)
ALPL	alkaline phosphatase liver, bone, kidney (corresponding gene to the ALP protein)
ANKH	ANKH inorganic pyrophosphate transport regulator
ann. temp.	annealing temperature
ANOVA	analysis of variance
APS	ammonium persulfate
ARS	Alizarin red S staining
autocl.	autoclaved
bi-dist.	bidistilled
BMD	bone mineral density
BMP	bone morphogenetic protein
BMPR	BMP receptor
bp	base pair
BSA	bovine serum albumin
C3H10T1/2	murine multipotent mesenchymal cell line
cDNA	complementary DNA
C/EBP	CCAAT/enhancer binding protein
CKD-MBD	chronic kidney disease-mineral and bone disorder
CO_2	carbon dioxide
COL1A1	collagen 1 A1
ctrl	control
d	day(s)
DAG	diacylglycerol
dist.	distilled
DKK	dickkopf (protein family of Wnt inhibitors)
DMEM	Dulbecco's modified eagle's medium

Continued on next page

Table 14.1 – *Continued*

DMP1	dentin matrix acidic phospho-protein 1
DMSO	dimethylsulfoxide
DNA	deoxyribonucleic acid
dNTPs	deoxynucleotide triphosphates
ECM	extracellular matrix
EDTA	ethylendiamintetraacetic acid
EEF1α	eukaryotic translocation elongation factor 1α
effic.	efficiency
e.g.	exempli gratia
ENPP1	ectonucleotide pyrophosphatase/phosphodiesterase 1
ERK1/2	extracellular signal-regulated kinases 1 and 2
et al.	et alia
FABP4	fatty acid binding protein 4, adipocyte (alias adipocyte protein 2 (aP2))
FACS	fluorescence activated cell sorting
FCS	fetal calf serum
FGF	fibroblast growth factor
FGFR	FGF receptor
fig.	figure
FRS2α	FGFR substrate 2α
g	constant of gravitation
GAB1	GRB2-associated-binding protein 1
GAPDH	glycerinaldehyde-3-phosphate dehydrogenase
GFP	green fluorescent protein
GRB2	growth factor receptor-bound protein 2
h	hour(s)
hASCs	human adipose-derived stromal cells
hBMSC	human bone marrow stromal cell
HCl	hydrochloric acid
HFD	high-fat diet
hFOB 1.19	human fetal osteoblastic cell line
hPA	primary human pre-adipocytes
HPLC	high performance liquid chromatography
HRP	horse radish peroxidase
HS	heparan sulfate

Continued on next page

Table 14.1 – *Continued*

HSPG	heparan sulfate proteoglycan
IBMX	3-isobutyl-1-methylxanthine
IBSP	integrin-binding sialoprotein
inh	inhibitor
IU	international unit/s
IP_3	inositol triphosphate
JNK	c-Jun N-terminal kinase
kb	kilobase
LPL	lipoprotein lipase
M	molar (mol per liter)
MAPK	mitogen-activated protein kinase
mASCs	murine adipose-derived stem cells
MC3T3-E1	murine calvarial pre-osteoblast cell line
MEK1/2	MAPK/ERK kinases 1 and 2 (alias mitogen-activated protein kinase kinases 1 and 2)
min	minute(s)
MLO-Y4	murine osteocyte cell line
mRNA	messenger RNA
N	normal concentration
NaCl	sodium chloride
NaOH	sodium hydroxide
NIH-3T3	Murine embryonic fibroblast cell line
OB1	murine osteoblast cell line
OC	osteocalcin (alias bone gamma-carboxyglutamate (Gla) protein (BGLAP))
OD	optical density
OPN	osteopontin (alias secreted phosphoprotein 1 (SPP1))
ORO	Oil red O staining
ost prediff	osteogenically pre-differentiated
p38-MAPK	p38-mitogen-activated protein kinase
PBS	phosphate buffered saline
PDGF	platelet-derived growth factor
PFA	paraformaldehyde
PHOSPHO-1	phosphoethanolamine/phosphocholine phosphatase
PI3K	phosphoinositide 3-kinase

Continued on next page

Table 14.1 – *Continued*

PIP_2	phosphatidylinositol 4,5-bisphosphate
PKC	protein kinase C
PLCγ	protein lipase Cγ
PMSF	phenylmethylsulfonylfluoride
PPARγ2	peroxisome proliferator-activated receptor γ2
Pref-1	pre-adipocyte factor 1
PTH	parathyroid hormone
PTPN11	protein tyrosine phosphatase, non-receptor type 11 (alias SHP2)
PVDF	polyvinylidenfluoride
qPCR	quantitative real-time reverse transcriptase PCR
RNA	ribonucleic acid
RPLP0 (alias 36B4)	ribosomal protein, large, P0
rpm	rounds per minute
RPS27A	ribosomal protein S27a
RT-PCR	semiquantitative reverse transcriptase polymerase chain reaction
RUNX2	runt-related transcription factor 2 (alias core-binding factor subunit alpha-1 (CBFA-1)
s	second
Saos-2	human osteoblast-like sarcoma cell line
SAPK	stress-activated protein kinase
SDS	sodium dodecyl sulfate
SDS-PAGE	sodium dodecyl sulfate polyacrylamide gel electrophoresis
SEM	standard error of the mean
SFRP1	soluble frizzled-related protein 1
SHP2 (alias PTPT11)	protein tyrosine phosphatase, non-receptor type 11
shRNA	small hairpin RNA
siRNA	small interfering RNA
SOS	son of sevenless homolog
Sost	sclerostin
TA1	murine adipose cell line
tab.	table
TAZ	transcriptional co-activator with PDZ-binding motif
TEMED	N,N,N,N-tetramethyl ethylenediamine
temp.	temperature

Continued on next page

Table 14.1 – *Continued*

TGF-β	transforming growth factor-β
TK	tyrosine kinase domain
U2OS	human osteoblast-like sarcoma cell line
undiff	undifferentiated
veh	vehicle (respective solvent)
vol.	volume
WHO	World Health Organization
w/o	without

List of Publication

Peer reviewed journal publications

Simann M, Schneider V, Le Blanc S, Dotterweich J, Zehe V, Krug M, Jakob F, Schilling T[1], Schütze N[1] ([1] contributed equally), 'Heparin affects human bone marrow stromal cell fate: Promoting osteogenic and reducing adipogenic differentiation and conversion', *Bone*, 78:102-113, May 2015. ISSN 87563282. doi 10.1016/j.bone.2015.04.039. Original research paper.

Dittmar K E J, **Simann M**, Zghoul N, Schön O, Meyring W, Hannig H, Macke L, Dirks W G, Miller K, Garritsen H S P, Lindenmaier W, 'Quality of Cell Products: Authenticity, Identity, Genomic Stability and Status of Differentiation', *Transfusion medicine and hemotherapy*, 37(2):57-64, April 2010. ISSN 1660-3796. doi 10.1159/000284401. Original research paper.

Manuscripts in preparation or under review

Simann M, Le Blanc S, Schneider V, Schilling T, Jakob F, Schütze N. 'FGF1 impedes adipogenic and osteogenic differentiation and conversion of hBMSCs via FGFR1 and ERK 1/2 signaling'. In preparation.

Le Blanc S, **Simann M**, Jakob F, Schütze N, Schilling T. 'Fibroblast growth factor 1 and 2 inhibit adipogenic differentiation of human bone marrow stromal cells in 3D collagen gels', *Exp Cell Res*. In revision.

Oral presentations

Simann M, Le Blanc S, Jakob F, Schütze N, Schilling T, 'Determining the role of FGF1 in adipogenic and osteogenic differentiation and conversion of hMSC', *PhD Training Course of the European Calcified Tissue Society (ECTS)*, Oxford - United Kingdom, Jun. 2014. (DAAD travel stipend)

Simann M, Le Blanc S, Schütze N, Schilling T, 'Untersuchung von FGF1-Signalwegen während der Konversion von Osteoblasten und Adipozyten als neuer Ansatz für die Osteoporose-Therapie', *Osteologie Conference*, Weimar - Germany, Mar. 2013. (DAdorW travel stipend)

Simann M, Le Blanc S, Schütze N, Schilling T, 'Fibroblast growth factor signaling during the adipogenic conversion of osteoblasts', *3rd International Conference 'Strategies in Tissue Engineering' of the Würzburger Initiative for Tissue Engineering e.V. (WITE)*, Würzburg - Germany, May 2012.

Poster presentations

Simann M, Le Blanc S, Jakob F, Schütze N, Schilling T, 'FGF1 impedes adipogenic and osteogenic differentiation and conversion of hBMSCs via FGFR1 and ERK 1/2 signaling', *4th International Conference 'Strategies in Tissue Engineering' of the Würzburger Initiative for Tissue Engineering e.V. (WITE)*, Würzburg - Germany, Jun. 2015.

Le Blanc S, **Simann M**, Jakob F, Schütze N, Schilling T. 'Inhibition of adipogenic and osteogenic differentiation of hBM-MSCs by FGF1 and FGF2 in 3D collagen gels', *Annual Meeting of the American Society for Bone and Mineral Research (ASBMR)*, Houston (Texas) - USA, Sep. 2014.

Simann M, Le Blanc S, Jakob F, Schütze N, Schilling T, 'Decrease of mineralization by FGF1 is linked to up-regulation of ANKH and OP in osteogenic differentiation and conversion', *Annual Meeting of the European Calcified Tissue Society (ECTS)*, Prague - Czech Republic, May 2014.

Simann M, Le Blanc S, Jakob F, Schütze N, Schilling T, 'Determining the role of FGF on osteogenic and adipogenic differentiation and conversion in mesenchymal stem cells', *Annual Meeting of the American Society for Bone and Mineral Research (ASBMR)*, Baltimore (Maryland) - USA, Oct. 2013.

Le Blanc S, **Simann M**, Schütze N, Schilling T. 'Adipogenic and osteogenic differentiation/conversion in 3D collagen gels as a model for osteoporosis research', *Annual Meeting of the American Society for Bone and Mineral Research (ASBMR)*, Baltimore (Maryland) - USA, Oct. 2013.

Le Blanc S, **Simann M**, Schütze N, Schilling T. 'Adipogenic and osteogenic differentiation of BM-MSC in type-I collagen gels as a model for osteoporosis research', *Osteologie Conference*, Weimar - Germany, Mar. 2013.

Le Blanc S, **Simann M**, Schütze N, Schilling T. 'Adipogenic differentiation of BM-MSC in type- I collagen gels', *Berlin-Brandenburg School for Regenerative Therapies PhD Students Symposium*, Berlin - Germany, Dec. 2012.

Simann M, Le Blanc S, Benisch P, Klotz B, Schütze N, Schilling T, 'Exploring signaling check points in conversion of osteoblasts and adipocytes as novel approaches for osteoporosis therapy', *Annual Meeting of the American Society for Bone and Mineral Research (ASBMR)*, Minneapolis (MN) - USA, Oct. 2012. (GSLS travel stipend)

Le Blanc S, **Simann M**, Schütze N, Schilling T. 'Adipogenic and osteogenic differentiation of hBM-MSC in type-I collagen gels', *GSLS Doctoral Researchers Symposium*, Würzburg - Germany, Oct. 2012.